Push-pull Tests to Quantify In-situ Naphthalene Phytoremediation Rates

Mark T. Pitterle

Thesis submitted to the faculty of Virginia Polytechnic Institute and State University in partial fulfillment of the requirements for the degree of

MASTER OF SCIENCE

in

ENVIRONMENTAL ENGINEERING

John T. Novak, Co-Chair
Mark A. Widdowson, Co-Chair
Charles Hagedorn

January 9th, 2004

Blacksburg, Virginia

Keywords: naphthalene, creosote, phytoremediation, poplar trees, push pull, injection withdrawal

Push-pull Tests to Quantify In-situ Naphthalene Phytoremediation Rates

by

Mark Pitterle

Committee Co-Chairs: John T. Novak, Mark A. Widdowson

Environmental Engineering

ABSTRACT

Ten strategically placed push-pull wells were installed to determine in-situ degradation rates at a creosote contaminated site and to assess the contribution of hybrid poplar trees to polynuclear aromatic hydrocarbon (PAH) remediation. Well positioning enabled comparison between contaminated and non-contaminated locations, as well as comparisons between locations with and without trees. Comparison of areas with and without trees enabled an improved understanding of the role that the phytoremediation system has on the overall degradation of PAHs at the site. Bromide, a conservative, non-reactive tracer, was injected in solution along with dissolved oxygen. Twelve push-pull tests (PPTs) were performed, of which three did not include naphthalene in the injection solution, so that the developed method could be evaluated, tested, and yield an initial set of rates to make seasonal and spatial varying in-situ comparisons. Method comparison used for rate analysis found the highest confidence in the method of Snodgrass and Kitanidis (1998) for zero order rates and the method of Haggerty et al. (1998) for first order rates. The largest zero and first order rates, 2.43 $mg_{naphthalene}$/L-hr and 1.25 1/hr, respectively, occurred at treed regions in June. Zero and first order winter rates at treed regions were greater by a factor of at least 2.5 when compared to non-treed regions. Degradation rates at treed regions were found to steadily increase by over four times from winter to summer. Results validate that decay variations attributed to phytoremediation can be detected with the push-pull method. PPTs performed at the Oneida site verified observed trends determined from six years of monitoring data, microbial characterization, and microcosm studies.

ACKNOWLEDGEMENTS

I would like to thank Dr. Novak for his endless advice and freedom in letting the student find their way. You have taught me far more than academics. I would also like to thank Dr. Widdowson for his support and critical help in groundwater concepts. Thank you, Dr. Hagedorn, for your humor and participation on my committee.

Thank you to the EPA Hazardous Waste Center for funding support that made this research possible. Thank you to the Edna Bailey Sussman Foundation for further financial support that helped initiate this research.

Above all, I would like to thank my always hard-working research partner Rikke, who supported half of everyone's load on the way. Your partnership on site trips and support along the way was essential. I couldn't have done it without you! And cheers of praise could not be any louder for the hard work and support of Julie Petruska and Jody Smiley. You make our research possible. And to Betty Wingate and Sherry Burke, without you, our department would fall apart. Thank you to Heather Rectanus and Ellis for their help on field trips and bringing things together in times of need. Thank you to John Haggard and Micah Leamer for their willingness to share their mathematical genius. Your comments and suggestions provided important insights to fully grasp concepts discussed in this paper. Thank you to the remaining friends in the environmental engineering department who have helped, supported, and gave advice along the way; there are so many of you that were so helpful that it is not possible to list all of you here, but nevertheless your help is greatly appreciated. And to the remaining cast of friends that helped maintain balance in my life.

Thank you to my parents, whose support, patience, and willingness to keep giving are a model to us all. All of you have made this work possible. I will truly miss all of you and my Blacksburg community! May we each learn to simply be.

TABLE OF CONTENTS

LIST OF FIGURES

APPENDIX B

APPENDIX C

LIST OF TABLES

1.0 INTRODUCTION

Quantifying in-situ degradation rates are necessary to optimize the design of future phytoremediation projects in contaminated areas, predict the bioremediation timeframe, and to minimize the risk of exposure of contaminants to the public and the surrounding environment. Accurately forecasting the rate and extent of remediation using various approaches, including phytoremediation, will enable engineers to make cost-effective design decisions. Site-specific data that supports design decisions may prove critical to the success of phytoremediation.

A number of methods have been developed to estimate subsurface microbial degradation rates including rate derived calculations from monitoring data and microcosm studies, the merits of which are discussed by Chapelle (1993). Generally, the determination of in-situ degradation rates is considered more representative of the actual aquifer conditions since a larger volume of aquifer can be investigated (Istok et al., 1997). The transferability of laboratory-derived rates to in-situ processes is complicated by possible disturbance of the in-situ microbial population as well as sample-sediment disturbance and fracture. Furthermore, the reproduction of field conditions in the laboratory can prove to be problematic. For example, laboratory procedures may cause unforeseen selective growth conditions, such as the selection of fast growing species when laboratory conditions are inadvertently more ideal than field conditions (Istok et al., 1997). Further difficulties arise when attempting to obtain representative samples, as well as scaling laboratory results to field-scale processes (e.g. scaling of particle size for sorption characterization can lead to great uncertainty, Drever and McKee, 1980). Laboratory methods, such as microcosms, can provide general trends that can then be verified through in-situ rate determination, but generally, confidence is only given to rates determined in-situ, such as via push-pull tests. Nonetheless, pairing laboratory approaches with the determination of in-situ degradation rates enables comparison of the accuracy of individual methods and ultimately the development of real-time remediation models capable of incorporating seasonal and spatial variations.

1.1 Push-pull Tests

Single-well injection-withdrawal tests, or push-pull tests (PPTs), involve the injection ("push") of a well-mixed solution consisting of a non-reactive, conservative tracer and an electron donor and/or a contaminant into the saturated zone of an aquifer. Following injection, extraction ("pull") of groundwater from the well occurs. The conservative tracer is subject only to advection and dispersion, whereas the other reactive solute(s) are additionally presumed to be subject to constant, irreversible attenuation processes. Prior to the initial injection, background samples are collected and analyzed. An incubation period may precede the extraction phase of the test solution, that includes a rest phase without pumping, to enable measurable changes in the degraded solute/contaminant to occur, such as during slower, anaerobic metabolism. Samples are collected during the injection and the extraction cycles to analyze the concentration of the solutes over time. The inert tracer is chosen so that the tracer and the electron acceptor and/or contaminant have similar retardation factors. A breakthrough curve (BTC) is created, where the normalized concentration is plotted versus the normalized volume of recovered fluid. Integration of the breakthrough curve enables calculation of the mass removal rate during the extraction phase when coupled with the mean residence time of the tracer. The mean residence time is defined as the elapsed time from the midpoint of the injection to the centroid of the tracer. Degradation rates can then be determined using the methods of Haggerty et al. (1998), Schroth et al. (2001), and Snodgrass and Kitanidis (1998).

PPTs have proven to be a useful tool to establish quantitative information essential for proper site characterization, risk assessment, and remedial design. PPTs' wide applicability is enabling this fast and cost-effective approach to become an important method in determining in-situ conditions including groundwater properties, microbial activity and pathways, as well as enabling the determination of in-situ degradation rates. PPTs offer many advantages over laboratory procedures as well as traditional, in-situ multi-well tracer test studies. Advantages of PPTs over laboratory procedures are described above as well as by Istok et al. (1997). Since only one well is required, considerable time and cost is saved during setup as well as during testing when compared to multi-well tracer test studies. Multi-well tracer test studies require

significantly longer test durations, as test solutions must migrate from the injection well to the various, down-gradient extraction wells.

Push-pull test results can provide accurate in-situ data for a spatial and seasonal variation model that potentially can provide accurate forecasts of plume reduction and elimination. The following uses the typical polynuclear aromatic hydrocarbon (PAH) contaminated site as an example. Generally, aerobic PAH degradation is more rapid than anaerobic processes, but given the slow mass transfer replacement of oxygen into the groundwater, anaerobic decay predominates at the center of the contaminant source (Norris et al., 1994; Morgan and Watkinson, 1992). Since a much larger contaminant mass is contained within the center, anaerobic portion of the plume, proper characterization of anaerobic transformation is essential. Although site dependent, a strong redox gradient typically exists at plume boundaries where aerobic conditions begin to dominate. Ease of PPT setup can enable optimal well placement to determine sharply varying redox conditions at the plume's fringe gradient, thus enabling accurate characterization of the aerobic/anaerobic contribution that is typical at plume boundaries. Careful manipulation of these observed trends provides accurate spatially varying conditions that are essential to model plume remediation.

PPTs have been used to determine a number of aquifer properties including development of an advection-dispersion equation during nonuniform flow (Hoopes and Harleman, 1967), longitudinal dispersivity (Gelhar and Collins, 1971; Bachmat et al., 1988), scale-dependent dispersion in a stratified aquifer (Pickens and Grisak, 1981), effective porosity (Bachmat et al., 1988), and flow velocity (Leap and Kaplan, 1988). Hall et al. (1991) drew upon previous work to develop equations to estimate effective porosity and groundwater velocity from push-pull results.

PPTs are useful in determining remediation rates for a variety of contaminant and attenuation processes. PPTs have been successfully applied to uranium immobilization and remobilization (Senko et al., 2002), benzene, toluene, ethylbenzene, and xylene (BTEX) transformation (Reinhard et al., 1997; Reusser et al., 2002), and non-aqueous phase liquid detection (Davis et al., 2002; Istok et al., 2002). PPTs have also been applied to determine cation exchange effects on surfactants (Field et al., 2000), sorption (Drever and McKee, 1980), solute retardation (Schroth et al., 2001), surfactant sorption

(Istok et al., 1999), surfactant enhanced solubilization (Field et al., 1999), microbial enzyme kinetics (Istok et al., 2001), microbial activity and diversity (Kleikemper et al., 2002), in-situ redox manipulation (Istok et al., 1999), and have even been applied to sulfide turnover rates in a meromictic alpine lake (Luthy et al., 2000).

Numerous studies have also applied PPTs to the determination of in-situ reaction processes and rates. Borden et al. (1989) utilized PPTs to study the effects of low oxygen concentrations on the biotransformation of polynuclear aromatics. Trudell et al. (1986) applied PPTs to determine in-situ denitrification rates. Schroth et al. (1998) examined spatial variability during aerobic and denitrifying conditions, while Reinhard et al. (1997) employed PPTs to nitrate and sulfate reducing conditions. Furthermore, aerobic and anaerobic microbial rate determination, including aerobic respiration, denitrification, sulfate reduction, methanogenesis, was addressed by Istok et al. (1997) and Schroth et al. (1998).

Traditionally, estimation of degradation rate coefficients determined from push-pull tests has relied upon fitting parameters to the data in a numerical transport model. Although numerical models have been carried out effectively, application of numerical models is often problematic. Even the best numerical algorithms, used to solve the transport equations, carry numerical errors in final results (Snodgrass and Kitanidis, 1998). Computer models also require knowledge of various aquifer parameters, including longitudinal dispersivity and effective porosity, none of which can be determined exactly and thus must be estimated. Therefore, numerical solutions of solute transport equations are only approximate and derived degradation rates carry this residual error (Snodgrass and Kitanidis, 1998). Methods developed by Haggerty et al. (1998) and Snodgrass and Kitanidis (1998), however, require no previous knowledge of regional groundwater flow or hydraulic parameters. Haggerty et al. (1998) developed a series of method-specific equations for determining zero and first order reaction-rate coefficients and Snodgrass and Kitanidis (1998) elaborated on this approach to apply to more generalized push-pull zero and first order reaction-rate coefficient determination.

Key assumptions to the methods of Haggerty et al. (1998) and Snodgrass and Kitanidis (1998) include: 1) the injected solutes are simultaneously introduced as well-mixed slugs; 2) the dominating processes are advection, dispersion, and spatially

homogeneous, constant coefficient, zero or first order irreversible reactions; 3) other processes such as sorption are negligible; 4) the retardation factors and boundary conditions of the conservative tracer and injected reactive solutes are similar, and 5) unless a modification of the method is performed, the background concentration of the conservative tracer and reactive solutes are negligible. In addition, Haggerty et al. (1998) showed that complete tracer recovery is not necessary for accurate quantification of rate coefficients.

Significant difficulties arise during PPTs when background concentrations are sufficiently high, creating ambiguous results when degradable test solutes are mixed with identical native solutes. Hageman et al. (2001) utilized a unique approach to detect trichloroethene (TCE) uptake by incorporating trichlorofluoroethene (TCFE) as the monitored solute. Fluoride was retained during reductive dechlorination, providing unambiguous rate determination when high background concentrations of TCE were present. Pombo et al. (2002) applied PPTs for phospholipid fatty acid (PLFA) and fluorescent in-situ hybridization (FISH) analyses and ^{13}C derived first order rate coefficients. The high expense and radioactivity of ^{13}C-labeled chemicals drove Reusser et al. (2002) to employ a less expensive approach where deuterated toluene and xylene were used to assess BTEX degradation. Rather than monitoring transformation of organic contaminants, Schroth et al. (2001) utilized stable sulfur isotope analyses to determine in-situ first order rate coefficients. Utilizing naturally occurring stable isotope analyses enables specific microbial characterization of sulfate-reducing conditions in the presence of high sulfate background concentrations and thus provides critical assessment of anaerobic contribution within the center of the plume. To date, little success has resulted from PPT attempts to characterize iron-reducing conditions, since the produced ferrous iron readily precipitates in the presence of sulfide. Thus, the monitored ferrous iron formation product produces ambiguous results and the terminal electron acceptor (TEA) process cannot be accurately distinguished.

PPTs have been used to address degradation attributed to fluctuations of the groundwater table. McGuire et al. (2002) assessed enhanced degradation caused from groundwater recharge carrying low concentrations of TEAs. PPTs, using tracer gases, rather than tracer solutes, have been applied to successfully determine the often

significant contribution of vadose zone volatilization (Amerson et al., 2001). It has been shown that vadose zone volatilization, although subject to changes in soil moisture, temperature, (Washington, 1996) atmospheric pressure, (Choi et al., 2002; Massmann and Farrier, 1992) as well as other weather characteristics including rainfall (Davis et al., 2001; Smith et al., 1996), can be the most significant removal mechanism in the early stages of remediation, when volatile compounds are found in their greatest proportion (Chaplin et al., 2002).

1.2 Phytoremediation

Natural attenuation and poplar tree phytoremediation systems have been shown to successfully mineralize PAH compounds, demonstrating that the combination of the two approaches can supplement one another through symbiosis to enable more rapid remediation of PAH contaminants (McCutcheon and Schnoor, 2003; Heitkamp and Cernigilia, 1988; Meuller et al., 1991; Walter et al., 1991; Weissefels et al., 1991; Milhelcic and Luthy, 1988; Leduc et al., 1992; McNally et al., 1998; Coates et al, 1996; Coates et al., 1997). Extending PPTs to quantify in-situ remediation in phytoremediated systems will further the applicability of phytoremediation to specific site characteristics.

Phytoremediation, or the use of plants to remove or degrade soil and groundwater contaminants, occurs through both direct and indirect mechanisms for organic pollutants. Direct phytoremediation involves the direct uptake of contaminants and subsequent accumulation of either the contaminant or non-toxic metabolites within the plant tissue. The contaminants or non-toxic metabolites can then be volatilized into the atmosphere in a process called phytovolatilization (Salt et al., 1998; Susarla et al., 2002). Indirect phytoremediation, or the rhizosphere effect, involves both: 1) the stimulation of microbial activity and transformation of xenobiotic contaminants caused by the release of enzymes and exudates into the rhizosphere and 2) enhanced mineralization of contaminants by microrhizal fungi and rhizosphere microbial consortia (Schnoor et al., 1995).

Phytoremediation serves as a cost-effective alternative to traditional groundwater remediation approaches, such as pump-and-treat systems or contaminated soil removal/landfilling. The non-intrusive nature of phytoremediated systems generally require little management while providing an aesthetically pleasing, publicly accepted

treatment technology. Application of phytoremediation is largely dependent upon the type of contaminant present and the discussion below is focused upon application of this technology to the amelioration of PAHs.

Degradation rates can be expected to increase when plants are used since plants provide tremendous root surface area for microbes to attach and grow and some species of plants transfer oxygen to the rhizosphere enabling aerobic mineralization of organics; increased microbial mineralization can also be attributed to the release of soluble exudates that include enzymes, aliphatics, aromatics, amino acids, sugars, and low-molecular-weight carbohydrates (Burken and Schnoor, 1996; Robinson, 2001). Symbiotic relationships with fungi and plant roots provide a wider array of enzymatic pathways that is not possible with bacteria alone (Schnoor et al., 1995). Jordahl et al. (1997) found significantly higher populations of denitrifiers, pseudomonads, and monoaromatic hydrocarbon degraders in soils taken from the rhizosphere of poplar trees when compared to non-vegetated soil. Microbial activity in the rhizosphere can be enhanced up to 100 times when compared to unvegetated soil (Reilley et al., 1996). Investigation of anthracene and pyrene, two PAHs found in creosote, showed 30 to 44% lower concentrations in vegetated soil (Reilley et al., 1996).

Bioavailability of PAHs limits direct phytoremediation to moderately hydrophobic compounds, such as naphthalene (log K_{ow} between 1.0 and 3.5) (Dietz and Schnoor, 2001); however, microbial consortia and mycorrhizal fungi degradation of two, three, and four ring PAHs have been shown to occur during aerobic (Heitkamp and Cernigilia, 1988; Meuller et al., 1991; Walter et al., 1991; Weissefels et al., 1991), denitrifying (Milhelcic and Luthy, 1988; Leduc et al., 1992; McNally et al., 1998), and sulfate reducing conditions (Coates et al, 1996; Coates et al., 1997). Monoaromatic hydrocarbon (Cozzarelli at al., 1990; Borden et al., 1995), and naphthalene (Anderson and Lovley, 1999) degradation has been shown to occur under iron-reducing conditions. Given the often-insoluble iron oxides common in the subsurface (Lovley, 1991), little research exists for iron-reducing degradation of PAHs. Lastly, previous laboratory work by Yeom and Ghosh (1998) has shown that mass transfer and dissolution kinetics in aged soils can be the limiting process in the mineralization of PAHs.

2.0 SCOPE OF PROJECT

To the best of our knowledge, PPTs have not been applied to assess degradation rates at a phytoremediation site. In this study, PPTs were applied to assess the contribution of a hybrid poplar tree phytoremediation system to the amelioration of PAHs at a creosote-contaminated site in Oneida, TN. The overall objective of this study is to develop, implement, and demonstrate a PPT method that can be used to determine in-situ degradation rates at the Oneida phytoremediation site.

2.1 Site Description

The phytoremediation system is located in Oneida, Tennessee at a facility formerly used to treat railroad ties with creosote. A large above-ground creosote tank ruptured during operation at the site discharging creosote into the subsurface soil and groundwater. Additional source contamination can be attributed to an unlined holding pond containing surplus creosote from railroad tie operations. Consequently, the site is severely contaminated with creosote constituents such as PAHs, benzene, toluene, ethylbenzene, xylene (BTEX), and other petroleum byproducts. The creosote, present as a dense non-aqueous phase liquid (DNAPL), sank to the bedrock, approximately 10-12 feet below the surface. Monitoring data has shown that the DNAPL has migrated towards Pine Creek to where it is presently located at a geologically low region of the bedrock. The subsurface is broadly characterized by a shallow, unconfined aquifer composed of three layers. The uppermost layer consists of several feet of gravel and coal fill, which overlays 5 to 6 feet of silty clay, followed by 4 to 5 feet of silty sand that rests upon shale bedrock. PAHs, which are carcinogens derived from the creosote contamination, warrant concern for local groundwater consumption and future land use as well as threaten the biodiversity and use of nearby Pine Creek and surrounding surface waters.

In 1997, over one thousand hybrid poplar trees, *Populus deltoides x nigra DN34*, were planted over 2.5 acres of the site to promote in-situ phytoremediation enhanced natural attenuation. Hybrid poplar trees were chosen based upon their evapotranspiration potential, growth rate, depth and distribution of roots, biomass yield, degradative enzyme production, and their ability to contain, degrade, and bioaccumulate contaminants (Al-

Yousfi et al., 2000). Capable of growing 3 meters per year, with roots reaching more than 20 feet in depth, hybrid poplar's phreatophitic nature enables them to uptake over 20 gallons of water per day (Matso, 1995). Thus, hybrid poplar trees are very useful for hydraulic control and lend themselves extremely useful to reduce the volume of groundwater in contact with the contaminant. The tree roots at the Oneida site have since penetrated the groundwater table and have reached the contamination plume.

In an effort to demonstrate phytoremediation of creosote with poplar trees, an extensive monitoring system including a series of monitoring wells and more than twenty multi-level samplers, with sampling ports at one-foot intervals, was constructed. Piezometers and pressure transducers are also employed within the site to measure the effect of the trees on groundwater flow patterns. In 1997, Virginia Tech began biannual groundwater and annual soil boring monitoring of 10 PAHs including 2-, 3-, 4-, and 5-ring PAHs that are representative of the large range of chemical properties and solubilities found in creosote. The 10 representative PAHs, which constitutes about 59% of the total mass of PAHs present in creosote, were chosen based upon initial site characterization data (Smartt, 2000; Robinson, 2001; Mueller et al., 1989). In addition, biannual monitoring of dissolved oxygen, nitrate, iron, sulfate, and hydrogen served to assess subsurface redox conditions. A map detailing the layout of the phytoremediation system, soil boring transects, monitoring wells, multi-level samplers (MLs), and push-pull test wells can be found in Figure 1.

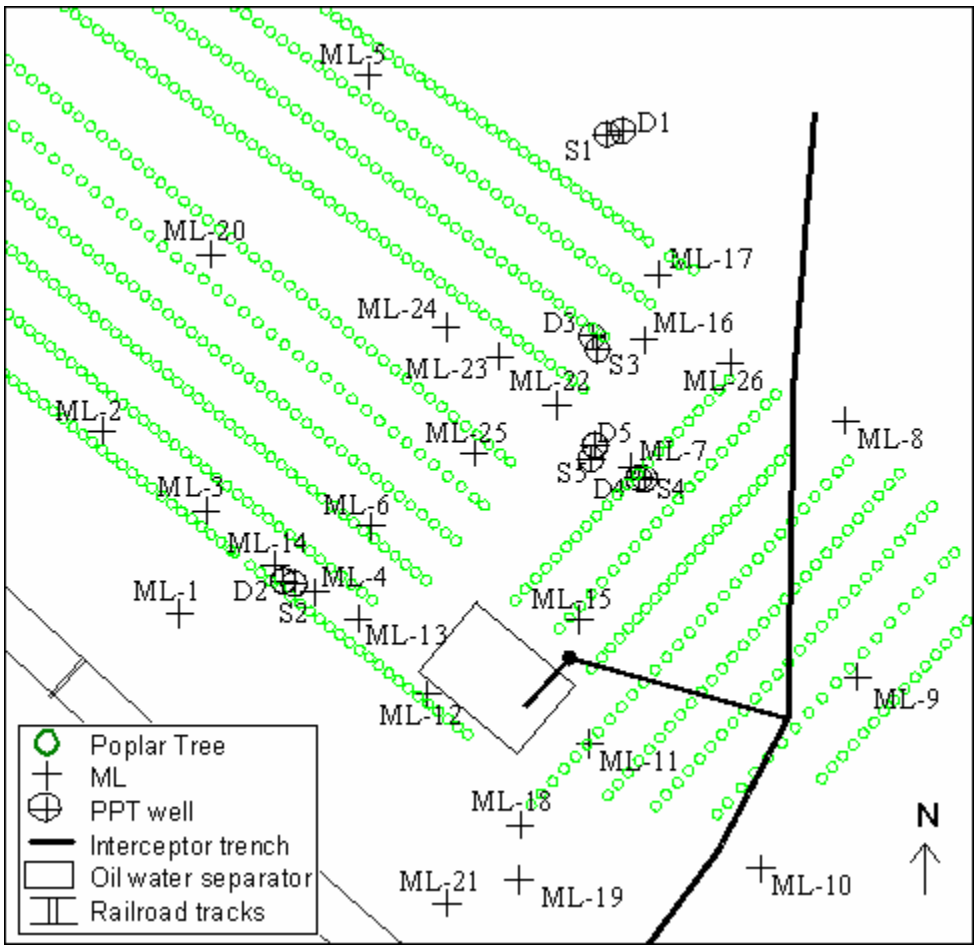

Figure 1: Oneida Phytoremediation and Monitoring System

2.2 Historic Data and Observed Trends

Marked drops in groundwater concentration and plume size over time have been observed in both shallow and deeper regions of the plume (Figure 2). An enrichment of high molecular weight compounds has been observed at the site. Figure 3 illustrates this observed trend at ML - 12. Figure 3 shows a marked decrease in naphthalene concentrations, as well as a slight decrease in acenaphthylene, another relatively low molecular weight PAH. Naphthalene, the most readily degradable PAH found in creosote, currently consists of about 65% of the PAHs found in the groundwater.

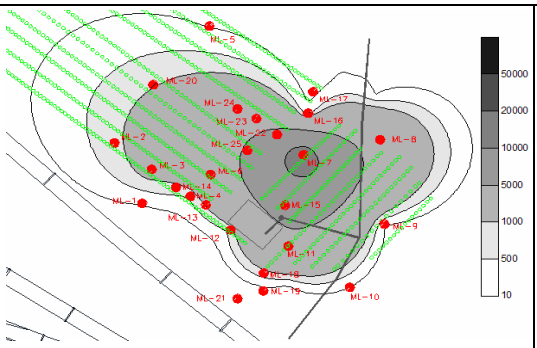

March 1998, Total PAH

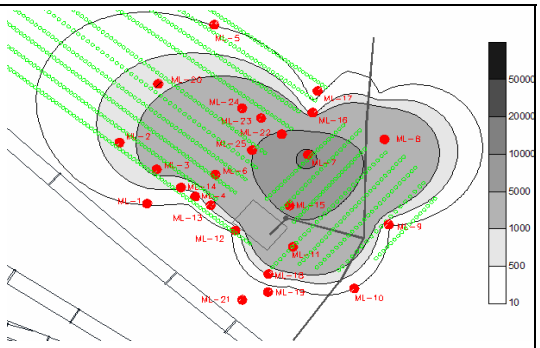

March 1998, Naphthalene Only

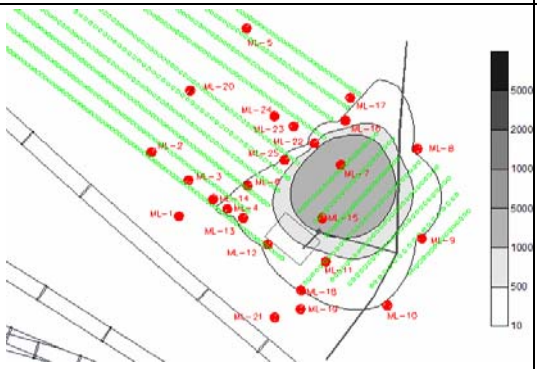

April 2003, Total PAH

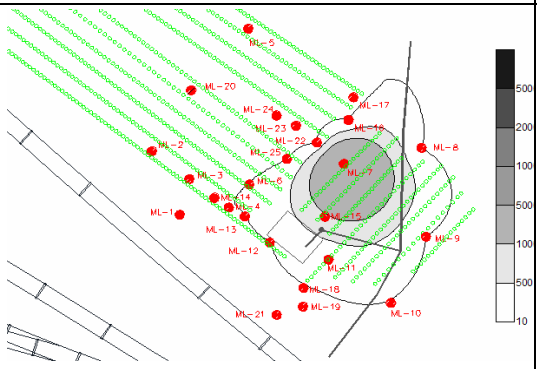

April 2003, Naphthalene Only

Figure 2: Average PAH Concentration [µg/L] in Groundwater 3-8 Feet Above Bedrock

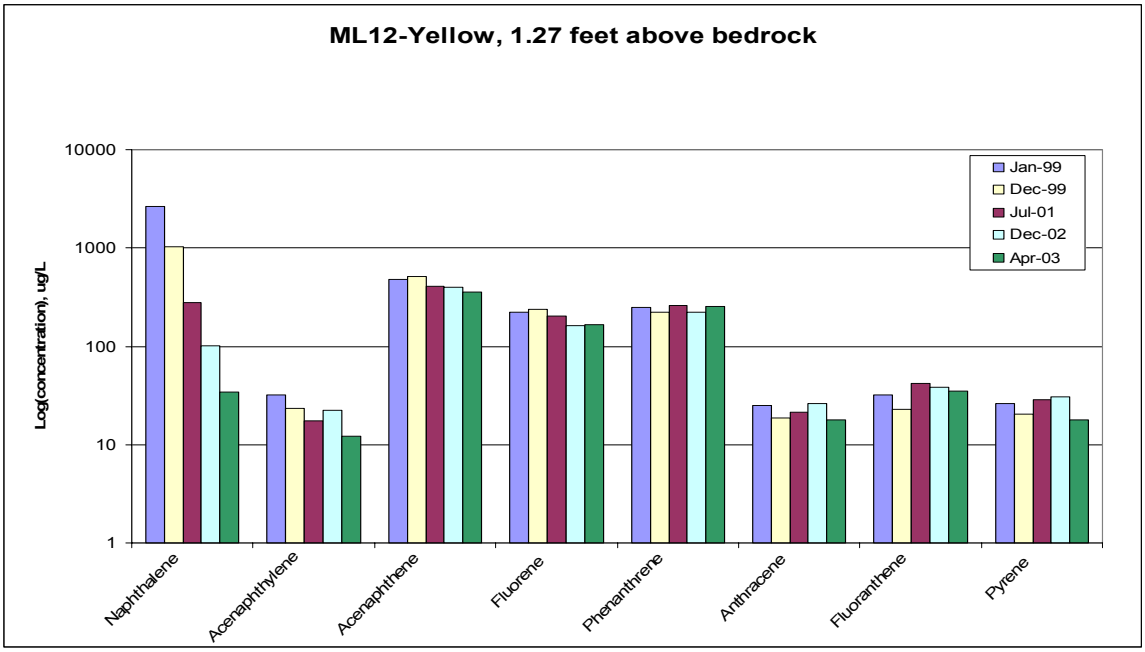

Figure 3: Distribution of PAHs in Groundwater with Time at MLS-12 , 1.27 Feet Above Bedrock [Log Scale]

Robinson (2001) identified increased diversity of PAH degraders in rhizosphere soil including fungal, actinomycetes, pseudomonads and bacillus species that are known aerobic, denitrifying, and ferrogenic PAH degraders. Observations of terminal electron acceptor (TEA) processes were further supported by dissolved hydrogen analysis. Microbial enumerations demonstrated an enhancement of microbial activity up to 100 times when compared to non-vegetated soils (Robinson, 2001). Presence of actinomycetes, a potential PAH degrader, were found to be approximately three times higher in rhizosphere soils as well, indicating the significant role that hybrid poplar trees' symbiotic relationships may have in PAH degradation (Robinson, 2001). Smartt (2002) found that dissolution kinetics is a rate-limiting process to amelioration of PAHs at the Oneida site.

The presence of naphthalene in root tissue and non-toxic metabolites in petioles and leaf buds suggest that hybrid poplar trees aid in the degradation of moderately hydrophobic PAHs (Robinson, 2001). These non-toxic metabolites, identified as sesquiterpenes (natural products with a naphthalene base) were not found in control trees located in an uncontaminated region (Robinson, 2001). At a later date, primary aromatics, including naphthalene-derivatives, phenols (including isoeugenol), and other aromatic compounds were found in buds, bark, and twig tissue all of which are not naturally occurring compounds found in poplar trees (Waters, 2002). In addition, moderate correlations were found to exist when unnaturally occurring primary aromatics identified in poplar tree tissue were used to predict the spatial distribution of the underlying PAH plume (Waters, 2002). To date, however, isolation of the mechanisms responsible for degradation, namely non-phytoremediated microbial transformation, plant uptake/transformation, rhizosphere microbial transformation, and vadose zone volatilization has not been assessed.

3.0 EXPERIMENTAL DESIGN

3.1 Push-pull Test In-Situ Method

Ten push-pull wells were installed to evaluate in-situ degradation rates at the creosote contaminated site in Oneida, TN. The 10 wells consisted of a shallow and deep well pair at five locations (Figure 1). Strategic well placement enabled comparison

between contaminated and non-contaminated locations, as well as comparisons between locations with and without trees. Comparison of areas with and without trees was designed to enable an improved understanding of the role that symbiosis in the rhizosphere has in the overall degradation of PAHs at the site.

S1 and D1, a shallow and deep well pair, respectively, was a control well outside the plume having no contamination. S2 and D2 were placed at a location near trees that has seen contamination but is no longer heavily contaminated. S3 and D3 were located at a fairly heavily contaminated part of the plume, adjacent to the largest tree on the site; this well demonstrates the best indicator of the contribution of phytoremediation. S4 and D4 were placed near trees in the most heavily contaminated part of the plume. S5 and D5 were also within the most heavily contaminated part of the plume, but are located at a maximum distance away from any tree, to assess degradation rates less affected by phytoremediation. It should be noted that the low groundwater velocity, only 7.5 inches/day, at the Oneida site made the use of multi-well tracer test studies impractical, which led to the use of PPTs to determine in-situ rates.

Twelve push-pull tests at the Oneida site were performed using bromide as the conservative tracer and a variety of reactive solutes. Reactants that were assessed include dissolved oxygen, ferrous iron, sulfate, sulfide, and nitrate (if present in background). Nine tests included the addition of naphthalene in the injection solution. The merit of naphthalene injection is described in 3.2 Proposed Testing Matrix below. All tests assume that the tracer and reactant have the same retardation factors, which signifies that the tracer and reactants have similar sorption to the aquifer sediment and similar solute transport throughout the aquifer. Schroth et al. (2001) has shown that bromide, dissolved oxygen, and sulfate exhibit similar transport behavior in a heterogeneous aquifer, thus validating this assumption.

3.2 Proposed Testing Matrix

Variations in the composition of the injection solution provide essential data to ensure experimental soundness. Overall, four varieties of the injection solution were considered: 1) bromide and dissolved oxygen (DO), 2) bromide, DO, and naphthalene, 3) bromide (anaerobic), and 4) bromide and naphthalene (anaerobic). The creation of

all injection solutions is discussed in 3.5.1 Contaminant Water Injection. Oxygen will be consumed prior to any other electron acceptor and thus wells located in aerobic regions will be predominantly composed of an aerobic consortium. Injecting an anaerobic solution into oxygenated wells would provide anaerobic electron acceptors available only to the insignificant anaerobic microbial fraction, potentially killing the aerobic microbes if oxygen remains depleted for a significant period of time. Furthermore, this does not test true, in-situ conditions. Therefore, options 1 and 2 are appropriate for wells that have a measurable background concentration of dissolved oxygen. Option 1 enables critical evaluation of DO utilization in the absence of PAHs in the control wells S1 and D1. DO uptake that occurs in wells S1 and D1 during option 1 can be attributed to the metabolism of background organic carbon.

Option 2 includes naphthalene in addition to bromide and DO. Naphthalene, the most readily degradable and most dominant PAH found in the plume at the Oneida site, was used to establish consistency and comparability throughout individual tests. In addition, the addition of naphthalene provides an assessment of degradation in control wells S1 and D1 by bacteria that have not been exposed to naphthalene or PAHs before and thus have not been adapted to PAH degradation. These bacteria also have no benefit of a symbiotic relationship with trees.

Options 3 and 4 are appropriate for wells that are anaerobic. Options 3 and 4 can provide critical data for anaerobic PAH metabolism and enable an improved understanding of the contribution of each electron acceptor that is already present at the site. Employment of options 3 and 4 typically occurs at the center of the plume where PAH concentrations are extremely high and thus, anaerobic conditions prevail. Naphthalene addition in option 4, again, enables consistency and comparability throughout individual tests. Options 1 and 3 also provide clues to the effects that injected naphthalene may have on retardation factors of other solutes. Variation in the retardation factors of any reactant caused by the composition of the injection solution can have a critical effect on the observed degradation rate and therefore demands a critical assessment.

The tests performed to date are illustrated in Table 1. It should be noted that only options 1 and 2 were employed in the initial Oneida PPTs, yielding quantitative aerobic

degradation rates. Future tests will employ options 3 and 4 to quantify anaerobic degradation rates.

Unlike previous studies of push-pull tests, excluding the addition of DO in options 1 and 2, reactants were not added to the injection solution. Rather, the analysis of iron, sulfate, nitrate, and sulfide were based upon the availability of native electron donors. The contribution of background electron donors potentially can provide a spatial representation of in-situ degradation, providing a real-time estimate of plume degradation and extinction. Furthermore, the addition of DO in options 1 and 2 provide an assessment of not only degradation where DO already exists, but also provides an estimate of degradation that occurs during seasonal fluctuations of the groundwater table.

Table 1: Number and Location of Push-pull Tests and Variation of Injection Constituents

	Option 1 Br, DO	Option 2 Br, DO, Naphthalene
D1	2	3
S3		1
D3	1	3
D4		2
S5		1

3.3 Well Construction

Wells were constructed using a hand auger, working from the least to the most heavily contaminated well. Soil samples corresponding to the screened depths for the shallow and deep pairs were collected for later microcosm construction. One-inch PVC wells were then installed at desired depths using a capped one-foot section of well casing that was coupled to rigid PVC pipe. Well depth selection was based upon the proximity of sandy soils below the groundwater table that was absent of free product (Table 2). Approximately one and a half feet of filter sand was then packed around the installed well. Next, one to two feet of bentonite was added to eliminate preferential channeling. The well was then backfilled with all-purpose sand and then capped at the surface with bentonite and the well itself, with a PVC well cap. Logs of soil borings performed during PPT well construction can be found in Appendix B.

Table 2: Depths of 10 Push-pull Wells at the Oneida site

Well	Depth*, ft
S1	7.29
D1	8.21
S2	8.29
D2	9.29
S3	7.29
D3	8.29
S4	5.82
D4	7.09
S5	5.75
D5	6.50

*All depths measured from the ground surface at each well.

Newly constructed wells were then conditioned by injecting a minimum of 50 L of clean water at a flowrate of approximately 0.5 L/min. The depth of water within the well was monitored using a groundwater depth indicator to ensure stabilization occurred once sufficient head was maintained to distribute flow out of the well casing. Flowrate was adjusted as necessary, but in all instances, a minimum flowrate of 0.5 L/min was feasible.

3.4 Pre-test Preparation

3.4.1 Solution Preparation

For each push-pull test, separate bromide and naphthalene concentrates were prepared. Chemical concentrated solutions were prepared to enable a concentration of 750 mg/L bromide and 2 mg/L naphthalene for 35 L of injection solution. The mass of sodium bromide, NaBr, needed to create 35 L solution of 750 mg/L Br^- was weighed and placed in a volatile organic analysis (VOA) U.S. Environmental Protection Agency (EPA) amber vial. The high volatility of naphthalene required a more involved procedure. A 25 ml volumetric flask was weighed. A minimum of 70 mg of naphthalene was then added to the flask in a fume hood to ensure a final concentration of 2 mg/L in the 35 L carboy. The flask was then filled with high-grade methanol and the concentration within the 25 ml flask was calculated. The volume of this concentrated solution that is necessary to create 35 L of 2 mg/L naphthalene was then added to a VOA EPA amber vial. The amber vial was then filled with methanol to prevent the creation of

a headspace and thus a volatile loss of naphthalene. Lastly, the amber vial was taped with Teflon™ tape to minimize any volatile loss and stored at 4° C.

3.4.2 Preparation of Feed Tank

Prior to field departure, carboys and chemical concentrated solutions were prepared. Carboys were first washed with soap and water to remove excess debris and contaminants. The carboys were then washed with a highly concentrated sodium chloride solution to enable ion exchange; sodium and chloride ions exchanged with potentially interfering ions used for gas chromatograph (GC) and ion chromatograph (IC) analysis. PPTs often employ a lag phase to allow time for slower anaerobic degradation to occur; however, tests performed at the Oneida site observed faster aerobic decay, while observing anaerobic trends that occurred after DO was consumed. Since a lag phase was not implemented, the high concentration of bromide was necessary to enable a longer test duration so that monitored reactive solute concentrations would approach zero as they were microbially metabolized.

A more detailed explanation of In-situ Test and Constituent Analysis as well as Data Analysis is contained in Appendix A.

3.5 In-situ Test and Constituent Analysis

3.5.1 Contaminant Water Injection

During PPTs, ferrous iron, sulfide, DO, bromide, sulfide, nitrate, and PAHs, particularly naphthalene, were analyzed. At the Oneida site, nitrate levels are often negligible, but nitrate should be assessed since this can interfere with microbial preference of TEAs during anaerobic PPTs. Samples for each constituent were taken at varying time intervals throughout both the injection and extraction phases of the test, based upon the varying flowrates that were a function of seasonal groundwater depth variation. In-situ field tests include DO, ferrous iron, and sulfide analysis and measurements were made using HACH™ kit methods. Dissolved oxygen was measured using a digital titrator and Winkler titration method with a method detection limit of 0.1 mg/L. Ferrous iron samples were first filtered using 0.45 μm filters and then were measured using a HACH™ DR/700 Colorimeter with a method detection limit of 0.03

mg/L. Absorbance was read and converted to a concentration using a standard curve that was constructed using ferrous sulfate. Total sulfides were measured by first filtering all samples with a 0.45 μm filter and then a HACH™ DR/700 Colorimeter reported concentration results in mg/L with a method detection limit of 0.02 mg/L. Scintillation vials were used to collect samples for IC analysis, which includes analysis of bromide, sulfate, and nitrate (if present), all with a method detection limit of 0.5 mg/L. VOA EPA amber vials are used to collect samples for PAH analysis. PAH samples were then extracted using methylene chloride and analyzed on a GC with flame ionization detection using a DB5-MS fused silica capillary column following the method of Fetterolf (1999). PAH characterization for PPTs focused upon naphthalene, the most readily degradable PAH found within creosote and the naphthalene method detection limit, based upon the noise in the baseline, was 9.5 μg/L. External standards were used for quantification.

Following collection of the groundwater background samples, 35 L of prepared injection solutions were injected at a flowrate of approximately 0.5 L/min. 35 L corresponds to the volume of water necessary to influence a minimum radius of one foot of aquifer material. Injection samples were then collected, after sufficient 'backflushing' of the extraction tubes, which ensures no contamination of the current sample from the previous sample. A minimum of 200 ml was backflushed to eliminate contamination potential. The 200 ml backflushing corresponds to greater than 1.5 pore volumes of the sampling tubes. The backflushed volume was recorded for flow balance calculations. Upon completion of injection, the total injection time was recorded. A more detailed version of Contaminant Water Injection, outlining specific field methods, can be found in Appendix A.

3.5.2 Contaminant Water Extraction

Immediately following completion of injection, extraction was initiated at a flowrate ranging from 200 ml/min to 350 ml/min. The flowrate between sampling intervals was calculated by recording the volume collected in a 4 L graduated cylinder during the recorded time interval. The volume of sample that was consumed for each DO, ferrous iron, and sulfide in-situ measurement is recorded for flow balance calculations (Appendix A). A more detailed explanation of flow balance calculations and

other PPT extraction details can be found in Appendix A. The total volume of extraction solution collected was recorded for later use in the flow balance calculations. Extraction was continued until either three times the injected volume was collected or until the DO and ferrous iron/sulfide measurements stabilized. Stabilization in general was determined as a concentration equivalent to background concentrations, but if variation continued, the test continued. This is especially true for both ferrous iron and sulfide, which serve as the products of electron acceptors ferric iron and sulfate, respectively. Thus, if ferric iron and sulfate were utilized as electron acceptors, ferrous iron and sulfide concentrations would exceed background concentrations. DO, ferrous iron, and sulfide field measurements served as the only indicator for the stability of other electron acceptors not analyzed in the field, including sulfate and nitrate.

4.0 DATA ANALYSIS

4.1 Flow Balance

A flow balance was constructed using the field-measured flowrates during the extraction phase and the volumes consumed during backflushing as well as sample collection. An adjusted total injection volume, V_{inj}, and total extraction volume, V_{ext}, were then calculated (Appendix A). The cumulative extraction volume was normalized by dividing by V_{inj} at each sampling time period, yielding V_{ext}/V_{inj} for each time interval. The calculated total extraction volume, based upon the flowrates measured in the field, was compared to the measured total extraction volume to ensure that they are within a minimum of ten percent error.

The total volume of aquifer that was investigated was then determined, assuming an equal porosity of the sand-pack and the aquifer:

$$V_t = \frac{V_{inj} - V_{well-casing}}{Porosity_{aquifer}} - \frac{V_{sand-pack}}{Porosity_{sand-pack}} \quad \textbf{(1)}$$

where: V_t = total volume of aquifer investigated, L
$V_{well-casing}$ = volume of well-casing, L
$Porosity_{aquifer}$ = porosity of the aquifer
$V_{sand-pack}$ = volume of the sand-pack, L
$Porosity_{sand-pack}$ = porosity of the sand-pack

4.2 Solute Constituent Balance

Bromide, DO, ferrous iron, sulfate, sulfide, and naphthalene were analyzed to determine degradation rates and the overall percent recovery. The average injection concentration for each constituent, C_{inj}, was calculated by a simple average of all injection concentration samples. The extraction concentration was normalized at each time period as shown:

$$\mathbf{C_{nor} = (C_{ext})/(C_{inj})} \qquad \mathbf{(2)}$$

where: C_{nor} = normalized extraction concentration
C_{ext} = extraction concentration for each sampling period, mg/L

When background concentration of any constituent was present, such as in control wells with sufficient DO, the extraction concentration was normalized as follows:

$$\mathbf{C_{nor} = (C_{ext} - C_B)/(C_{inj} - C_B)} \qquad \mathbf{(3)}$$

where: C_{nor} = normalized extraction concentration
C_{ext} = extraction concentration for each sampling period, mg/L
C_B = background concentration, mg/L

A breakthrough curve (BTC) was formulated by plotting C_{ext}/C_{inj} (or $(C_{ext} - C_B)/(C_{inj} - C_B)$ if background present) versus V_{ext}/V_{inj}. BTCs provide visual details of how degradable solutes behave relative to conservative tracers. BTCs also aid in determination of the overall mass removed during the extraction period. To minimize the effects of measurement error in observed constituent concentrations, a best-fit line was used to determine the corrected normalized extraction concentrations at each ten-minute interval. Thus, all degradation rates were assessed using values from the best-fit line, which enabled smaller time intervals to be utilized for improved mass removal calculations. By removing the effects of experimental error from calculations, a better representation of true in-situ conditions was enabled. The equations from the best-fit lines were used to obtain normalized concentrations for each ten-minute interval. The corrected concentration at each ten-minute interval was then calculated by solving for C_{ext} in Equations 2 and 3, depending upon the presence of background solutes. Data were then analyzed to determine zero and first order degradation rates.

4.3 Zero Order Reaction Rates

4.3.1 Method of Istok et al. (1997)

Istok et al. (1997) provide a method to determine zero order degradation rates for PPTs. The method's zero order rate calculation involves dividing the mass of the degradable solute that is consumed (injected mass – extracted mass) or produced (extracted mass) by the total volume of the injected solution, V_{inj}, and by the mean residence time, θ, which is the elapsed time from the midpoint of injection to the bromide centroid (Istok et al., 1997). Using the extraction flow rate for each time interval, a flow weighted extracted mass and a cumulative sum of the removed flow weighted mass was determined (Appendix A). These calculations ultimately produced M_{ext}, the total extracted mass, and M_{inj}, the total injected mass, yielding a flow weighted percent recovery (Appendix A).

Zero order degradation rates for naphthalene, DO, and sulfate (Equation 4) as well as zero order production rates for ferrous iron and sulfide (Equation 5) were then determined:

$$\mathbf{R_{Istok} = M_{net}/(V_{inj} * \theta)} \quad \mathbf{(4)}$$

where: R_{Istok} = zero order degradation rate calculated using the method of Istok et al. (1997), mg/(L-hr)
$M_{net} = M_{inj} - M_{ext}$ = mass consumed, mg
θ = mean residence time = elapsed time from the midpoint of injection to the bromide centroid, hr
Bromide centroid = time when half of the injected bromide mass was recovered, hr

$$\mathbf{R_{Istok}' = M_{net}'/(V_{inj} * \theta)} \quad \mathbf{(5)}$$

where: R_{Istok}' = zero order production rate calculated using the method of Istok et al. (1997), mg/(L-hr)
$M_{net}' = M_{ext} - M_{inj}$ = mass created, mg

4.3.2 Method of Snodgrass and Kitanidis (1998)

Snodgrass and Kitanidis (1998) provide an alternative method to determine zero order degradation rates for PPTs. The method requires no prior knowledge of aquifer parameters, such as hydraulic conductivity. Additional assumptions to the method, not

stated above in 1.1 Push-pull Tests, are the injection time is short relative to the extraction time, and if the flow field is highly heterogeneous, more weight should be given to early measurements. The method of Snodgrass and Kitanidis (1998) heavily relies upon a short injection phase when compared to the duration of the extraction phase, since it assumes that degradation of the injected solutes during the injection phase is insignificant. Also, in highly heterogeneous flow fields, the method becomes unstable as the concentration of reactants approach zero. This is in part due to the fact that measurement error is a larger proportion of measured values at low concentrations. Instability as concentrations approach zero can also be explained by heterogeneity in the flow field, where mixing and subsequent extraction of injected solutes with native groundwater at the fringe of the zone of influence of the test is not uniform. At the end of the test, native groundwater, having a reactant concentration of zero, may return to the well-casing before some of the injected solutes. The method, however, is valid prior to effects at the injected solute-native groundwater interface, which occurs throughout the majority of the test. Snodgrass and Kitanidis (1998) have produced similar results to a computer-based model employed by Reinhard et al. (1997), which requires inputs of various aquifer parameters, thus validating the method.

The method involves transforming measured concentrations to remove the effects of dilution whose decrease (or increase, such as with ferrous iron and sulfide,) in concentration is due only to degradation. Measured concentrations are transformed, regardless of the advection and dispersion, as follows (Snodgrass and Kitanidis, 1998):

$$\hat{C}_r(t) = C_r^0 \left(\frac{C_r^m(t)}{C_r^0} - \frac{C_t^m(t)}{C_t^0} + 1 \right) \qquad \textbf{(6)}$$

where: $\hat{C}_r(t)$ = transformed reactive solute concentration at time t, mg/L
C_r^0 = reactive solute concentration during injection = C_{inj} for the reactive solute, mg/L
C_t^0 = non-reactive, tracer solute concentration during injection = C_{inj} for the tracer solute, mg/L
$C_r^m(t)$ = reactive solute concentration at time t = C_{ext} for the reactive solute, mg/L
$C_t^m(t)$ = non-reactive, tracer solute concentration at time t = C_{ext} for the tracer solute, mg/L
t = elapsed time from the beginning of extraction, min

Zero order degradation rates for naphthalene, DO, and sulfate as well as first order production rates for ferrous iron and sulfide can be calculated by plotting $\hat{C}_r(t)$ versus t, described in the equation below (Snodgrass and Kitanidis, 1998):

$$\hat{C}_r(t) = C_r^0 - \alpha t \quad \textbf{(7)}$$

where: α = zero order degradation rate calculated using the method of Snodgrass and Kitanidis (1998), mg/(L-hr)

When zero order degradation is occurring, a plot of $\hat{C}_r(t)$ versus t will yield a straight line, with slope α. It should be noted that a slope of –α results for reactants that are consumed (DO, sulfate), whereas a slope of α results for reactants that are produced (ferrous iron, sulfide).

4.3.3 Transforming Zero Order Rates

The observed zero order reactant rate constants were converted to degradation rate constants for naphthalene using stoichiometric equations. In any heterotrophic microbial growth reaction, the metabolism of an organic substrate is fractionated between cell growth and the creation of useful cellular energy. To account for all of the factors involved in microbial cellular functions, an overall stoichiometric equation is developed consisting of three individual half reactions. Letting R represent the overall stoichiometric equation, the sum of the half-reactions is (Grady et al., 1999):

$$\mathbf{R = R_d - f_e{*}R_a - f_s{*}R_c} \quad \textbf{(8)}$$

where: R_d = half reaction of the electron donor
R_a = half reaction of the electron acceptor
R_c = half reaction for cell material
f_e = fraction of the electron donor that is coupled with the electron acceptor
f_s = fraction of the electron donor that is captured through biomass synthesis

The general electron donor half reaction for hydrocarbons is given by (Stumm and Morgan, 1996):

$$\frac{1}{(4a+b)}C_aH_b+\frac{2a}{(4a+b)}H_2O\rightarrow\frac{a}{(4a+b)}C\,O_2+H^++e^- \quad \textbf{(9)}$$

where: a = number of carbon atoms in the original hydrocarbon
b = number of hydrogen atoms in the original hydrocarbon

Equation 9 was used to develop a half reaction for naphthalene. This approach assumes that naphthalene is the sole electron donor and is completely mineralized to carbon dioxide.

In order for Equation 9 to balance:

$$\mathbf{f_e + f_s = 1.0} \quad \textbf{(10)}$$

Equation 10 is the equivalent of stating that electrons from the electron donor end up either in the electron acceptor (f_e) or in the biomass synthesized (f_s). The creation of biomass is treated as an end product and is denoted with the empirical formula $C_5H_7O_2N$. This approach employs the creation of a biomass yield coefficient, which accounts for the amount of biomass produced for a given amount of substrate. When ammonia is the nitrogen source, the biomass yield coefficient is equivalent to f_s (Grady et al., 1999). Theoretical estimates for the average biomass yield coefficient during PAH oxidation have been established. During aerobic and sulfate-reducing conditions, the average biomass yield coefficients have been shown to be 0.33 $g_{biomass}/g_{PAH}$ and 0.06 $g_{biomass}/g_{PAH}$, respectively, when using a bioenergetic model that assumes ammonia as the non-limiting nitrogen source (Brauner, 2000). Estimates for the amount of electron acceptor to degrade a known amount of naphthalene, or the electron acceptor utilization coefficient, were then calculated following the method of Brauner (2000) and the balanced stoichiometric equations are shown in Table 3. Results for dissolved oxygen and sulfate are 2.007 $mg_{O2}/mg_{naphthalene}$ and 4.226 $mg_{SO4}/mg_{naphthalene}$, respectively. Dividing the zero order degradation rates, which are in terms of the electron acceptor, by the electron acceptor utilization coefficient yields a naphthalene degradation rate.

Table 3: Balanced Stoichiometric Equations for Naphthalene Mineralization to Carbon Dioxide through Dissolved Oxygen and Sulfate Electron Acceptor Pathways

$C_{10}H_8 + 8.04\ O_2 + 0.792\ HCO_3^- + 0.792\ NH_4^+ \rightarrow 0.792\ C_5H_7O_2N + 3.208\ H_2O + 6.832\ CO_2$
$C_{10}H_8 + 5.64\ SO_4^- + 0.144\ HCO_3^- + 0.144\ NH_4^+ + 8.46\ H^+ \rightarrow 0.144\ C_5H_7O_2N + 3.856\ H_2O + 9.424\ CO_2 + 2.82\ H_2S + 2.82\ HS^-$
Balanced equations use heterotrophic growth, assuming non-limiting ammonia nitrogen source. Yield coefficients ($mg_{biomass}/mg_{naphthalene}$) for aerobic and sulfate-reducing conditions were 0.33 and 0.06, respectively (Brauner, 2000).

4.4 First Order Reaction Rates

4.4.1 Method of Haggerty et al. (1998)

Haggerty et al. (1998) and Schroth et al. (2001) provide a method to determine first order degradation rates for PPTs. The method is based upon tracer and reactant transport as the radial flow field fluctuates from divergence during injection and convergence during extraction. The method assumes typical first order decay where $dC_r/dt = -kC_r$, where C_r is the reactant concentration and k is the rate constant. The method assumes that retardation factors of the tracer and reactants are similar. In addition, the method assumes that the injected solution is well mixed within the aquifer, that spatially homogenous reaction rates exist, that identical reaction rates exist in the mobile and immobile aqueous and sorbed phases, and that measurement errors are small, random, independent, and have a mean value of zero (Haggerty et al., 1998). These assumptions prelude that advection-dispersion-sorption transport properties of the tracer and reactants are similar (Schroth et al., 2001). By employing a t^* term, the elapsed time from the end of the injection phase, the method of Haggerty et al. (1998) can allow for a lag time between injection and extraction. The y-intercept in Equation 11 accounts for degradation that occurs during the injection period, thus reducing reliance upon an assumption commonly employed in PPT data analysis – that the duration of the injection phase is short relative to the extraction phase. First order degradation rates for naphthalene, DO, and sulfate as well as first order production rates for ferrous iron and sulfide can be determined from (Haggerty et al., 1998):

$$\ln\left[\frac{C_r^*(t^*)}{C_t^*(t^*)}\right] = \ln\left[\frac{(1-e^{-k t_{inj}})}{k t_{inj}}\right] - k t^* \quad \textbf{(11)}$$

where: C_r^* = normalized concentration of the reactant at time t^*
C_t^* = normalized concentration of the tracer at time t^*
t^* = elapsed time from the end of the injection phase, min
t_{inj} = total time of the injection phase, min
k = first order degradation rate calculated using the method of Haggerty et al. (1998), min^{-1}

If the reactive solute is decaying at a first order rate, a plot of $\ln(C_r^*(t^*)/C_t^*(t^*))$ versus t^* produces a straight line with slope –k and y-intercept of $\ln[(1-e^{-ktinj})/(kt_{inj})]$. It should be noted that a slope of –k results for reactants that are consumed (DO, sulfate), whereas a slope of k results for reactants that are produced (ferrous iron, sulfide).

4.4.2 Method of Snodgrass and Kitanidis (1998)

Snodgrass and Kitanidis (1998) provide an alternative method to determine first order degradation rates for PPTs. Additional assumptions to the method, not stated above in 1.1 Push-Pull Tests, are the injection time is short relative to the extraction time, and if the flow field is highly heterogeneous, more weight should be given to early measurements. The method is similar to the approach of Haggerty et al. (1998), except observed concentrations are plotted versus time rather than normalized concentrations. The methods also differ in approach through the calculation of the y-intercept term and the Snodgrass and Kitanidis (1998) method does not allow for a lag phase between the injection and extraction phases. The y-intercept term in Equation 12 assumes that the concentration of injected reactants within the aquifer at the beginning of the extraction phase is identical to the average injection concentration. Therefore, the method of Snodgrass and Kitanidis (1998) heavily relies upon a short injection phase when compared to the duration of the extraction phase, assuming that degradation of the injected solutes during the injection phase is insignificant. Further elaboration of the merits of these two additional assumptions in the Snodgrass and Kitanidis method can be found above in 4.3 Zero Order Reaction Rates.

First order degradation rates for naphthalene, DO, and sulfate as well as first order production rates for ferrous iron and sulfide can be determined from (Snodgrass and Kitanidis, 1998):

$$\ln\left(\frac{C_r^m(t)}{C_t^m(t)}\right) = \ln\left(\frac{C_r^0}{C_t^0}\right) - \beta t \qquad \textbf{(12)}$$

where: β = first order degradation rate calculated using the method of Snodgrass and Kitanidis (1998), mg/(L-hr)

If the reactive solute is decaying at a first order rate, a plot of $\ln(C_r^m(t)/C_t^m(t))$ versus t produces a straight line with slope –β. It should be noted that a slope of – β results for reactants that are consumed (DO, sulfate), whereas a slope of β results for reactants that are produced (ferrous iron, sulfide).

5.0 RESULTS AND DISCUSSION

Results of the twelve PPTs performed at the Oneida site yielded quantitative rates for aerobic conditions at the Oneida site. The date, location, option employed, background concentrations for DO and naphthalene, as well as the injection and extraction volumes and flowrates for the twelve PPTs are summarized in Table 4. Efforts to monitor anaerobic degradation, based upon native electron acceptors not added to the injected solution, did not produce measurable rates. Monitoring of anaerobic electron acceptors is explained in further detail in 8.3 Anaerobic Assessment.

Table 4: Summary of Push-pull Test Parameters

Test Number	Location	Date	Option	Background Concentrations		Injection		Extraction	
				DO	Naphthalene	Q_{inj}	V_{inj}	Average Q_{ext}	V_{ext}
				mg/L	µg/L	L/min	L	L/min	L
1	D3	12/14/2002	2	0.0	378.8	0.50	35	0.30	42.4
2	D4	12/14/2002	2	0.1	8604.2	0.50	35	0.30	62.6
3	D1	2/23/2003	1	3.3	0.0	0.50	35	0.34	76.7
4	D4	2/23/2003	2	0.0	10697.0	0.58	35	0.39	109.7
5	S3	2/24/2003	2	0.0	5.7	0.44	35	0.35	91.5
6	S5	2/24/2003	2	0.0	2501.9	0.50	35	0.26	61.1
7	D1 1	4/17/2003	1	4.1	0.0	0.58	35	0.35	110.2
8	D3 1	4/17/2003	1	0.0	1517.0	0.50	35	0.31	105.2
9	D1 2	4/18/2003	2	3.1	0.0	0.32	35	0.32	108.2
10	D3 2	4/18/2003	2	0.0	388.3	0.55	35	0.36	107.4
11	D1	6/6/2003	2	0.3	7.6	0.54	35	0.38	110.0
12	D3	6/6/2003	2	0.0	1594.7	0.55	35	0.29	116.6

5.1 Breakthrough Curves

Breakthrough curves (BTCs) provide visual details of how degradable solutes behave relative to conservative tracers, which enable observation of trends pertaining to degradation rates. BTCs are formulated by plotting C_{ext}/C_{inj} (or $(C_{ext} - C_B)/(C_{inj} - C_B)$ if background DO is significant) versus V_{ext}/V_{inj}. When normalized concentrations resulted in an initial extraction value greater than one, C_{inj} was adjusted to the maximum value of C_{ext}. When points of high influence greatly distorted BTC regression lines (i.e. plotted data did not follow a typical dilution curve), the outliers were excluded from regression analysis and the outlying data points are indicated on BTC graphs. One PPT, D4 December, experienced a large number of data points that diverged from the typical BTC (Appendix C: Figure C2). These outliers were removed, but given the large number of outlying data points, less confidence is given to the results from D4 December and future tests should verify observed trends at D4 during December. BTCs serve as the first tool in data analysis of PPTs to observe whether degradation is occurring, particularly whether the degradation is zero or first order.

Rates are determined from the relative difference between the non-reactive tracer, bromide, and the reactive solute. In this study, aerobic degradation rates were derived using PPTs performed at the Oneida site. Figure 4 illustrates an example BTC which details where degradation is occurring. Zero order rates are determined simply from either the mass difference between the bromide and DO BTCs (Istok et al., 1997) or by transforming the concentration of the reactive solute to remove the effects of dilution, by incorporating the reactive solutes relativity to the tracer (Snodgrass and Kitanidis, 1998).

Both methods address the mass difference between the bromide and DO BTCs to determine rates and this mass difference is illustrated in Figure 4.

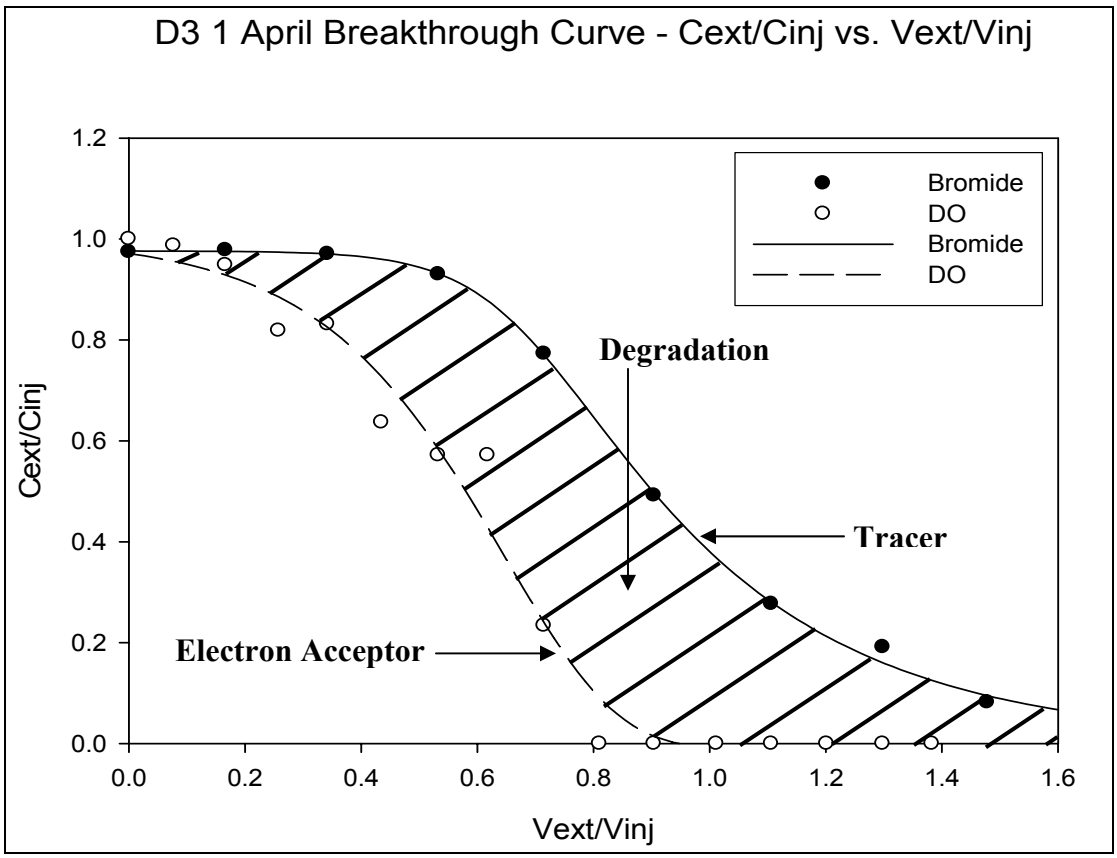

Figure 4: Example Breakthrough Curve – Zero Order Degradation

First order rate determination employs a similar approach to assess degradation. Whether analyzing the normalized relative difference in tracer and reactive solute concentrations (Haggerty et al., 1998) or simply analyzing the measured relative difference in tracer and reactive solute concentrations (Snodgrass and Kitanidis, 1998), first order degradation occurs when the tracer curve diverges vertically from the reactive solute curve. The faster the curves diverge, the greater is the calculated first order degradation rate. Vertical divergence of the tracer and reactive solute curves is illustrated in Figure 5.

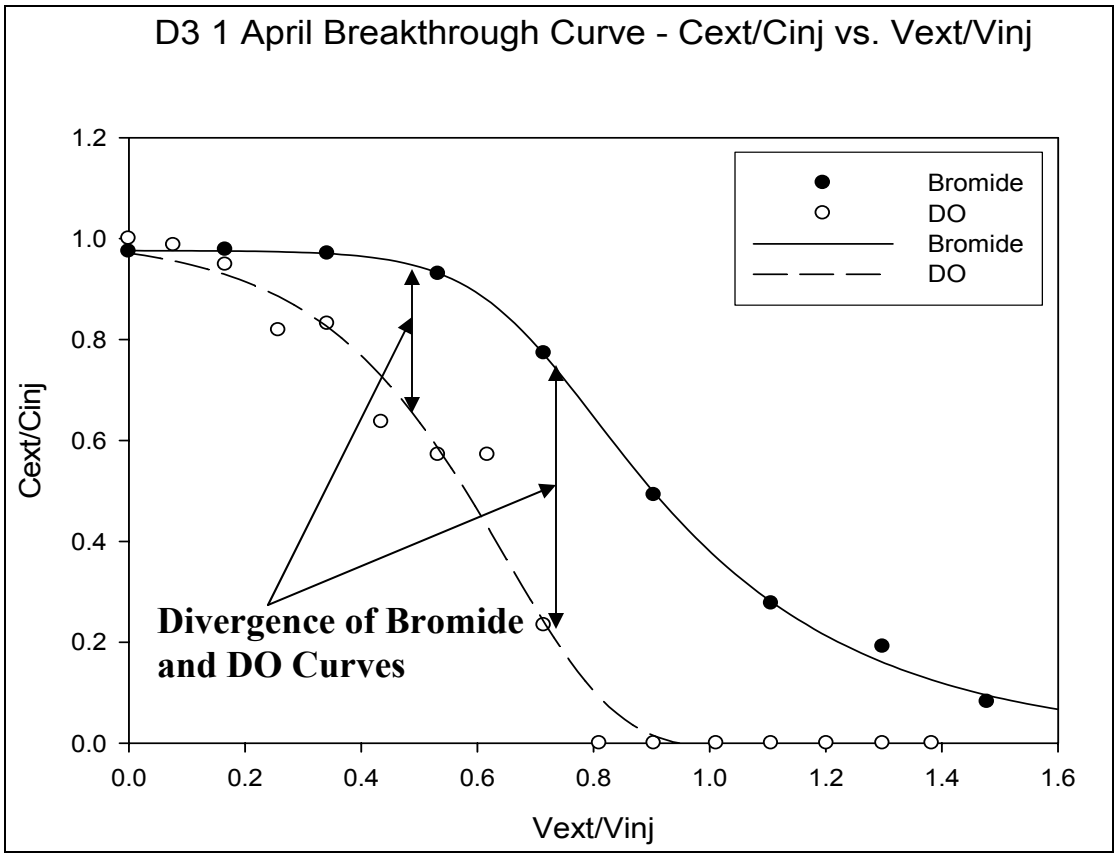

Figure 5: Example Breakthrough Curve – First Order Degradation

5.2 Regression Analysis

The methods of Snodgrass and Kitanidis (1998) and Haggerty et al. (1998) involve plotting data to determine zero and first order rates. As explained above, the method of Istok et al. (1997) does not plot zero order rate data to determine zero order degradation rates. Rather, the method of Istok et al. (1997) calculates the mass difference between bromide and DO BTCs. For the methods of Snodgrass and Kitanidis (1998) and Haggerty et al. (1998), zero and first order decay is presumed to be occurring where the plotted data produces a straight line. A linear least squares approach was used to evaluate data believed to be exhibiting zero or first order decay, producing an equation and R^2 value for the best-fit line. In the case of electron acceptor consumption, such as with DO utilization, data points that did not exhibit a negatively-sloped, straight line were excluded from regression line analysis.

Application of the methods of Snodgrass and Kitanidis (1998) and Haggerty et al. (1998) to Oneida PPT data, however, did not always exhibit a straight line when it was

believed that degradation was occurring. Experimental error, particularly measurement error, is intrinsic in all experimental procedures and results in a non-ideal representation of data exhibiting known phenomena. Heterogeneous conditions of the Oneida site aquifer contribute to non-ideal behavior of PPTs. When combined, the effects of experimental error and heterogeneous aquifer characteristics can result in a non-ideal representation of solute behavior during PPTs. As a result, BTCs do not always respond as anticipated and cause data plotted for rate determination to not always exhibit a straight line when zero or first order degradation is occurring. Consequently, when plotted data did not exhibit a straight line, regression line analysis included non-linear datasets. This qualitative approach to data analysis is explained in greater detail in 6.0 Summary of Data Evaluation Methods.

5.3 Modifying Data Analysis Methods

Modification of the methods of Istok et al. (1997), Snodgrass and Kitanidis (1998), and Haggerty et al. (1998) were performed for determination of degradation rates at the Oneida site. Modifications executed include: 1) setting a minimum reactive solute concentration for first order decay [methods of Snodgrass and Kitanidis (1998) and Haggerty et al. (1998)], 2) adjusting concentrations when significant background solute concentrations were present [for all zero and first order methods], 3) adapting rate regression line analysis to cases where a clear microbial lag-phase was present [for the zero and first order methods of Snodgrass and Kitanidis (1998) and Haggerty et al. (1998)], and 4) not force-fitting regression lines through calculated y-intercept values [for the zero and first order methods of Snodgrass and Kitanidis (1998)].

First order rates, using the methods of Snodgrass and Kitanidis (1998) and Haggerty et al. (1998), were calculated for data with a DO concentration greater than 1 mg/L. At DO concentrations less than 1 mg/L, the oxygen becomes limiting and first order kinetics no longer apply. Setting a minimum level of 1mg/L for DO first order rate analysis is supported in the protocol in *Standard Methods for the Examination of Water and Wastewater* for biological oxygen demand analysis (Clesceri et al., 1998).

The methods of Istok et al. (1997), Snodgrass and Kitanidis (1998), and Haggerty et al. (1998) were adapted to situations where background concentrations are significant.

Modifications of the rate determination methods were performed at the Oneida site when significant background concentrations of DO were present, particularly at the control wells D1 and S1 which are located outside of the contaminant groundwater plume. Since no contamination is present near the control wells, background DO concentrations typically existed between 3-4 mg/L and consequently were normalized as described in Equation 3. Figure 6 compares the BTCs at control well D1 when background concentration is (Fig. 6b) and is not (Fig. 6a) addressed. All PPTs at the Oneida site removed background concentration from the analysis, enabling bromide and DO curves to be directly compared for rate determination.

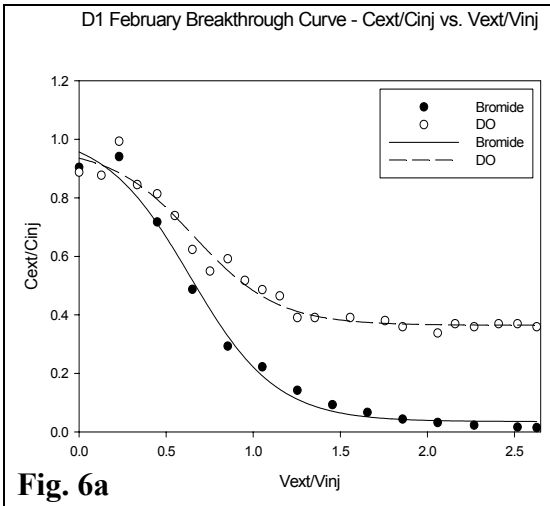

Fig. 6a

NO BACKGROUND DO REMOVED

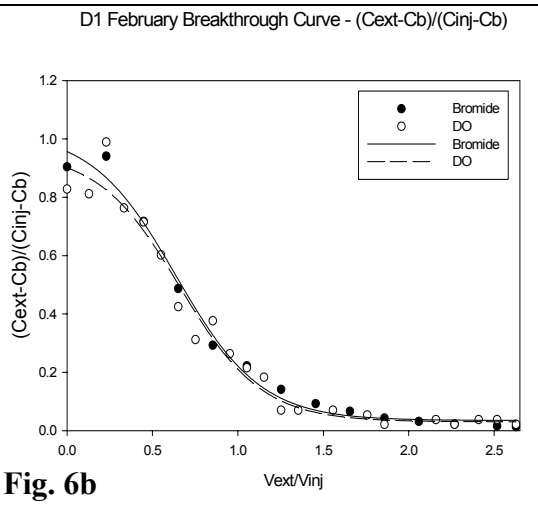

Fig. 6b

BACKGROUND DO REMOVED

Figure 6: Comparing Breakthrough Curves When Background Concentrations Are Significant

If background concentrations are not removed from analysis, rates can not be determined since a positive slope results (when a negative slope should exist for DO consumption). The positive slope results from the DO curve lying above the bromide curve, as depicted in Fig. 6a. Figure 7 compares the effects of removing background concentration during rate determination, using the method of Snodgrass and Kitanidis (1998) for zero order rate determination as an example. Similar results occur with the methods of Snodgrass and Kitanidis (1998) and Haggerty et al. (1998) for first order rate determination.

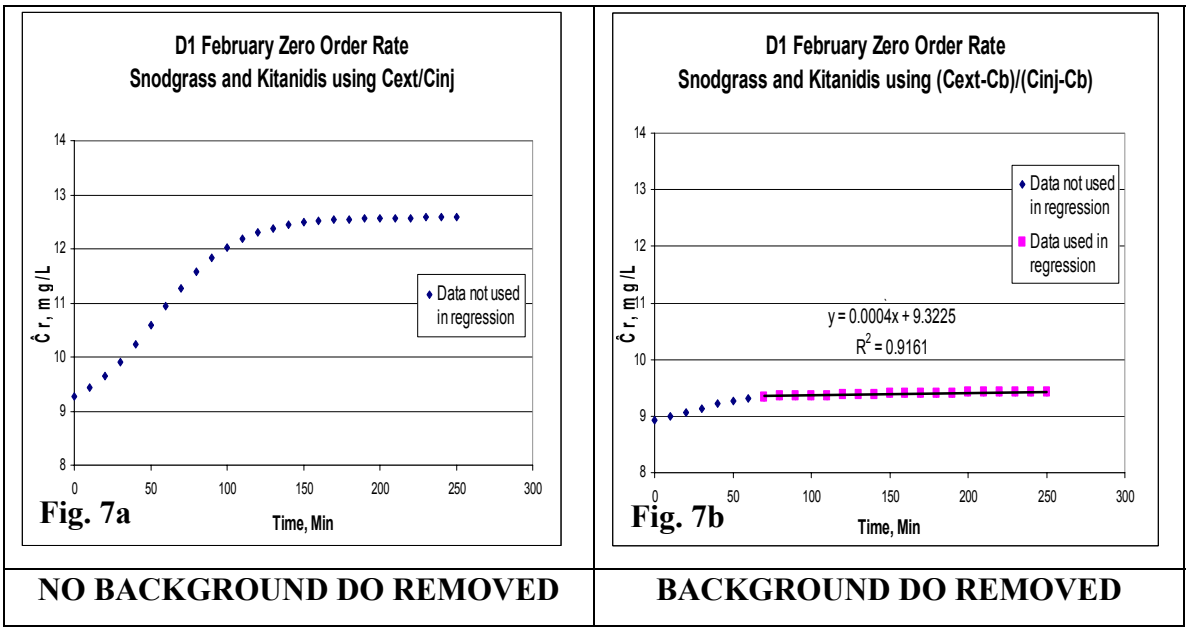

Figure 7: Example Comparison of Normalizations That Account and Do Not Account for Background Concentration – Snodgrass and Kitanidis (1998) Zero Order Rate Determination

The methods of Snodgrass and Kitanidis (1998) and Haggerty et al. (1998) were adapted to incorporate cases where a microbial lag-phase was evident. The methods of Snodgrass and Kitanidis (1998) and Haggerty et al. (1998) have defined y-intercept values as detailed in Equations 7, 11, and 12. The equations assume that decay occurs immediately at the beginning of the extraction phase. However, a lag phase often exists during microbial degradation processes. Lag phases are most common when either a contaminant is introduced to microbes that have never seen the contaminant before or when redox conditions change rapidly (Madigan et al., 2000). When redox conditions rapidly change from an anaerobic state to an aerobic state, such as with the introduction of oxygenated water to anaerobic zones, microbial populations must adjust to the redox change and this adjustment is commonly seen as a lag phase. Lag phases appeared to exist for five of the PPTs at the Oneida site. When a lag phase did occur, the initial 'lag' data points were ignored in regression line analysis and rates were determined only from data that exhibited decay. The response of the zero order plot (Fig. 8b), used as an example, to the D3 2 April PPT BTC (Fig. 8a) is illustrated in Figure 8, which shows a PPT where a lag-phase was evident. Data after time 60 min. (V_{ext}/V_{inj} = 0.689) was not used in analysis since a positive slope existed in plotted zero order data. Similar lag-

phase calculations were employed for the zero and first order methods of Snodgrass and Kitanidis (1998) and Haggerty et al. (1998).

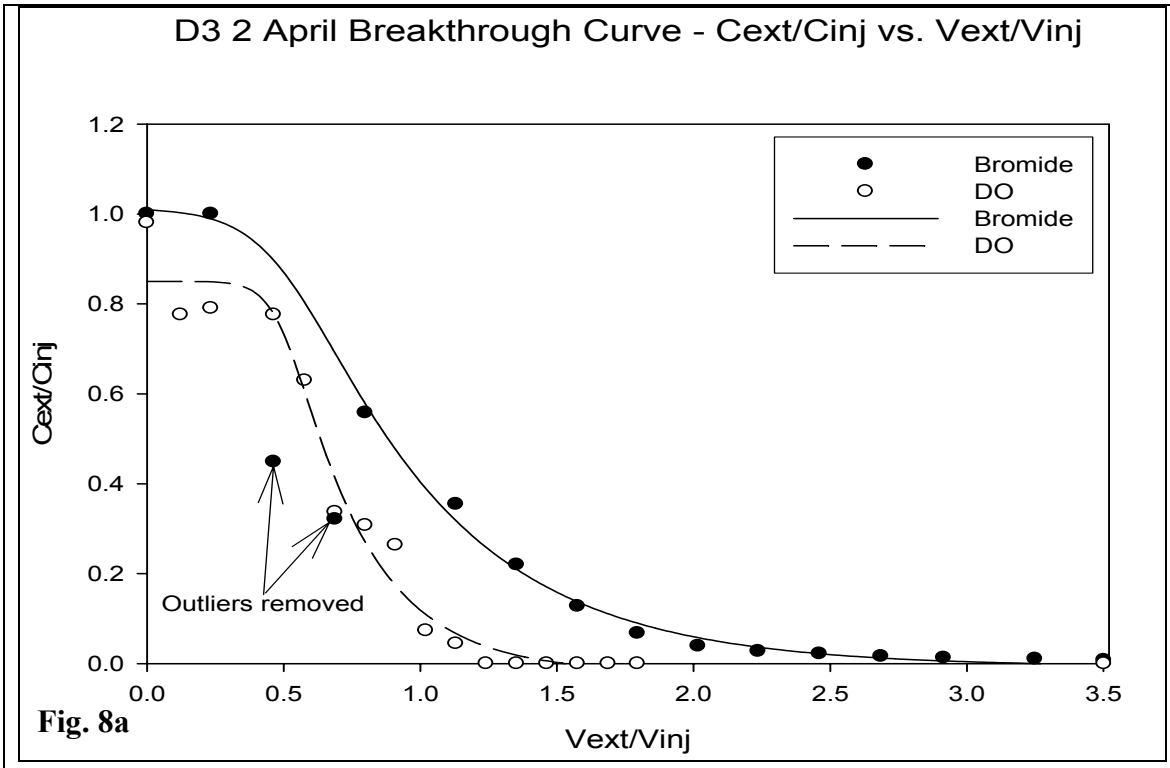

Fig. 8a

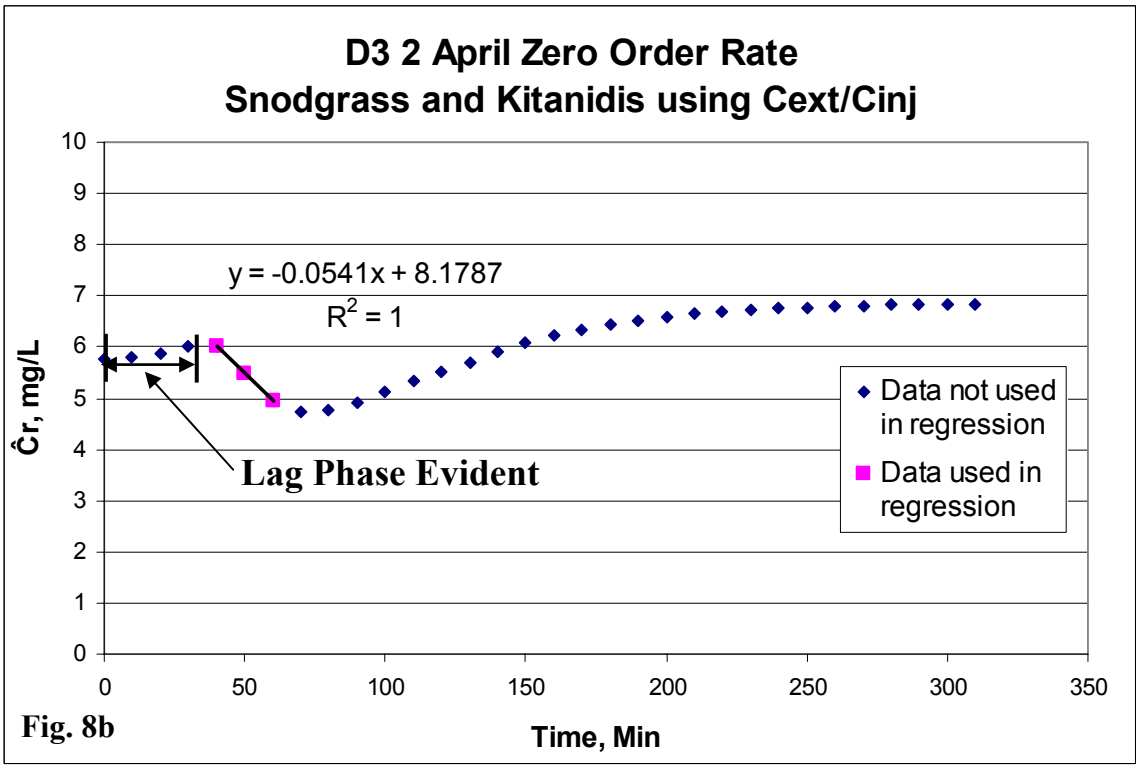

Fig. 8b

Figure 8: Lag-Phase Rate Calculation Example

Regression lines, used in calculation of degradation rates, were not force-fit through the calculated y-intercept as required by Equations 7, 11, and 12. The calculated y-intercept using the method of Haggerty et al. (1998), however, always returns a y-intercept value that is identical to the y-intercept of the best fit line. This is because the y-intercept term in Equation 11 includes k, the slope of the best fit line, and a linear least squares approach applied to a plot of Equation 11 always yields a y-intercept term equivalent to the y-intercept of the best-fit line.

The method of Snodgrass and Kitanidis (1998), however, always results in a y-intercept term of the best-fit line that differs from the calculated y-intercept term that employs injection concentration (Equations 7, 12). Snodgrass and Kitanidis (1998) applied their method to an ideal computer-simulated PPT and consequently did not need to address whether the best-fit line of plotted data was forced through the calculated y-intercept. With real data, the average injection concentration, termed C_r^0 and C_t^0 in Equations 7 and 12, is rarely equal to the time zero extraction concentration, $C_r^m(0)$ and $C_t^m(0)$. This results in a plot whose time zero value differs from the calculated y-intercept value obtained in Equations 7 and 12. In addition, linear least squares analysis of real data does not produce a y-intercept value that is identical to the calculated y-intercept value from Equations 7 and 12. If the plotted data did force the regression line through the calculated y-intercept value, the y-intercept would have a large influence on the regression line, strongly affecting calculated degradation rates and reducing the R^2 fit-measuring parameter. An example comparison of rate calculation that did (Fig. 9a) and did not (Fig. 9b) force the regression line through the calculated y-intercept is shown in Figure 9. The regression line that did not force fit the y-intercept term resulted in an R^2 value of 0.9444, when compared to the force-fit R^2 value of 0.6564. As a result of these phenomena, regression analysis did not force-fit regression lines through the calculated y-intercept values when employing the zero and first order methods of Snodgrass and Kitanidis (1998) and Haggerty et al. (1998). Instead, trends in plotted data were used to determine degradation rates.

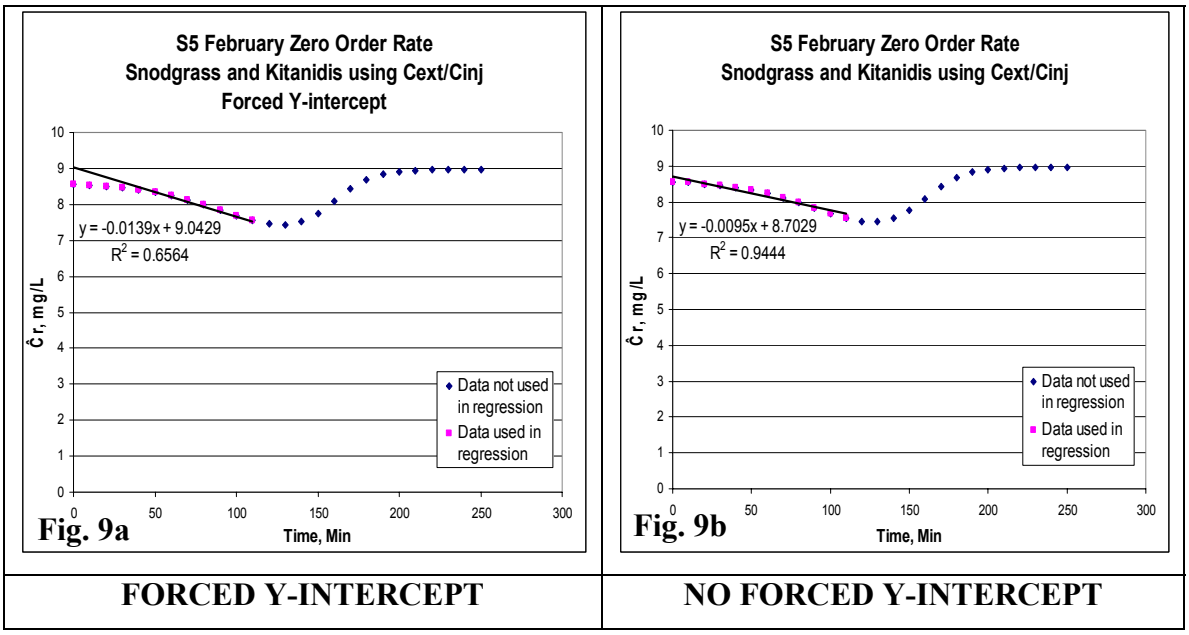

Figure 9: Comparison of Force-fitting Calculated Y-intercept Values

5.4 Overview of Rate Analysis Methods

The methods of Snodgrass and Kitanidis (1998) and Haggerty et al. (1998) produce zero and first order rates through regression analysis. To aid in further discussion of these methods, an example of each type of regression is illustrated in Figures 10, 11, and 12. Plotted data used Equation 2 for normalization when background concentrations were low and when background concentrations were high Equation 3 was used. Figure 10 displays the method of Snodgrass and Kitanidis (1998) used to determine zero order degradation rates. When Equation 7 is plotted, the regression line has a slope of α, as depicted. Given discrepancies between calculated y-intercept terms and time zero extraction concentrations, as explained above, the Snodgrass and Kitanidis (1998) zero order degradation graphs are not force-fit through the y-intercept. It should be noted that the method of Snodgrass and Kitanidis (1998) for zero order rate calculations can become highly variable as the solute concentrations approach zero. As a result, when irregularity was observed (i.e. plotted data diverged from a straight line), the regression analysis was stopped at the last point of stability (Fig. 10b).

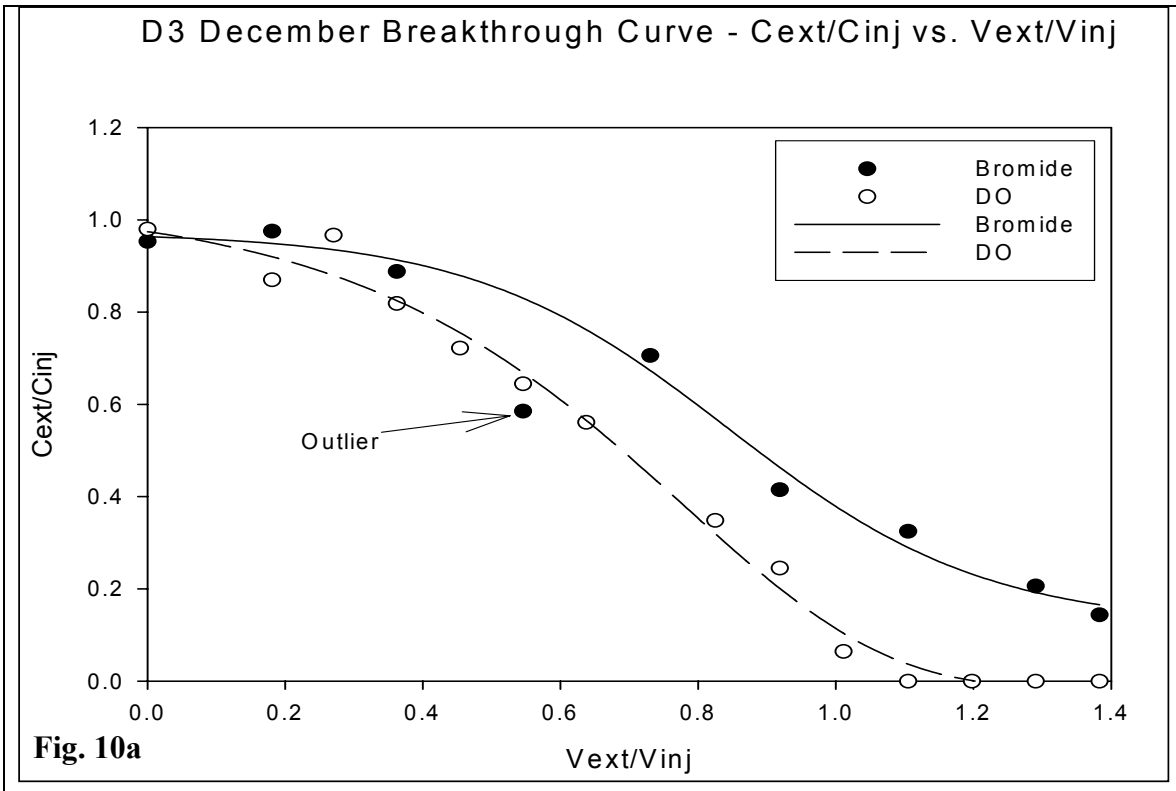

Fig. 10a

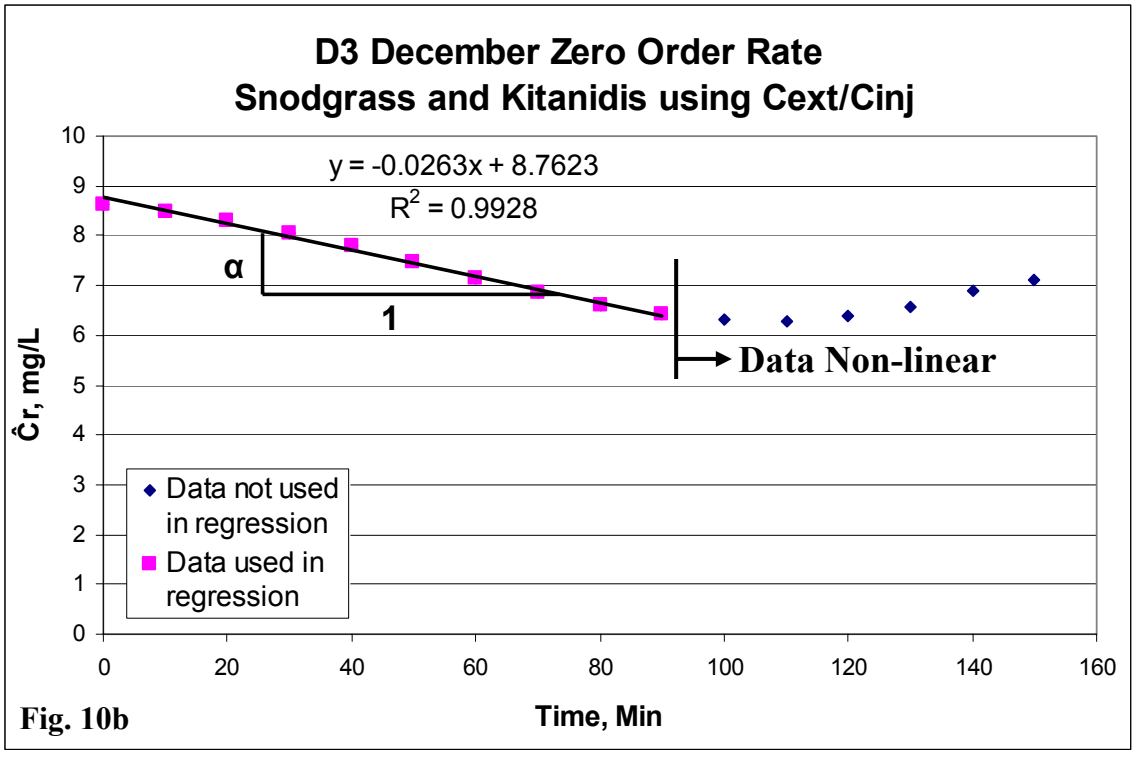

Fig. 10b

Figure 10: Example Snodgrass and Kitanidis (1998) Zero Order Rate Graph

Figure 11 illustrates the method of Haggerty et al. (1998) used to determine first order degradation rates. When Equation 11 is plotted, the regression line has a slope of k and a y-intercept of $\ln[(1-e^{-ktinj})/(kt_{inj})]$, as depicted (Fig. 11b). Since the method of Haggerty et al. (1998) uses the least squares approach to simultaneously determine the slope, k, and the y-intercept value, the plotted regression line will always intersect the y-intercept. Fig. 11b serves as an example where regression analysis stopped when the DO was less than 1 mg/L. It should be noted that the data point at time zero (i.e. the y-intercept data point) is used only for illustrative purposes and is not part of the plotted data series used to determine R^2 values.

Figure 12 displays the method of Snodgrass and Kitanidis (1998) used to determine first order degradation rates. When Equation 12 is plotted, the regression line has a slope of β (Fig. 12b). Fig. 12b serves as another example where regression analysis stopped when the DO was less than 1 mg/L. In situations where plotted data became non-linear prior to reaching a minimum DO concentration of 1 mg/L, regression analysis ceased at the last linear plotted data point, which is explained in greater detail in 5.2 Regression Analysis. Removal of outliers, such as with the D4 December PPT BTC (Fig. 12a), is discussed in greater detail in 5.1 Breakthrough Curves. Given differences between calculated y-intercept terms and time zero extraction concentrations, as explained above, the Snodgrass and Kitanidis (1998) first order degradation graphs are not force-fit through the y-intercept.

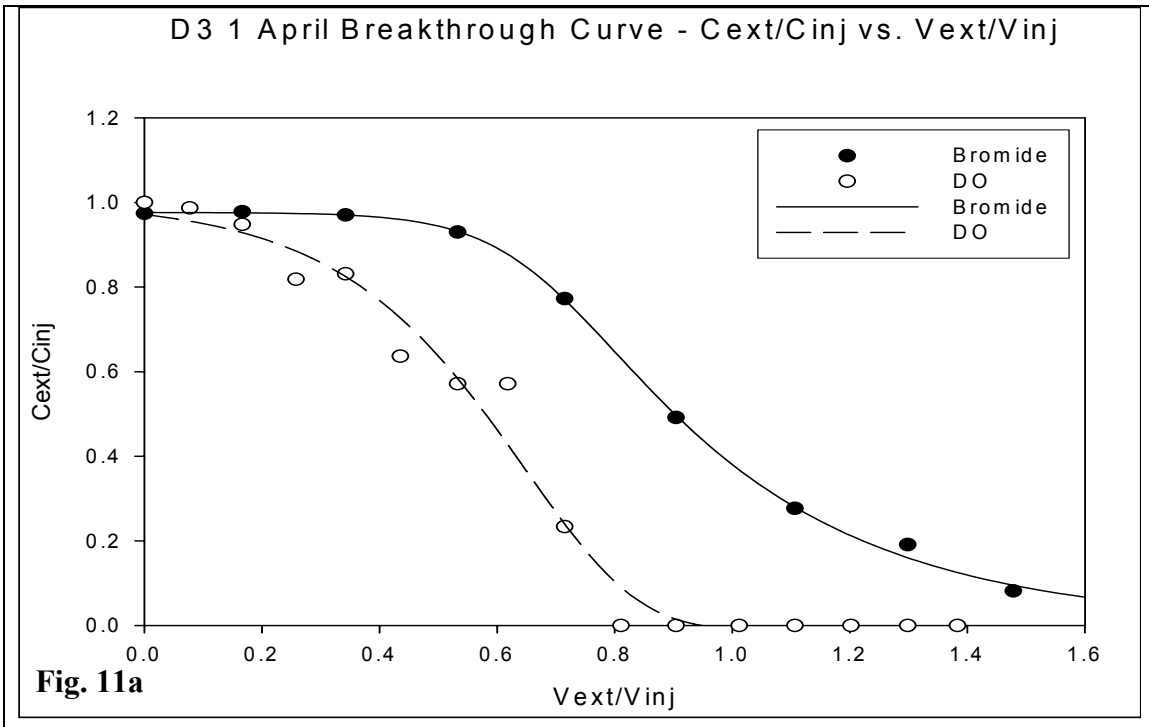

Fig. 11a

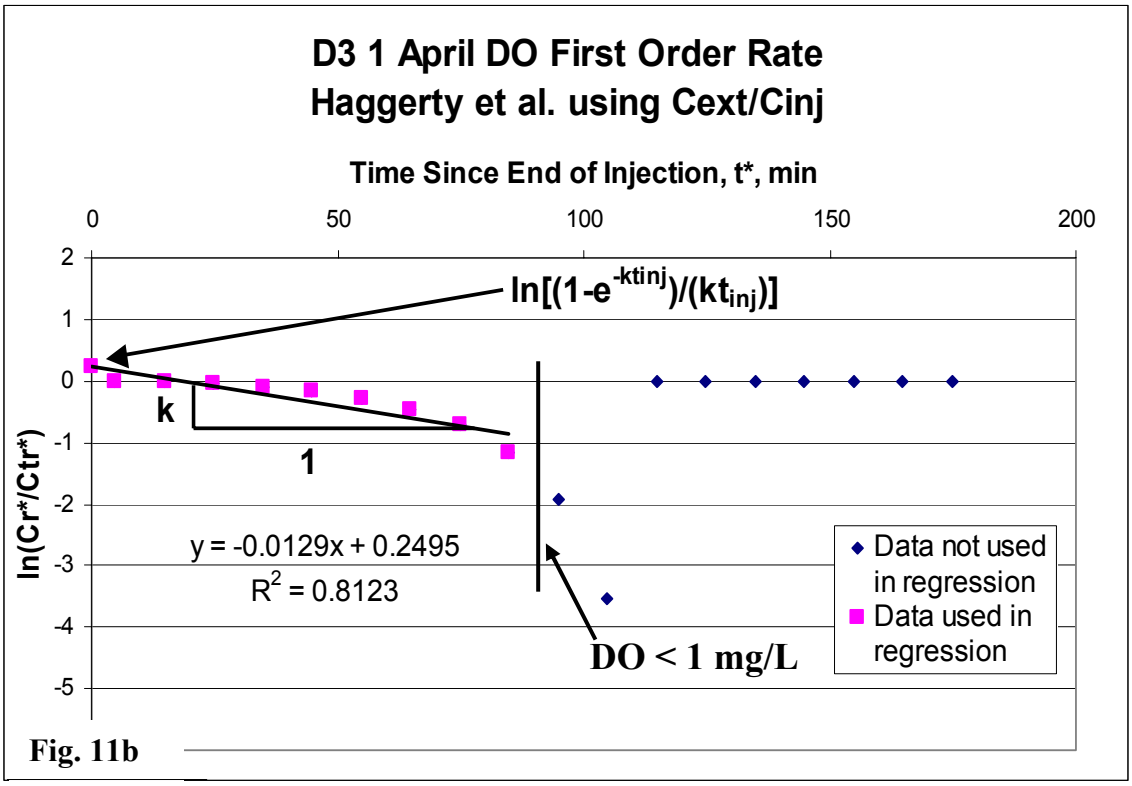

Fig. 11b

Figure 11: Example Haggerty et al. (1998) First Order Rate Graph

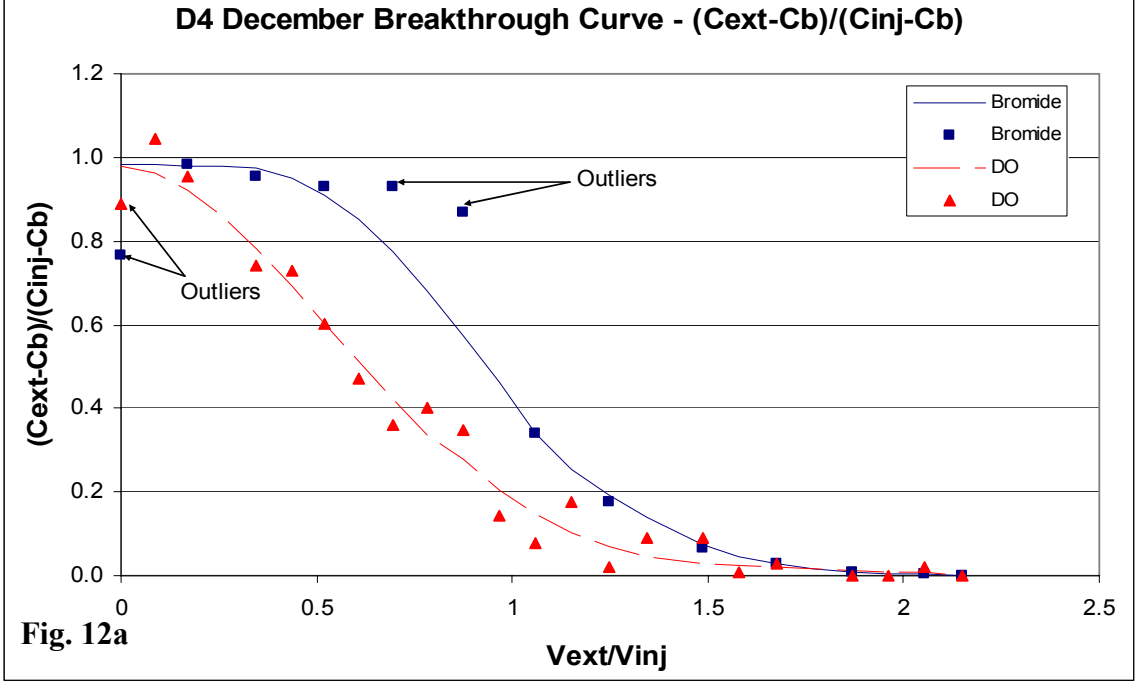

Fig. 12a

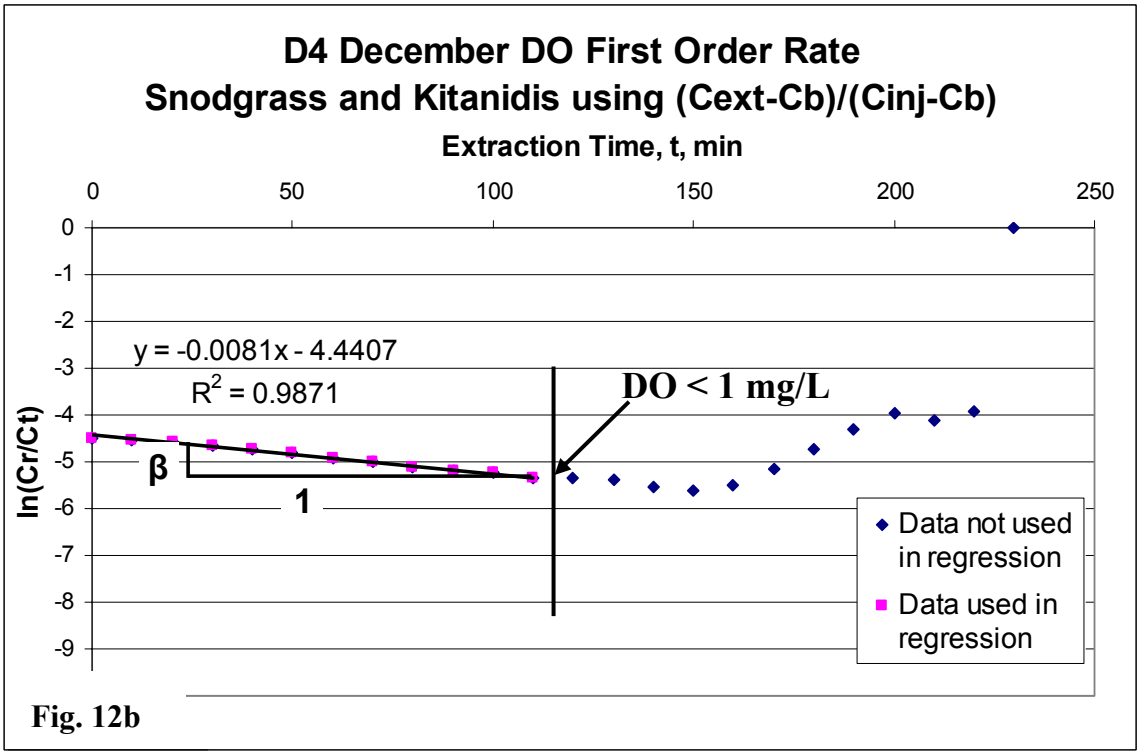

Fig. 12b

Figure 12: Example Snodgrass and Kitanidis (1998) First Order Rate Graph

5.5 General Trends in Push-pull Test Data

5.5.1 Control Wells

5.5.1.1 Option 1

Initial analysis of BTCs provide general trends that show PPTs are a valid method to discern degradation characteristics at the Oneida site. As expected, little to no measurable degradation was observed at the control well, D1, when only DO and bromide were injected (option 1). Employing option 1 at the control well provides an understanding of oxygen uptake of natural total organic carbon (TOC) in the soil and groundwater. TOC represents all organic carbon sources present in the natural groundwater, some of which exhibit biological oxygen demand. When TOC is high, DO utilization can be significant without the introduction of contaminants.

Accurately characterizing the proportion of DO utilized when natural TOC is degraded is essential. If natural TOC utilization is not addressed, rates calculated in contaminated regions may be overestimated since the rates do not remove the proportion of DO that is consumed for natural TOC degradation. In addition, DO can be consumed by other abiotic processes. PPTs using option 1 at control wells provide an indication of DO that is consumed for TOC degradation and other abiotic processes. If significant DO utilization occurs at control wells employing option 1, rates located within contaminated regions must be adjusted by subtracting the proportion of DO that is consumed for TOC degradation and other abiotic processes. Figure 13 shows the observed difference between a control (Fig. 13a) and contaminated (Fig. 13b) well. The area under the contaminated breakthrough curves for DO and bromide differ significantly, indicating consumption of DO.

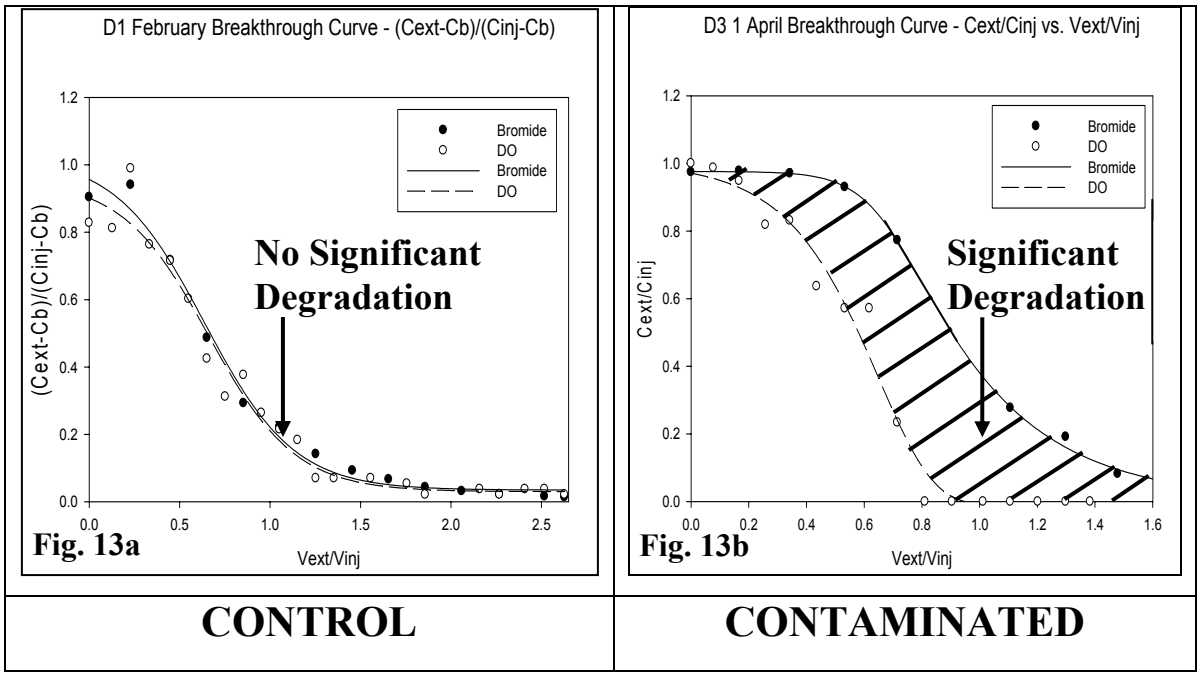

Figure 13: Comparison of Control and Contaminated Push-pull Tests

Control well results employing option 1 did not detect significant amounts of DO uptake, except for the D1 1 April PPT. The D1 1 April PPT occurred during a major rain event. Rates calculated for this test were the highest rates observed at the Oneida site. Rather than being a true control test, the D1 1 April test shows the effects of a groundwater recharge event. Contrary to expectations, the results suggest that rain events at the Oneida site remove DO from the aquifer, rather than replenish DO. However, the control well is downstream from an exposed bed of coal and runoff could leach coal-derived contaminants, particularly reduced iron, into the aquifer, thereby readily depleting DO. Because the D1 1 April PPT occurred during a major rain event, the test cannot be directly compared to other PPTs, thus the results were not incorporated into analysis of option 1 at control wells. Since the remaining option 1, control well PPT, D1 February, was unable to detect any degradation, rates determined within the contaminated region were not adapted to remove the contribution of DO utilization for natural TOC and abiotic processes.

The method of Istok et al. (1997) used in zero order rate calculations resulted in significant rates for DO uptake at the control well; however, this is a consequence of the methods inability to accurately remove background concentrations from the analysis.

Even when the method of Istok et al. (1997) is applied using Equation 3, which removes the contribution of background solutes, significant rates result when visual inspection of the BTC indicates that little to no degradation is occurring. The method of Istok et al. (1997) calculates the mass difference of the bromide and DO BTCs. If the curves are a significant distance apart, a significant rate will be calculated. However, visual inspection of the control well BTC in Fig. 13a shows the bromide and DO curves are not a significant distance apart. Furthermore, a comparison of the control well BTC (Fig. 14a) with a BTC that occurred at a contaminated well where no background concentration (Fig. 14b) was observed provides further details of the method's inability to accurately handle tests where significant background concentrations exist (Figure 14). It is clear that there is a significant distance between the bromide and DO BTCs at the contaminated S5 well (Fig. 14b). The control well shows no significant distance between the two curves (Fig. 14a). Thus, based on the mass difference under the BTCs of the two tests, it can be concluded that the zero order rate at the contaminated S5 well should be significantly larger than the rate at the control well. However, when employing the method of Istok et al. (1997) to calculate zero order rates, the control well results in a larger zero order rate (0.5387 $mg_{naphthalene}$/L-hr) when compared to the contaminated S5 well (0.4541 $mg_{naphthalene}$/L-hr). Therefore, it can be concluded that the method of Istok et al. (1997) cannot be used to determine zero order rates at PPT wells that have significant background concentrations.

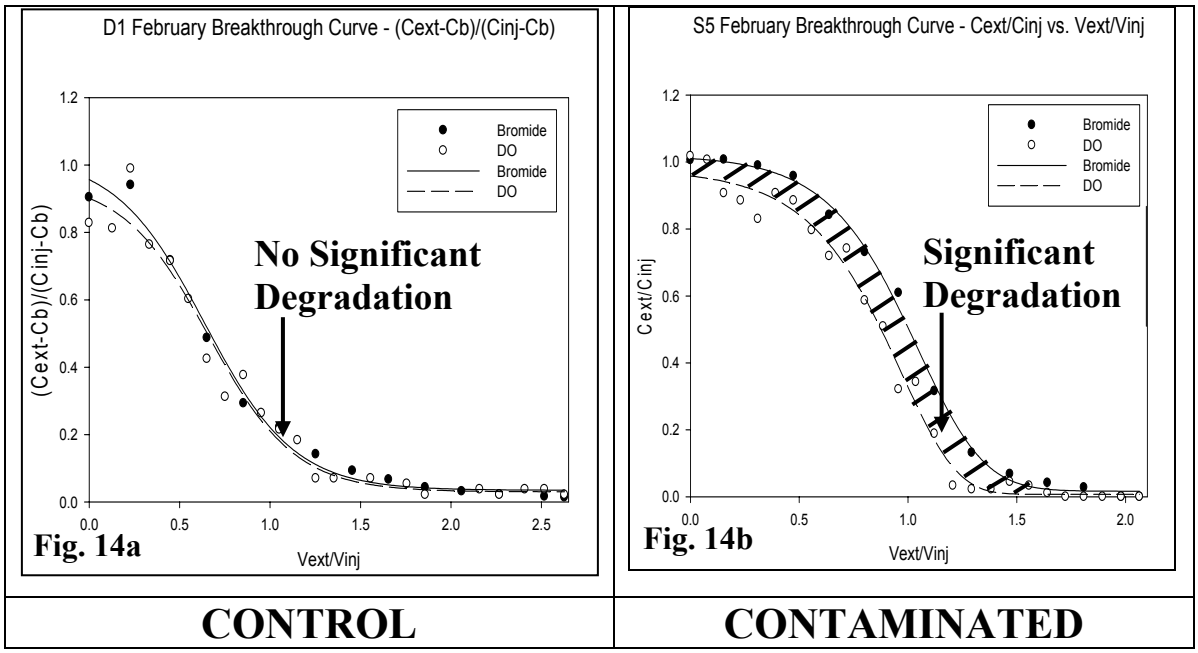

Figure 14: Additional Comparison of Control and Contaminated Push-pull Tests

5.5.1.2 Option 2

When naphthalene was included in the injection solution (option 2) at the control well, no significant amount of degradation occurred. Two of the four PPTs performed at the control well employed option 2, namely PPTs D1 June and D1 2 April. The purpose of performing an option 2 test at a control well was to ensure that injection of naphthalene does not erroneously modify PPT rate results. It can be anticipated that little degradation of naphthalene will occur at the control well since microbes near the control well have not adapted and developed pathways that enable degradation of this xenobiotic contaminant. If DO is readily consumed at naphthalene-injected control wells, results would suggest that options 1 and 2 cannot be directly compared for rate analysis, since the naphthalene is altering an unknown aspect of the test that affects rate determination.

Figure 15 shows the resulting BTC of one of the tests performed at the control well where naphthalene was injected, PPT D1 June. It can be clearly seen that no significant degradation occurred at the control well when naphthalene was injected. This indicates that microbes near the vicinity of the control well are not adapted to degradation of naphthalene. First order rates at naphthalene injected control wells were undetectable using the methods of Snodgrass and Kitanidis (1998) and Haggerty et al. (1998). Zero

order rates at naphthalene injected control wells, using the methods of Istok et al. (1997) and Snodgrass and Kitanidis (1998), were detected, but were small when compared to rates determined from wells located within the contaminated region of the site (Table 6, Figure 21). It is possible that microbes can quickly adapt to the contaminant injection, which would result in a lag-phase in degradation. A lag-phase was evident in only one of the two tested naphthalene-injected control wells, as shown in Figure 16.

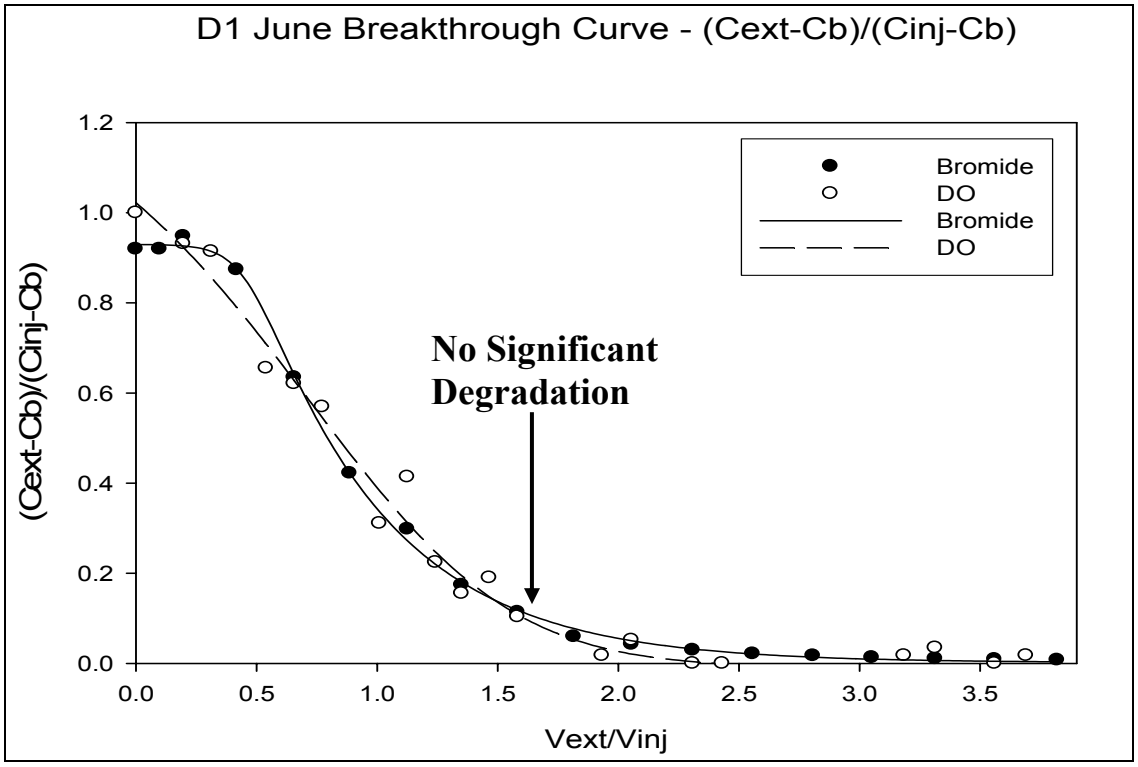

Figure 15: Control Well Breakthrough Curve Response to Naphthalene Injection

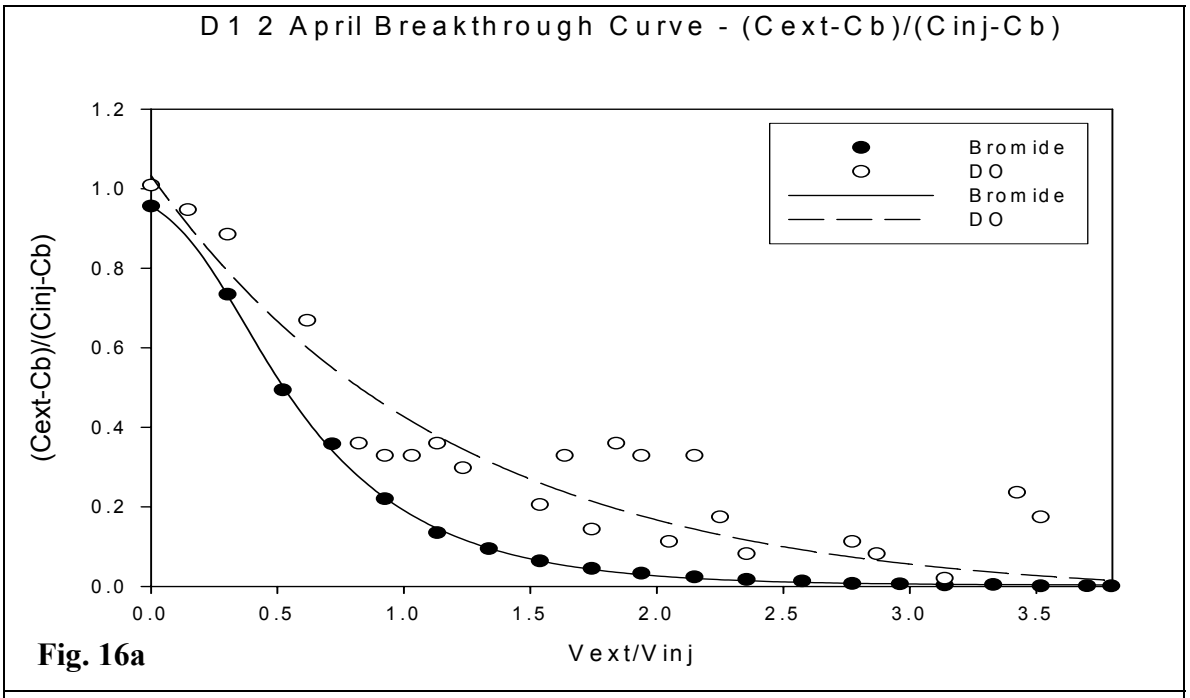

Fig. 16a

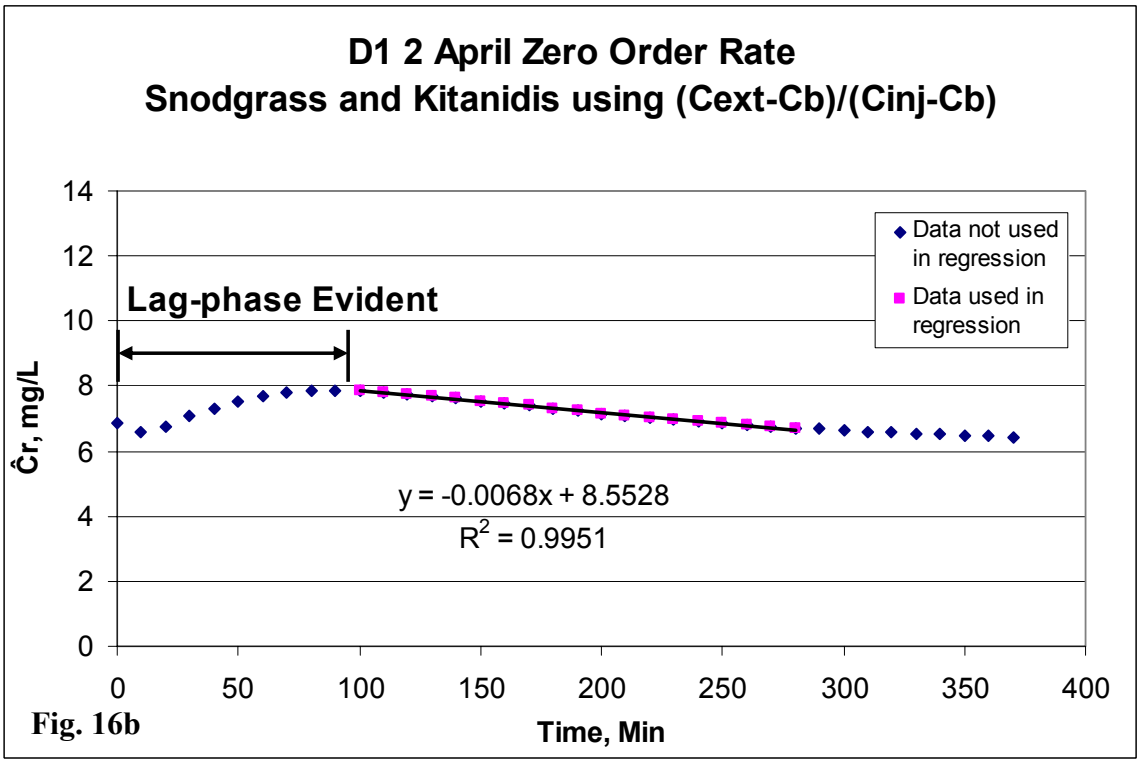

Fig. 16b

Figure 16: Lag-phase Evident at Naphthalene Injected Control Well – Zero Order Rate

Collectively, it is clear that microbes at the control wells were unable to degrade naphthalene at significant rates, thus demonstrating that the PPT method can accurately

characterize areas with no degradation. In addition, the contribution of DO consumed at control wells for TOC is insignificant. Table 5 illustrates the percent total organic matter (TOM) observed from soils taken from Oneida PPT wells during well construction using the method of Andersen and Christensen (1998). TOC can be estimated by doubling the observed TOM (Andersen and Christensen, 1998). Estimated TOC values obtained at other PPT wells were similar in magnitude to TOC values obtained at the control wells (Table 5). As a result, the effect of DO uptake for TOC degradation at wells within the contaminated area can be expected to be similar to the results obtained at the control wells. However, it is possible that DO uptake for TOC degradation at anaerobic wells would be greater than at control wells, since the TOC present is not in an oxidized form. Reduced TOC could erroneously inflate derived degradation rates. Since in-situ conditions do not exist where the aquifer is anaerobic, but without contamination, this could not be addressed. Since natural TOC content was primarily less than two percent in all but one instance, the small amount of TOC present in the Oneida site soils will not significantly contribute to DO uptake (Andersen and Christensen, 1998; Schwarzenbach et al., 1993). Thus, the effects of DO uptake for TOC degradation during anaerobic conditions is likely to be very small and consequently no attempts were made to adjust rates for this insignificant portion of DO uptake at anaerobic wells. Overall, the PPT results at the control well D1 validate that rate adjustments for TOC at contaminated wells is unnecessary, naphthalene-injection does not alter test results, and consequently options 1 and 2 can be compared directly.

Table 5: Percent Total Organic Matter and Total Organic Carbon in Push-pull Test Soils

	S1	D1	S2	D2	S3	D3	S4	D4	S5	D5
TOM Content	0.30%	0.97%	0.51%	0.60%	0.31%	0.67%	0.89%	1.01%	0.79%	0.99%
TOC Content	0.60%	1.93%	1.01%	1.20%	0.63%	1.33%	1.77%	2.03%	1.58%	1.98%

5.5.2 Comparing Options 1 and 2

Three PPTs employed option 1 to determine whether the inclusion of naphthalene in injected solutions had an effect on results. Naphthalene, when included in the injection solution, could potentially alter the test results, such as impacting retardation factors of other injected solutes. As explained above in 5.5.1 Control Wells, PPTs performed at the

control well, D1, suggest that the addition of naphthalene in injection solutions caused little change in results. A more concrete example occurs with the PPTs performed at a contaminated well, D3, during April. The April tests, D3 1 April and D3 2 April, were performed only a day apart, with similar weather conditions. Thus, the tests can be directly compared without interference of seasonal variations. Results for the two tests (Table 6), show that rates calculated with options 1 and 2 are very similar. Application of the methods of Snodgrass and Kitanidis (1998) and Haggerty et al. (1998) result in a percent error between the two tests of less than 3%. The zero order rate method of Istok et al. (1997) produces a percent error less than 10%. The larger error associated with the method of Istok et al. (1997) is most likely due to the data variability that influenced the shape of the BTC for D3 2 April (Appendix C). In addition, an error of less than 10% is still within the error associated with flow balance calculations. As a result, it can be concluded that options 1 and 2 have no affect on the PPT results and options 1 and 2 can be directly compared to determine in-situ rates.

5.5.3 Treed and Untreed Regions

Oneida PPTs have shown that degradation of naphthalene attributed to phytoremediation can be detected with the push-pull method. Higher degradation rates were observed at regions of the site located adjacent to trees (Fig. 17a), when compared to regions away from trees (Fig. 17b). The overall rate summary for zero and first order methods can be found in Table 6. These results suggest that phytoremediation at the Oneida site enhances degradation and thus decreases the overall remediation timeframe.

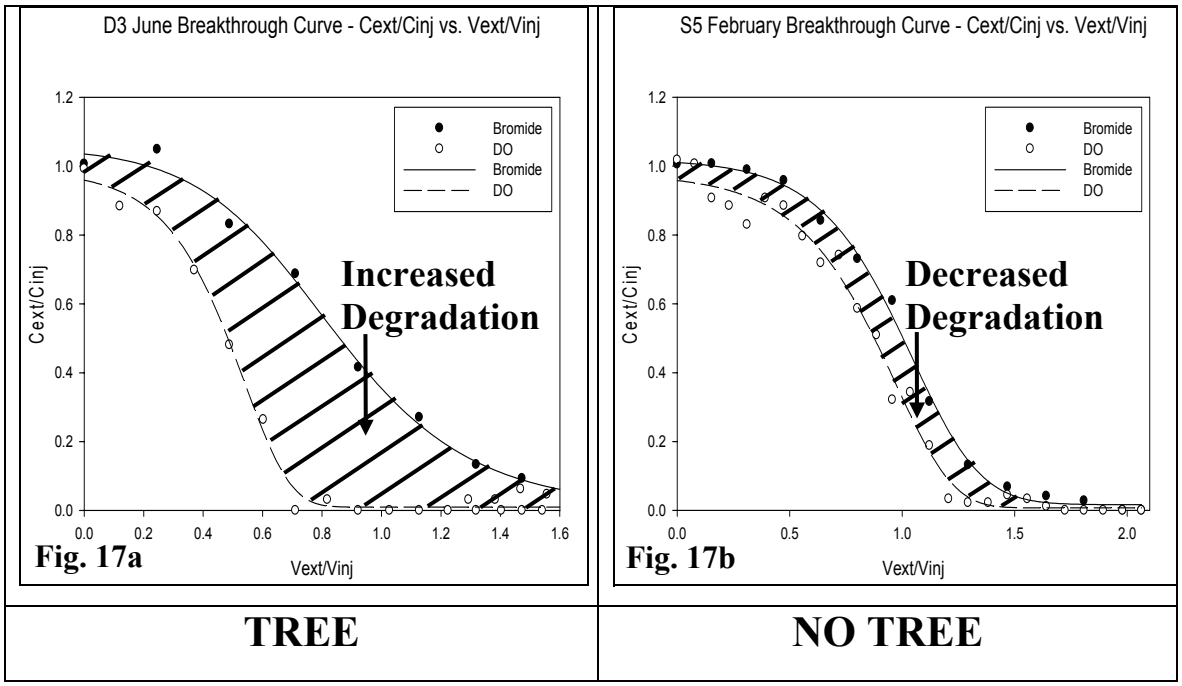

Figure 17: Push-pull Comparison of Trees and No Trees

6.0 SUMMARY OF DATA EVALUATION METHODS

6.1 Breakthrough Curve Crossing

Poor results for zero and first order rate analysis are produced when the bromide and DO BTCs cross one another. When the normalized DO concentration exceeds the normalized bromide concentration, the DO and bromide BTCs cross one another (Figure 18). When two solutes have similar retardation factors, the BTC of the two solutes should be nearly identical. Theoretically, if one of the solutes is a non-reactive tracer (bromide) and the other solute is subject to decay (DO), the non-reactive tracer BTC should always have a normalized concentration equal to or greater than the degrading solute. This was observed for nearly all of the PPTs, but four of the tests exhibited instances where the normalized DO concentration exceeded the normalized bromide concentration, causing the bromide and DO BTCs to cross one another. Of the four PPTs that exhibited BTC crossing, three of the tests occurred at the control well. Since little to no degradation was observed at the control well, the relative difference between the normalized DO and bromide concentrations is small. Thus, the three PPTs at the control wells that exhibited BTC crossing were due only to slight changes in normalized concentrations, which can be attributed to measurement variability. The remaining PPT

that exhibited BTC crossing, S3 February, however, occurred at a well within the contaminated region of the site where the relative difference between the normalized bromide and DO concentrations is expected to be large.

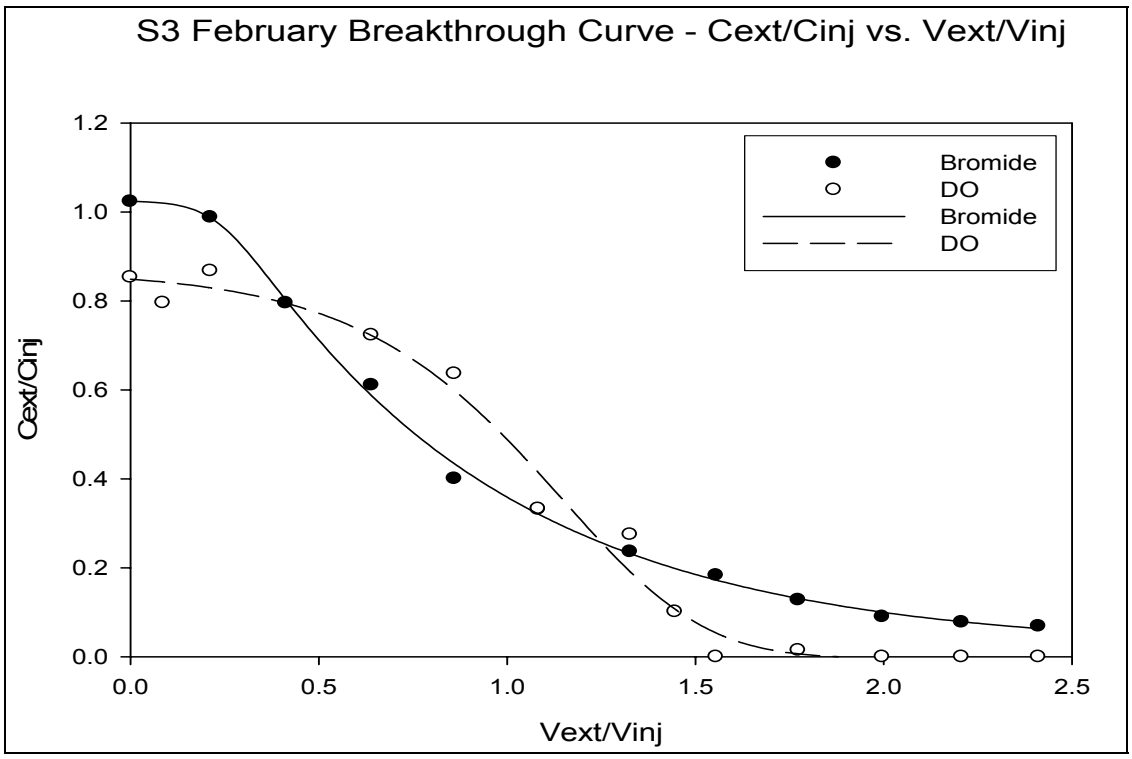

Figure 18: Example Bromide and Dissolve Oxygen Crossing Breakthrough Curve

The exact cause of the bromide and DO BTC crossing at the contaminated well, S3, is unclear. Because Istok et al. (1997) and Haggerty et al. (1998) showed that the retardation factors of bromide and DO are similar, explanation of BTC crossing must be accounted for by other means. Since BTC crossing occurred during four PPTs, particularly one at a contaminated well, it can be deduced that BTC crossing was not well specific. It is likely that this effect occurred as a result of a combination of experimental error and performing PPTs at a heterogeneous aquifer. The latter of which is an intrinsic part of the assumption that the dominating processes are advection, dispersion, and spatially homogeneous, constant coefficient, zero or first order irreversible reactions. Istok et al. (1997), Haggerty et al. (1998) and others have successfully applied PPTs to heterogeneous aquifers, but it is possible that heterogeneous factors can sometimes affect PPT results.

When the non-ideal, crossing BTCs are applied to the methods of Istok et al. (1997), Snodgrass and Kitanidis (1998), and Haggerty et al. (1998), plotted data does not produce a straight line where it is likely that either zero or first order decay is occurring. When bromide and DO BTCs converge towards one another, a positive slope results (when a negative slope should exist). When the bromide and DO BTCs finally cross one another and normalized DO concentrations are greater than normalized bromide concentrations, plotted rate data exceed values obtained prior to the BTC crossing (Fig. 19b, 19c). If the bromide and DO curves then begin to diverge from one another, ultimately to where the normalized DO concentration is less than the normalized bromide concentration, a negative slope results. Figure 19 illustrates the effects of BTC crossing (Fig.19a) on both zero (Fig. 19b) and first order (Fig. 19c) degradation rate regression analysis. When BTC crossing occurs, a sinusoidal shape results in plotted data, making degradation rates very difficult to determine. The sinusoidal shape increases with the greater number of BTC crossings, thus furthering rate analysis complexity. Therefore, PPTs that exhibit BTC crossing, particularly when large differences are expected between the tracer and the reactive solute, can have a large amount of embedded error in rate results and very little confidence is given to PPTs that exhibit BTC crossing. As a consequence, rates determined from PPT S3 February can only be used for initial comparison, very little confidence is given to the BTC crossing S3 February results, and future tests should be performed at S3 to confirm initial results.

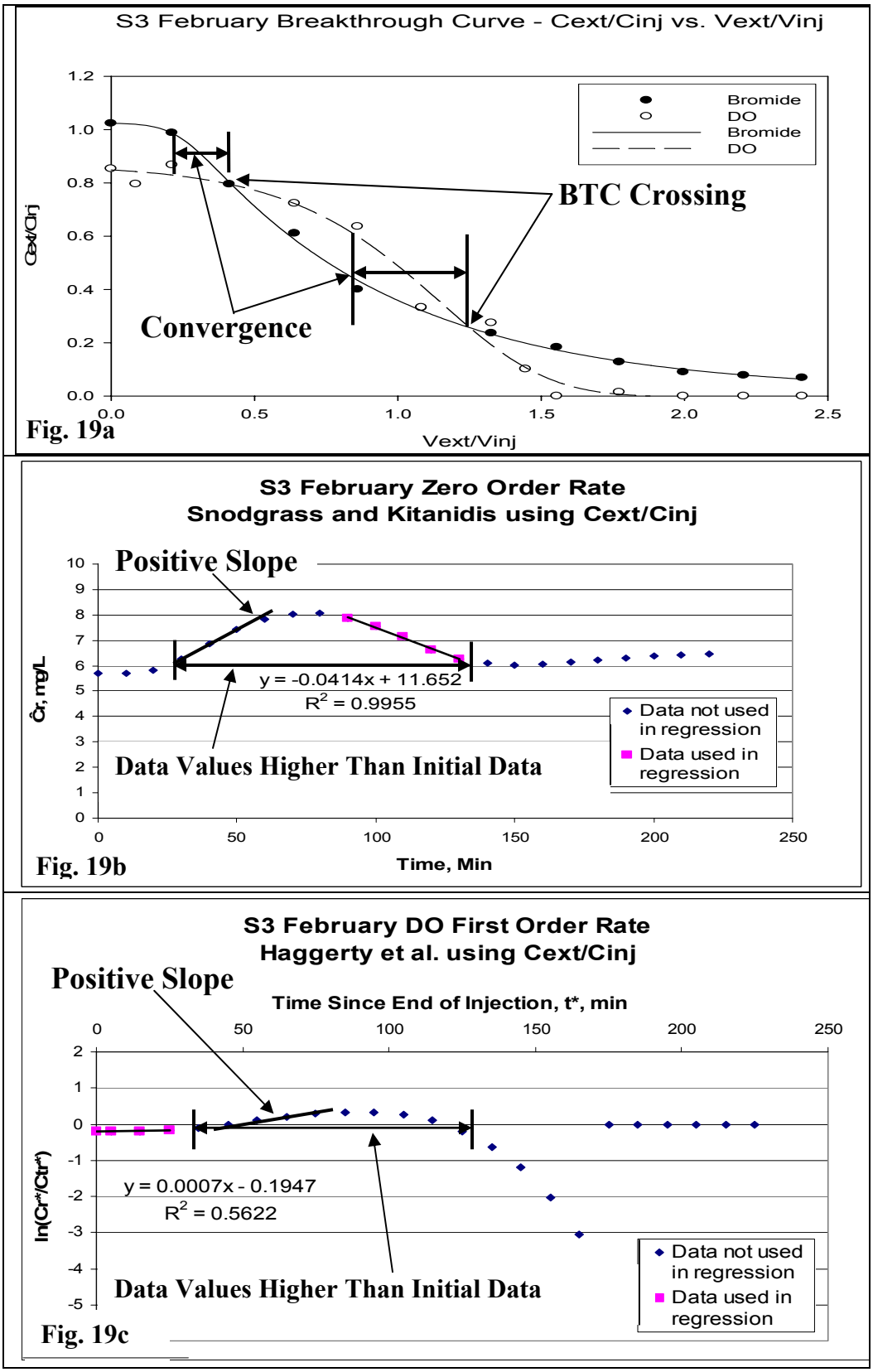

Figure 19: Effects of Breakthrough Curve Crossing

6.2 Zero Order Degradation Rates

6.2.1 Method of Istok et al. (1997)

The method of Istok et al. (1997) was shown to poorly calculate degradation rates when significant background concentrations existed, even after applying the normalization of Equation 3, as explained in 5.5.1 Control Wells. Furthermore, the method performed poorly for determining rates when little to no degradation was observed in BTCs, such as in PPT D4 February. As an example, the method of Istok et al. (1997) calculated a zero order rate of 0.8245 $mg_{naphthalene}$/L-hr for the D4 February test when little degradation was observed from the BTC (Figure 20, Table 6). The method also poorly accounted for the rapid degradation of DO at PPT D1 1 April, which occurred during a major rain event. The resultant zero order rate for D1 1 April was lower than all rates calculated for tests at D3 and D4; however, this is most likely a consequence of the bromide and DO BTCs crossing one another, as explained in the previous section. The method was able to detect relative trends that occurred at D3 throughout the varying seasons (Figure 21); however these rates differed significantly from the zero order rates determined from the method of Snodgrass and Kitanidis (1998). Therefore, the method of Istok et al. (1997) is excluded from further Oneida PPT analysis and conclusions.

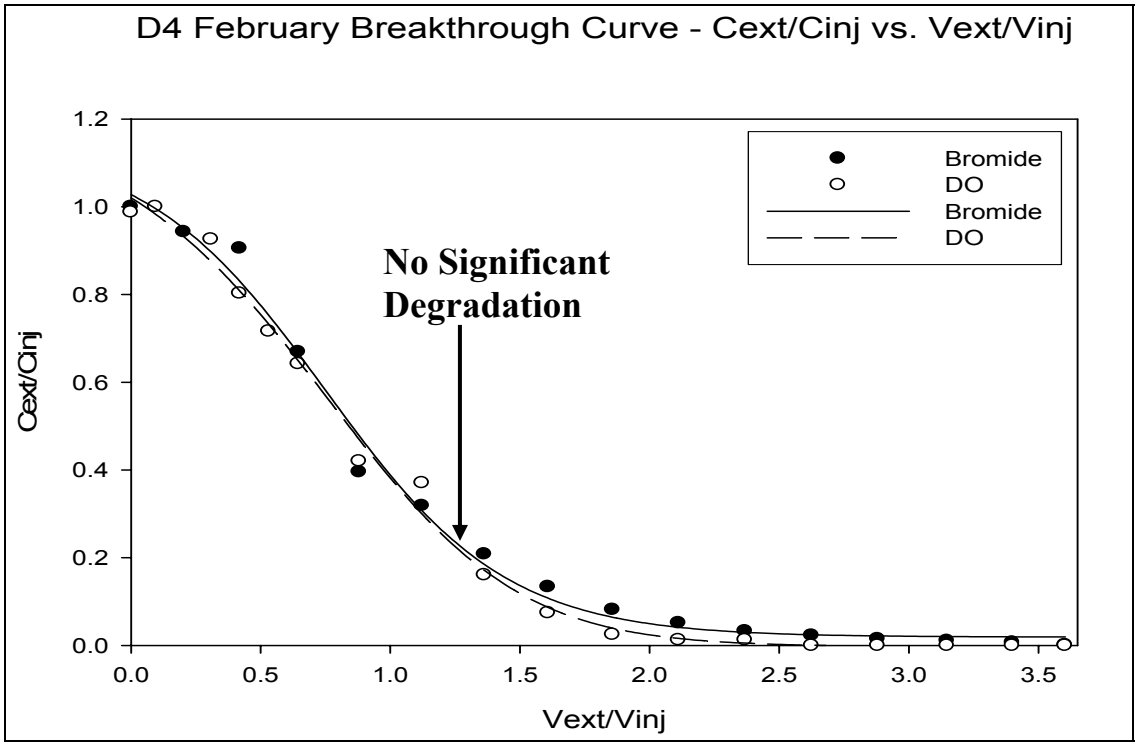

Figure 20: D4 February Breakthrough Curve

6.2.2 Method of Snodgrass and Kitanidis (1998)

The zero order rate determination method of Snodgrass and Kitanidis (1998) performed well when discerning rates under a multitude of conditions. The method produced rates close to zero when little to no degradation was observed in BTCs. For example, the D4 February PPT returned a degradation rate of 0.003 $mg_{naphthalene}$/L-hr when the BTC indicated little to no degradation was occurring (Table 6, Figure 20). The method was also able to account for general trends during seasonal variation at D3 (Fig. 25a). The method was also able to account for the rapid uptake of DO that occurred at PPT D1 1 April (Appendix C).

6.2.3 Zero Order Rate Methods Conclusion

The plotting method of Snodgrass and Kitanidis (1998) enables selection of data points that exhibit a straight-line, whereas the method of Istok et al. (1997) is limited to simple mass difference calculations under the entire breakthrough curve. The method of Istok et al. (1997) provides no approach to select boundaries to where data may or may not be exhibiting zero order kinetics. Being forced to select the entire mass difference under the bromide and DO BTCs causes errors in rate calculations and consequently obscures true rates. Therefore, the highest confidence is placed in the method of Snodgrass and Kitanidis (1998) to determine zero order rate coefficients.

6.3 First Order Rates

Only one PPT resulted in differing first order rates when the methods of Snodgrass and Kitanidis (1998) and Haggerty et al. (1998) were applied. Both methods found very similar rates since the plotted data from Equations 11 and 12 are very similar. Equation 11 plots normalized data according to Equations 2 and 3, whereas Equation 12 plots non-normalized C_{ext} data. The PPT that produced a different first order rate was D4 February.

6.3.1 Differing First Order Rate Results at PPT D4 February

Only PPT D4 February produced different first order rates when applying the methods of Haggerty et al. (1998) and Snodgrass and Kitanidis (1998). For all PPTs performed, the two methods evaluated the same time boundaries when plotting natural

log concentration data thus enabling direct comparison of the two methods. For PPT D4 February, the R^2 value was smaller (0.1938) using the method of Haggerty et al. (1998) than the R^2 value (0.1938) using the method of Snodgrass and Kitanidis (1998). The low R^2 values are misleading. When plotted data is nearly linear, the relative scatter between data points is small, but is magnified in the R^2 value due to squaring of residuals during R^2 calculations. The rates detected at D4 (February) were 0.012 1/hr and 0.006 1/hr for the methods of Haggerty et al. (1998) and Snodgrass and Kitanidis (1998), respectively. Thus, a 50% error occurs between the rates, which can lead to a significant error when extrapolated over a long time, as is common with site remediation forecasting.

The observed difference at D4 February can be attributed to variations in how the rates were calculated. Concentration data used for rate analysis was based upon the regression line-fit in BTCs, which aided in removing measurement error from calculated rates (as explained in 4.2 Solute Constituent Balance). Regression line equations from BTCs return normalized concentrations, C_{ext}/C_{inj} [or $(C_{ext}-C_b)/(C_{inj}-C_b)$ if background present], evaluated as a function of V_{ext}/V_{inj}. Therefore, C_{inj} concentrations for bromide (tracer) and DO (reactive solute) must be used to back-calculate the $C_r^m(t)$ and the $C_t^m(t)$ values (These values are simply the C_{ext} values of bromide and DO evaluated at time t) from Snodgrass and Kitanidis (1998) Equation 12. Using the C_{inj} term to derive Snodgrass and Kitanidis (1998) first order rates incorporates more experimental error into the calculation, when compared to the method of Haggerty et al. (1998), which uses normalized concentrations, C_{ext}/C_{inj} [or $(C_{ext}-C_b)/(C_{inj}-C_b)$ if background present], directly in Equation 11. As a result, despite opposing conclusions based on R^2 values, more confidence is placed in the Haggerty et al. (1998) D4 February first order rate simply due to how data was analyzed to aid in removing experimental error. It should be noted, however, that the 95% confidence interval for the Haggerty et al. (1998) first order rate is 0.012 +/- 0.006 1/hr (using Equation 13A in Appendix A). Thus, although the Snodgrass and Kitanidis rate incorporates more measurement error, the calculated rate is still within the 95% confidence interval of the Haggerty et al. (1998) first order rate. Overall, this suggests that the mathematical approach used to determine Snodgrass and Kitanidis (1998) is appropriate, which is certainly supported by eleven of the twelve PPTs

producing identical first order rates, when employing the methods of Snodgrass and Kitanidis (1998) and Haggerty et al. (1998).

6.3.2 Clearly Elucidating Breakthrough Curve Crossing

The first order method of Haggerty et al. (1998) has potential advantages, when compared to the first order method of Snodgrass and Kitanidis (1998), to elucidate when BTC crossing is occurring. Equation 11 of the method of Haggerty et al. (1998), defines plotted values to be greater than zero when $C_r > C_t$; this situation occurs when BTC crossing is occurring (Fig. 19c). When $C_r > C_t$, degradation cannot be occurring and these data should not be evaluated in determining degradation rates. When using the method of Snodgrass and Kitanidis, however, it is more difficult to discern when $C_r > C_t$ since Equation 12 does not define this to occur at a known, set value (Appendix C: Figure C5). Therefore, the method of Haggerty et al. (1998) aids in assessment of when BTC crossing is occurring.

6.3.3 First Order Rate Conclusions

It can be concluded that the methods of Snodgrass and Kitanidis (1998) and Haggerty et al. (1998) produce very similar first order rate results. In the single instance where the calculated rates differed, more confidence was given to the rates derived using the method of Haggerty et al. (1998). In addition, the method of Haggerty et al. (1998) provides an improved indication of when BTC crossing is occurring. The method of Haggerty et al. (1998) also enables incorporation of a lag-phase that is common in anaerobic PPTs, by using the t* term (Equation 11), but the method of Snodgrass and Kitanidis (1998) is limited to tests that do not utilize a lag-phase. Although the two first order methods produced nearly identical results, the method of Haggerty et al. (1998) provides slight advantages over the method of Snodgrass and Kitanidis (1998). As a result, slightly more confidence is given to the method of Haggerty et al. (1998) to determine first order rate coefficients.

7.0 OVERALL RESULTS

Twelve push-pull tests were performed, utilizing either option 1 or 2, so that the method could be evaluated and tested. The PPTs yielded an initial set of rate data that enabled comparison of seasonal and spatial varying in-situ conditions. Modifications to the methods of Istok et al. (1997), Snodgrass and Kitanidis (1998), and Haggerty et al. (1998) explained in 5.3 Modifying Data Analysis Methods were performed and the results of the twelve PPTs are displayed in Table 6. Zero order degradation rates were converted to $mg_{naphthalene}$/L-hr as explained in 4.3.3 Transforming Zero Order Rates. First order degradation rates are reported as 1/hr. As mentioned previously, Haggerty et al. (1998) showed that complete tracer recovery is not necessary for accurate quantification of rate coefficients. Tests are divided chronologically by the well and time at which the test took place with asterisks indicating whether option 1 or 2 was employed. Four tests were performed during April at two wells, D1 and D3. The first pair of tests, denoted D1 1 April and D3 1 April, employed option 1, whereas the second pair of tests, denoted D1 2 April and D3 2 April, employed option 2 (naphthalene included in injection).

All rate values reported for DO utilization should be positive; however, negative values are reported indicating the applied method failed to determine a rate when it is known that degradation is occurring. This occurred only with two tests, S3 February and D1 2 April. S3 February was the most severe BTC crossing (Fig. 19a) observed and consequently limited first order rate regression line analysis only to the first few points where a near zero slope occurred as shown above in the Haggerty et al. (1998) graph (Fig. 19c). A negative value also occurred using the method of Istok et al. (1997) to determine a zero order rate coefficient at D1 2 April. The method of Istok et al. (1997) is unable to accurately produce degradation rates when significant background concentrations are present, which is explained in 6.0 Summary of Data Evaluation Methods, as a shortcoming to the method of Istok et al. (1997). In addition, when regression analysis produced slightly positive-slopes for tests where little to no degradation was observed from BTCs, the resultant negative-valued rate was forced to a value of zero. D1 2 April resulted in a BTC where the normalized DO concentration was greater than the bromide curve at each time. Consequently first order rates could not be calculated for D1 2 April since plotted data yielded a positive slope.

Table 6: Rate Summary of Twelve Oneida Push-pull Tests

Monitoring Well - Time		Br	DO	R^2 Values
*D3 - December***	**Percent Recovery**	87.76%	65.68%	
	Istok et al. (1997) Zero Order Rate, $mg_{naphthalene}/L\text{-}hr$		0.8784	N/A
	Snodgrass and Kitanidis (1998) Zero Order Rate, $mg_{naphthalene}/L\text{-}hr$		**0.7863**	**0.9928**
	Haggerty et al. (1998) First Order Rate, 1/hr		**0.3000**	**0.9273**
	Snodgrass and Kitanidis (1998) First Order Rate, 1/hr		0.3000	0.9273
*D4 - December***	**Percent Recovery**	94.61%	65.90%	
	Istok et al. (1997) Zero Order Rate, $mg_{naphthalene}/L\text{-}hr$		0.8712	N/A
	Snodgrass and Kitanidis (1998) Zero Order Rate, $mg_{naphthalene}/L\text{-}hr$		**1.2916**	**0.9750**
	Haggerty et al. (1998) First Order Rate, 1/hr		**0.4860**	**0.9871**
	Snodgrass and Kitanidis (1998) First Order Rate, 1/hr		0.4860	0.9871
*D1 - February**	**Percent Recovery**	74.95%	71.96%	
	Istok et al. (1997) Zero Order Rate, $mg_{naphthalene}/L\text{-}hr$		0.5387	N/A
	Snodgrass and Kitanidis (1998) Zero Order Rate, $mg_{naphthalene}/L\text{-}hr$		**0.0000**	**0.9161**
	Haggerty et al. (1998) First Order Rate, 1/hr		**0.0024**	**0.0098**
	Snodgrass and Kitanidis (1998) First Order Rate, 1/hr		0.0024	0.0098
*D4 - February***	**Percent Recovery**	94.51%	87.79%	
	Istok et al. (1997) Zero Order Rate, $mg_{naphthalene}/L\text{-}hr$		0.3357	N/A
	Snodgrass and Kitanidis (1998) Zero Order Rate, $mg_{naphthalene}/L\text{-}hr$		**0.0030**	**0.0147**
	Haggerty et al. (1998) First Order Rate, 1/hr		**0.0120**	**0.1938**
	Snodgrass and Kitanidis (1998) First Order Rate, 1/hr		0.0060	0.3392
*S3 - February***	**Percent Recovery**	93.95%	86.83%	
	Istok et al. (1997) Zero Order Rate, $mg_{naphthalene}/L\text{-}hr$		0.2736	N/A
	Snodgrass and Kitanidis (1998) Zero Order Rate, $mg_{naphthalene}/L\text{-}hr$		1.2378	0.9955
	Haggerty et al. (1998) First Order Rate, 1/hr		-0.0420	0.5622
	Snodgrass and Kitanidis (1998) First Order Rate, 1/hr		-0.0420	0.5622
*S5 - February***	**Percent Recovery**	99.27%	82.45%	
	Istok et al. (1997) Zero Order Rate, $mg_{naphthalene}/L\text{-}hr$		0.4541	N/A
	Snodgrass and Kitanidis (1998) Zero Order Rate, $mg_{naphthalene}/L\text{-}hr$		**0.2840**	**0.9444**
	Haggerty et al. (1998) First Order Rate, 1/hr		**0.0960**	**0.8653**
	Snodgrass and Kitanidis (1998) First Order Rate, 1/hr		0.0960	0.8653

*** = Option 1 – Bromide, DO Injected**
**** = Option 2 – Bromide, DO, Naphthalene Injected**

Table 6 (cont.): Rate Summary of Twelve Oneida Push-pull Tests

Monitoring Well - Time		Br	DO	R^2 Values
*D1 1 - April**	Percent Recovery	86.14%	50.64%	
	Istok et al. (1997) Zero Order Rate, $mg_{naphthalene}/L\text{-}hr$		0.5371	N/A
	Snodgrass and Kitanidis (1998) Zero Order Rate, $mg_{naphthalene}/L\text{-}hr$		6.2187	0.9814
	Haggerty et al. (1998) First Order Rate, 1/hr		5.8020	0.9909
	Snodgrass and Kitanidis (1998) First Order Rate, 1/hr		5.8020	0.9909
*D1 2 - April***	Percent Recovery	66.44%	113.83%	
	Istok et al. (1997) Zero Order Rate, $mg_{naphthalene}/L\text{-}hr$		-0.1108	N/A
	Snodgrass and Kitanidis (1998) Zero Order Rate, $mg_{naphthalene}/L\text{-}hr$		**0.2033**	**0.9951**
	Haggerty et al. (1998) First Order Rate, 1/hr		**Positive slope - Forced to 0.0**	**Not evaluated**
	Snodgrass and Kitanidis (1998) First Order Rate, 1/hr		Positive slope - Forced to 0.0	Not evaluated
*D3 1 - April**	Percent Recovery	96.02%	53.92%	
	Istok et al. (1997) Zero Order Rate, $mg_{naphthalene}/L\text{-}hr$		1.0683	N/A
	Snodgrass and Kitanidis (1998) Zero Order Rate, $mg_{naphthalene}/L\text{-}hr$		**1.5846**	**0.9411**
	Haggerty et al. (1998) First Order Rate, 1/hr		**0.7740**	**0.8123**
	Snodgrass and Kitanidis (1998) First Order Rate, 1/hr		0.7740	0.8123
*D3 2 - April***	Percent Recovery	101.24%	62.68%	
	Istok et al. (1997) Zero Order Rate, $mg_{naphthalene}/L\text{-}hr$		0.9679	N/A
	Snodgrass and Kitanidis (1998) Zero Order Rate, $mg_{naphthalene}/L\text{-}hr$		**1.6174**	**1.0000**
	Haggerty et al. (1998) First Order Rate, 1/hr		**0.6000**	**0.7309**
	Snodgrass and Kitanidis (1998) First Order Rate, 1/hr		0.6000	0.7309
*D1 - June***	Percent Recovery	91.13%	88.00%	
	Istok et al. (1997) Zero Order Rate, $mg_{naphthalene}/L\text{-}hr$		0.2367	N/A
	Snodgrass and Kitanidis (1998) Zero Order Rate, $mg_{naphthalene}/L\text{-}hr$		**0.0359**	**0.0750**
	Haggerty et al. (1998) First Order Rate, 1/hr		**0.0000**	**0.1605**
	Snodgrass and Kitanidis (1998) First Order Rate, 1/hr		0.0000	0.1605
*D3 - June***	Percent Recovery	91.73%	45.79%	
	Istok et al. (1997) Zero Order Rate, $mg_{naphthalene}/L\text{-}hr$		1.3264	N/A
	Snodgrass and Kitanidis (1998) Zero Order Rate, $mg_{naphthalene}/L\text{-}hr$		**2.4277**	**0.9810**
	Haggerty et al. (1998) First Order Rate, 1/hr		**1.2540**	**0.7766**
	Snodgrass and Kitanidis (1998) First Order Rate, 1/hr		1.2540	0.7766

*** = Option 1 – Bromide, DO Injected**

**** = Option 2 – Bromide, DO, Naphthalene Injected**

7.1 Zero Order Results

Results from application of the methods evaluated for zero and first order decay were plotted in chronological order, separated by tests performed at each well. Figure 21 displays the results obtained for zero order degradation. As explained above, more confidence is given to the results using the method of Snodgrass and Kitanidis (1998) and therefore, the following conclusions are drawn solely from the rates determined from the method of Snodgrass and Kitanidis (1998). Comparison of the D3 1 (1.58 $mg_{naphthalene}$/L-hr) and D3 2 (1.62 $mg_{naphthalene}$/L-hr) April PPT rates, employing options 1 and 2 respectively, indicate that tests using either options 1 or 2 are not significantly different and can be used for direct comparison, as explained above in greater detail. Observed magnitudes of degradation, as high as 6.22 $mg_{naphthalene}$/L-hr during the rain event at D1 1 April, are reasonable and certainly within zero order decay of naphthalene observed at wastewater treatment plants and other naphthalene-remediation sites. When the test at D1 1 April is excluded, it is evident that the highest zero order rates occur at well D3, which serves as the best indicator of the contribution of trees to remediation. The largest rate found at D3, 2.43 $mg_{naphthalene}$/L-hr, occurred in June when the contribution of the trees is largest, while the lowest rate at D3, 0.79 $mg_{naphthalene}$/L-hr, occurred in December when trees are not active and thus their contribution to remediation is the smallest at this time of the year. After D3, the next highest rates were found at D4 (December) and the shallow well S3, located adjacent to D3 (Figure 1), respectively. The D4 well is also located adjacent to trees and the high observed rate (2.25 $mg_{naphthalene}$/L-hr) can be attributed to the added benefit of phytoremediation; the D4 December PPT is discussed in further detail below. The zero order rate at S3 February was 1.24 $mg_{naphthalene}$/L-hr. This rate is greater than the rate observed at D3 in December, but less than the rates determined at both tests at D3 in April. Again, this fits into the seasonal variation and bio-activeness of trees, where the contribution of trees to remediation is lowest in the coldest winter months (December) and then gradually increases to a peak in the warmest summer months (June-August). These results are further supported by the calculated rate that occurred at S5, located within the access road the furthest distance possible away from trees, but still within the contaminated region of the site. Rates observed at S3 during February were more than four times the rates observed at the untreed S5 well

(Figure 22); it should be noted that the S3 February PPT exhibited BTC crossing and therefore the low confidence in results must be validated by future PPTs that compare treed and untreed regions. In general, zero order winter rates at treed regions were greater by a factor of at least 2.5 when compared to non-treed regions. Since no tests were performed to compare treed and untreed regions during peak summertime performance, the exact peak enhancement factor of trees to remediation is still unknown. It should also be noted that PPTs could not be performed in August since the groundwater table dropped to depths below the PPT wells (see 8.1 Push-pull Tests During Drought and Summer Conditions for further explanation). Future research can determine this ratio, but for now, it is only known that trees enhance remediation by over four times during months were the poplar trees do not have leaves and are not active. All zero order results indicate that not only can the PPT method discern differences between treed and non-treed regions, but also seasonal variations of phytoremediation, whose effects are rapidly increasing in-situ degradation and remediation.

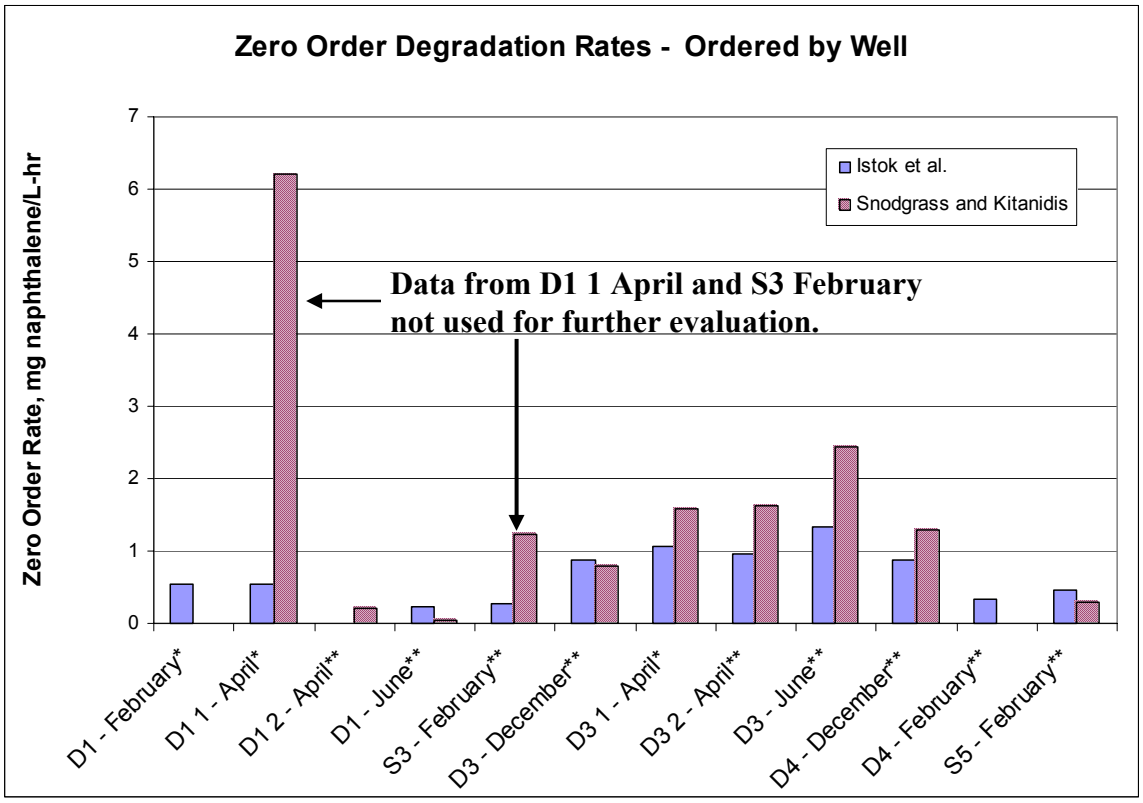

Figure 21: Zero Order Degradation Rates – Ordered by Chronological Well
*** = Option 1 – Bromide, DO Injected**
**** = Option 2 – Bromide, DO, Naphthalene Injected**

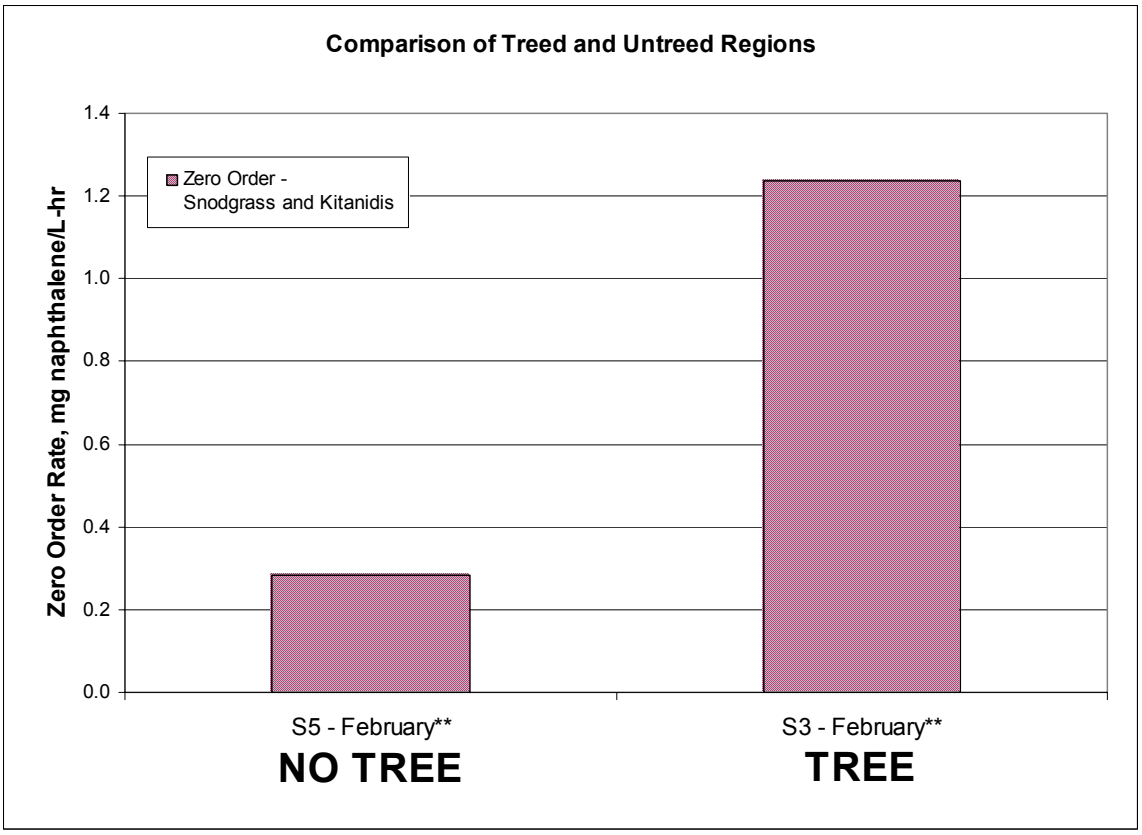

Figure 22: Comparison of Treed and Untreed Regions
*** = Option 1 – Bromide, DO Injected**
**** = Option 2 – Bromide, DO, Naphthalene Injected**

Figure 21 also provides information about control well, D1. Excluding the test performed at D1 1 April during the rain event, little to no degradation was observed at the control well. No degradation was observed at D1 when option 1 was employed, while slight degradation, up to 0.20 $mg_{naphthalene}$/L-hr, was observed at D1 when naphthalene was injected (option 2). A lag-phase was evident in the D1 2 April PPT, but was not clearly observed at the D1 June PPT (Figure 16; Appendix C). Zero order results support that the control well functioned properly as a control well, that levels of TOC consumed during PPTs are an insignificant contribution to DO depletion during PPTs, and that options 1 and 2 can be used for direct comparison.

Figure 21 and Table 6 show that the zero order rate at well D4, a highly contaminated well, in February did not produce observable degradation. Since initially the well was extremely anaerobic (having a DO of 0 mg/L) and a impulse input of DO was introduced during injection (much like a step-input function), the microbes adjacent

to D4 who had adapted to extremely anaerobic conditions, were likely 'shocked' by the introduction of DO. Many anaerobic microbes cannot live when any oxygen is introduced into their environment (Madigan et al., 2000). The anaerobic microbes were unable to adapt to the rapid change in the redox conditions and consequently did not contribute to observed degradation. If this conclusion is correct and results obtained from D4 February were a result of microbial shock and not experimental error, this test provides further support that DO uptake for natural TOC at wells that were previously subject to anaerobic conditions is insignificant. If DO utilization for natural TOC degradation was significant during tests that injected DO into anaerobic wells, a significant degradation rate would have been observed at the D4 February PPT. The rate calculated by Snodgrass and Kitanidis (1998) is 0.003 $mg_{naphthalene}$/L-hr, which is extremely low. As a result, it can be concluded that rate adjustments for natural TOC is not necessary for all PPTs, including wells that were both aerobic and anaerobic prior to injection.

A higher zero order rate (1.29 $mg_{naphthalene}$/L-hr) was observed at D4 December, when compared to D4 February (0.003 $mg_{naphthalene}$/L-hr), which can be attributed to seasonal fluctuations of the groundwater table (GWT). The GWT is at its lowest in late August-September, but does not recover significantly until later in the winter. As a result, the microbes at D4 during December were exposed to aerobic conditions for a longer, more recent time-period, while the microbes at D4 during February were subject to anaerobic conditions when the GWT is at its highest. As a result, it can be expected that degradation during aerobic PPTs will be faster during the D4 December test since microbes are already acclimated to aerobic conditions. Although the trees are not active in December, the contribution of trees is expected to be higher than non-treed regions even when trees are not active, as was observed at D3 above. Rates determined at PPT D4 December are slightly higher than rates determined at D3 December; however, variations between the two tests could be attributed to the lower confidence placed in the D4 December PPT and future tests must validate whether this trend is indeed occurring.

7.2 First Order Results

The methods used to determine first order rates agree in all instances except for one where more confidence is given to the rates determined with the method of Haggerty et al. (1998). Results show that seasonal variation occurs at PPT well D3, which supports trends observed in zero order rate calculations, where phytoremediation effects were observed to increase during warmer months when trees are more active (Figure 23). First order rate comparison of PPTs S3 February with S5 February is not possible due to the BTC crossing found in PPT S3 February and consequently future tests should address comparisons between these treed and non-treed regions to determine the peak enhancement factor associated with phytoremediation-enhanced degradation.

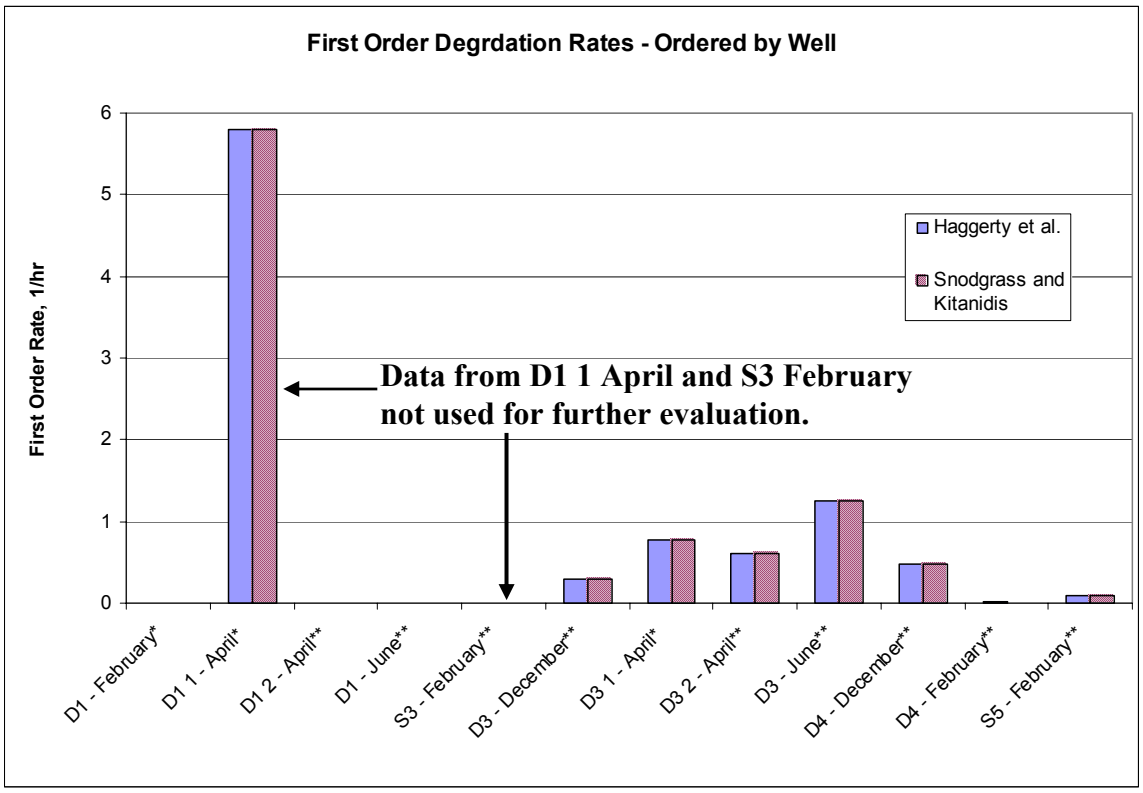

Figure 23: First Order Degradation Rates – Ordered by Chronological Well
*** = Option 1 – Bromide, DO Injected**
**** = Option 2 – Bromide, DO, Naphthalene Injected**

Neither first order method was able to detect first order decay at the control wells, when the non-characteristic D1 1 April is excluded. These results further support that the control wells did indeed function as good controls, TOC oxygen uptake is insignificant, and naphthalene addition in option 2 does not alter test results, as explained in 5.5

General Trends in Push-pull Test Data. Anaerobic wells, introduced to an aerobic injection solution, does not contribute to noticeable TOC oxygen uptake, which is supported by the low first order rate found at D4 February, 0.0024 1/hr. Adjusting observed rates to remove the contribution of the potential overestimation of 0.0024 L/hr, which involves TOC degradation rather than naphthalene degradation is unnecessary since 0.0024 L/hr falls within the 95% confidence interval for all tests (Equation 13A in Appendix A).

7.3 Qualitative Confidence Ratings

Qualitative levels of confidence were applied to PPT results to aid in deciphering overall test conclusions. Low confidence was given to two PPTs; S3 February, exhibited BTC crossing, whereas another PPT, D1 1 April, exhibited minor BTC crossing, but more importantly occurred during a major rain event, consequently preventing direct comparison to other tests (Appendix C). As a result, both of these PPTs are excluded from further comparison.

7.4 Removing Low Confidence Methods and Tests

Low confidence was given to two PPT results as well as to the zero order method of Istok et al. (1997) and the first order method of Snodgrass and Kitanidis (1998). Removing the low confidence tests results and methods clarifies observed trends. Figure 24 and Table 7 display the zero (Fig. 24a) and first (Fig. 24b) after removing the low confidence PPTs as well as the less satisfactory zero order method of Istok et al. (1997) and first order method of Snodgrass and Kitanidis (1998). As discussed previously, control well tests were unable to detect degradation when option 1 was employed. The lowest zero order rates were observed at control well tests using option 2 (naphthalene injected). First order degradation for option 2 control well tests did not detect degradation. Figures 24 and 25 clearly indicate that PPTs D3 1 April and D3 2 April, using options 1 and 2, respectively, produced nearly identical zero and first order rates, thus validating that options 1 (without injected naphthalene) and 2 (with injected naphthalene) can be directly compared. The highest rates were observed at D3, the best indicator for the influence of phytoremediation. Figure 25 illustrates the observed

seasonal variation at D3; zero order (Fig. 25a) and first order (Fig. 25b) rates increased by a factor of three and four, respectively, from winter to summer. Figure 25 also shows that zero and first order winter rates at treed regions were greater by a factor of at least 2.5 when compared to non-treed regions.

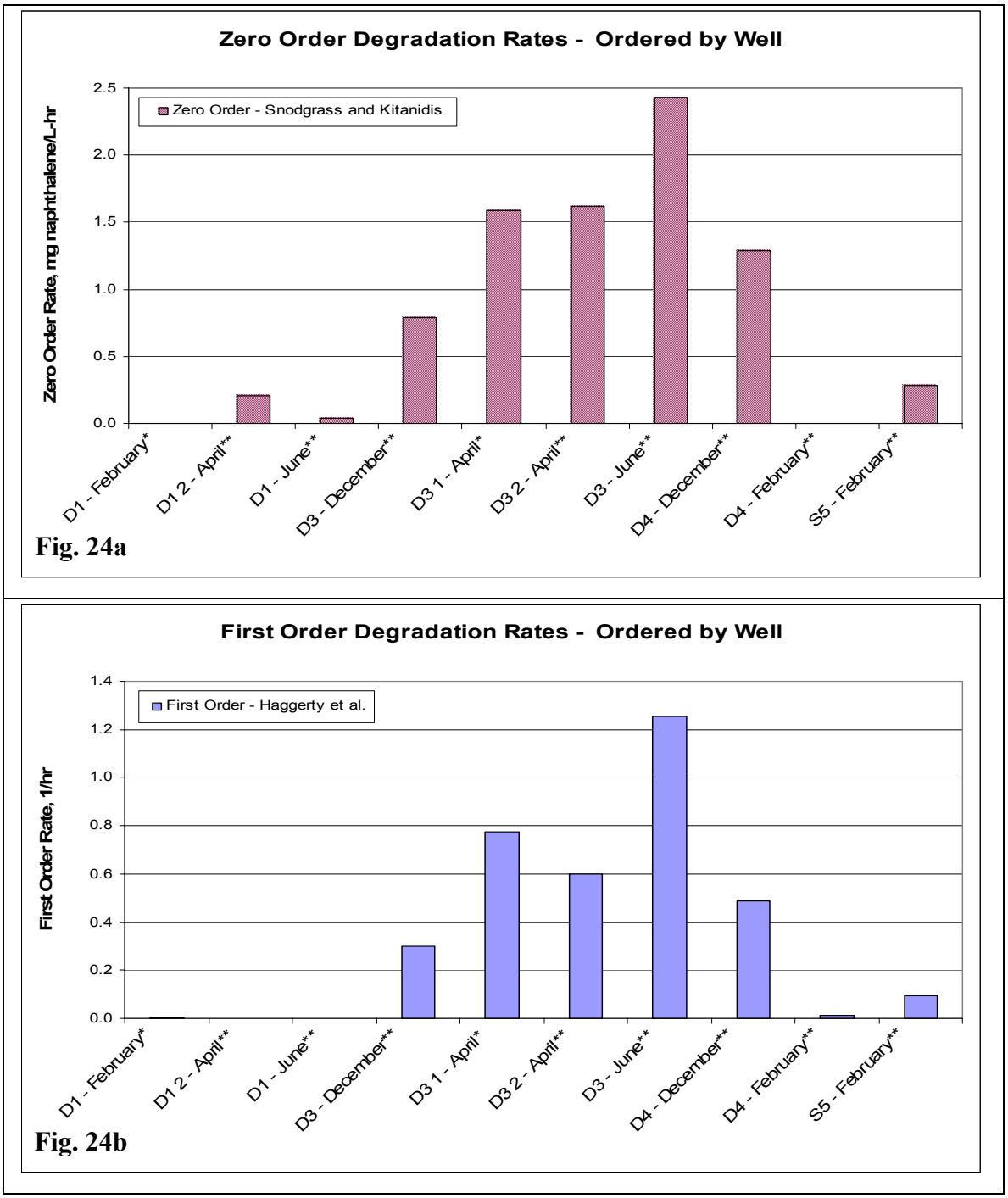

Figure 24: Zero and First Order Degradation Rates
*** = Option 1 – Bromide, DO Injected**
**** = Option 2 – Bromide, DO, Naphthalene Injected**

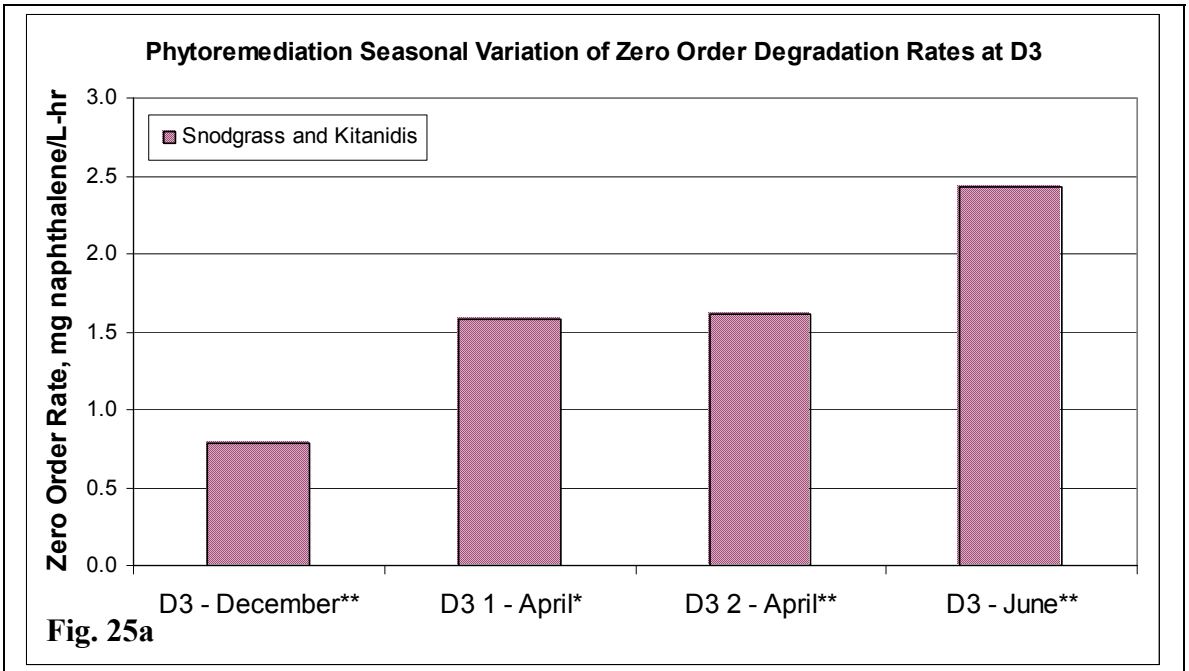

Fig. 25a

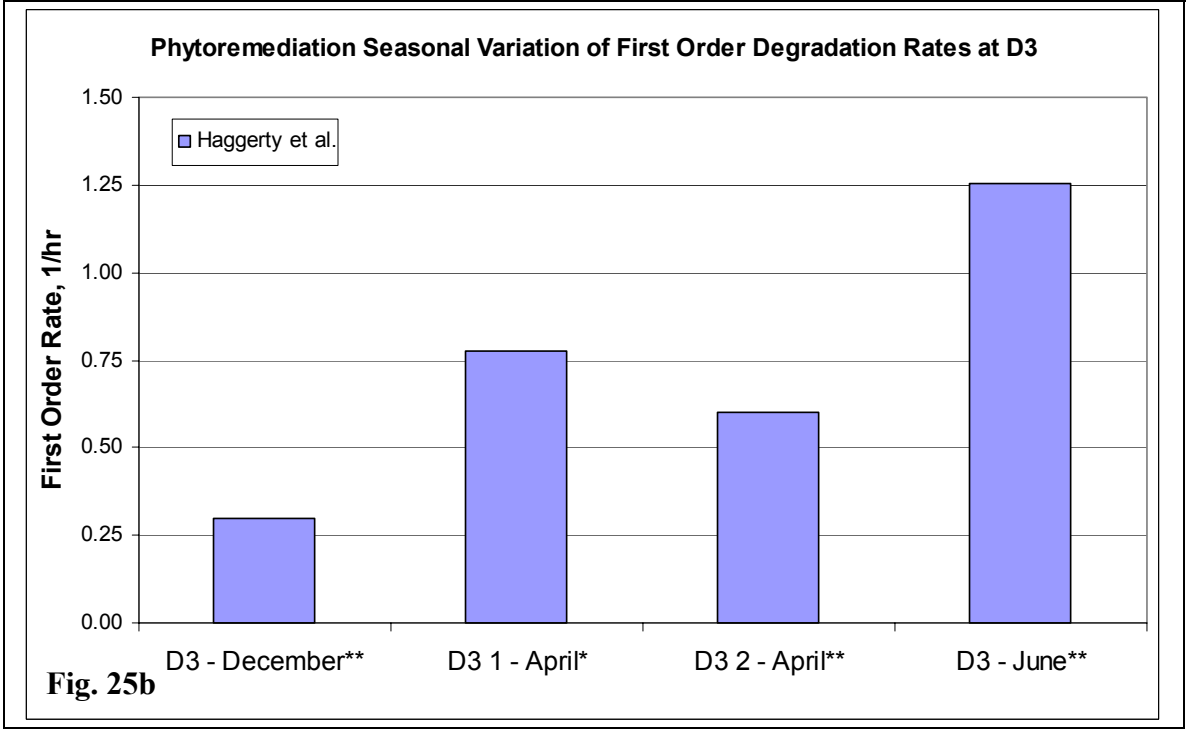

Fig. 25b

Figure 25: Phytoremediation Seasonal Variation of Zero and First Order Degradation Rates

*** = Option 1 – Bromide, DO Injected**

**** = Option 2 – Bromide, DO, Naphthalene Injected**

Table 7: Zero and First Order Degradation Rates

Monitoring Well - Time		Br	DO	R^2 Values
*D3 - December***	Percent Recovery	87.76%	65.68%	
	Snodgrass and Kitanidis (1998) Zero Order Rate, $mg_{naphthalene}/L\text{-}hr$		0.7863	0.9928
	Haggerty et al. (1998) First Order Rate, 1/hr		0.3000	0.9273
*D4 - December***	Percent Recovery	94.61%	65.90%	
	Snodgrass and Kitanidis (1998) Zero Order Rate, $mg_{naphthalene}/L\text{-}hr$		1.2916	0.9750
	Haggerty et al. (1998) First Order Rate, 1/hr		0.4860	0.9871
*D1 - February**	Percent Recovery	74.95%	71.96%	
	Snodgrass and Kitanidis (1998) Zero Order Rate, $mg_{naphthalene}/L\text{-}hr$		0.0000	0.9161
	Haggerty et al. (1998) First Order Rate, 1/hr		0.0024	0.0098
*D4 - February***	Percent Recovery	94.51%	87.79%	
	Snodgrass and Kitanidis (1998) Zero Order Rate, $mg_{naphthalene}/L\text{-}hr$		0.0030	0.0147
	Haggerty et al. (1998) First Order Rate, 1/hr		0.0120	0.1938
*S5 - February***	Percent Recovery	99.27%	82.45%	
	Snodgrass and Kitanidis (1998) Zero Order Rate, $mg_{naphthalene}/L\text{-}hr$		0.2840	0.9444
	Haggerty et al. (1998) First Order Rate, 1/hr		0.0960	0.8653
*D1 2 - April***	Percent Recovery	66.44%	113.83%	
	Snodgrass and Kitanidis (1998) Zero Order Rate, $mg_{naphthalene}/L\text{-}hr$		0.2033	0.9951
	Haggerty et al. (1998) First Order Rate, 1/hr		Positive slope - Rate ~ 0.0	Not evaluated
*D3 1 - April**	Percent Recovery	96.02%	53.92%	
	Snodgrass and Kitanidis (1998) Zero Order Rate, $mg_{naphthalene}/L\text{-}hr$		1.5846	0.9411
	Haggerty et al. (1998) First Order Rate, 1/hr		0.7740	0.8123
*D3 2 - April***	Percent Recovery	101.24%	62.68%	
	Snodgrass and Kitanidis (1998) Zero Order Rate, $mg_{naphthalene}/L\text{-}hr$		1.6174	1.0000
	Haggerty et al. (1998) First Order Rate, 1/hr		0.6000	0.7309
*D1 - June***	Percent Recovery	91.13%	88.00%	
	Snodgrass and Kitanidis (1998) Zero Order Rate, $mg_{naphthalene}/L\text{-}hr$		0.0359	0.0750
	Haggerty et al. (1998) First Order Rate, 1/hr		0.0000	0.1605
*D3 - June***	Percent Recovery	91.73%	45.79%	
	Snodgrass and Kitanidis (1998) Zero Order Rate, $mg_{naphthalene}/L\text{-}hr$		2.4277	0.9810
	Haggerty et al. (1998) First Order Rate, 1/hr		1.2540	0.7766

*** = Option 1 – Bromide, DO Injected**
**** = Option 2 – Bromide, DO, Naphthalene Injected**

7.5 Comparison of Zero and First Order Rates

Historically, bioremediation rates are typically presumed to exhibit first order rate kinetics, but little effort has been undertaken to evaluate whether first order rate kinetics is always occurring. Comparison of the zero order rate method of Snodgrass and

Kitanidis (1998) with the first order method of Haggerty et al. (1998) enables evaluation of whether first order kinetics is always occurring. When plotted data, employing the method of Haggerty et al. (1998), exhibits a straight line, first order kinetics is occurring. When plotted first order data does not exhibit a straight line, zero order kinetics could be occurring, which is confirmed when plotted zero order data, using the method of Snodgrass and Kitanidis (1998), exhibits a straight line.

Evaluation of all the first order graphs using the method of Haggerty et al. (1998) shows that linear portions of plotted data existed in all but three of the PPTs and to a lesser extent at a fourth test, demonstrating that first order kinetics predominated site degradation characteristics. The three tests that did not exhibit a clear straight line of plotted first order data were D3 1 April, D3 2 April, and D3 June (Figure 26). The fourth test, D1 June, exhibited BTC crossing and resulted in a slightly sinusoidal shape to plotted data. Relative differences between the bromide and DO BTCs are small during D1 June, as explained above in 6.1 Breakthrough Curve Crossing and consequently it can be expected that there will be little to no degradation occurring. The plotted first order data, even though slightly sinusoidal and having a positively sloped, best-fit line, produces a rate that is very close to zero. Thus, it can be deduced that the first order rate for D1 June is zero. All first order plots, using the method of Haggerty et al. (1998), can be found in Appendix C.

Figure 26 illustrates the three PPTs, D3 1 April (Fig. 26a), D3 2 April (Fig. 26b), and D3 June (Fig. 26c), which did not exhibit a straight line when first order data was plotted. The first order R^2 value of PPTs D3 1 April, D3 2 April, and D3 June were 0.8123, 0.777, and 0.8326, respectively. The non-linearity of plotted data from PPT D3 2 April is partly due to the slightly irregular BTC. Since the irregular BTC only affects the first five plotted data points and non-linearity continues past this time (time 40 minutes), it is likely that first order kinetics did not exist at this test. The other non-linear first order PPTs exhibited normal BTCs and therefore provide no indication to question results. Therefore, results from the three non-linear first order PPTs, D3 1 April, D3 2 April, and D3 June, suggest that first order kinetics are not occurring at these tests. A closer examination of the plotted zero order data will indicate whether zero order kinetics predominates instead.

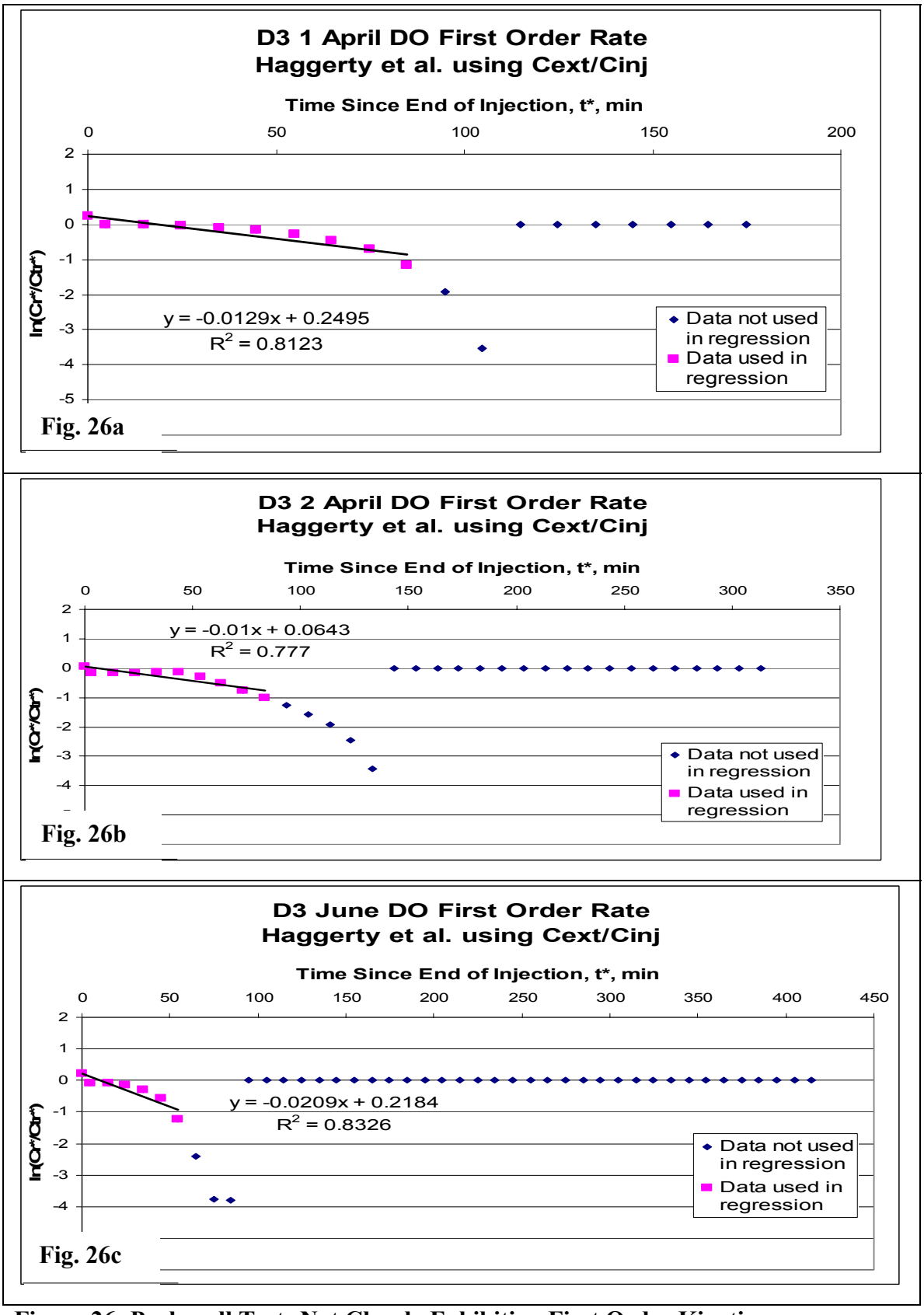

Figure 26: Push-pull Tests Not Clearly Exhibiting First Order Kinetics

Plotted zero order data for the three non-linear first order PPTs D3 1 April (Fig. 27a), D3 2 April (Fig. 27b), and D3 June (Fig. 27c) showed improved correlation. For the three tests, the R^2 value for plotted zero order kinetics was higher for PPTs D3 1 April, D3 2 April, and D3 June when compared to plotted first order data, resulting in zero order R^2 values of 0.9411, 1.0, and 0.981, respectively. As a result, it can be concluded that all PPTs except for D3 1 April, D3 2 April, and D3 June exhibited first order kinetics and PPTs D3 1 April, D3 2 April, and D3 June are likely undergoing zero order kinetics. D3 is highly contaminated and since both substrate and oxygen are unlimited, observation of zero order kinetics agrees with the Monod kinetic model (Grady et al., 1999). Figure 28 and Table 8 illustrate the first order rates at all tests except for zero order rates at PPTs D3 1 April, D3 2 April, and D3 June. Only the PPTs for the higher confidence zero and first order methods of Snodgrass and Kitanidis (1998) and Haggerty et al. (1998), respectively, are reported.

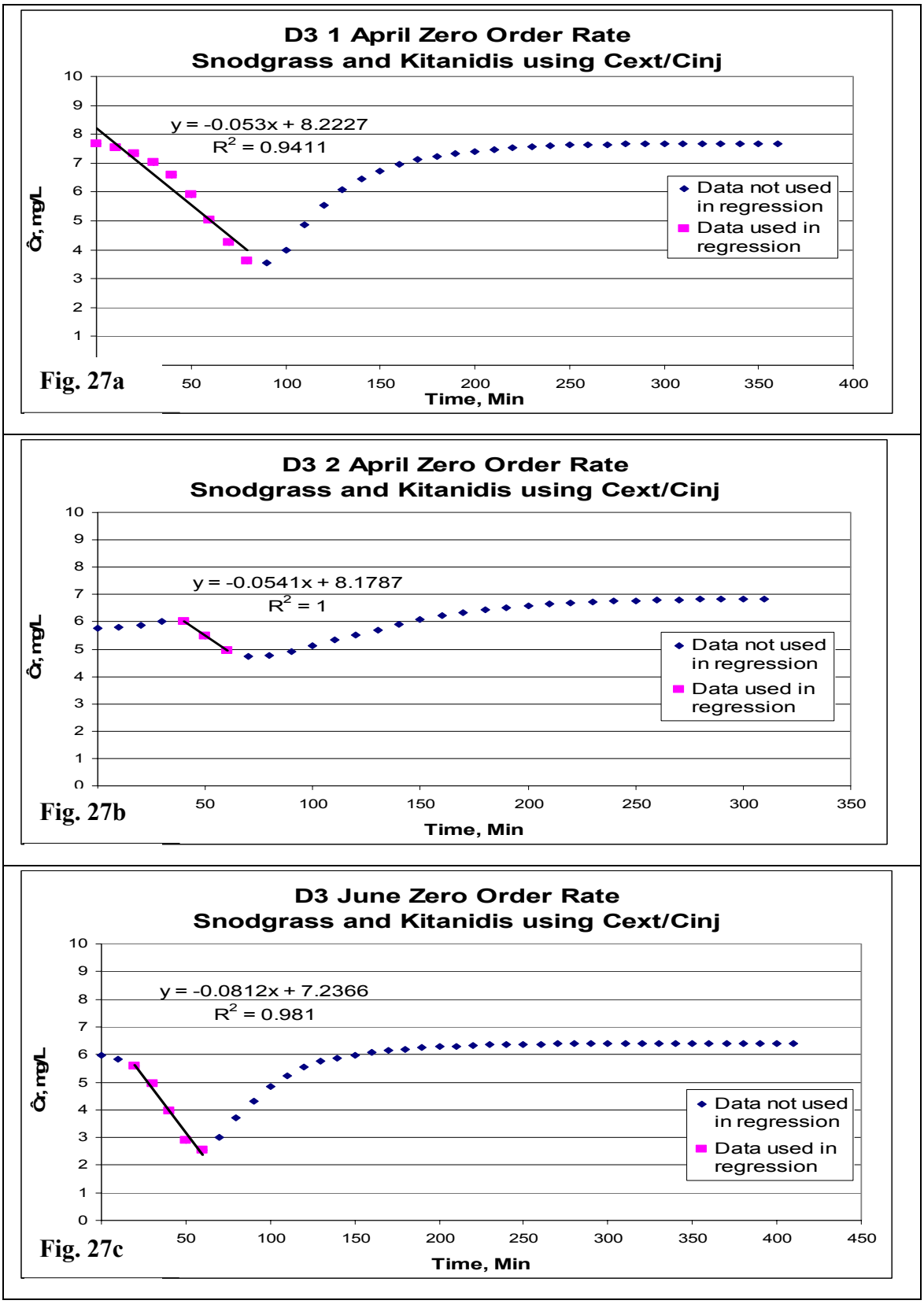

Figure 27: Push-pull Tests That Exhibited Zero Order Kinetics

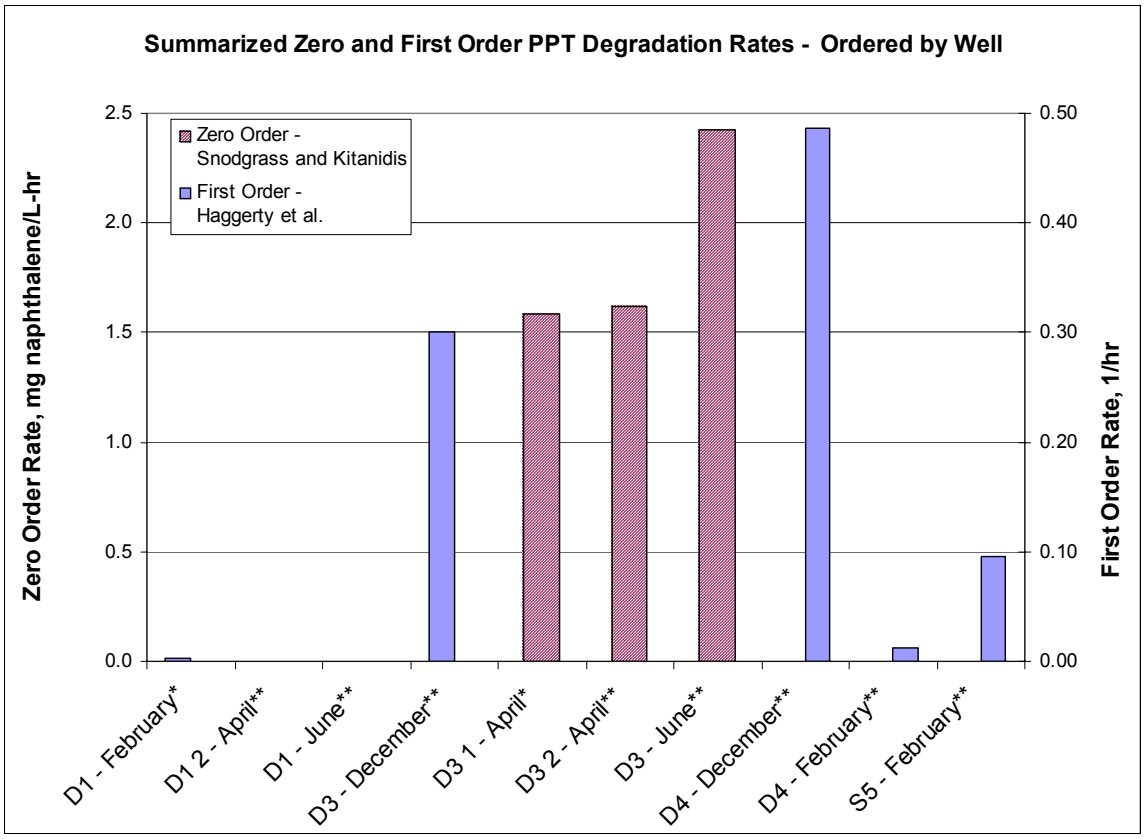

Figure 28: Summarized Zero and First Order Push-pull Test Degradation Rates

*** = Option 1 – Bromide, DO Injected**

**** = Option 2 – Bromide, DO, Naphthalene Injected**

Table 8: Summarized Zero and First Order Push-pull Test Results

Monitoring Well - Time		Br	DO	R^2 Values
*D3 - December***	Percent Recovery	87.76%	65.68%	
	Haggerty et al. (1998) First Order Rate, 1/hr		0.3000	0.9273
*D4 - December***	Percent Recovery	94.61%	65.90%	
	Haggerty et al. (1998) First Order Rate, 1/hr		0.4860	0.9871
*D1 - February**	Percent Recovery	74.95%	71.96%	
	Haggerty et al. (1998) First Order Rate, 1/hr		0.0024	0.0098
*D4 - February***	Percent Recovery	94.51%	87.79%	
	Haggerty et al. (1998) First Order Rate, 1/hr		0.0120	0.1938
*S5 - February***	Percent Recovery	99.27%	82.45%	
	Haggerty et al. (1998) First Order Rate, 1/hr		0.0960	0.8653
*D1 2 - April***	Percent Recovery	66.44%	113.83%	
	Haggerty et al. (1998) First Order Rate, 1/hr		Positive slope - No rate evaluated	Not evaluated
*D3 1 - April**	Percent Recovery	96.02%	53.92%	
	Snodgrass and Kitanidis (1998) Zero Order Rate, $mg_{naphthalene}/L$-hr		1.5846	0.9411
*D3 2 - April***	Percent Recovery	101.24%	62.68%	
	Snodgrass and Kitanidis (1998) Zero Order Rate, $mg_{naphthalene}/L$-hr		1.6174	1.0000
*D1 - June***	Percent Recovery	91.13%	88.00%	
	Haggerty et al. (1998) First Order Rate, 1/hr		0.0000	0.1605
*D3 - June***	Percent Recovery	91.73%	45.79%	
	Snodgrass and Kitanidis (1998) Zero Order Rate, $mg_{naphthalene}/L$-hr		2.4277	0.9810

*** = Option 1 – Bromide, DO Injected**
**** = Option 2 – Bromide, DO, Naphthalene Injected**

8.0 RECOMMENDATIONS FOR FUTURE PUSH-PULL TESTS

A multitude of approaches were taken to develop a PPT method at the Oneida site and in the laboratory before the current method, which monitors TEA uptake and production, was adopted. Each approach encountered various obstacles; however, each variation provided critical insights that lead to the development of the adopted Oneida PPT method. Initially, methods addressed overcoming drought and low groundwater tables, monitoring naphthalene with the non-conservative, sorbing tracer 2,4,5-trichlorophenol (2,4,5-TCP), and evaluating native anaerobic solutes to determine anaerobic degradation rates.

8.1 Push-pull Tests During Drought and Summer Conditions

The high evapotranspiration rate of poplar trees limits applicability of PPTs during drought and summer conditions. Initial proposed PPTs were unable to be performed due to low levels of groundwater within the monitoring well, particularly in the summer. Annually, the groundwater table rises to a maximum during the winter months and decreases to a minimum during the summer. Fluctuations in the GWT can be attributed to the combined influence of annual weather cycles, particularly hot, dry summers, and high poplar tree evapotranspiration rates that peak during summer months. As a result, the localized GWT can drop below the depth of the deepest PPT well (9.29 feet from the surface). At each location, PPT wells were placed at the deepest possible depth above the free-phase DNAPL, while assuring that the well screens coincided with porous sand lenses. Attempts were made to artificially raise the localized GWT through an overnight clean water injection of ~800 L in a phytoremediated area, but only a very insignificant change of two inches was observed in the localized GWT. As discussed in Appendix A, it is recommended that the GWT is at least one foot above the bottom of the PPT well, but ideally 1.5-2 feet above the well bottom. This ensures that PPTs can be compared and rate determination is not influenced by the cone of depression that occurs during the extraction phase. Initial method development PPTs (data not shown) were planned several days after rain events to maximize the effects of an increased GWT, but to prevent variable flow and site conditions due to precipitation. Future tests at the Oneida site may have to employ a similar strategy, especially to obtain peak phytoremediation enhancement factors that occur during the summer months of July and August.

8.2 Push-pull Tests Monitoring Naphthalene Uptake

Initial method development PPTs (data not shown) attempted to monitor degradation from carbon uptake rather than through TEA utilization. Naphthalene was injected along with a conservative bromide tracer and a non-reactive, sorbing tracer 2,4,5-TCP. 2,4,5-TCP has a similar octanol-water partitioning coefficient, K_{ow}, when compared to naphthalene and served as a means to assess sorption during the test since 2,4,5-TCP is extremely recalcitrant. The non-reactive 2,4,5-TCP tracer is subject to

similar sorption/desorption processes as naphthalene due to its K_{ow}. Multiple push-pull tests were performed, but variation in the resulting breakthrough curves caused development of an alternative method that is more applicable to all contaminated sites. Inconsistencies between naphthalene and TCP BTCs provoked an alternative method to be considered, which lead to the adoption of PPTs that monitor TEAs to assess degradation.

Naphthalene was monitored at all PPTs to gain an improved understanding of the response of sorbing compounds during PPTs. Plotted naphthalene data sometimes returned typical BTC response, but often naphthalene concentrations would either jump about sporadically throughout the test or the concentration would decrease with time and then increase in concentration at late times, potentially indicating a sorption/desorption period. It is suspected that sorption properties of naphthalene is highly irregular in the heterogeneous Oneida aquifer and consequently efforts to monitor naphthalene uptake will produce ambiguous results unless an alternative to the method explained above is employed.

8.3 Anaerobic Assessment

To date, push-pull tests have focused upon the determination of aerobic degradation rates; however, anaerobic electron acceptors, namely nitrate and sulfate, as well as degradation products of electron acceptors, namely ferrous iron and sulfide, were monitored throughout all Oneida PPTs. Nitrate and sulfide levels were not detected during any PPT. Although it is likely that sulfide was being produced during anaerobic conditions, sulfide was most likely not detectable due to immediate precipitation with native iron species. As mentioned previously, if ferric iron and sulfate were utilized as electron acceptors, ferrous iron and sulfide concentrations would exceed background concentrations, while sulfate concentrations would be less than background concentrations. The extremely low solubility of ferric iron prevents monitoring of ferric iron. Ferrous iron and sulfate concentrations vary throughout the site and are highest in the anaerobic center of the DNAPL.

Significant background levels of ferrous iron and sulfate exist at the Oneida site. Background ferrous iron concentrations were found to range from 5 to 35 mg/L in

contaminated wells S3, D3, D4, and S5. Background ferrous iron was below detection limits at the control well, D1. Background sulfate concentrations were found to be as high as 1000 mg/L in the DNAPL center, but typically ranged from 300 to 600 mg/L during PPTs at S3, D3, D4, and S5. Background sulfate iron concentrations were significantly lower at the control well, typically less than 100 mg/L.

All PPTs attempted to monitor native anaerobic TEAs and their degradation products, without spiking injection solutions with additional anaerobic TEAs. Since all PPTs performed involved aerobic injection, PPTs monitored solutes beyond the time at which all DO was consumed when anaerobic conditions prevailed. Since ferrous iron was the only anaerobic solute that was monitored in-situ, tests continued until ferrous iron stabilized at a steady concentration. Ferrous iron served as the only means to assess when other TEAs, that were not monitored in-situ, stabilized to steady concentrations.

The high background levels of ferrous iron and sulfate complicate observing small changes in concentration that is typical with slower anaerobic degradation during the short duration of push-pull tests. Rates were difficult to discern during anaerobic processes since degradation was obscured by incorporation of high concentrations found in the native groundwater. Measurement error associated with measuring high concentrations, coupled with the inherent inaccuracies of Hach Kit™ tests, further complicate analysis since large dilutions were necessary for solute samples to fall within the standard curve. Often a drop in concentration of TEAs (or rise in concentration for TEA degradation products) was observed for short time periods during PPTs. The large volume of native groundwater in the PPT wells quickly obscured these observed trends; although degradation could be observed adjacent to the well for small time intervals, native groundwater quickly predominates the extraction solution, causing observed trends to only be observed for short time intervals. This is due to the fact that background concentrations were significant and small changes in concentration were difficult to discern, especially after undergoing large dilutions. Furthermore, since anaerobic solutes were not added to the injection solution, typical BTC analysis is complicated, and is explained in greater detail in 8.4.1 Future Oneida Push-pull Test Method. The drop (or rise) in concentration typically occurred at only a few data points, making rate calculations unfeasible, but suggesting that it is likely that sulfate reduction or

ferrogenesis was occurring. Single data point drops in sulfate concentration were found to exist at PPTs S3 February, S5 February, and D4 February, indicating sulfate utilization was likely. Figure 29 illustrates the observed temporary decrease in sulfate concentration at PPT S3 February.

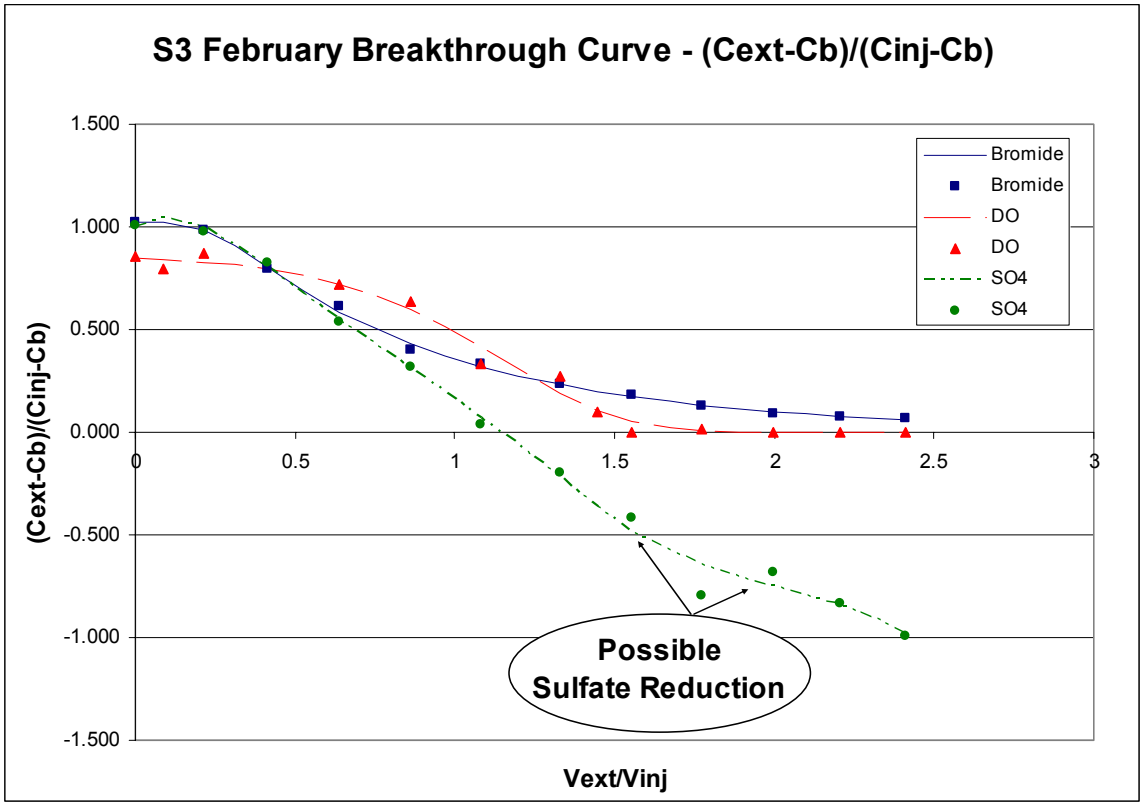

Figure 29: Example of Possible Sulfate Reduction

PPT D4 February observed a temporary decrease in sulfate concentrations over a moderate four data point range; however, the sulfate levels never returned to background levels (Figure 30). A zero order rate from these data could not be calculated since a positive slope is produced (when a negative slope should result for TEA consumption). It should also be noted that DO concentrations in the bulk phase were slightly above zero mg/L during this time interval, causing doubt in the observed trend since redox conditions were slightly aerobic. Calculation of a first order rate is not possible since natural log transformation (Equation 12) of the negative, normalized concentrations (i.e. when the sulfate concentration exceeds background) is not feasible.

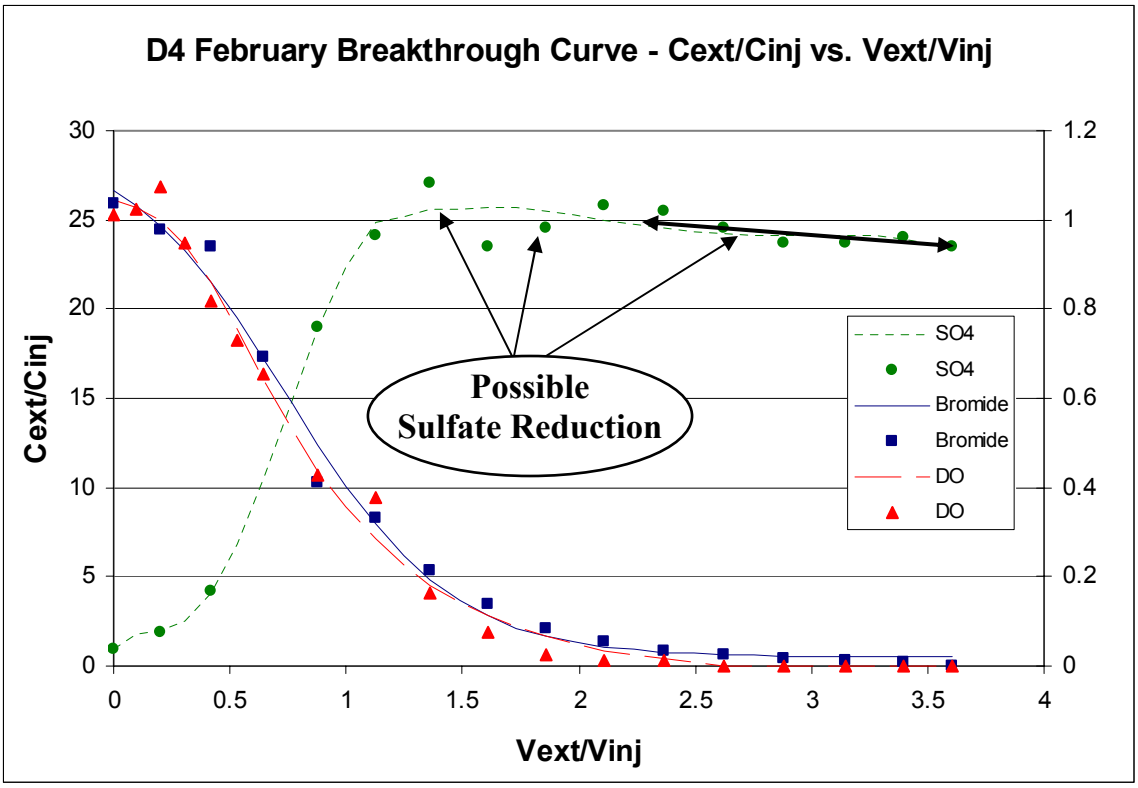

Figure 30: Another Example of Possible Sulfate Reduction

PPTs D4 February, D3 1 April, D3 2 April observed a temporary increase in iron concentrations throughout a longer time interval. Ferrous iron serves as a TEA degradation product and consequently ferrous iron present at levels higher than background concentrations demonstrates ferrogenic degradation has occurred. Fig. 31a illustrates a BTC for PPT D3 1 April where ferrous iron was measured at concentrations greater than background levels, C_b. The trend is most easily observed from a C_{ext} BTC curve (Fig. 31a); however, rate analysis employs normalization according to Equation 3 $[(C_{ext}-C_b)/(C_{inj}-C_b)]$ (Fig. 31b). C_{ext} is employed since normalization according to C_{ext}/C_{inj} cannot be computed since iron was not detected in the injection solution (i.e. C_{inj} = 0 mg/L) and normalization according to $(C_{ext}-C_b)/(C_{inj}-C_b)$ obscures the location of C_b. Both DO and iron are plotted on the secondary axis. DO is not properly scaled when plotted in this manner, but was included only to note when all DO was consumed, causing anaerobic conditions to prevail. Using the method of Snodgrass and Kitanidis (1998), zero order transformed iron concentrations were plotted and results are shown in Figure 31b. Only ferrous iron concentrations greater than background that exhibited a

positively sloped line were used in regression analysis. Positive slopes should result since ferrous iron is a TEA degradation product and concentrations should exceed background during ferrogenic processes. A zero order rate of 0.03 mg_{iron}/L-hr resulted from the regression analysis, producing a positively sloped regression line well after all DO was consumed. Again, first order rate analysis was not feasible.

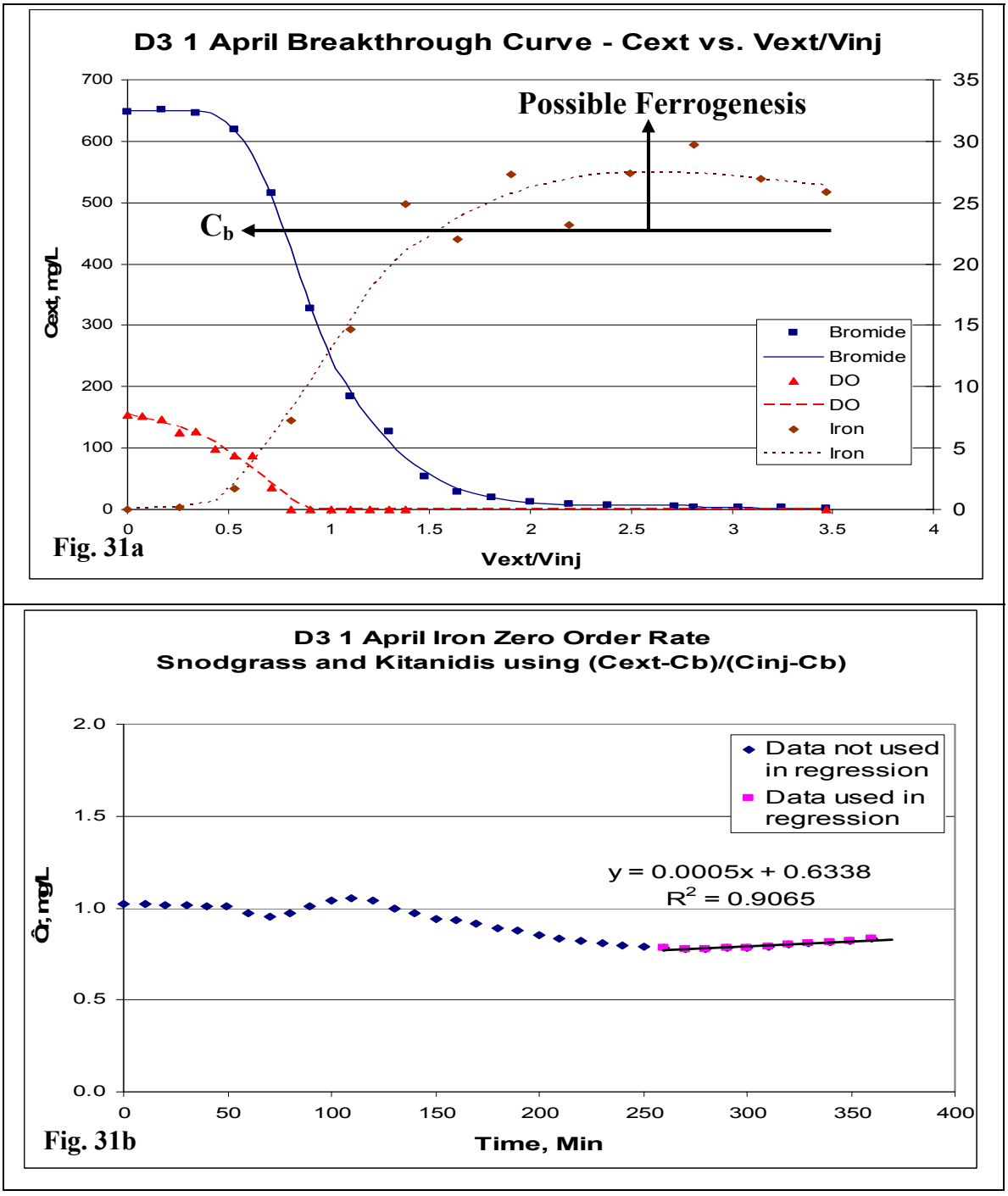

Figure 31: Example of Possible Ferrogenesis

A similar trend occurred at the D3 2 April PPT. The resulting C_{ext} vs. V_{ext}/V_{inj} BTC is shown in Fig. 32a and the zero order regression plot is shown in Fig. 32b. Again, DO is not properly scaled and rates were evaluated using the normalization from Equation 3. Results show that a positive slope was found, well after all the DO was consumed. A zero rate of 0.0042 mg_{iron}/L-hr resulted from the regression analysis. Again, a first order rate analysis was not possible.

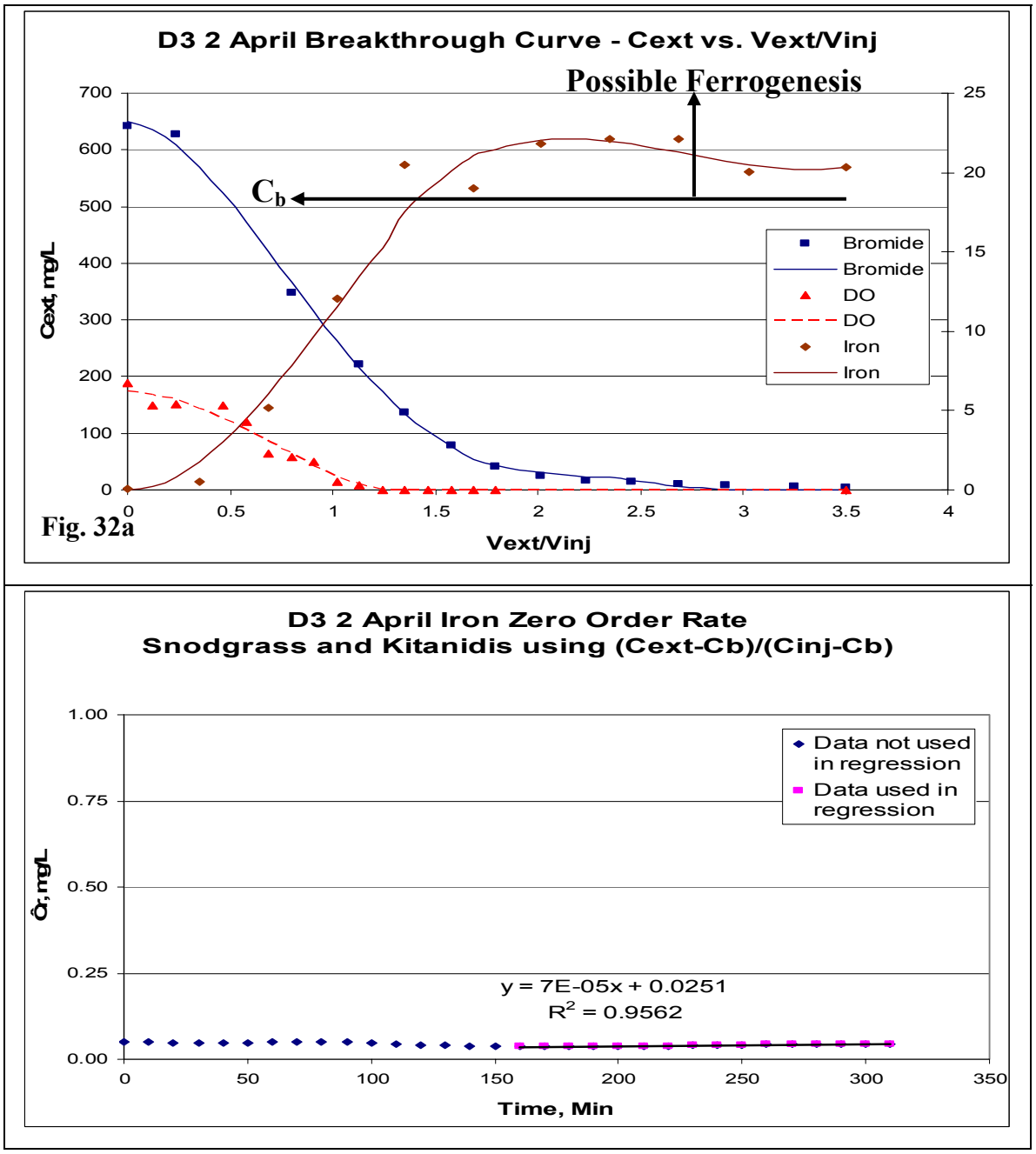

Figure 32: Another Example of Possible Ferrogenesis

8.3.1 Anaerobic Analysis Conclusions

Monitoring of native anaerobic TEAs resulted in observation of sulfate reduction and ferrogenesis, but typically during very short time intervals. High background concentrations, coupled with experimental error, obscured rate analysis. Degradation rate determination was only possible for two PPTs and was limited to only ferrogenic rates. PPTs D3 1 April and D3 2 April resulted in ferrogenic zero order rates of 0.03 and 0.0042 mg_{iron}/L-hr, respectively. Since large dilutions were necessary for solute analysis, large amounts of experimental error occurred as extraction concentrations approached the high background levels. Large amounts of measured data variability were observed, as evident in Figures 29-32. As a result, observed trends could possibly be due to experimental error. Also, extraction concentrations often did not return to background concentrations, which further supports that experimental error could be the cause of observed trends. Figure 33 shows an example where ferrous iron, although in excess of background levels, exhibited large measured concentration variability. Although anaerobic processes were observed for small time intervals, results could be obscured by experimental error, suggesting improvements of the current method are necessary.

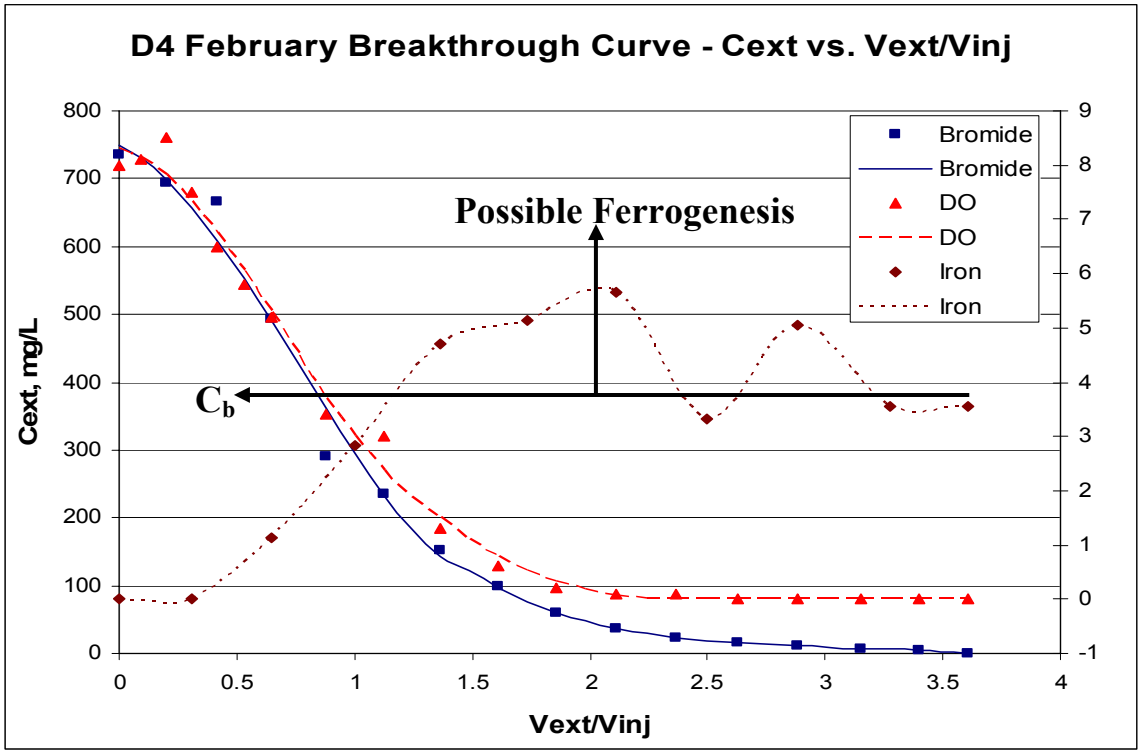

Figure 33: Example of Large Uncertainty in Measured Iron Concentrations

8.4 Future Suggestions

Unable to calculate anaerobic degradation rates for all but two tests forces future PPTs to consider a modified method. High background concentrations obscure trends and lead to increased experimental error. Monitoring of native anaerobic TEAs, rather than injected solutes, has shown that anaerobic degradation can be observed and rate evaluation is typically not feasible. Future tests should not attempt to combine aerobic tests with anaerobic tests. Instead, anaerobic tests should monitor spiked injected anaerobic solutes to enable most of the mass removal to be observed before extraction concentrations approach high background levels. This method will reduce experimental error since dilutions will not be nearly as large during the initial part of the PPT. Furthermore, monitoring spiked solute injection enables a significant concentration to be degraded at early extraction times, while simultaneously simplifying BTC analysis. Since injection concentrations, C_{inj}, would be significant, typical normalization, as outlined in Equations 2 and 3, can be applied to BTC analysis rather than being forced to plot C_{ext} vs. V_{ext}/V_{inj} as was done in all analysis of iron.

8.4.1 Future Oneida Push-pull Test Method

Employing separate anaerobic and aerobic PPTs has many advantages. Aerobic PPTs can be performed during a considerably smaller time interval, since the test only needs to continue until DO returns to background levels. Also, aerobic PPTs can use a lower concentration of bromide to evaluate rates, thus minimizing potential contamination for future tests. Bromide concentrations should be lowered to ensure that at the end of the aerobic PPT, nearly all of the bromide is recovered, which again prevents future contamination problems. Istok et al. (1997), Haggerty et al. (1998), and Schroth et al. (1998) have all successfully used 100 mg/L bromide for injection solutions; however, an incremental decrease in bromide concentration from the current 750 mg/L is recommended to ensure that bromide will be present while DO is being consumed.

Certain parameters of aerobic tests must be modified to perform anaerobic PPTs. Anaerobic PPTs should use a diffuse ‘aerator’ attached to a nitrogen gas feed that strips DO from the injection solution, replacing it with inert nitrogen gas, as detailed in Schroth et al. (1998). In addition, anaerobic decay is typically a much slower process than

aerobic decay, particularly for the degradation of PAHs. As a result, a lag phase should be utilized to monitor anaerobic processes over a longer time period. Lag-phases are also typically complimented by the injection of a much larger volume (~1000 L) of injection solution to ensure a significant proportion of injected solutes remains near the injection well and are not carried away downstream. Larger injection volumes also permit an increased number of sampling periods over a longer time interval. The exact injection volume employed depends upon the desired duration of the PPT and this volume can be calculated. For example, 1100 L must be injected for an anaerobic PPT duration of 1 week. 1100 L maintains the one foot radius of tested aquifer material, detailed in 3.5 In-situ Test and Constituent Analysis, while ensuring test solutes are not carried downstream [Required radius for appropriate injection volume = radius affected by the Oneida groundwater velocity of 7.5 inches/day over 1 week + one foot radius of tested aquifer material + radius of sand-pack = 7 days * 7.5 inches/day * 1 ft./12 in. + 1 ft + 0.14375 ft = 5.52 ft; Required injection volume = required radius^2 * π * 1 ft. of well-casing * porosity = (5.52 ft)^2 * π * 1 ft * 0.4 * 1 ft^3/28.317 L = 1083.8 L]. Additional adjustments must be made to address the high background concentrations of anaerobic TEAs at the Oneida site.

Anaerobic tests at the Oneida site are limited by high background concentrations and possibly warrant a different approach. Anaerobic tests have been successful when injecting anaerobic solutes ranging from 25-50 mg/L NO_3^- – N (Schroth et al., 1998; Reusser et al., 2002; Reinhard et al., 1997) and 80-100 mg/L SO_4 (Reusser et al., 2002; Kleikemper et al., 2002; Schroth et al., 2001). Although nitrate is typically not present in the native groundwater at the Oneida site, denitrification processes could be occurring at a steady-state equilibrium where denitrifiers immediately consume any nitrate that is present in the native groundwater. As a result, although nitrate is typically non-detectable in native groundwater, denitrification processes could be significant and therefore should be addressed. As discussed in a previous section, little success has resulted from monitoring ferrogenic processes since the produced ferrous iron readily precipitates with native solutes, particularly sulfide. Similar complications can result when sulfate is monitored.

Sulfate consumption or sulfide product formation is complicated by abiotic transformations, dissolution/precipitation of gypsum, or by sulfide precipitation as iron sulfide (Schroth et al., 2001; Stumm and Morgan, 1996). Sulfate analysis can be improved through application of the method of Schroth et al. (2001), which monitors stable isotopes that are produced during degradation processes. Microbial sulfate reduction typically produces significant isotope fractionation, resulting in an enrichment of ^{34}S in unconsumed sulfate and an enrichment of ^{32}S in produced sulfides (Schroth et al., 2001). Kleikemper et al. (2002) also successfully used stable sulfur isotope analysis to determine isotope enrichment factors to assess sulfate reduction. At the Oneida site, monitoring the preferential fractionation of sulfate can elude sulfate reduction processes and provide reliable degradation rates even when significant background concentrations exist.

Eluding the ferrogenic processes at the Oneida site still presents some complications and the development of new, reliable methods is critical. Since ferric iron is preferentially used as a TEA over sulfate, it is possible that a standard approach (monitoring solely sulfate consumption and not sulfate fractionation) to monitoring sulfate reduction in the presence of ferric iron will result in an overestimation of degradation rates if the contribution of ferrogenesis is not accounted. However, the method of Schroth et al. (2001) can accurately account for sulfate reduction in the presence of ferric iron, since this method monitors preferential, stable sulfur isotope fractionation. Monitoring only ferrous iron can result in an underestimation of degradation rates, since it is likely that a significant quantity of produced ferrous iron will readily precipitate as iron sulfide. Therefore, a combination of approaches described thus far may yield accurate ferrogenic degradation rates.

Coupling the stable sulfur isotope fractionation method of Schroth et al. (2001) with monitoring naphthalene uptake may provide reliable iron degradation rates. A number of possibilities exist to produce a method that accounts for the sorption/desorption processes of naphthalene. In an approach similar to the naphthalene monitoring described in 8.2 Push-pull Tests Monitoring Naphthalene Uptake, naphthalene can be added to the injection solution, along with a non-reactive tracer with a similar K_{ow}. The non-reactive tracer will be subject to similar sorption/desorption

processes as naphthalene due to its K_{ow}. Use of 2,4,5-TCP as a sorbing tracer is not recommended. Not only is 2,4,5-TCP is highly recalcitrant and therefore polluting, it may also be difficult to obtain the appropriate permits for in-situ field application. Alternatives to the highly recalcitrant 2,4,5-TCP sorbing tracer exist, such as the use of sorbing tracer dyes. Borden and Bedient (1987), Wiedemeier et al. (1996), Sabatini and Austin (1991), Davis et al. (1980), Smart and Laidlaw (1977), and Leitao et al. (1996) discuss the multitude of sorbing tracers that can be used as an alternative to 2,4,5-TCP. Selection of the appropriate tracer requires additional tracer tests studies, which can follow the method of Jin et al. (1995, 1997). Additional studies pertaining specifically to in-situ rate assessment that account for sorption of creosote compounds, particularly naphthalene, are discussed in Rugge et al. (1999), Wise and Charbeneau (1994), and Thierrin et al. (1995).

Since naphthalene is already present in significant background concentrations, analysis would be improved by using deuterated naphthalene in the injection solution. When this approach is coupled with the method of Schroth et al. (2001), ferrogenic processes can be discerned even when sulfate reduction is occurring simultaneously. The method of Schroth et al. (2001) enables calculation of the contribution of sulfate reduction. Monitoring of naphthalene or deuterated naphthalene provides the overall degradation. Therefore, if no other anaerobic processes, such as denitrification, are occurring, ferrogenic rates can be calculated by subtracting the fraction of sulfate degradation from the overall degradation.

Given the complexities observed at the Oneida site when monitoring injected naphthalene (8.2 Push-pull Tests Monitoring Naphthalene Uptake), an alternative approach similar to the method of Hageman et al. (2001) could be employed. Hageman et al. (2001) monitored the transformation of TCFE in TCE contaminated groundwater. When TCFE was degraded in the presence of high background concentrations of TCE, fluorine product formation was monitored to detect degradation rates. Similarly, a halogenated naphthalene compound could be injected, producing a non-reactive, non-sorbing degradation product, such as fluorine or chlorine, which can be used to determine in-situ degradation rates, providing the produced degradation product is not present in native groundwater. Selection of the halogenated naphthalene must address typical

naphthalene degradation pathways, to ensure the degradation product is released when degradation occurs. Again, when halogenated naphthalene is coupled with sulfate isotope fractionation studies, iron degradation rates can be calculated. Collectively, application of sulfur stable isotope analysis coupled with one of the aforementioned approaches to determine naphthalene degradation can produce reliable ferrogenic rates.

9.0 PUSH-PULL TEST COMPARISON TO MICROCOSM RATES

Trends observed in microcosm studies, derived from the ten PPT well soils, agree well with observations from Oneida PPTs. Microcosm studies, created and analyzed by Rikke Granum Andersen, used soils from the five shallow wells to create aerobic microcosms, while soils from deep wells were used for anaerobic microcosms. A 10 ml headspace of air ensured sufficient oxygen for aerobic microcosms. Anaerobic microcosms added K_2SO_4 to obtain a concentration of sulfate of 150 mg/l, typical for sulfate concentrations at the Oneida site. Iron was not added to the microcosms since the soil serves as a reservoir for ferric iron. 8 ml of autoclaved deionized water and 3 grams of the relevant soil spiked with a hexane solution containing 250 mg/L naphthalene and 50 mg/l of acenapthylene, acenapthene, flourene, flouranthene, anthracene, pyrene and chrysene (and the hexane was allowed to evaporate off in a fume hood) were added to 20 ml vials with rubber septa crimp caps. This resulted in initial concentrations of naphthalene ranging from 500-700 mg/kg_{soil} and 20-50 mg/kg_{soil} of the other PAHs. Anaerobic microcosms were constructed identically inside a nitrogen-purged anaerobic glove-box. The microcosms were placed on a vortex shaker and then incubated at a constant temperature of 20ºC in the dark on a slow agitating table that mimicked the slow groundwater flowrate at the site. The aerobic microcosms were placed on a vortex shaker once a week to avoid diffusion limitations of oxygen into the water phase. Microcosms were sacrificed in triplicate approximately every second week. Samples were extracted with methylene chloride and analyzed along with external standards on a gas chromatograph with flame ionization detection and DB5-MS fused silica capillary column for PAH analysis. Like PPTs, microcosm monitoring focused on the degradation of naphthalene, the most readily degradable PAH found at the Oneida site.

No attempt was made to convert microcosm rates, calculated as $mg_{naphthalene}/kg_{soil}$-day, to $mg_{naphthalene}/L_{water}$-hr to enable direct comparison with PPT units, since microcosm creation used water greatly in excess of soil saturation. Approximately 7 ml (of the 8 ml) of water lied above the saturated soil and had no direct contact with the water. The excess water used in the microcosms served solely as a means to measure iron and sulfate. Since the large volume of water used for the microcosms differs from saturated in-situ aquifer conditions, rates obtained from the microcosms could not be converted to $mg_{naphthalene}/L_{water}$-hr and directly compared to PPTs. Microcosms, as discussed in 1.0 Introduction, are useful tools to observe general trends, but little confidence is given to the magnitude of the degradation rate since laboratory bias is introduced that varies from true in-situ conditions. An alternative normalization was made to compare microcosm and PPT results.

Aerobic microcosms and PPT results were normalized to enable comparison of trends between the microcosm and PPT degradation rates. Microcosms were normalized by dividing each zero (or first) order rate (R) by the maximum of the zero (or first) order rates (R_{max}). PPTs were normalized similarly, normalizing each averaged well rate (R) with respect to the largest observed PPT rate result (R_{max}). Aerobic PPT rate results for each prospective well pair were averaged (e.g. average the zero order rates of all PPTs performed at wells D3 and S3) and compared to aerobic microcosms obtained from the shallow well. Figure 34 illustrates a comparison of the aerobic PPT and microcosm zero (Fig. 34a) and first (Fig. 34b) order rates using R/R_{max} for all comparisons. Since PPTs were not performed at all of the shallow wells, a direct comparison of all shallow PPTs cannot be made with the aerobic microcosm rates obtained from shallow well soils. It is recommended that future tests observe rates at shallow wells to support generalized conclusions made at each well pair and to enable a more direct comparison with microcosm trends. Rate comparison excluded the anomaly rain event at PPT D1 1 April.

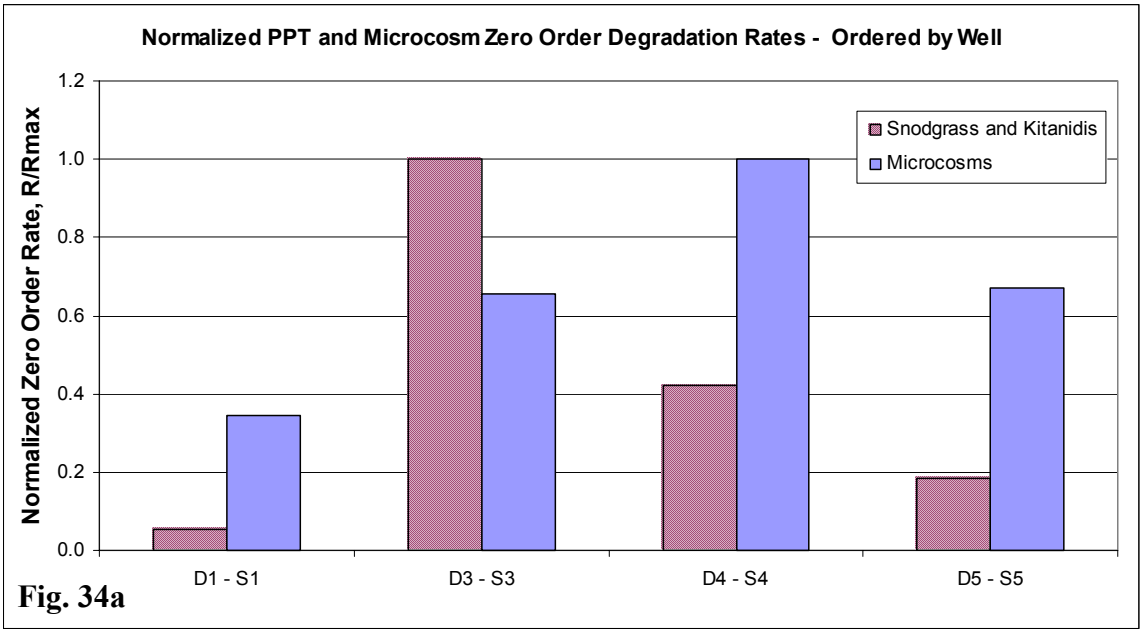

Fig. 34a

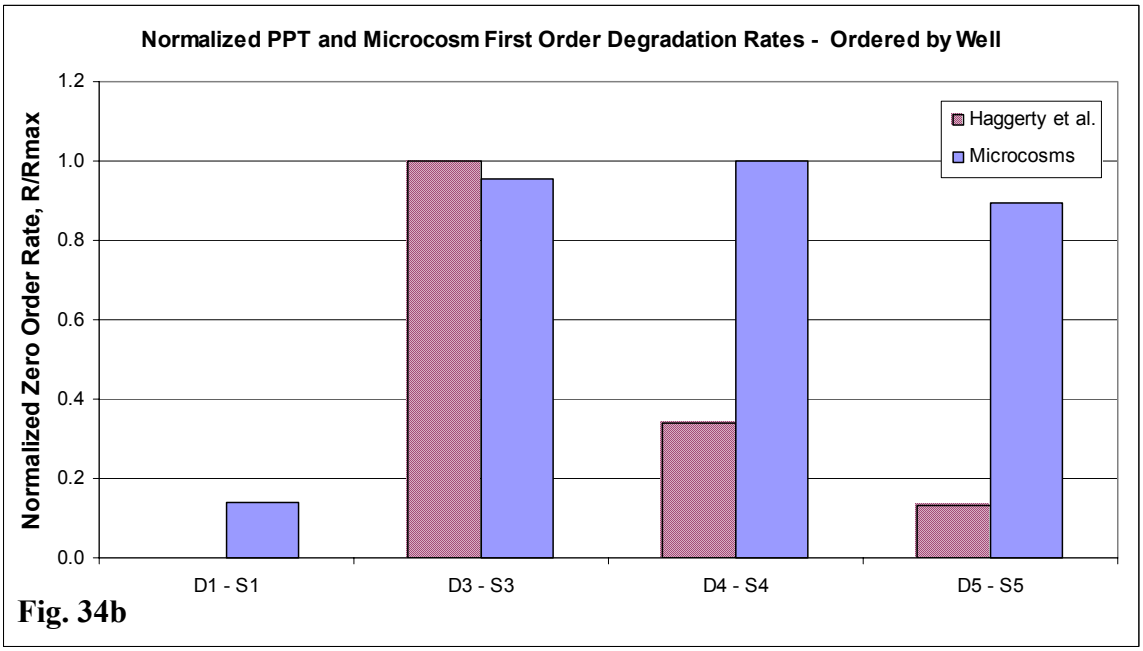

Fig. 34b

Figure 34: Normalized Push-pull Test and Microcosm First Order Degradation Rates

Results show a very good correlation at D3 for first order rates, but zero order microcosm rates at S3-D3 were only 2/3 of the observed normalized PPT zero order rate at S3-D3. Other normalized well comparison show poor correlation when comparing magnitude; however, overall trends are still very similar. The lowest observed rates for both PPTs and microcosms were found at the control well pair, S1-D1. PPT results show

degradation is highest at S3-D3, then S4-D4, S5-D5, and S1-D1, respectively (Figure 34). Microcosm results show a very similar sequence, except the microcosms show degradation rates are highest at S4-D4 instead of S3-D3. Although S3-D3 serve as the best indicator of phytoremediation, since this well pair is located adjacent to the largest poplar tree, both S4-D4 and S3-D3 are under the influence of phytoremediation. Therefore, it can be expected that the results from the two well pairs are very similar. Since only two tests were performed at D4 during winter months, it can be expected that future tests will show larger rates at D4 that agree with microcosm results.

Results from both studies verified trends observed from over 6 years of monitoring data. Monitoring data has shown an enrichment of heavier PAHs within the phytoremediated zone of the site, due to increased mineralization of naphthalene once poplar tree roots reached the DNAPL. PPTs and microcosms confirm these observations, since the largest degradation rates were observed in phytoremediated areas of the site, namely S3-D3 and S4-D4. Although more pronounced in the PPT results, both PPT and microcosm results show that degradation at S5-D5, a well pair subject to minimal influence of phytoremediation, was less than degradation that occurred in phytoremediated zones of the site, S3-D3 and S4-D4.

Overall, PPT results verified trends observed from PPT soil microcosms and six years of monitoring data. The highest degradation rates were observed at phytoremediated regions of the site and the lowest degradation rates were observed at the control well. Results show that poplar trees are effective in ameliorating PAHs, particularly naphthalene, which is supported by heavier PAH enrichment found from monitoring data, as well as increased degradation rates in contaminated regions observed in both PPTs and microcosms.

10.0 SUMMARY AND CONCLUSIONS

10.1 Method Development and Conclusions

Twelve push-pull tests were performed, utilizing either option 1 or 2, so that the method could be evaluated and tested. The PPTs yielded an initial set of rate data that enabled comparison of seasonal and spatial varying in-situ conditions. The highest confidence in zero order rate methods was given to the method of Snodgrass and

Kitanidis (1998). The first order rate methods of Haggerty et al. (1998) and Snodgrass and Kitanidis (1998) agreed very well, but when they differed, the highest confidence was placed in the method of Haggerty et al. (1998). PPTs that exhibit BTC crossing cannot be confidently used for analysis and conclusions and as a result, rate results from PPT S3 February must be verified by future PPTs at S3.

No significant degradation was observed at the control well, D1, when the non-characteristic D1 1 April rain event test was removed from analysis. Overall, the PPT results at the control well D1 validate that rate adjustments for TOC at contaminated wells is unnecessary, naphthalene-injection does not alter test results, and consequently options 1 and 2 can be compared directly. No adjustment for natural TOC DO uptake is further supported by the initial anaerobic conditions found at PPT D4 February. Anaerobic wells, introduced with an aerobic injection slug, do not contribute to noticeable natural TOC oxygen uptake, which is supported by the low first order rate found at D4 February, 0.0024 1/hr.

All zero order results indicate that not only can the PPT method discern differences between treed and non-treed regions, but also seasonal variations of phytoremediation, whose effects are rapidly increasing in-situ degradation and remediation. First order rate data further supports conclusions between treed and non-treed regions. PPT well D3 served as the best indicator of the contribution of phytoremediation in enhancing in-situ degradation. The largest zero order rate, 2.43 $mg_{naphthalene}$/L-hr, occurred at D3 in June when the contribution of the trees is largest. The winter rate at D3 decreased to 0.79 $mg_{naphthalene}$/L-hr, during December when trees are not active and thus their contribution to remediation is the smallest at this time of the year. The largest first order rate was also found at D3 in June, resulting in a rate of 1.25 1/hr. The zero and first order winter rate at D3 was greater by a factor of at least 2.5 when compared to all tests performed at any well outside of the influence of phytoremediation, particularly tests performed at D1 and S5. Treed and untreed zero order rates were compared during the month of February, where S3, the best indicator of phytoremediation, resulted in a rate over four times higher than the rate at S5, which occurs at a contaminated region of the site farthest away from the influence of trees. Comparison of February S3 and S5 PPTs for first order rates could not be made due to

BTC crossing. Seasonal variation of degradation rates at treed regions were found to steadily increase by a factor of four from winter to summer.

A PPT method was successfully developed and applied to the Oneida site. Control wells and other well comparisons validated the method. Seasonal and spatial variations, as well as enhanced degradation due to phytoremediation, can be detected with the PPT method. Poplar tree induced phytoremediation increases in-situ degradation rates and thus reduces the remediation timeframe.

10.2 Future Tests

Both aerobic and anaerobic PPTs should be performed. Both tests can use lower injection concentrations of bromide (~100 mg/L). Anaerobic tests should begin by applying the method of Schroth et al. (2001) to assess sulfate utilization through stable sulfate isotope analysis. Iron reduction rates can be assessed by combining stable sulfate isotope analysis with monitoring of halogenated naphthalene compounds. Lag phases and large injection volumes (~1100 L) should be employed to detect slower anaerobic degradation rates.

Aerobic PPTs already performed at the Oneida site have gathered initial seasonal varying degradation rates at D3, but little to know data exists for these changes at S3, S4-D4, and S5-D5. Initial tests have also failed to gather rate data for S3-D3 in August, the time when the trees are at their peak, because of extremely low summertime groundwater depths. Future PPTs at the Oneida site should take full advantage of abnormally wet summers to test variations between treed (S3-D3, S4-D4) and untreed (S5-D5) regions to determine the peak enhancement factor of phytoremediation when compared to in-situ natural attenuation. Wet summer testing should also be performed at shallow wells to gain an improved spatial depth understanding, while also improving comparisons between aerobic microcosm and PPT trends. Summer testing may be forced to occur a few days after rain events to take advantage of the temporarily high GWT.

PPTs should be performed to compare variations of degradation as a function of seasonal variation (winter, spring, summer, fall), particularly for S4-D4 and S5-D5 to improve understanding of rates in treed and untreed regions throughout the year. Future tests can also examine night/day variations as well as short-term weather variations such

as sunny, cloudy, and rain-event conditions. Collectively, it is desired to develop degradation rates at the Oneida site that occur under a multitude of the varying spatial, diurnal, and seasonal conditions at the site so that a model can be developed that accurately reflects real-time changes in degradation characteristics, thus providing detailed forecasts of plume reduction and elimination.

LITERATURE CITED

Al-Yousfi, A. B.; Chapin, R. J.; King, T. A.; Shah, S. I. Phytoremediation – the natural pump-and-treat and hydraulic barrier system. *Practice Periodical of Hazardous, Toxic, and Radioactive Waste Management* **2000**, 4, 73.

Amerson, I. L.; Bruce, C. L.; Johnson, P. C.; Johnson, R. L. A multi-tracer push-pull diagnostic test for in-situ air sparging systems. *Biorem. J.* **2001**, 5, 4, 349-362.

Andersen, R. G.; Christensen, J. S. Intrinsic bioremediation of Hjorring gas plant site: microcosm degradability study for benzene, phenols, MTBE – appendix. **1998**. *M.S. Dissertation Thesis. Aalborg University*. DK.

Anderson, R. T.; Lovley, D. R. Naphthalene and benzene degradation under Fe(III)-reducing conditions in petroleum-contaminated aquifers. *Bioremediation J.* **1999**, 3, 121.

Bachmat, Y.; Mandel, S.; Bugayevski, M. A single-well tracer technique for evaluating aquifer parameters, I. Theoretical work. *J. of Hydrol.* **1988**, 99, 143.

Borden, R. C.; Bedient, P. B. In-situ measurement of adsorption and biotransformation at a hazardous waste site. *Water Resources Bulletin*. **1987**, 23, 4, 629-636.

Borden, R. C.; Gomez, C. A.; Becker, M. T. Geochemical indicators of intrinsic bioremediation. *Ground Water* **1995**, 33, 180.

Borden, R. C.; Lee, M. D.; Thomas, J. M.; Bedient, P. D.; Ward C. H. In-situ measurement and numerical simulation of oxygen limited biotransformation, *Ground Water Monitoring Review* **1989**, Winter, 83.

Brauner, J. S. Impacts of sequential microbial electron accepting processes on natural attenuation of selected petroleum hydrocarbons in the subsurface environment. *Ph.D. Dissertation. Virginia Polytechnic and State University.* **2000**. Blacksburg, Virginia.

Burken, J. G.; Schnoor, J. L. Phytoremediation: Plant Uptake of Atrazine and Role of Root Exudates. *J. of Environ. Eng.* **1996**, 122, 11, 958-963.

Chapelle, F. H. Ground-Water Microbiology and Geochemistry. John Wiley & Sons, Inc., NY. **1993**.

Chapelle, F. H.; McMahon, P. B.; Dubrovsky, N. M.; Fuji, R. F.; Oaksford, E. T.; Vroblesky, D. A. Deducing the distribution of terminal electron-accepting processes in hydrologically diverse groundwater systems. *Water Res. Research* **1995**, 31, 359-371.

Chaplin, B. P.; Delin, G. N.; Baker, R. J.; Lahvis, M. A. Long-term evolution of biodegradation and volatilization rates in a crude oil-contaminated aquifer. *Biorem. J.* **2002**, 6, 3, 237-255.

Choi, J.; Tillman, F. D.; Smith, J. A. Relative importance of gas-phase diffusive and advective trichloroethene (TCE) fluxes in the unsaturated zone under natural conditions. *Environ. Sci. Tech.* **2002**, 35, 14, 3157-3164.

Clesceri, L. S.; Grenberg, A. E.; Easton, A. D. *Standard methods for the examination of water and wastewater*. 20th ed. **1998**. American Public Health Association, Washington D.C.

Coates, J. D.; Anderson, R. T.; Lovley, D. R. Anaerobic oxidation of polycyclic aromatic hydrocarbons under sulfate-reducing conditions. *Appl. Environ. Microbiol.* **1996**, 62, 1099.

Coates, J. D.; Woodward, J.; Allen, J.; Philp, P.; Lovley, D. R. Anaerobic degradation of polycyclic aromatic hydrocarbons and alkanes in petroleum-contaminated marine harbor sediments. *Appl. Environ. Microbiol.* **1997**, 63, 3589.

Cozzarelli, I. M.; Eganhouse, R. P.; Baedecker, M. J. Transformation of monoaromatic hydrocarbons to organic-acids in anoxic groundwater environment. *Environ. Geology Water Sci.* **1990**, 16, 135.

Davis, B. M., Istok, J. D., Semprini, L. Push-pull partitioning tracer tests using radon-222 to quantify non-aqueous phase liquid contamination. *J. of Cont. Hydrol.* **2002**, 58, 129.

Davis, L. C.; Pitzer, C.; Castro, S.; Erickson, L. E. Henry's constant, Darcy's law, and contaminant loss. *Proceedings of the 2001 Conference on Environmental Research.* **2001**, 2-15.

Davis, S. N.; Thompson, G. M.; Bentley, H. W.; Stiles, G. Ground water tracers – a short review. Ground Water **1980**, 18, 14-23.

Dietz, A. C.; Schnoor, J. L. Advances in Phytoremediation. *Environ. Health Perspectives* **2001**, 109, 163.

Drever, J. I.; McKee, C. R. The push-pull test: a method of evaluating formation adsorption parameters for predicting the environmental effects on in-situ coal gasification and uranium recovery. *In Situ* **1980**, 4, 181.

Fetterolf, J. G. Characterization of a creosote-contaminated tie yard site and the effects of phytoremediation. *M.S. Thesis. Virginia Polytechnic and State University.* **1998**. Blacksburg, Virginia.

Field, J. A.; Istok, J. D.; Schroth, M. H.; Sawyer, T. E.; Humphrey, M. D. Laboratory investigation of surfactant-enhanced trichloroethene solubilization using single-well, "push-pull" tests. *Ground Water* **1999**, 37, 581.

Field, J. A.; Sawyer, T. E.; Schroth, M. H.; Humphrey, M. D.; Istok, J. D. Effect of cation exchange on surfactant-enhanced solubilization of trichloroethene. *J. Contam. Hydrol.* **2000**, 46, 131.

Gelhar, L. W.; Collins, M. A. General analysis of longitudinal dispersion in nonuniform flow. *Water Resources Research* **1971**, 7, 1511.

Grady, C. P. L.; Daigger, G. T.; Lim, H. C. *Biological Wastewater Treatment*. 2nd ed. Marcel Dekker Inc., NY. **1999**.

Hageman, K. J.; Istok, J. D.; Field, J. A.; Buscheck, T. E.; Semprini, L. In-situ anaerobic transformation of trichlorofluoroethene in trichloroethene-contaminated groundwater. *Environ. Sci. Technol.* **2001**, 35, 1729.

Haggerty, R.; Schroth, M. H.; Istok, J. D. Simplified method of "push-pull" test data analysis for determining in-situ reaction rate coefficients. *Ground Water* **1998**, 36, 314.

Hall, S. H.; Luttrell, S. P.; Cronin, W. E. A method for estimating effective porosity and ground-water velocity. *Ground Water* **1991**, 29, 171.

Heitkamp, M. A.; Cernigliz, C. E. Microbial metabolism of polycyclic aromatic hydrocarbons: isolation and characterization of a pyrene-degrading bacterium. *Appl. Environ. Microbiol.* **1988**, 54, 2549.

Hoopes, J. A.; Harleman, D. R. Dispersion in radial flow from a recharge well. *J. of Geophysical Research* **1967**, 72, 3595.

Istok, J.D.; Amonette, J. E.; Cole, C. R.; Fruchter, J. S.; Humphrey, M. D.; Szecsody, J. E.; Teel, S. S.; Vermeul, V. R.; Williams, M. D.; Yabusaki, S. B. In-situ redox manipulation by dithionite injection: intermediate-scale laboratory experiments. *Ground Water* **1999**, 37, 884.

Istok, J. D.; Field, J. A.; Schroth, M. H.; Davis, B. M.; Dwarakanath, V. Single-well "push-pull" partitioning tracer test for NAPL detection in the subsurface. *Environ. Sci. Technol.* **2002**, 36, 2708.

Istok, J. D.; Field, J. A.; Schroth, M. H. In-situ determination of subsurface microbial enzyme kinetics. *Ground Water* **2001**, 39, 348.

Istok, J. D.; Field, J. A.; Schroth, M. H.; Sawyer, T. E.; Humphrey, M. D. Laboratory and field investigation of surfactant sorption using single-well, "push-pull' tests. *Ground Water* **1999**, 37, 589.

Istok, J. D.; Humphrey, M. D.; Schroth, M. H.; Hyman, M. R.; O'Reilly, K. T. Single-well, "push-pull" test for in-situ determination of microbial activities. *Ground Water* **1997**, 35, 619.

Jin, M.; Delshad, M.; Dwarakanath, V.; McKinnery, D. C.; Pope, G. A.; Sepehrnoori, K.; Tilburg, C. E. Partitioning tracer test for detection, estimation, and remediation performance assessment of subsurface nonaqueous phase liquids. *Water Resources Res*. **1995**, 31, 5, 1201-1211.

Jin, M.; Butler, G. W.; Jackson, R. E.; Mariner, P. E.; Pickens, J. F.; Pope, G. A.; Brown, C. L.; McKinney, D. C. Sensitivity models and design protocol for partitioning tracer tests in alluvial aquifers. *Ground Water*. **1997**, 35, 6, 964-972.

Jordahl, J. L.; Foster, L.; Schnoor, J. L.; Avarex, P. J. J. Effect of hybrid poplar trees on microbial populations important to hazardous waste bioremediation. *Environ. Toxicol. Chem.* **1997**, 16, 1318.

Kleikemper, J.; Schroth, M. H.; Sigler, W. V.; Schmucki, M.; Bernasconi, S. M.; Zeyer, J. Activity and diversity of sulfate-reducing bacteria in a petroleum hydrocarbon-contaminated aquifer. *Appl. Environ. Microbiol.* **2002**, 68, 1516.

Leap, D. I.; Kaplan, P. G. A single-well tracing method for estimating regional advective velocity in a confined aquifer: theory and preliminary laboratory verification. *Water Resources Research* **1988**, 24, 993.

Leduc, R.; Samson, R.; Al-Bashir, B.; Al-Hawari, J.; Cseh, T. Biotic and abiotic disappearance of four PAH compounds from flooded soil under various redox conditions. *Water Sci. Technol.* **1992**, 26, 51.

Leitao, T. E.; Lobo-Ferreira, J. P.; Valocchi, A. J. Application of a reactive transport model for interpreting non-conservative tracer experiments: the Rio Maior case-study. *J. Cont. Hydrol.* **1996**, 24, 167-181.

Lovley, D. R. Dissimilatory Fe(III) and Mn(IV) reduction. *Microbiol. Rev.* **1991**, 55, 259.

Lüthy, L.; Fritz, M. Bachofen, R. In-situ determination of sulfide turnover rates in a meromictic alpine lake. *App. Environ. Microb.* **2000**, 66, 712.

Madigan, M. T.; Martinko, J. M.; Parker, J. *Brock: biology of microorganisms*. 9th ed. Prentice Hall, Upper Saddle River, N.J.

Massmann, J.; Farrier, D. F. Effects of atmospheric pressures on gas transport in the vadose zone. *Water Res. Research* **1992**, 28, 3, 777-791.

Matso, K. Mother Nature's Pump and Treat. *Civil Engineering – ASCE* **1995**, 65, 46.

McCutcheon, S. C.; Schnoor, J.L. *Phytoremediation: Transformation and Control of Contaminants*. John Wiley & Sons, Inc., Hoboken, NJ. **2003**.

McGuire, J. T.; Long, D. T.; Klug, M. J.; Haack, S. K. Hyndman, D. W. Evaluating behavior of oxygen, nitrate, and sulfate during recharge and quantifying reduction rates in a contaminated aquifer. *Environ. Sci. Technol.* **2002**, 36, 2693.

McNally, D. L.; Mihelcic, J. R.; Lueking, D. R. Biodegradation of three- and four-ring polycyclic aromatic hydrocarbons under aerobic and denitrifying conditions. *Environ. Sci Technol.* **1998**, 32, 2633.

Mihelcic, J. R.; Luthy, R. G. Degradation of polycyclic aromatic hydrocarbon compounds under various redox conditions in soil-water systems. *Appl. Environ. Microbiol.* **1988**, 54, 1182.

Morgan, P.; Watkinson, R. J. *Water Res.* **1992**, 26, 73-78.

Muck, A. J. Creosote migration in the subsurface at the Oneida Tie-Yard. M.S. Research Report. *Virginia Polytechnic and State University.* **2000**. Blacksburg, Virginia.

Mueller, J. G.; Chapman, P.; Pritchard, P. Creosote-contaminated sites – their potential for bioremediation. *Environ. Sci. Technol.* **1989**, 23, 97-120.

Mueller, J. G.; Lantz, S. E.; Blattmann, B. O.; Chapman, P. J. Bench-scale evaluation of alternative biological treatment processes for the remediation of pentachlorophenol- and creosote-contaminated materials: solid phase bioremediation. *Environ. Sci. Technol.* **1991**, 25, 1045.

Norris, R. D.; Hinchee, R. E.; Brown, R.; McCarthy, P. L.; Semprini, L.; Wilson, J. T.; Kampell, D. H.; Reinhard, M.; Bouwer, E. J.; Borden, R. C.; Vogel, T. M.; Thomas, J. M.; Ward, C. H. *The Handbook of Bioremediation* Lewis Publishers: Boca Raton, FL, **1994**.

Pickens, J. F.; Grisak, G. E. Scale-dependent dispersion in a stratified granular aquifer. *Water Resources Research* **1981**, 17, 1191.

Pombo, S. A.; Pelz, O.; Schroth, M. H.; Zeyer, J. Field-scale ^{13}C-labelling of phospholipid fatty acids (PLFA) and dissolved inorganic carbon: tracing acetate assimilation and mineralization in a petroleum hydrocarbon-contaminated aquifer. *FEMS Microb. Ecology* **2002**, 41, 259.

Reilley, K. A.; Banks, M. K.; Schwab, A. P. Organic chemicals in the environment: dissipation of polycyclic aromatic hydrocarbons in the rhizosphere. *J. Environ. Quality* **1996**, 25, 212.

Reinhard, M.; Shang, S.; Kitanidis, P. K.; Orwin, E.; Hopkins, G. D.; Lebron, C. A. In-situ BTEX biotransformation under enhanced nitrate- and sulfate-reducing conditions. *Environ. Sci. Technol.* **1997**, 31, 28.

Reusser, D. E.; Istok, J. D.; Beller, H. R.; Field, J. A. In-situ transformation of deuterated toluene and xylene to benzylsuccinic acid analogues in BTEX-contaminated aquifers. *Environ. Sci. Technol.* **2002**, 36, 4127.

Robinson, S. Phytoremediation mechanisms of a creosote-contaminated site. *M.S. Thesis. Virginia Polytechnic and State University.* **2001**. Blacksburg, Virginia.

Rugge, K.; Bjerg, P. L.; Pederson, J. K.; Mosbaek, H.; Christensen, T. H. An anaerobic field injection experiment in a landfill leachate plume, Grindsted, Denmark: 1. Experimental setup, tracer movement, and fate of aromatic and chlorinated compounds. *Water Resources Bulletin*. **1999**, 35, 4 1231-1246.

Sabatini, D. A.; Austin, T. A. Characteristics of rhodamine WT and fluorescein as adsorbing ground-water tracers. *Ground Water*. **1991**, 29, 341.

Salt, J. L.; Smith, R. D.; Raskin, I. Phytoremediation. *Annual Review of Plant Physiology and Plant Molecular Biology* **1998**, 49, 643.

Schnoor, J. L.; Licht, L. A.; McCutcheon, S. C.; Wolfe, N. L.; Carreira, L. H. Phytoremediation of organic and nutrient contaminants. *Environ. Sci. Technol.* **1995**, 29, 318.

Schroth, M. H.; Istok, J. D.; Conner, G. T.; Hyman, M. R.; Haggerty, R.; O'Reilly, K. T. Spatial variability in in-situ aerobic respiration and denitrification rates in a petroleum-contaminated aquifer. *Ground Water* **1998**, 36, 924.

Schroth, M. H.; Istok, J. D.; Haggerty, R. In-situ evaluation of solute retardation using single-well push-pull tests. *Advances in Water Research* **2001**, 24, 105.

Schroth, M. H., Kleikemper, J., Bolliger, C., Bernasconi, S. M., Zeyer, J. In-situ assessment of microbial sulfate reduction in a petroleum-contaminated aquifer using push-pull tests and stable sulfur isotope analyses. J. of Cont. Hydrol. **2001**, 51, 179.

Schwarzenbach, R.P.; Gschwend, P.M.; Imboden, D.P. *Environmental Organic Chemistry*. John Wiley & Sons, NY. **1993**.

Senko, J. M., Istok, J. D.; Suflita, J. M.; Krumholz, L. R. In-situ evidence for uranium immobilization and remobilization. *Environ. Sci. Technol.* **2002**, 36, 1491.

Smart, P. L.; Laidlaw, I. M. An evaluation of some fluorescent dyes for water tracing. *Water Resources Res*. **1977**, 13, 1, 15-33.

Smartt, H. A. Effects of the desorption and dissolution of polycyclic aromatic hydrocarbons on phytoremediation at a creosote-contaminated site. *M.S. Thesis. Virginia Polytechnic and State University.* **2002**. Blacksburg, Virginia.

Smith, J. A.; Tisdale, A. K.; Cho, J. H. Quantification of natural vapor fluxes of trichloroethene in the unsaturated zone at Picatinny Arsenal, New Jersey. *Environ. Sci. Tech.* **1996**, 30, 7, 2243-2250.

Snodgrass, M. F.; Kitanidis, P. K. A method to infer in-situ reaction rates from push-pull experiments. *Ground Water* **1998**, 36, 645.

Stumm, W.; Morgan, J. J. Aquatic Chemistry: Chemical Equilibria and Rates in Natural Waters. 3rd ed. John Wiley & Sons, Inc., NY. **1996**.

Susarla, S.; Medina, V. F.; McCutcheon, S. C. Phytoremediation: An ecological solution to organic chemical contamination. *Ecol. Eng.* **2002**, 18, 647-658.

Thierrin, J.; Davis, G. B.; Barber, C. A ground-water tracer test with deuterated compounds for monitoring in-situ biodegradation and retardation of aromatic hydrocarbons. *Ground Water.* **1995**, 33, 3, 469-475.

Trudell, M. R.; Gillham, R. W.; Cherry, J. A. An in-situ study of the occurrence and rate of denitrification in a shallow unconfined aquifer. *J. Hydrol.* **1986**, 83, 251-268.

Walter, U.; Beyer, M.; Klein, J.; Rehm, H. J. Degradation of pyrene by *Rhodococcus* sp. UW1. *Appl. Microbiol. Biotechnol.* **1991**, 34, 671.

Washington, J. W. Gas partitioning of dissolved volatile organic compounds in the vadose zone: principles, temperature effects and literature review. *Ground Water* **1996**, 34, 4, 709-717.

Weissenfels, W. D.; Beyer, M.; Klein, J.; Rehm, H. J. Microbial metabolism of fluoranthene: isolation and identification of ring fission products. *Appl. Microbiol. Biotechnol.* **1991**, 34, 528.

Wiedemeier, T. H.; Swanson, M. A.; Wilson, J. T.; Kampbell, D. H.; Miller, R. N.; Hansen, J. E. Approximation of biodegradation rate constants for monoaromatic hydrocarbons (BTEX) in ground water. *GWMR*. **1996**. Summer, 186-194.

Wise, W. R.; Charbeneau, R. J. In-situ estimation of transport parameters: a field demonstration. *Ground Water.* **1994**, 32, 3, 420-430.

Yeom, I.; Ghosh, M. M. Mass transfer limitation in PAH-contaminated soil remediation. *Wat. Sci. Tech.* **1998**, 37, 111.

APPENDIX A: METHOD DESCRIPTION AND INSTRUCTIONS

The following are detailed instructions specific to the field tests performed at the Oneida phytoremediation site. The contents are addressed primarily to future researchers at the Oneida site and are not intended for universal application to other sites. It is recommended that the reader first fully understands specific site characteristics and then adapts the following method to the intended site.

A.1 Contaminant Water Injection

It is ideal to perform push-pull tests with an assistant so that two tests can be performed simultaneously, which are offset by the injection period. Field setup typically takes one to one and a half hours. To maximize efficiency in the field, detailed instructions for push-pull setup are explained below.

Upon arrival at the site, the two graduated carboys marked injection solution are filled to 35 L using tap water, while the other partner prepares in-situ field test setup. In-situ field tests include dissolved oxygen, ferrous iron, and sulfide analysis and measurements were made using HACH kit methods. *Field and laboratory tests need only be performed on solutes contained in the injection solution.* An *exception* applies to anaerobic tests, where dissolved oxygen (DO) and other more preferential electron acceptors must be monitored to ensure higher preference electron acceptors are not erroneously incorporated into monitored reactive solute rate calculations. DO was measured using a digital titrator and Winkler titration method. Ferrous iron samples were first filtered using 0.45 um filters and then were measured using a HACH™ DR/700 Colorimeter. Absorbance was read and converted to a concentration, mg/L, using a standard curve that was constructed using ferrous sulfate. Total sulfides were measured by first filtering all samples with a 0.45 um filter and then a HACH™ DR/700 Colorimeter reported concentration results in mg/L. HACH™ provides detailed instructions for performing the above in-situ methods. Future tests can include hydrogen production analysis to gain an improved understanding of anaerobic redox conditions. A gas chromatograph (GC) with reduction gas detector can be used to measure hydrogen following the method of Chapelle et al. (1995); however, this method has not yet been deployed for PPTs. Scintillations vials are used to collect samples for ion chromatograph (IC) analysis, which includes analysis of bromide, sulfate, and nitrate (if present). Volatile organic analysis (VOA) EPA amber vials are used to collect samples for PAH analysis. Samples are

placed in ice-packed coolers until return to the laboratory, where they are then stored at 4°C until analysis. PAH samples were then extracted using methylene chloride and analyzed on a GC with flame ionization detection using a DB5-MS fused silica capillary column following the method of Fetterolf (1999). External standards were used for quantification.

For aerobic tests, the injection solution is prepared by first placing the submersible mixing pump, to which the injection-in Teflon™ tube is attached, within the injection carboy containing 35 L of water and then placing an aerator within the carboys for sufficient time to enable the DO concentration to reach a maximum. The injection-in Teflon™ tube is attached to the submersible mixing pump to ensure that the tube does not float to the surface. For anaerobic tests, a similar approach is used, except the diffuse 'aerator' is attached to a nitrogen tank. After sufficient time has elapsed, bromide and naphthalene contained in the amber vials are carefully poured into the injection carboy. The EPA amber vials containing the concentrated solution are then rinsed several times using deionized water spray bottles and the rinse-water is poured into the carboy. Several alternating layers of Parafilm™, secured with duct tape, are placed over the carboy lid to prevent volatile loss. Shake the carboy gingerly assuring no water reaches the Parafilm™ seal. Then allow sufficient time for the solution to equilibrate.

Next, prepare the pumps for the first test. The two six foot sections of ¼ - 20 rod are connected using the coupler. Three extraction-in tubes are necessary to compensate for the slower flowrates associated with the Masterflex® L/S™ Standard Drive pumps. The three extraction-in tubes are attached to the ¼ - 20 rod six inches from the end. The injection-out tube is then attached to the rod three inches above the extraction-in tubes for a total of nine inches from the end of the rod. The rod is then measured and marked corresponding to the total depth of the test well; for example, if the well is eight feet deep to the bottom, the rod is marked at eight feet. The rod is then placed in the well. The marking ensures that the rod is lowered to the bottom of the well and ensures that the rod does not get 'hung up' at the coupler in such a manner that the observer mistakenly believes it has reached the bottom of the well. The injection in/out tubes as well as the extraction in/out tubes are then attached to the appropriate pumps. The extraction-out

tubes are placed in the 2 L graduated cylinder for later 'backflushing.' The appropriate pump flow directions are then determined (clockwise/counterclockwise).

Meanwhile, the groundwater depth indicator is used to determine the depth of groundwater within the well-casing. It is recommended that a minimum of one foot of groundwater is contained within the well-casing to perform a PPT, preferably two feet or more. The volume of water within the well-casing is then calculated. After removing a minimum of three-pore volumes of the water contained in the well-casing, duplicate background samples are taken for TOC (total organic carbon), IC, GC, and ferrous iron analysis using the extraction pump. It should be note that previous tests have confirmed that sulfide production cannot be accurately measured for PPTs most likely due to precipitation as ferrous sulfide. Background DO samples are taken in triplicate to ensure stability. DO and ferrous iron sampling is continued until a stable concentration is observed. Record the weather conditions and the pH and the temperature of the background samples after iron/sulfide samples have been removed. The groundwater depth indicator is then placed at a minimum of one foot from the surface of the test well. If the indicator beeps during the injection, the flowrate must be lowered *immediately* to ensure the injection solution does not overflow the test well.

It is imperative that all solutions containing injected solutes are collected and recorded for flow balance calculations, as detailed below. Once extraction solution carboys are filled, they must be placed in the oil-water separator to prevent contamination of bromide tracers to the Oneida site. Failure to follow this instruction will prevent future PPTs from using bromide as a tracer due to the presence of bromide in background samples.

Once stable background ferrous iron and DO measurements are achieved, the desired solution is injected at an approximate flowrate of 0.5 L/min (~9.4 RPM for the green Portable Masterflex® L/S™ Sampling Pump) and the stopwatch is begun at injection time zero. Prior to each sampling period, a minimum of 200 ml of water is 'backflushed' to ensure removal of fluid within the sampling tube from the previous sampling period; this backflushed volume is then recorded for flow balance calculations and the solution is placed in the extraction solution carboy. DO and IC samples are collected each 10 minute interval. GC, iron, and sulfide samples are collected every other sampling time,

corresponding to injection times 10, 30, 50, and so on. The volume of sample collected for the ferrous iron analysis is recorded. Following completion of the ferrous iron tests, the remaining sample volume that was not consumed during the field tests is measured, recorded, and then the remaining solution is added to the extraction solution carboy for later flow balance calculations. Before the remaining injection 30-minute iron sample (i.e. the portion of the sample remaining after completion of the iron/sulfide measurements) is added to the extraction solution carboy, the pH and the temperature is measured and recorded. *It is imperative to carefully monitor injection throughout the duration to ensure that injection is not interrupted, such as if the injection-in tube rises to the surface.* The carboy may have to be tilted as the injection solution nearly runs out to inject the entire 35 L. Once the injection period is complete, the total time of injection is recorded; however, the stopwatch must be reset and started to account for the elapsed time between injection and extraction periods.

A.2 Contaminant Water Extraction

When free time is available during the extraction period for the first well, the green Portable Masterflex® L/S™ Sampling Pump can be transferred to the second well. The procedure for testing and setup are identical, except that only one extraction in/out pair is needed. The single pair of extraction in/out tubes is attached to the Masterflex® L/S™ Standard Drive pump during the injection phase for sample collection. Following the completion of the injection phase, the extraction in/out tubes are then moved from the Masterflex® L/S™ Standard Drive pump to the green Portable Masterflex® L/S™ Sampling Pump and the flowrate is lowered from 0.5 L/min to 0.25 -0.35 L/min. The important point to note is that three pairs of tubing used with the Masterflex® L/S™ Standard Drive pumps are necessary to produce the desired flowrate that is achievable with one pair of tubing with the green Portable Masterflex® L/S™ Sampling Pump. The groundwater depth indicator should be transferred to the second well prior to injection to prevent overflow of injection solution from the second test well.

Immediately following the completion of the injection phase, the extraction pump flowrate is adjusted between 250 and 350 ml/min (~5 RPM for green Portable Masterflex® L/S™ Sampling Pump and ~ 8 RPM for the Masterflex® L/S™ Standard

Drive pump). After backflushing extraction tubes for the final time, extraction time zero samples are collected for GC, IC, ferrous iron, and DO analysis. Again, the backflushed volume is recorded. Upon completion of extraction time zero sample collection, the time elapsed since the completion of injection is recorded. The stopwatch is then reset, the extraction tubes are placed within the 4 L graduated cylinder, and the extraction pump is then turned on marking the beginning of the extraction phase. Every ten minutes, the volume collected in the 4 L graduated cylinder is recorded during a recorded time interval for later flowrate calculations. The extracted solution collected in the 4 L graduated cylinder is then placed in the extraction carboy. DO and IC samples are collected every ten minutes, while GC and ferrous iron are collected every 30 minutes. The volume of sample collected for the ferrous iron analysis is recorded. Following completion of the ferrous iron tests, the remaining sample volume that was not consumed during the field tests is measured, recorded, and then the remaining solution is added to the extraction solution carboy for later flow balance calculations. The total volume of extraction solution collected in the extraction carboy was recorded for later use in the flow balance calculations. *It is important to note that two extraction solution carboys are needed for each test.* Once one carboy becomes full, the extraction solution can then be placed in the remaining extraction solution carboy. When time is available, the full extraction solution carboy is then emptied at the sump-pump for later oil/water separation to minimize environmental impact. As each carboy becomes full, the volume collected in the extraction solution carboy is recorded. The extraction phase is complete when either three times the injected volume is extracted (105 L) OR the DO concentration stabilize to a value equal to or less than background concentrations and iron concentrations stabilize to a value equal to or greater than the background concentrations. Record the total volume and the time to the completion of the extraction phase.

A.3 Flow Balance

A flow balance was constructed by calculating the flowrate between sampling intervals from the recorded volume for each sampling time interval, which was collected in a 4 L graduated cylinder. The summed volumes used for backflushing, DO samples,

and ferrous iron/sulfide samples were tallied. The total injection volume, V_{inj}, was calculated as shown:

$$\mathbf{V_{inj} = 35\ L - V_{backflushing} - V_{DO\text{-}inj} - V_{Fe\text{-}inj\_rem} - V_{IC\text{-}inj} - V_{GC\text{-}inj}} \quad \mathbf{(1A)}$$

where: V_{inj} = total injection volume, L
$V_{backflushing}$ = total volume removed during backflushing, L
$V_{DO\text{-}inj}$ = total volume removed for DO samples during injection, L
$V_{Fe\text{-}inj\_rem}$ = total volume removed for iron samples during injection, L
$V_{IC\text{-}inj}$ = total volume removed for IC samples during injection, L
$V_{GC\text{-}inj}$ = total volume removed for GC samples during injection, L

Utilizing field measured flow rates, the total extraction volume, V_{ext}, was calculated. The extracted volume measured in the field includes the volume of water used for backflushing during the injection phase and the volume of iron samples that was not consumed during the injection phase and thus must be subtracted from the overall total. The total volumes used for samples during extraction for DO, iron, IC and GC were summed as shown:

$$\mathbf{V_{ext} = V_{field} - V_{backflushing} - V_{Fe\text{-}inj\_rem} + V_{Fe\text{-}inj} + V_{DO\text{-}ext} + V_{Fe\text{-}ext} + V_{IC\text{-}ext} + V_{GC\text{-}ext}} \quad \mathbf{(2A)}$$

where: V_{ext} = total extraction volume, L
$V_{backflushing}$ = total volume removed during backflushing, L
$V_{DO\text{-}ext}$ = total volume removed for DO samples during extraction, L
$V_{Fe\text{-}inj}$ = total volume consumed for iron samples during injection, L
$V_{Fe\text{-}ext}$ = total volume consumed for iron samples during extraction, L
$V_{IC\text{-}ext}$ = total volume removed for IC samples during extraction, L
$V_{GC\text{-}ext}$ = total volume removed for GC samples during extraction, L

Extraction flow rates were used to determine a cumulative volume extracted at the time of sampling for each sampling period. The cumulative extraction volume was normalized by dividing by V_{inj} at each sampling time period, yielding V_{ext}/V_{inj} for each time interval.

The total volume of aquifer that was investigated was determined, assuming an equal porosity of the sand-pack and the aquifer. The porosity chosen was 0.4 which has been shown to be an appropriate value for porosity of both the sand-pack and the sand lenses contained at the Oneida site (Muck, 2000).

$$V_t = \frac{V_{inj} - V_{well-casing}}{Porosity_{aquifer}} - \frac{V_{sand-pack}}{Porosity_{sand-pack}} \quad \textbf{(3A-1[1])}$$

where: V_t = total volume of aquifer investigated, L
$V_{well\text{-}casing}$ = volume of well-casing, L
$Porosity_{aquifer}$ = porosity of the aquifer
$V_{sand\text{-}pack}$ = volume of the sand-pack, L
$Porosity_{sand\text{-}pack}$ = porosity of the sand-pack

A.4 Solute Constituent Balance

Bromide, DO, ferrous iron, sulfate, and naphthalene were analyzed to determine degradation rates and the overall percent recovery. The average injection concentration for each constituent, C_{inj}, was calculated by a simple average of all injection concentration samples. The extraction concentration was normalized at each time period as shown:

$$\mathbf{C_{nor} = (C_{ext})/(C_{inj})} \quad \textbf{(4A-2)}$$

where: C_{nor} = normalized extraction concentration
C_{ext} = extraction concentration for each sampling period, mg/L

When background concentration of any constituent was present, such as in control wells with sufficient DO, the extraction concentration was normalized as follows:

$$\mathbf{C_{nor} = (C_{ext} - C_B)/(C_{inj} - C_B)} \quad \textbf{(5A-3)}$$

where: C_{nor} = normalized extraction concentration
C_{ext} = extraction concentration for each sampling period, mg/L
C_B = background concentration, mg/L

A breakthrough curve (BTC) was formulated by plotting C_{ext}/C_{inj} (or $(C_{ext} - C_B)/(C_{inj} - C_B)$ if background present) versus V_{ext}/V_{inj}. BTCs provide visual details of how degradable solutes behave relative to conservative tracers. BTCs also aid in determination of the overall mass removed during the extraction period. To minimize the effects of measurement error in observed constituent concentrations, a best-fit line was used to determine the corrected normalized extraction concentrations at each ten-minute

[1] The equation numbers in Appendix A designate where the same equation was referred to in the main text. For example, Equation 3A-1 is the third equation in Appendix A and the identical equation was referred to as Equation 1 in the main text.

interval. Thus, all degradation rates were assessed using values from the best-fit line, which enabled smaller time intervals to be utilized for improved mass removal calculations. By removing the effects of experimental error from calculations, a better representation of true in-situ conditions was enabled. The equations from the best-fit lines were used to obtain normalized concentrations for each ten-minute interval. The corrected concentration at each ten minute interval was then calculated by solving for C_{ext} in Equations 4A-2 and 5A-3, depending upon the presence of background solutes. Data were then analyzed to determine zero and first order degradation rates.

A.5 Zero Order Reaction Rates

A.5.1 Method of Istok et al. (1997)

Istok et al. (1997) provide a method to determine zero order degradation rates for PPTs. The method's zero order rate calculation involves dividing the mass of the degradable solute that is consumed (injected mass – extracted mass) or produced (extracted mass) by the total volume of the injected solution, V_{inj}, and by the mean residence time, θ, which is the elapsed time from the midpoint of injection to the bromide centroid (Istok et al., 1997). Details of this calculation are explained below.

Using the extraction flow rate for each ten minute interval, a flow weighted extracted mass removal rate was determined:

$$\mathbf{R_{flow\ weighted\_ext} = C_{ext\_corrected} * Q_n} \qquad \mathbf{(6A)}$$

where: $R_{flow\ weighted\_ext}$ = flow weighted extracted mass removal rate for the individual sampling interval, mg/min
$C_{ext\_corrected}$ = corrected extraction concentration, mg/L
Q_n = flowrate for the n^{th} sampling interval, L/min

To determine the overall percent recovery of each constituent, the injected mass and extracted mass were calculated. The extracted mass removed during each ten minute interval was determined, by applying the trapezoidal rule to the flow weighted extracted mass removal rate multiplied by ten minutes. Next, a cumulative sum of the mass removed was determined, yielding M_{ext}, the total extracted mass. The total injected mass, M_{inj}, was calculated by multiplying C_{inj} by V_{inj}. The percent recovery was then determined:

$$\textbf{Percent recovery} = M_{ext}/M_{inj} * 100\% \quad \textbf{(7A)}$$

Zero order degradation rates for naphthalene, DO, and sulfate as well as zero order production rates for ferrous iron and sulfide were then determined:

$$R_{Istok} = M_{net}/(V_{inj} * \theta) \quad \textbf{(8A-4)}$$

where: R_{Istok} = zero order degradation rate calculated using the method of Istok et al. (1997), mg/(L-hr)
$M_{net} = M_{inj} - M_{ext}$ = mass consumed, mg
θ = mean residence time = elapsed time from the midpoint of injection to the bromide centroid, hr
Bromide centroid = time when half of the injected bromide mass was recovered, hr

$$R_{Istok}' = M_{net}'/(V_{inj} * \theta) \quad \textbf{(9A-5)}$$

where: R_{Istok}' = zero order production rate calculated using the method of Istok et al. (1997), mg/(L-hr)
$M_{net}' = M_{ext} - M_{inj}$ = mass created, mg

A.5.2 Method of Snodgrass and Kitanidis (1998)

Snodgrass and Kitanidis (1998) provide an alternative method to determine zero order degradation rates for PPTs. The method involves transforming measured concentrations to remove the effects of dilution whose decrease (or increase, such as with Fe^{+2} and H_2S,) in concentration is due only to degradation. Measured concentrations are transformed as follows (Snodgrass and Kitanidis, 1998):

$$\hat{C}_r(t) = C_r^0\left(\frac{C_r^m(t)}{C_r^0} - \frac{C_t^m(t)}{C_t^0} + 1\right) \quad \textbf{(10A-6)}$$

where: $\hat{C}_r(t)$ = transformed reactive solute concentration at time t, mg/L
C_r^0 = reactive solute concentration during injection = C_{inj} for the reactive solute, mg/L
C_t^0 = non-reactive, tracer solute concentration during injection = C_{inj} for the tracer solute, mg/L
$C_r^m(t)$ = reactive, tracer solute concentration at time t = C_{ext} for the tracer solute, mg/L
$C_t^m(t)$ = non-reactive, tracer solute concentration at time t = C_{ext} for the tracer solute, mg/L
t = elapsed time from the beginning of extraction, min

Zero order degradation rates for naphthalene, DO, and sulfate as well as first order production rates for ferrous iron and sulfide can be calculated by plotting $\hat{C}_r(t)$ versus t, described in the equation below (Snodgrass and Kitanidis, 1998):

$$\hat{C}_r(t) = C_r^0 - \alpha t \quad \textbf{(11A-7)}$$

where: α = zero order degradation rate calculated using the method of Snodgrass and Kitanidis (1998), mg/(L-hr)

When zero order degradation is occurring, a plot of $\hat{C}_r(t)$ versus t will yield a straight line, with slope α. It should be noted that a slope of –α results for reactants that are consumed (DO, sulfate), whereas a slope of α results for reactants that are produced (ferrous iron, sulfide).

A.6 First Order Reaction Rates

A.6.1 Method of Haggerty et al. (1998)

Haggerty et al. (1998) provide a method to determine first order degradation rates for PPTs. First order degradation rates for naphthalene, DO, and sulfate as well as first order production rates for ferrous iron and sulfide can be determined from (Haggerty et al., 1998):

$$\ln\left[\frac{C_r^*(t^*)}{C_t^*(t^*)}\right] = \ln\left[\frac{(1 - e^{-k\,t_{inj}})}{k\,t_{inj}}\right] - k\,t^* \qquad \textbf{(12A-11)}$$

where: C_r^* = normalized concentration of the reactant at time t^*
C_t^* = normalized concentration of the tracer at time t^*
t^* = elapsed time from the end of the injection phase, min
t_{inj} = total time of the injection phase, min
k = first order degradation rate calculated using the method of Haggerty et al. (1998), min^{-1}

If the reactive solute is decaying at a first order rate, a plot of $\ln(C_r^*(t^*)/C_t^*(t^*))$ versus t^* produces a straight line with slope –k and y-intercept of $\ln[(1-e^{-ktinj})/(kt_{inj})]$. It should be noted that a slope of –k results for reactants that are consumed (DO, sulfate), whereas a slope of k results for reactants that are produced (ferrous iron, sulfide). Although not employed in the analysis in this report, the variance of k can be calculated to determine a 95% confidence interval for k ($k +/- 2\sigma_k$), σ_k from (Schroth et al., 1998):

$$\sigma_k^2 = \sigma^2 \left\{ \sum_{i=1}^{n} \left[\frac{1 - e^{kt_{inj}} + kt_{inj})}{k(e^{kt_{inj}} - 1)} - t^* \right]^2 \right\}^{-1} \qquad \textbf{(13A)}$$

where: n = Total number of observations
σ^2 = variance of errors in $\ln(C_r^*/C_t^*)$

A.6.2 Method of Snodgrass and Kitanidis (1998)

Snodgrass and Kitanidis (1998) provide an alternative method to determine first order degradation rates for PPTs. First order degradation rates for naphthalene, DO, and sulfate as well as first order production rates for ferrous iron and sulfide can be determined from (Snodgrass and Kitanidis, 1998):

$$\ln\left(\frac{C_r^m(t)}{C_t^m(t)}\right) = \ln\left(\frac{C_r^0}{C_t^0}\right) - \beta t \qquad \textbf{(14A-12)}$$

where: β = first order degradation rate calculated using the method of Snodgrass and Kitanidis (1998), mg/(L-hr)

If the reactive solute is decaying at a first order rate, a plot of $\ln(C_r^m(t)/C_t^m(t))$ versus t produces a straight line with slope $-\beta$. It should be noted that a slope of $-\beta$ results for reactants that are consumed (DO, sulfate), whereas a slope of β results for reactants that are produced (ferrous iron, sulfide).

A.7 Laminated Instructions for Push-pull Tests

Variations of the constituents contained in the injection solutions for push-pull testing exists. The method below describes the bromide/naphthalene/dissolved oxygen injection and assumes two push-pull tests will be performed simultaneously, offset by the injection phase. Concentrated solution preparation must be carried out prior to field departure. If anaerobic injection solutions are desired, a diffuse 'aerator' must be attached to nitrogen tanks and placed within the carboy. Other variations simply involve leaving out one of the above constituents.

Field and laboratory tests need only be performed on solutes contained in the injection solution. An ***exception*** applies to anaerobic tests, where dissolved oxygen (DO) and other more preferential electron acceptors must be monitored to ensure higher preference electron acceptors are not erroneously incorporated into monitored reactive solute rate calculations.

HACH™ kits are used for DO and ferrous iron in-situ measurements. Scintillation vials are used for IC analysis including bromide, sulfate, and nitrate (if present). EPA VOA amber vials are used for GC analysis for PAHs, particularly naphthalene. Hydrogen analysis may later be incorporated into the push-pull analysis, particularly to assess anaerobic redox conditions, which requires use of the field GC and hydrogen sampling equipment. Samples are placed in ice-packed coolers until return to the laboratory, where they are then stored at 4°C until analysis.

It is important to note that two extraction solution carboys are needed for each test. Upon arrival to the site, first determine the height of the groundwater in the proposed testing wells. A minimum of one foot of water from the bottom of the well casing is required, but it is suggested that at least two feet of water head is present. During summer months, PPTs often cannot be employed due to extremely low groundwater tables and high evapotranspiration rates of the poplar trees. Use caution when less than two feet of head is present, as air bubbles can enter the extraction out tubes and disrupt tested solute concentrations. If air bubbles are noticed, immediately lower the pumping flowrate until no bubbles are present.

It is imperative to carefully monitor injection throughout the duration to ensure that injection is not interrupted, such as if the injection-in tube rises to the surface. It is also imperative that all solutions containing injected solutes are collected and recorded for flow balance calculations, as detailed below. Once extraction solution carboys are filled, they must be placed in the oil-water separator sump-pump to prevent contamination of bromide tracers to the Oneida site. ***Failure to follow this instruction will prevent future PPTs from using bromide as a tracer due to the presence of bromide in background samples.***

Materials

Well Installation

- Soil auger and extensions
- 2 pipe wrenches to disconnect auger
- Pry/digging bar
- Soil boring paper/clipboard
- Bentonite

- 1 foot section 2" PVC well screens per well
- 10 feet 2" PVC solid wall pipes per well
- 2 2" PVC caps per well
- 1 2" PVC coupler per well
- Sand – All Purpose – Backfill – ~1 bag per well
- Sand – Filter Sand – ~3 bags per well
- Weighted tape measure/sand packer
- PVC wire pipe cutter
- Saw
- Tape measure
- Spatula/knife/stake for soil removal from auger
- Soil auger cleaning kit
- Plastic bags, mason jars, and lids for soil collection
- Cooler with ice for soil storage
- Heavy work gloves

Push-pull Test

- Chemical concentrated solutions for 35 L injection solution – 750 mg/L bromide, optional 2 mg/L naphthalene → **Prepare prior to leaving**
- 3 carboys per well – 1 for injection solution, 2 for extraction solution → **Clean prior to leaving**
- 2 carboys filled with nanopure
- DO/other waste solution carboy
- Green Portable Masterflex® L/S™ Sampling Pump and 2 Masterflex® L/S™ Standard Drive pumps + spare fuses
- Masterflex® Tubing
- Water depth indicator + batteries
- Hach Kits™ (for DO, Fe^{+2}) + batteries (refer to general site trip materials list)
- Hach Kit™ Instructions
- pH meter + batteries
- Thermometer
- 2 mixing pumps
- Twist ties to attach injection in tubes to mixing pump
- 2 aquarium air bubblers
- Nitrogen tanks and diffuse aerator (for anaerobic tests only)
- Extension cords
- Circuit breaker or equivalent multi-plug extension cord
- Teflon tubing for two wells
- 30 40 ml EPA VOA amber vials per well
- 60 Scintillation vials per well
- 2 400 ml graduated cylinders for flow balance
- 2 200 ml graduated cylinders for flow balance
- 10 ml and 5 ml graduated cylinders for iron analysis
- 1 L beaker for adjusting clean water solution for injection

- Directions to site
- Weather forecast
- Well depth table
- PPT site map
- Background notes, flushing tables, clipboard
- Calculator
- 2 stopwatches
- Gloves – plastic, Viton™
- Minimum of 2 pairs of safety goggles
- Nanopure spray bottles
- Parafilm™
- Kim Wipes™
- Hard hats, first aid, sun tan lotion, bug spray, rain jackets
- Tool Boxes – must include a wrench to remove stubborn well caps, a knife to cut tubing, and pliers to turn the broken spigot for clean water for injection solution creation
- Tent
- Tarps
- Lab notebooks
- Sharpies
- Masking/labeling tape; duct tape for Parafilm™
- 3 coolers with ice for samples
- Snacks/water
- Paper towels
- Garbage bags

Injection

1. One partner fills the two injection solution carboys to 35 L with tap water, while the other partner begins setting up in-situ constituent Hach kit analysis and pump setup. Caution should be used when filling the carboys to ensure spigot corrosion products do not enter the clean water used for injection solution creation. Blank IC and GC samples should be collected from the tap water for quality control. In-situ analysis includes DO, and ferrous iron and may eventually include hydrogen gas analysis.
2. Place aerators within the 35 L solution to enable a maximum DO concentration.
3. Adjust flow rate of the green Portable Masterflex® L/S™ Sampling Pump, the preferred injection pump, to 0.5 L/min, which is marked at approximately 9.4 RPM.
4. Laminated Hach Kit™ instructions provide the details of how to perform the DO and ferrous iron analysis.
5. Prepare individual carboy with concentrate. First, place injection-in Teflon™ tubing with attached submersible mixing pump into the injection solution carboy. Note the side of the carboy that the injection-in tube is placed (for tilting the carboy later). Next, empty bromide solid into the injection carboy first, rinsing several times with DI water. Next, empty naphthalene concentrate solution into the carboy, rinsing several times with DI water. Rinse water is placed within the injection solution

carboy. Place several layers of Parafilm™ on top of lid, securing with duct tape. Shake gingerly to avoid spilling. Allow time to stabilize.

6. Determine the depth of groundwater within the well-casing using the groundwater depth indicator.
7. Calculate the volume of groundwater located within the well-casing.
8. Join the two six foot sections of ¼ - 20 rod with the coupler. Attach the three extraction-in tubes so they are 6" from the bottom of the rod. Attach the injection-out tube 3" above the extraction-in tubes for a total of 9" from the bottom of the rod. Mark the rod at a distance from the end of the rod that is equivalent to the total depth of the test well. Insert the rod into the well, making sure the mark on the rod lines up with the top of the well (The rod can become 'hung up' on the coupler prior to the perforated well-casing).
9. The extraction in/out tubes are then attached to the Masterflex® L/S™ Standard Drive pump, observing the direction (clockwise/counterclockwise) that is needed for sample collection. The free end of the extraction-out tube is then placed in the 2 L graduated cylinder for measurement of backflushing volume. The injection in/out tubes are then attached to the green Portable Masterflex® L/S™ Sampling Pump and the direction switch is set to ensure injection of the solution.
10. Confirm pump flow directions are correct.
11. Perform the identical setup for the second test well, keeping in mind that the green Portable Masterflex® L/S™ Sampling Pump and the groundwater depth indicator will be moved to the second well upon completion of the injection phase from the first well.
12. Remove a minimum of three pore volumes of the groundwater located within the well-casing from the test well, prior to background sample collection.
13. Collect duplicate background samples for ferrous iron, IC, and GC analysis.
14. Triplicate DO background samples should be collected and injection should not begin until stable results exist for DO, and ferrous iron measurements.
15. Once sampling is complete for the iron background samples, the temperature and pH is measured and recorded. At this time, record the weather conditions at the site.
16. The groundwater depth indicator is placed a minimum of one foot from the surface of the test well. If the indicator beeps, the injection flowrate must be lowered immediately to prevent overflow.
17. Begin injecting contaminant and monitor time with a stopwatch. It is imperative to ensure that the injection is not interrupted. Simply confirm periodically that the pump is indeed pumping water and not air.
18. At each ten minute interval, a minimum of 200 ml must be backflushed from the extraction tube to prevent contamination from the previous sampling period. The volume backflushed is then recorded and the solution is placed in the extraction solution carboy.
19. IC and DO samples are collected every ten minutes. DO results are recorded.
20. GC and ferrous iron samples are collected every 20 minutes, which corresponds to injection times 10, 30, 50, and so on. The volume of sample removed for the iron samples is recorded. Once analysis is complete, the volume of iron sample remaining is recorded and the remaining solution is placed in the extraction solution carboy. Iron results are then recorded.

21. Before the unused portion of the injection 30 minute iron sample is added to the extraction solution carboy, the pH and the temperature is measured and recorded.
22. Continue sampling IC and DO every 10 minutes and iron and GC every 20 minutes. When the injection solution carboy is nearly depleted, tilt the carboy to the side where the injection-in tube was placed to ensure that the entire 35 L is injected.
23. Once injection is complete, record the time for the completion of the injection phase. Reset and start the stopwatch immediately.

Extraction

1. Immediately following completion of injection, adjust the flow rate of the Masterflex® L/S™ Standard Drive pump to between 0.25 – 0.35 L/min, which is approximately 8 RPM for the Masterflex® L/S™ Standard Drive pump and 5 RPM for the green Portable Masterflex® L/S™ Sampling Pump.
2. Remove the green Portable Masterflex® L/S™ Sampling Pump injection pump.
3. During a lull in the extraction phase, setup the green Portable Masterflex® L/S™ Sampling Pump and the groundwater depth indicator at the second test well. Follow the identical procedure outlined in these instructions, except only one pair of extraction in/out tubes is needed in the second well. Following completion of the injection phase, the extraction in/out tubes are transferred from the Masterflex® L/S™ Standard Drive pump to the green Portable Masterflex® L/S™ Sampling Pump. The flowrate on the green Portable Masterflex® L/S™ Sampling Pump is then lowered to between 0.25 – 0.35 L/min, which is approximately 5 RPM.
4. Perform the final backflushing and record the volume.
5. Collect IC, GC, DO, and iron extraction time zero samples.
6. Stop the stopwatch and record the time between the injection and extraction phases.
7. Reset and start the stopwatch, while turning the extraction pump on. Place the extraction-out tubes in the 4 L graduated cylinder.
8. At each ten minute interval, collect DO and IC samples. Place the extraction-out tubes temporarily in the extraction solution carboy. Record the volume collected in the 4 L graduated cylinder and the time interval during the collection. Place the collected solution in the extraction solution carboy.
9. Place the extraction-out tubes in the 4 L graduated cylinder and record the time of the beginning of the new flowrate measurement.
10. Collect GC and iron samples every 30 minutes, corresponding to extraction times 0, 30, 60, and so on.
11. When the first extraction solution carboy is full, transfer the extraction-out tubes into the second extraction solution carboy. Empty the full extraction solution carboy into the sump pump for the oil/water separator. Record the volume collected as each carboy becomes full.
12. The extraction phase is complete when either 3 times the injected volume is extracted (105 L) OR the DO concentration stabilize to a value equal to or less than background concentrations and iron/sulfide concentrations stabilize at a value equal to or greater than the background concentrations.
13. Record the total volume of extraction solution collected and the time to complete the test.

APPENDIX B: SOIL BORING LOGS

Appendix B contains the five soil boring logs created during well construction. Each soil boring log refers to a well pair. For example, the first soil log is for the control well pair, S1 and D1. Wells were created using a soil auger. The depth to the groundwater table (GWT) was recorded. The depth to the bottom of the well casing (BS) was recorded. A minimum of 1.5 feet of filter sand was added and the depth to the top of the filter sand (FS) was recorded. A minimum of one foot of bentonite was added to remove preferential channeling and the depth to the top of the bentonite (BT) was recorded. The well boring was then backfilled with multi-purpose sand and capped with bentonite. Greater detail of well construction can be found in 3.3 Well Construction.

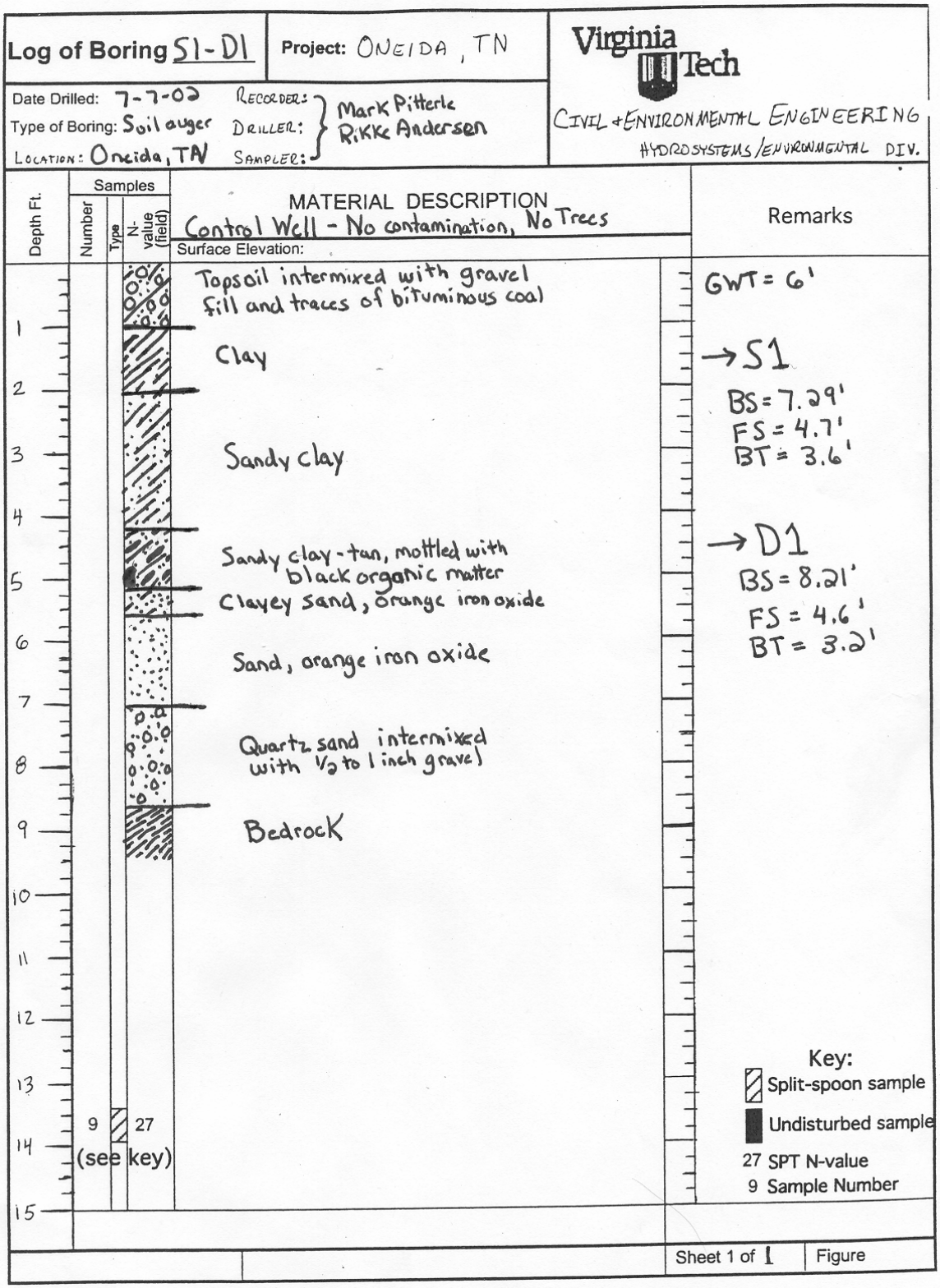

Figure B1: Soil Boring Log of Push-pull Test Well Pair S1-D1

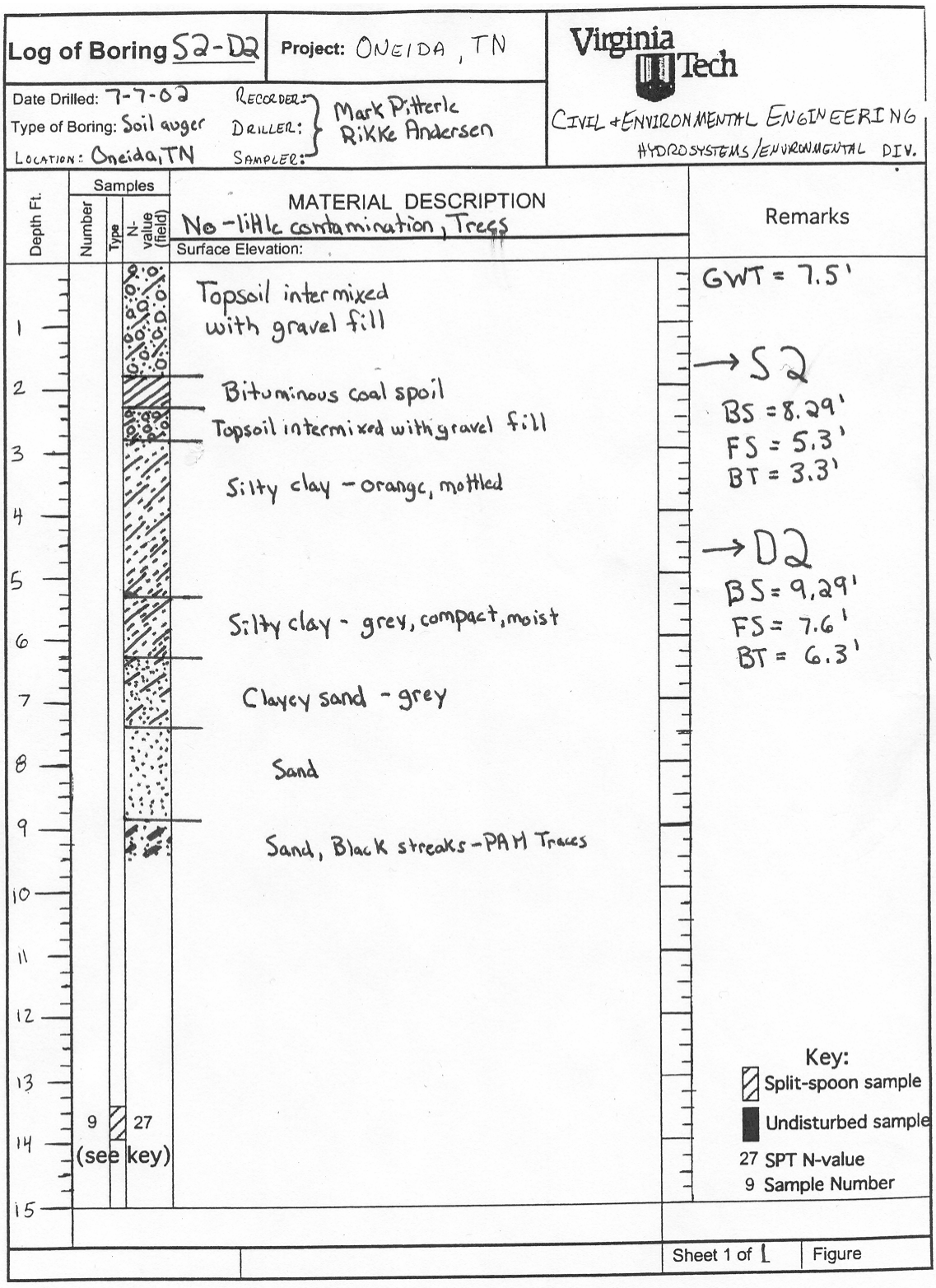

Figure B2: Soil Boring Log of Push-pull Test Well Pair S2-D2

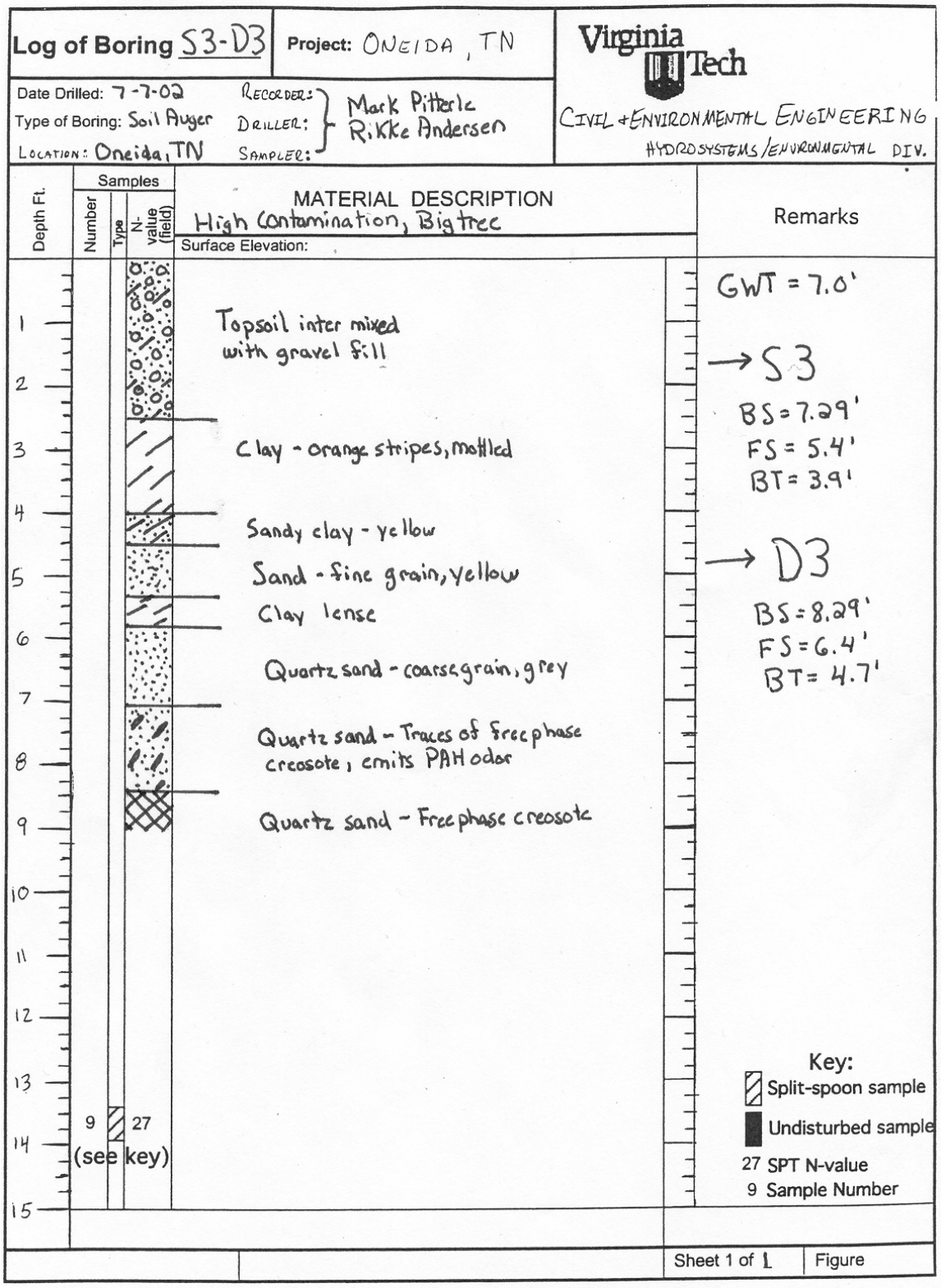

Figure B3: Soil Boring Log of Push-pull Test Well Pair S3-D3

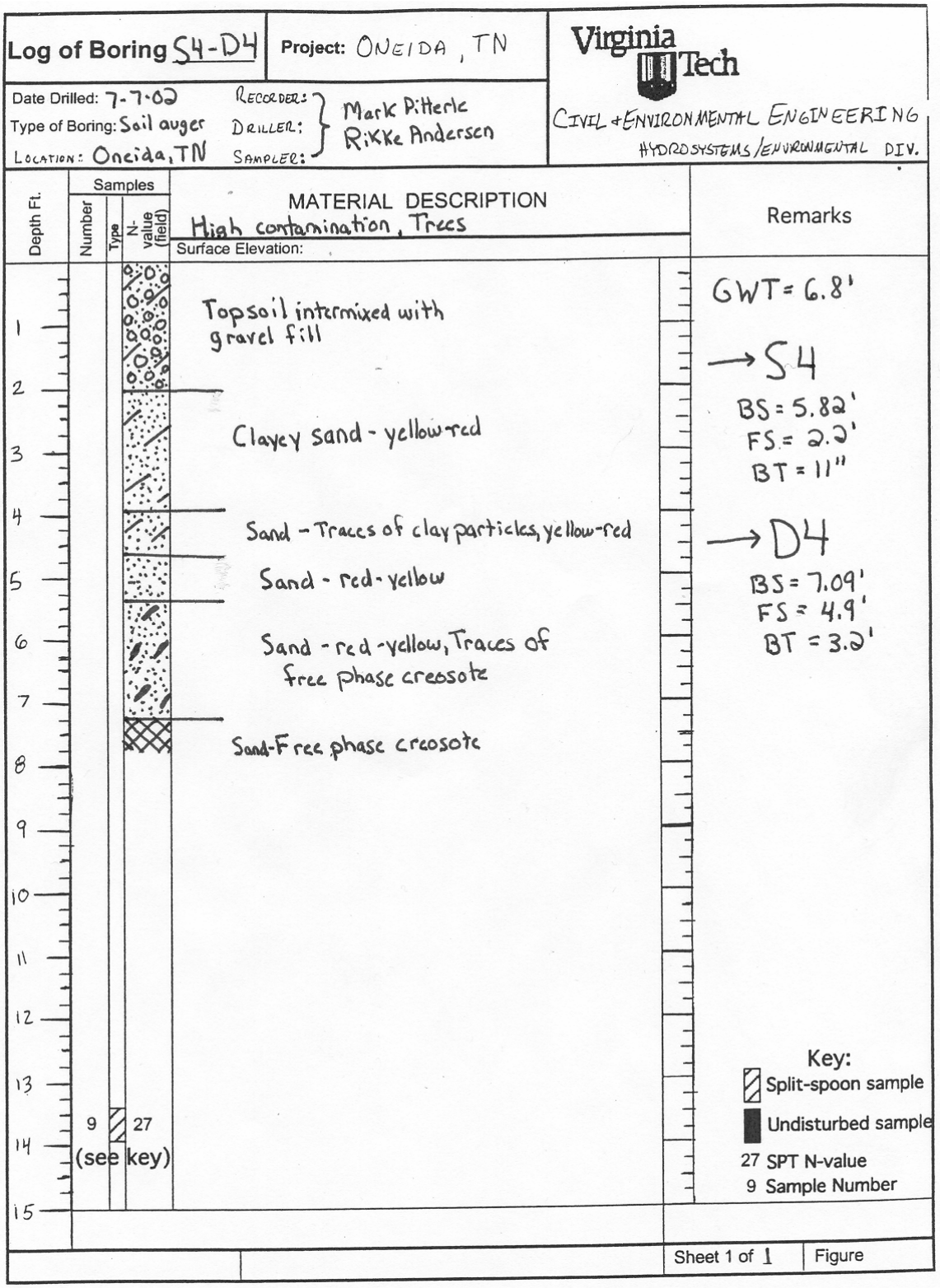

Figure B4: Soil Boring Log of Push-pull Test Well Pair S4-D4

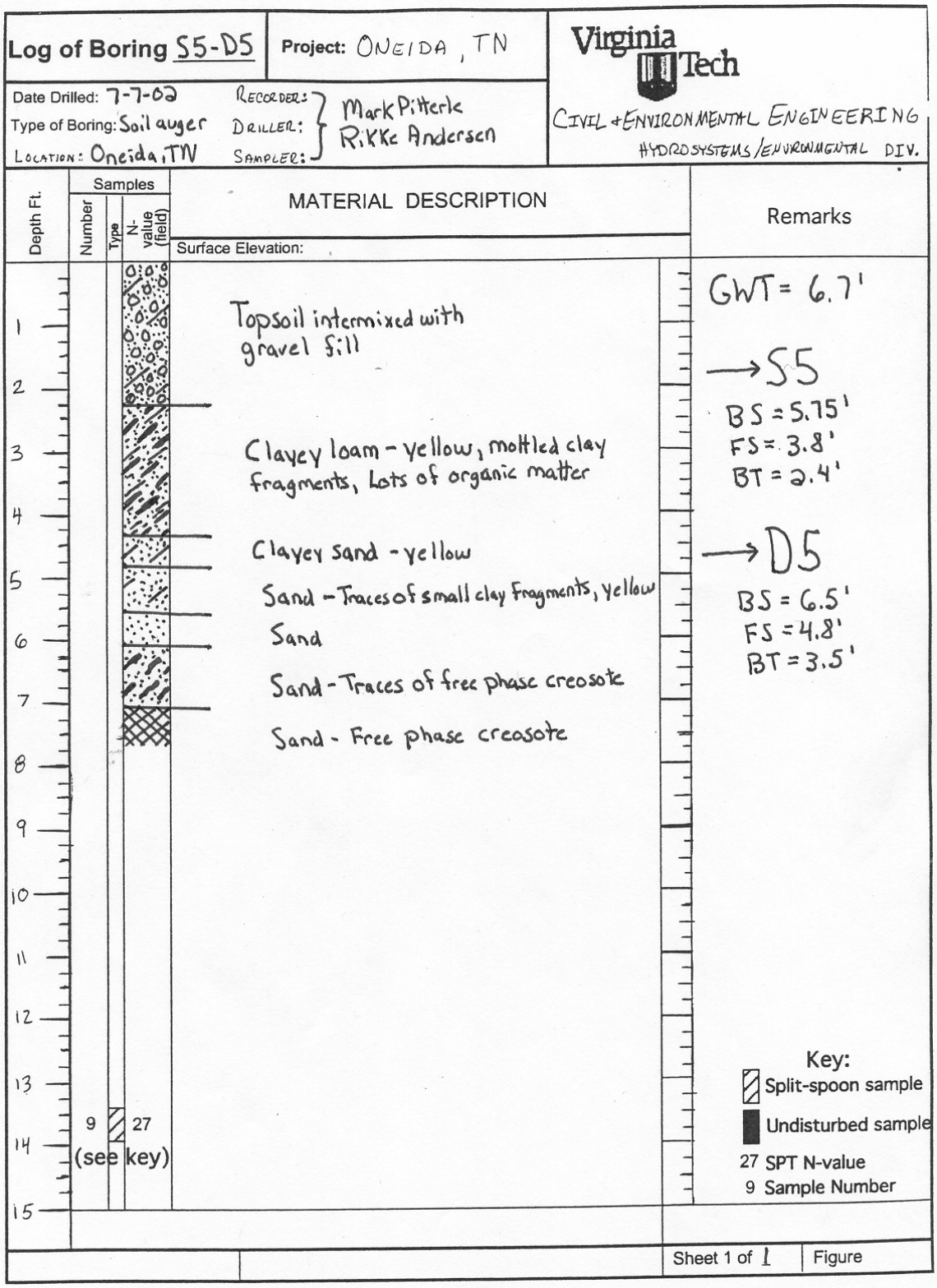

Figure B5: Soil Boring Log of Push-pull Test Well Pair S5-D5

APPENDIX C: PUSH-PULL TEST BREAKTHROUGH CURVES AND ZERO AND FIRST ORDER PLOTS

Appendix C chronologically displays all PPT BTCs and the zero and first order regression analysis plots for the methods of Snodgrass and Kitanidis (1998) and Haggerty et al. (1998). For each test, four graphs are divided on two separate pages. The specific PPT BTC and the Snodgrass and Kitanidis (1998) zero order regression analysis plot is on the first page and the first order regression analysis plots for the methods of Snodgrass and Kitanidis (1998) and Haggerty et al. (1998) are displayed on the second page, respectively. For Haggerty et al. (1998) first order plots, it should be noted that the y-intercept data point (i.e. the data point at time zero) is used for illustrative purposes only and this data point was not used in regression analysis or R^2 calculations.

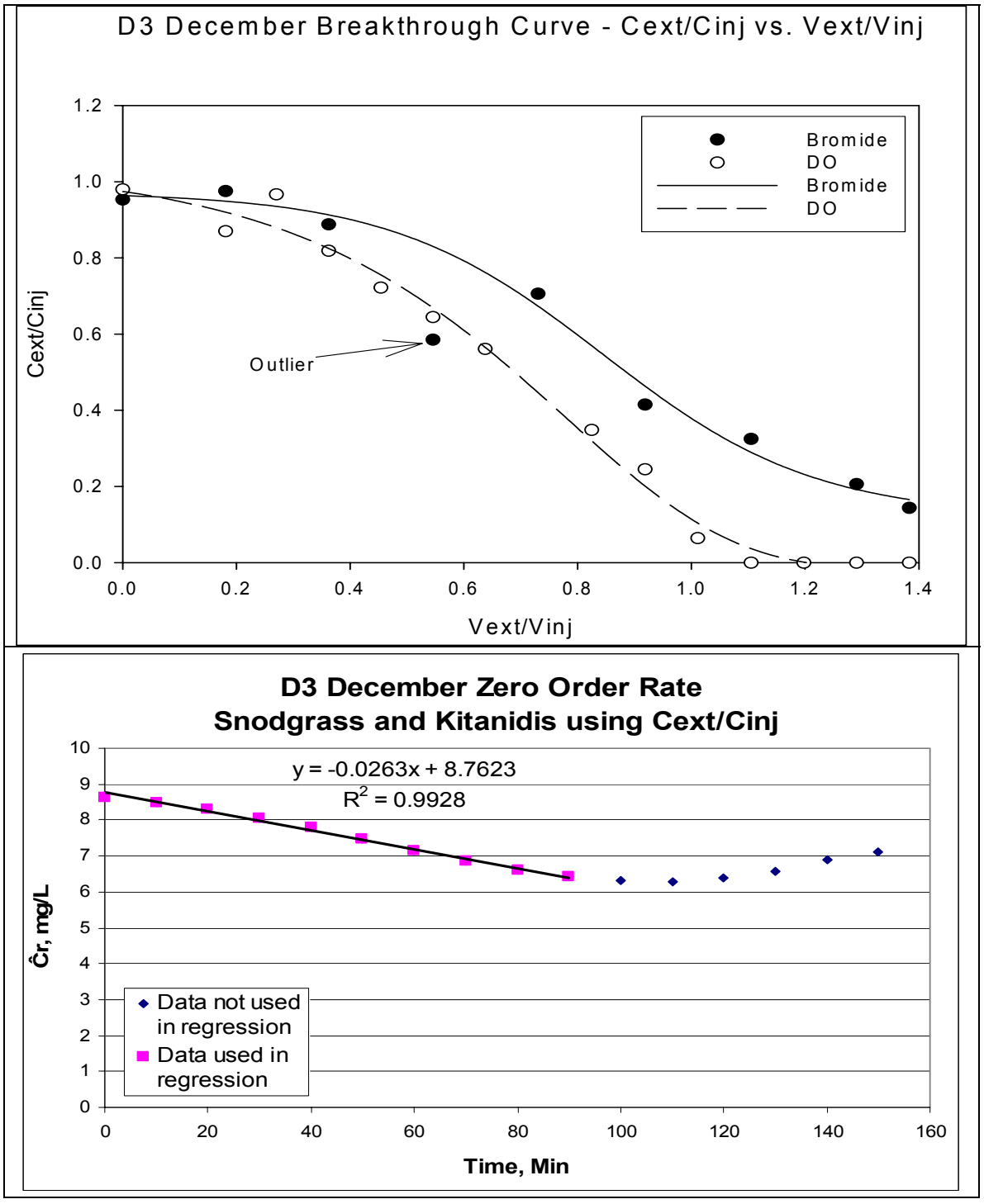

Figure C1: Push-pull Test D3 December

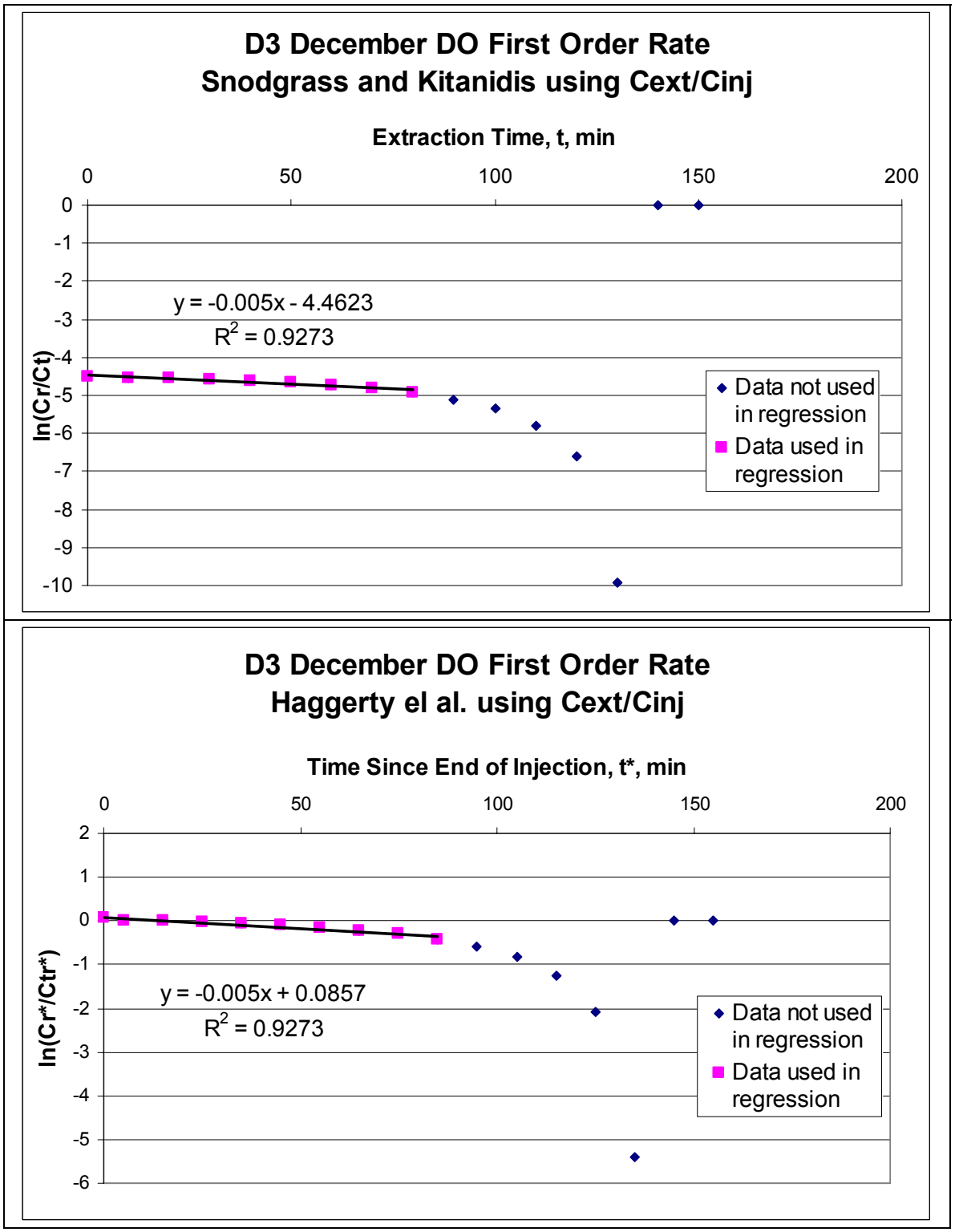

Figure C1 (cont.): Push-pull Test D3 December

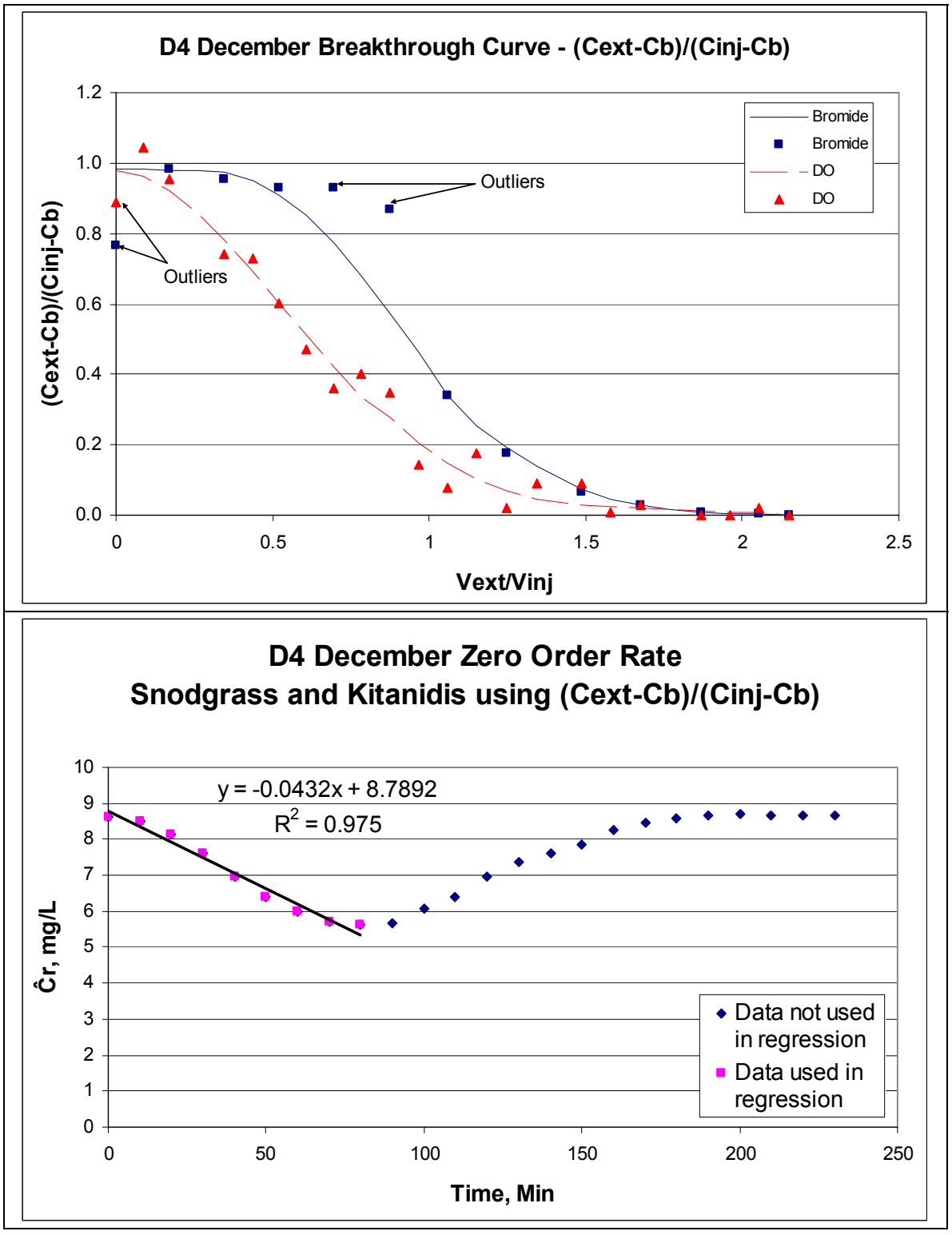

Figure C2: Push-pull Test D4 December

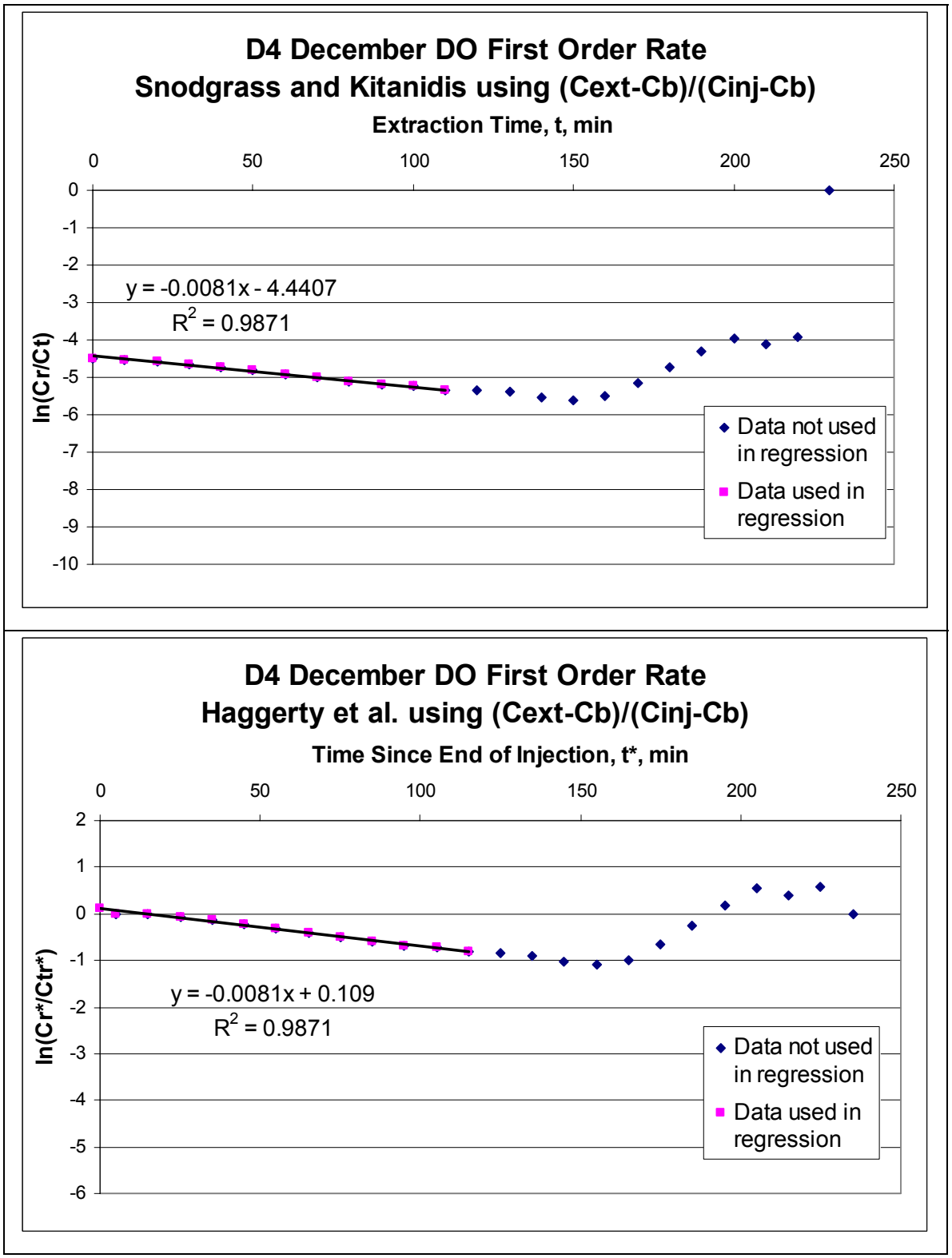

Figure C2 (cont.): Push-pull Test D4 December

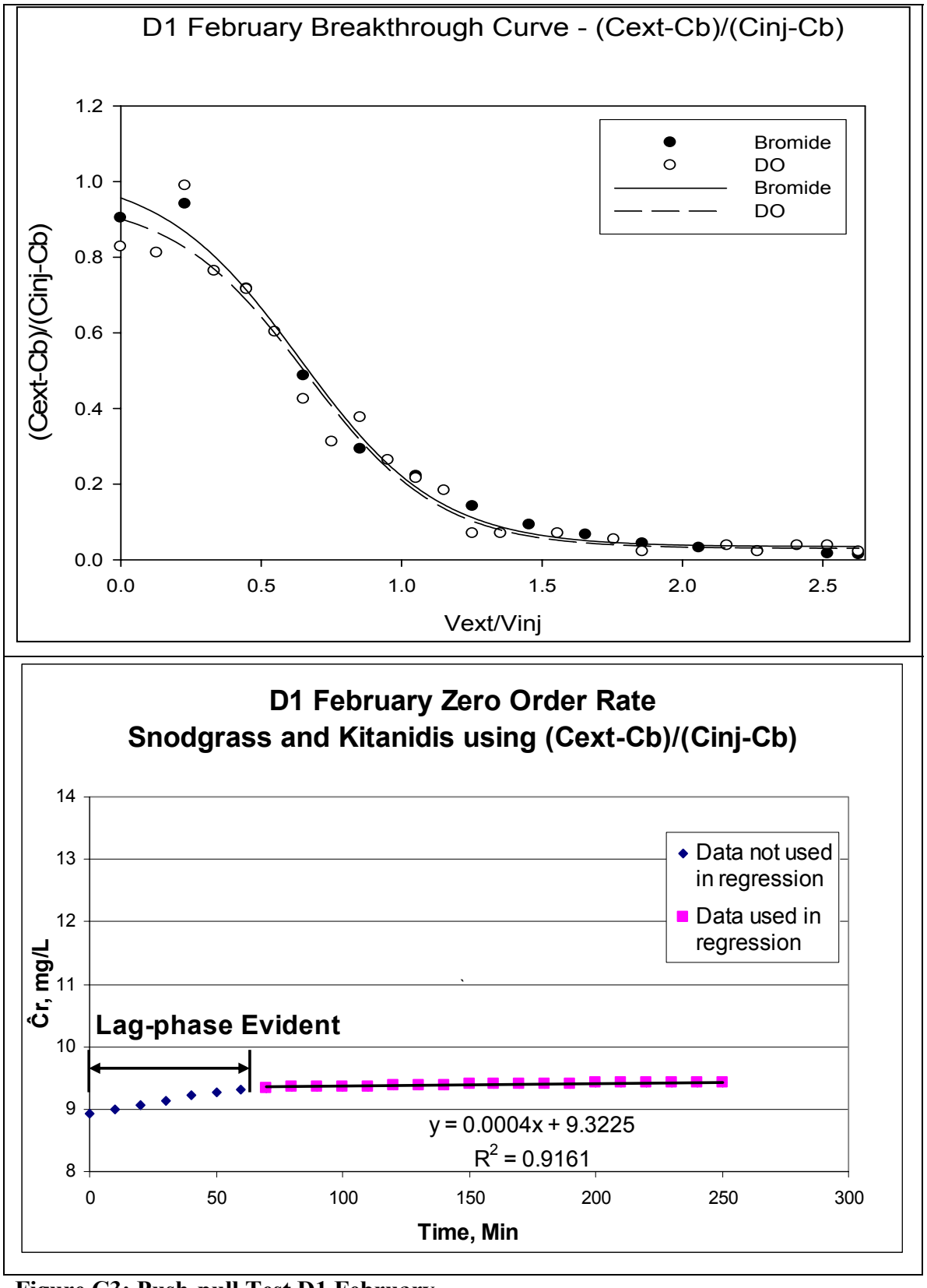

Figure C3: Push-pull Test D1 February

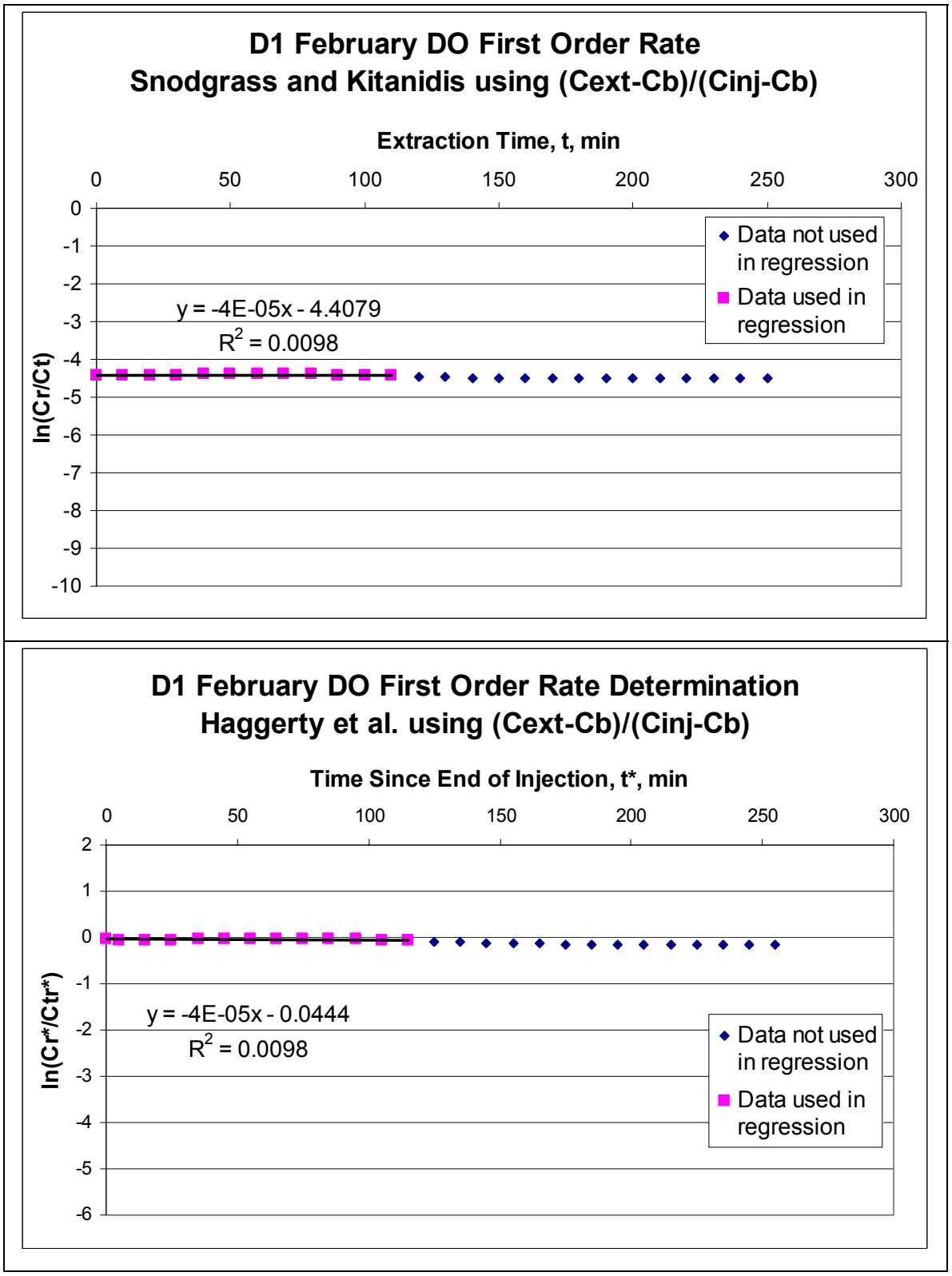

Figure C3 (cont.): Push-pull Test D1 February

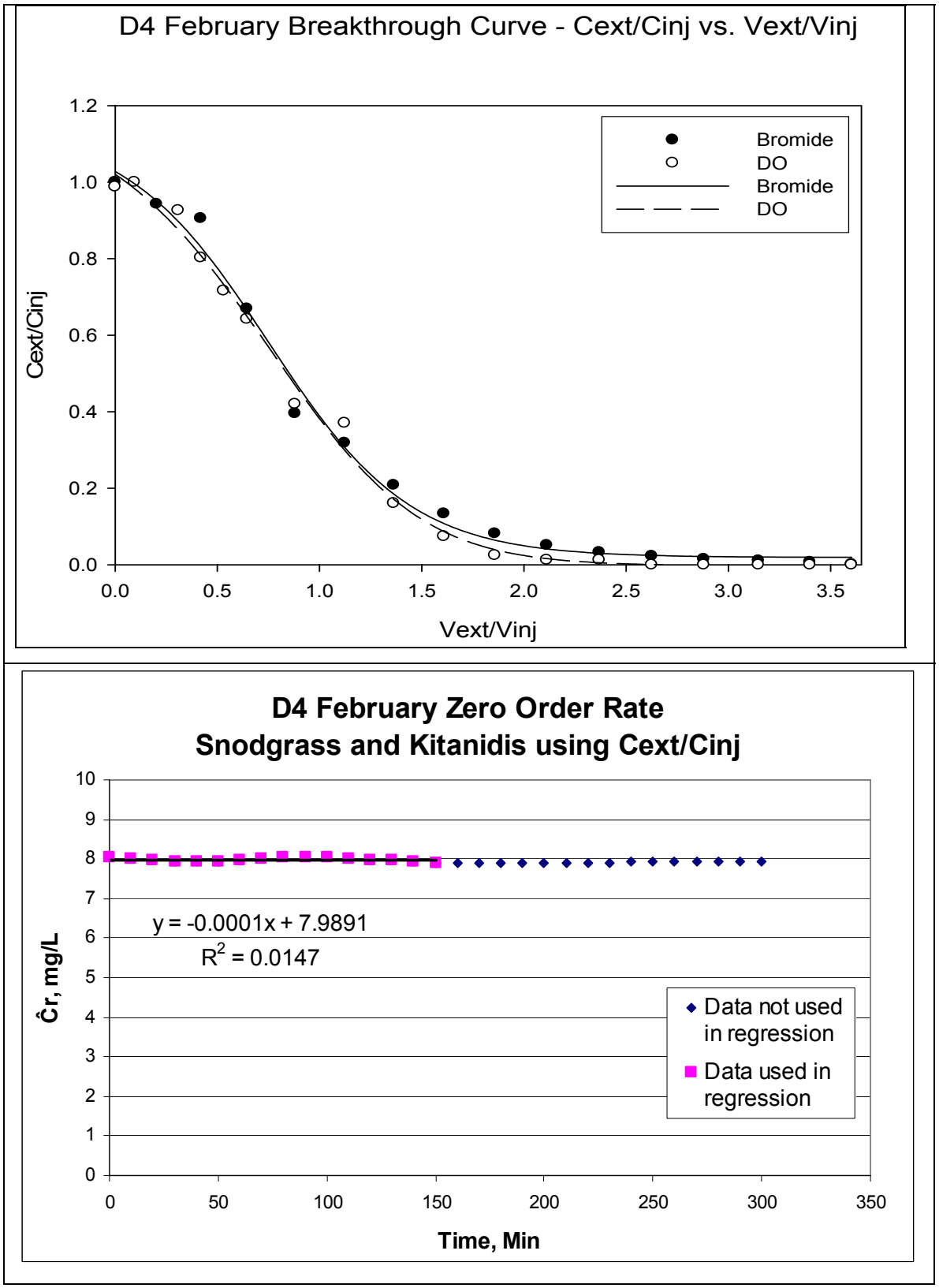

Figure C4: Push-pull Test D4 February

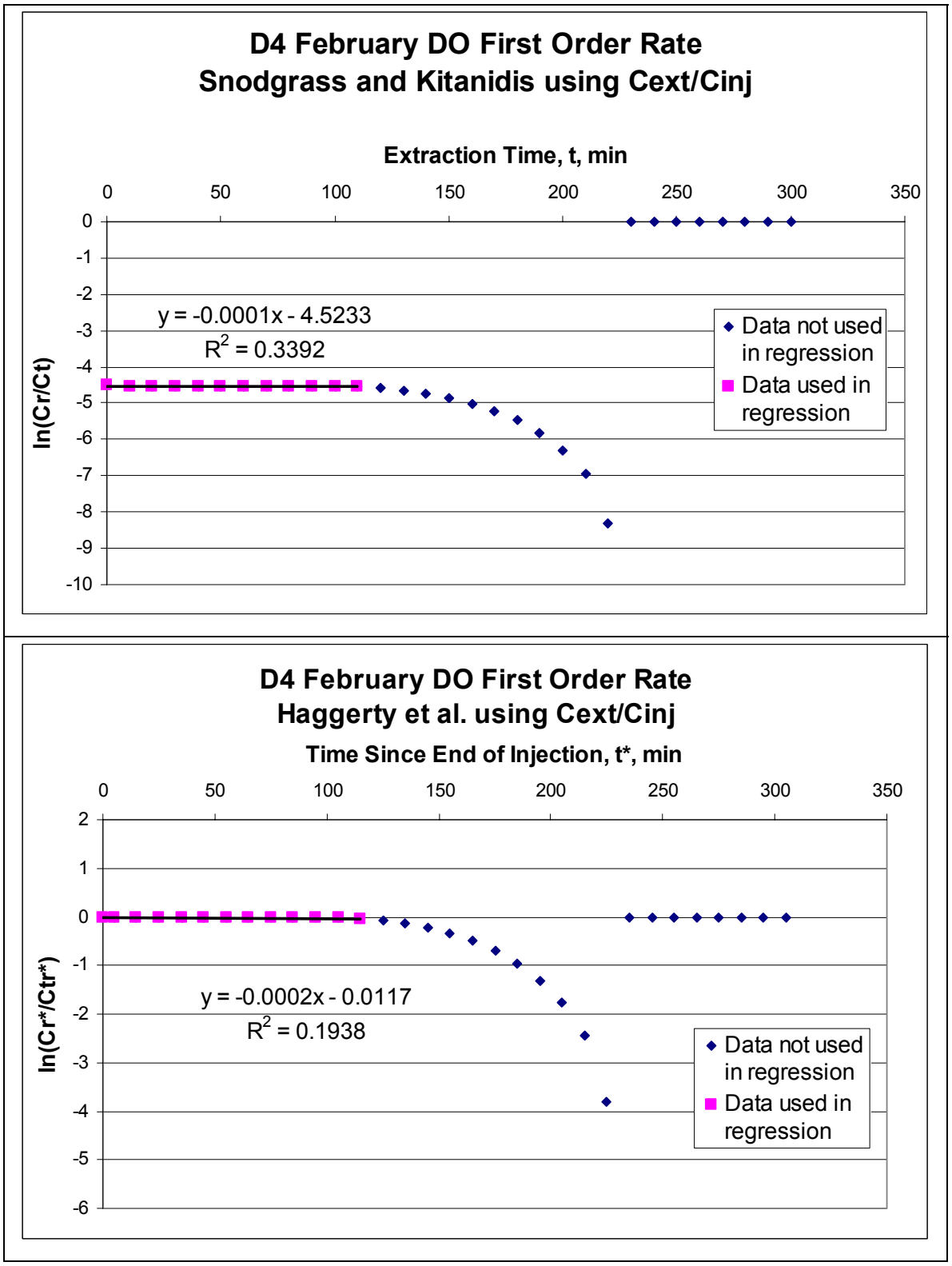

Figure C4 (cont.): Push-pull Test D4 February

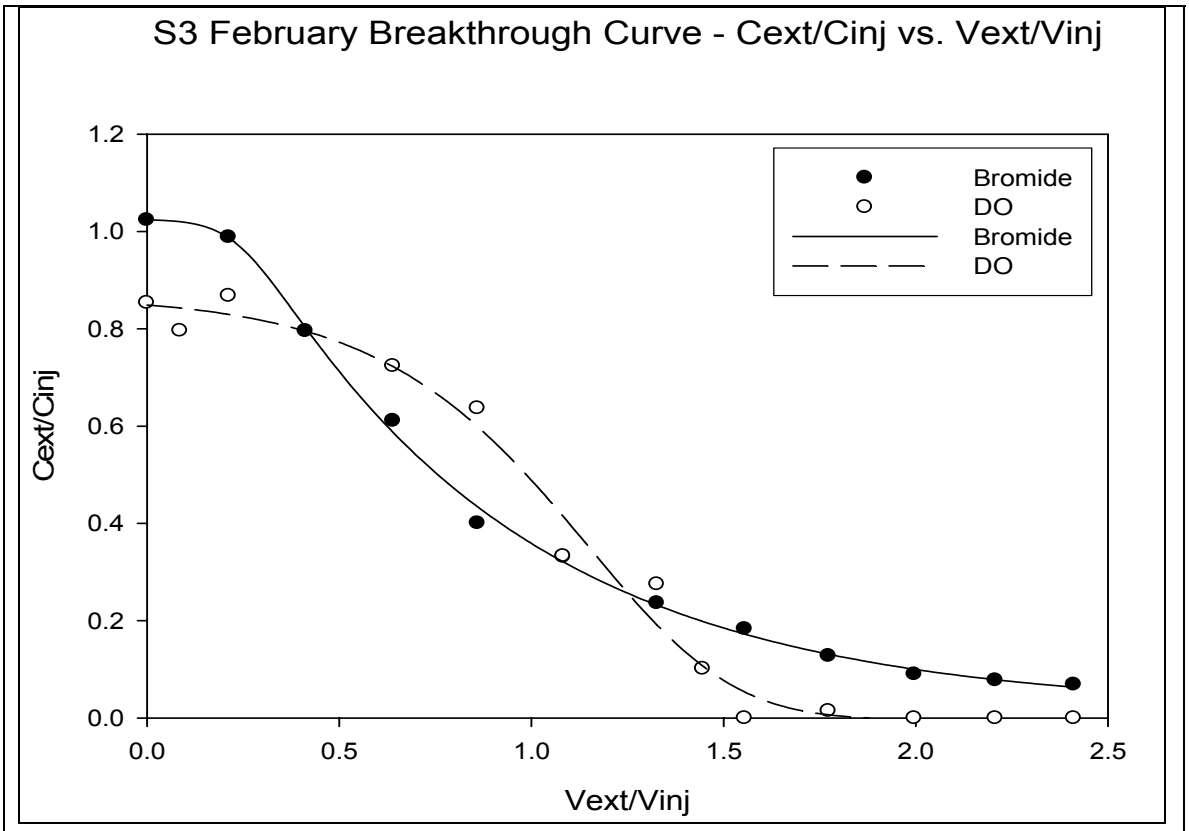

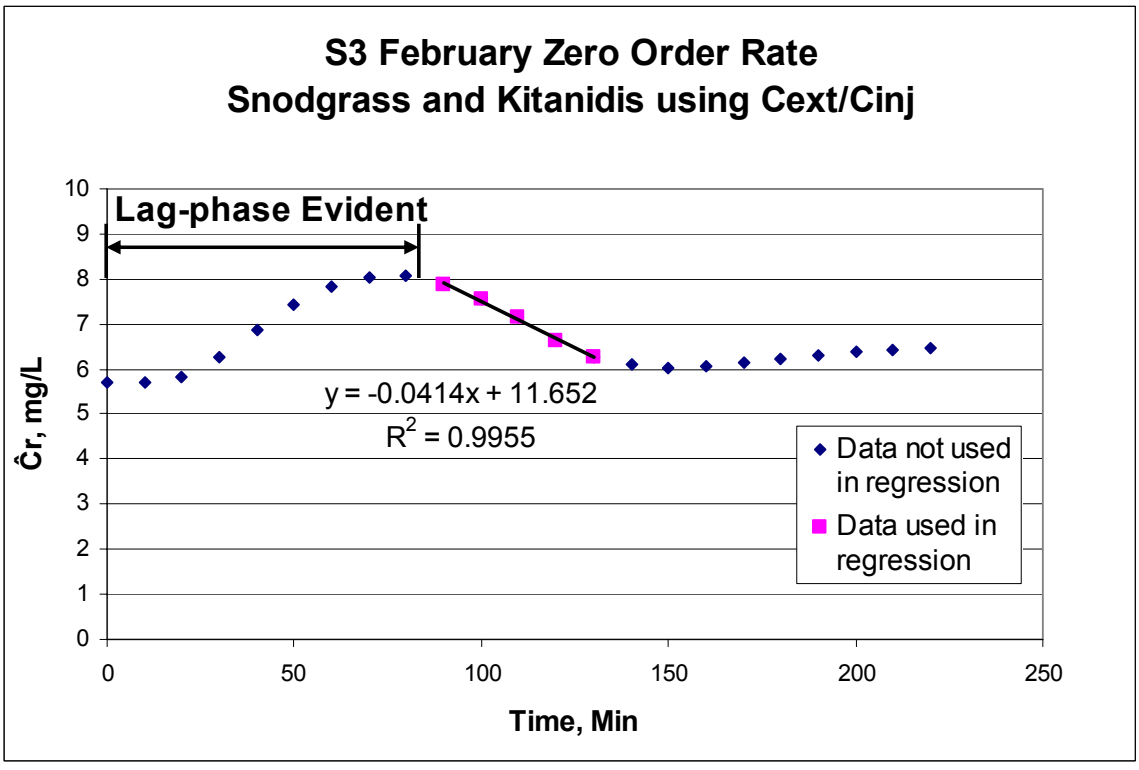

Figure C5: Push-pull Test S3 February

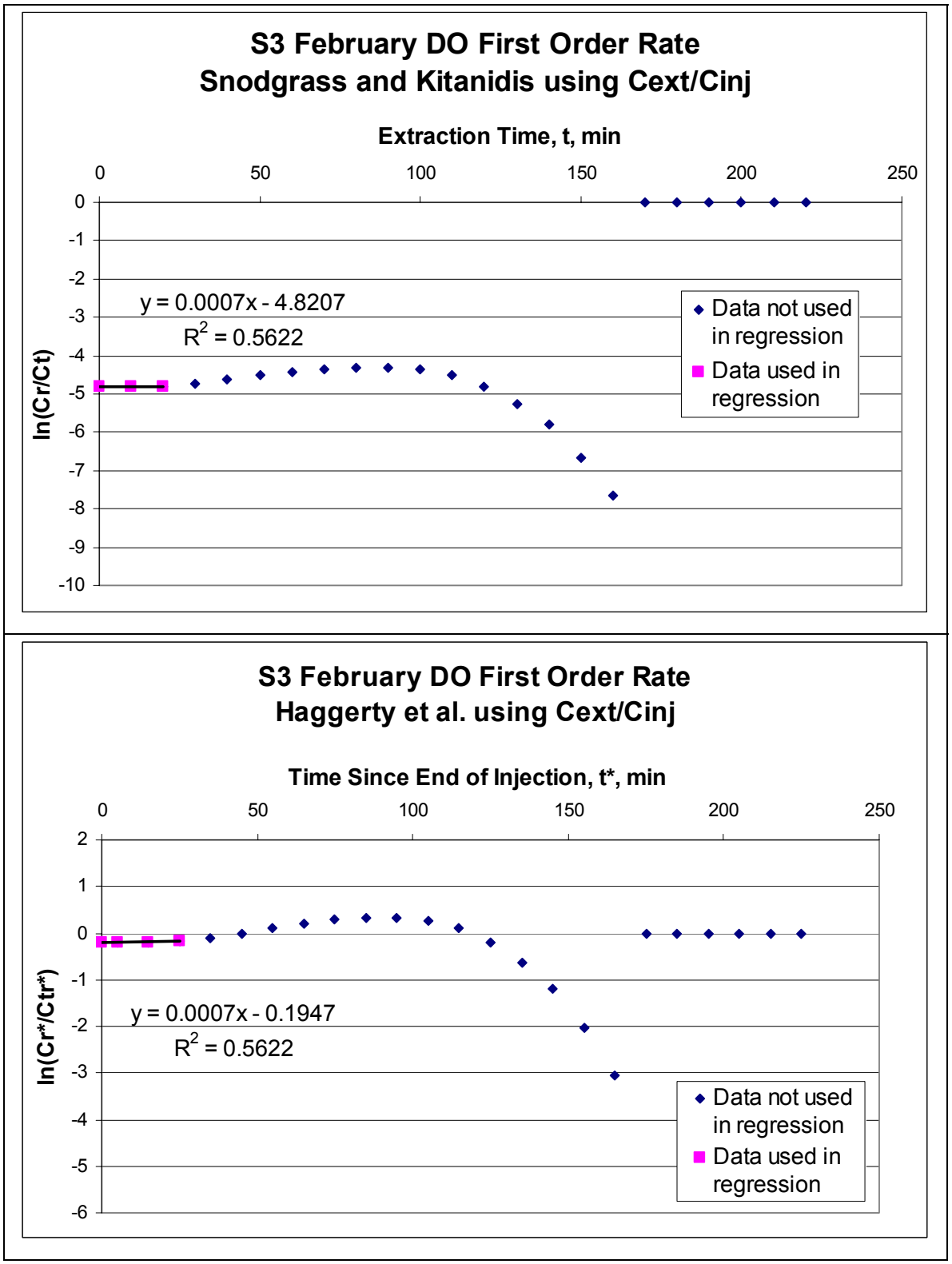

Figure C5 (cont.): Push-pull Test S3 February

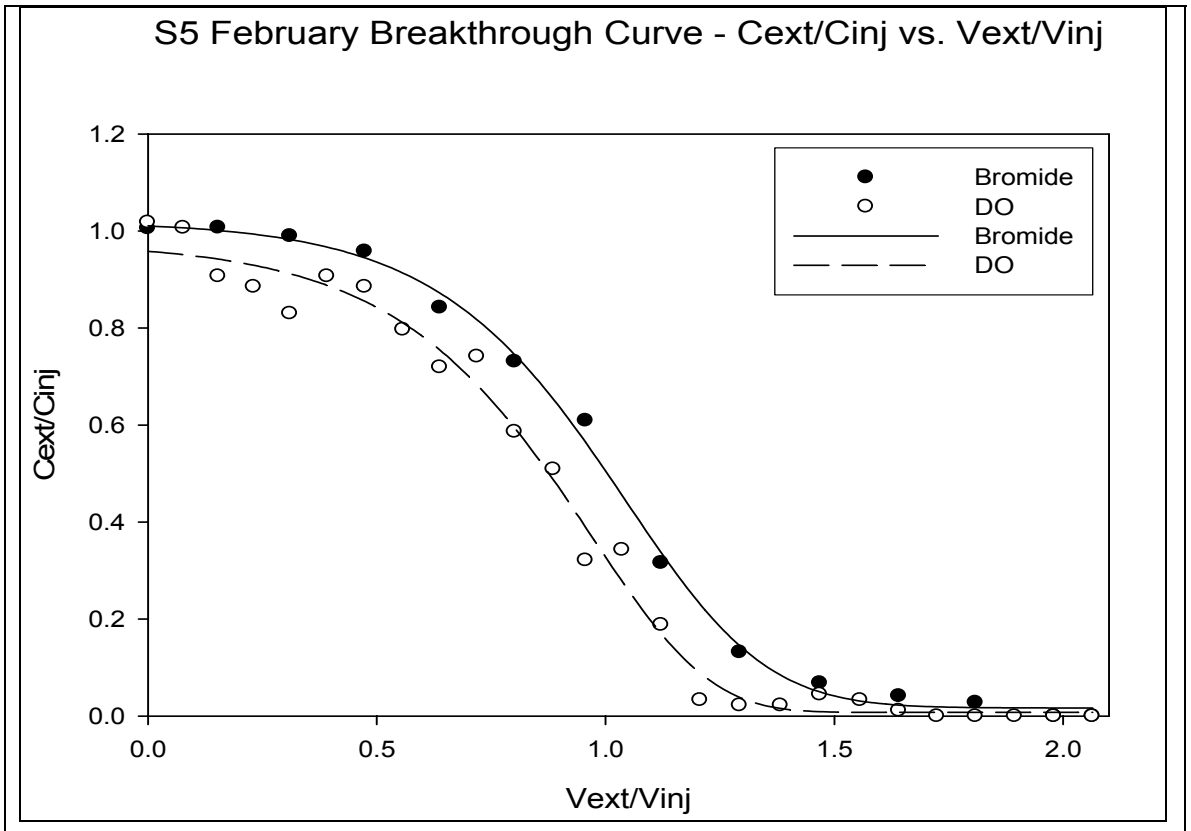

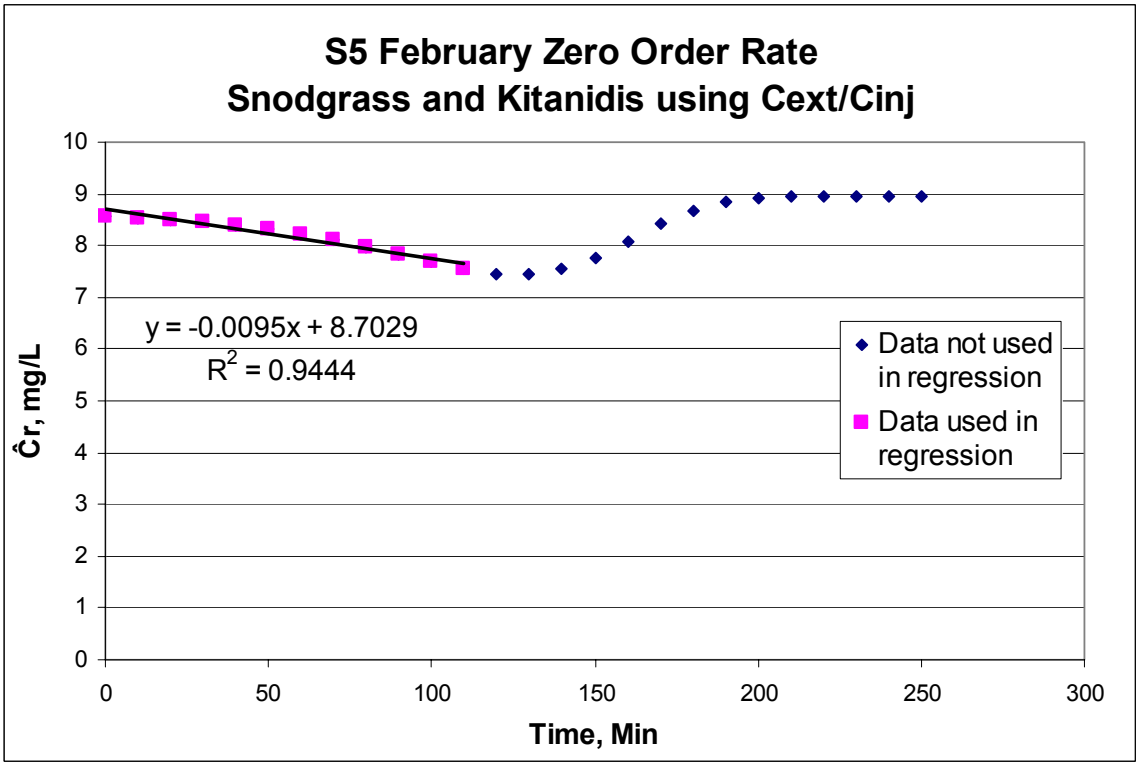

Figure C6: Push-pull Test S5 February

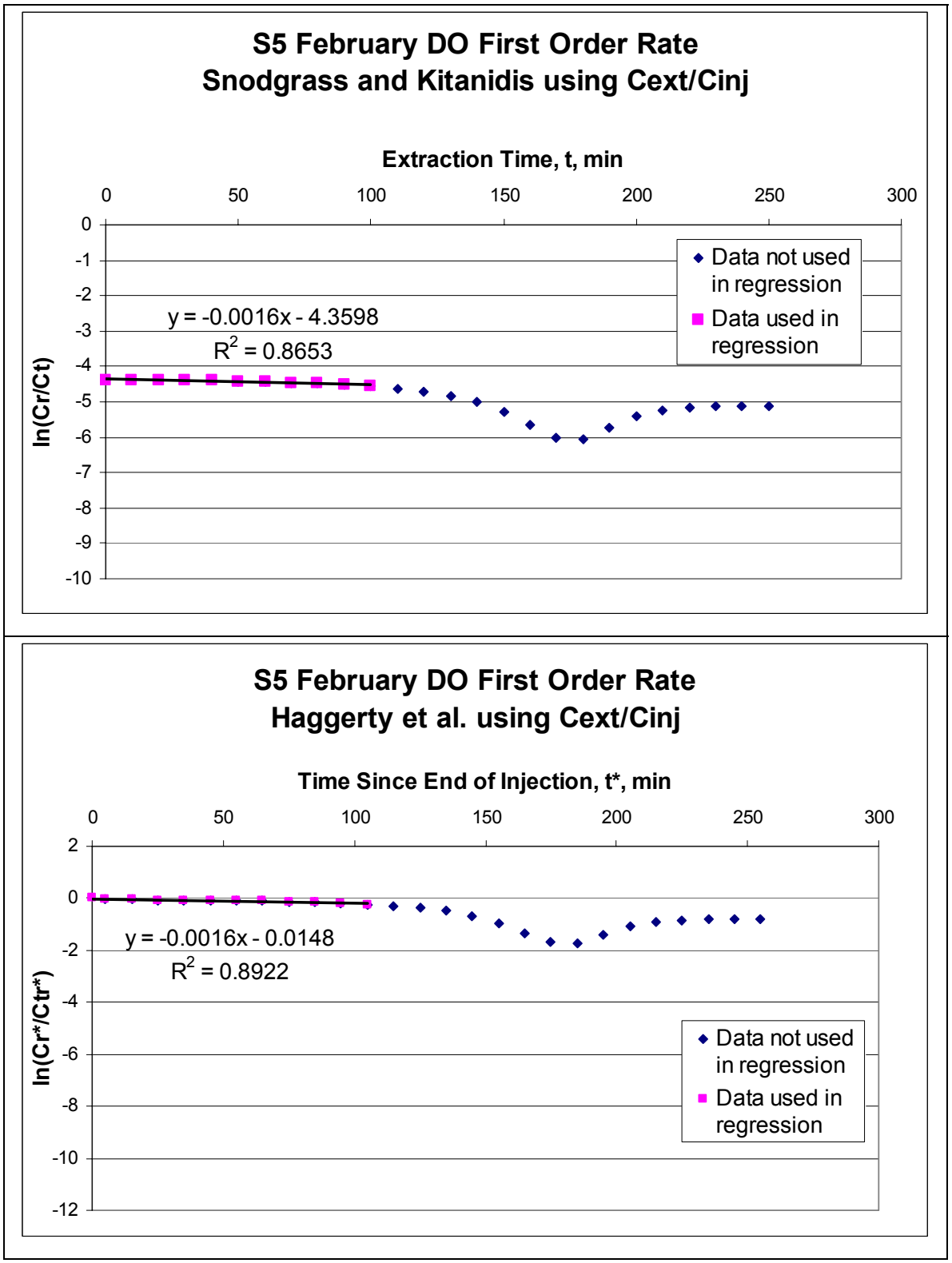

Figure C6 (cont.): Push-pull Test S5 February

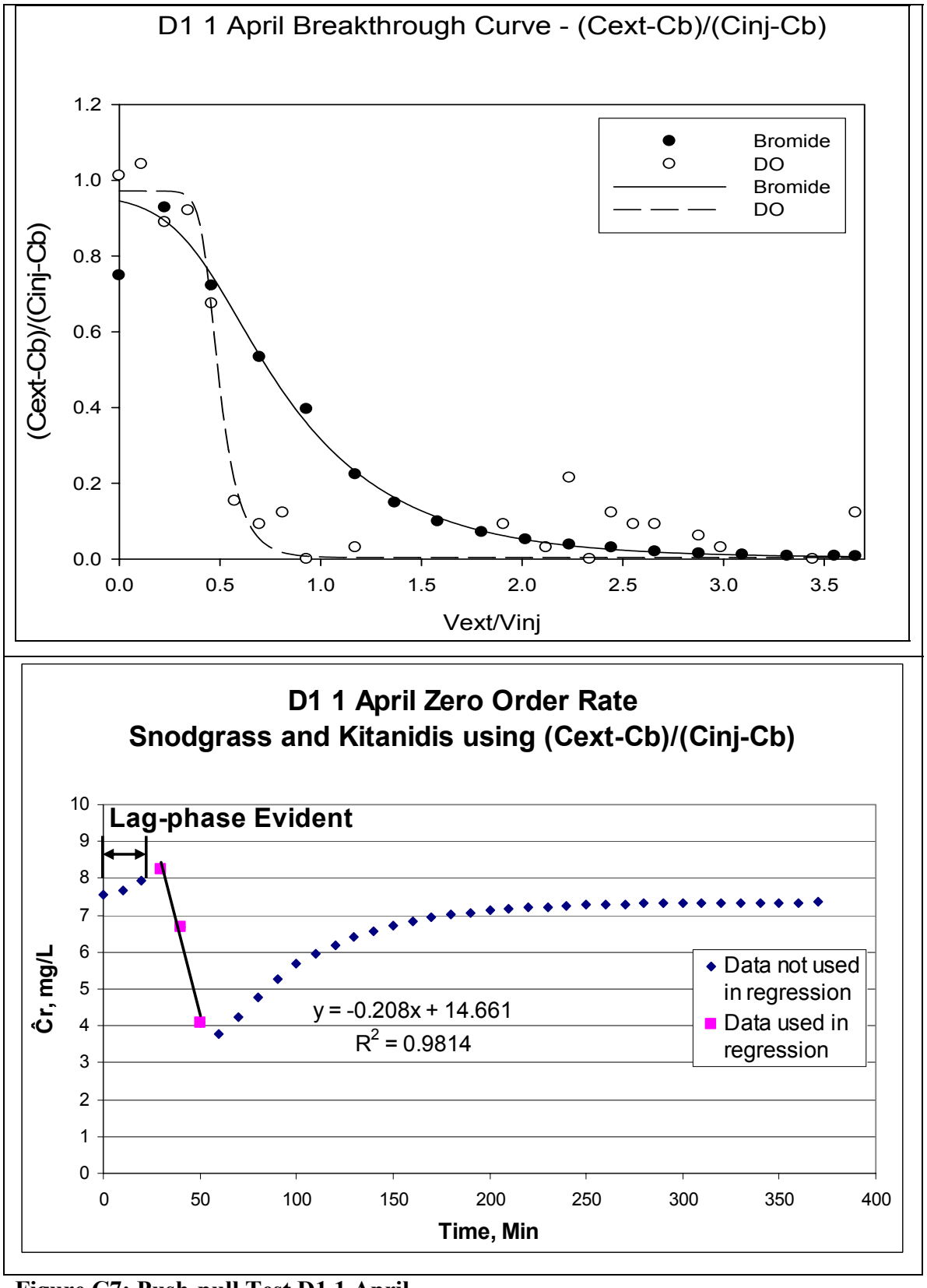

Figure C7: Push-pull Test D1 1 April

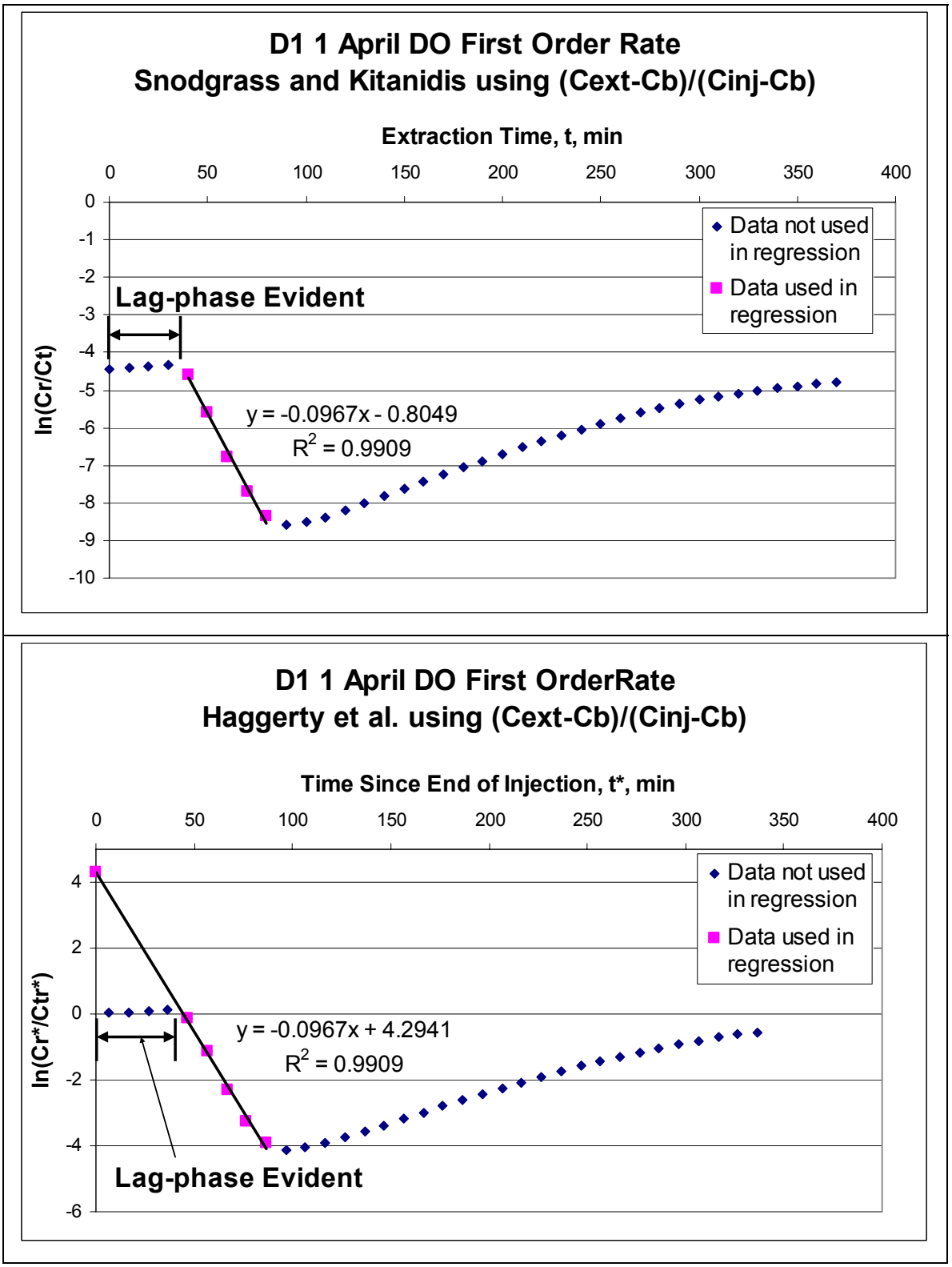

Figure C7 (cont.): Push-pull Test D1 1 April

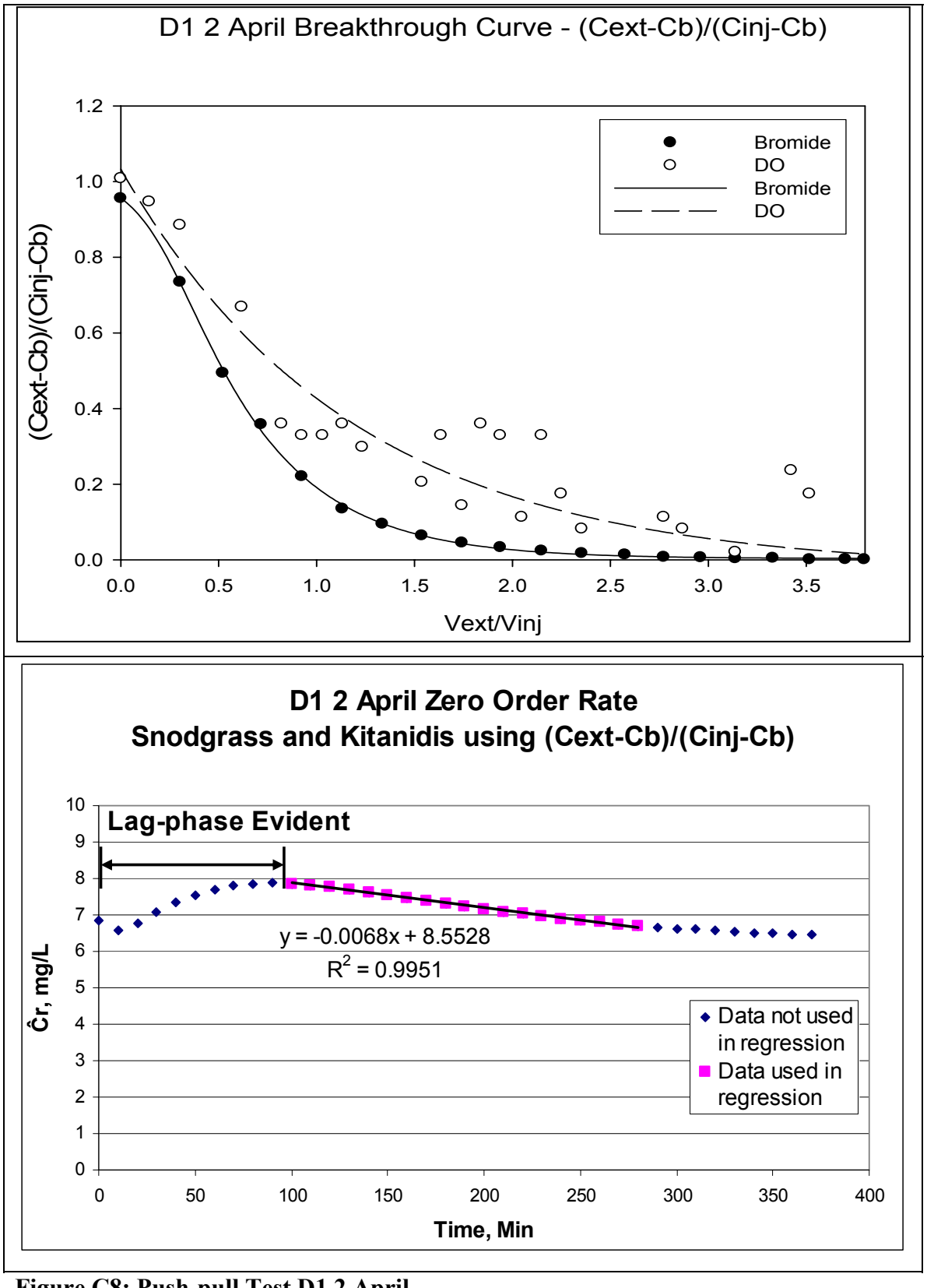

Figure C8: Push-pull Test D1 2 April

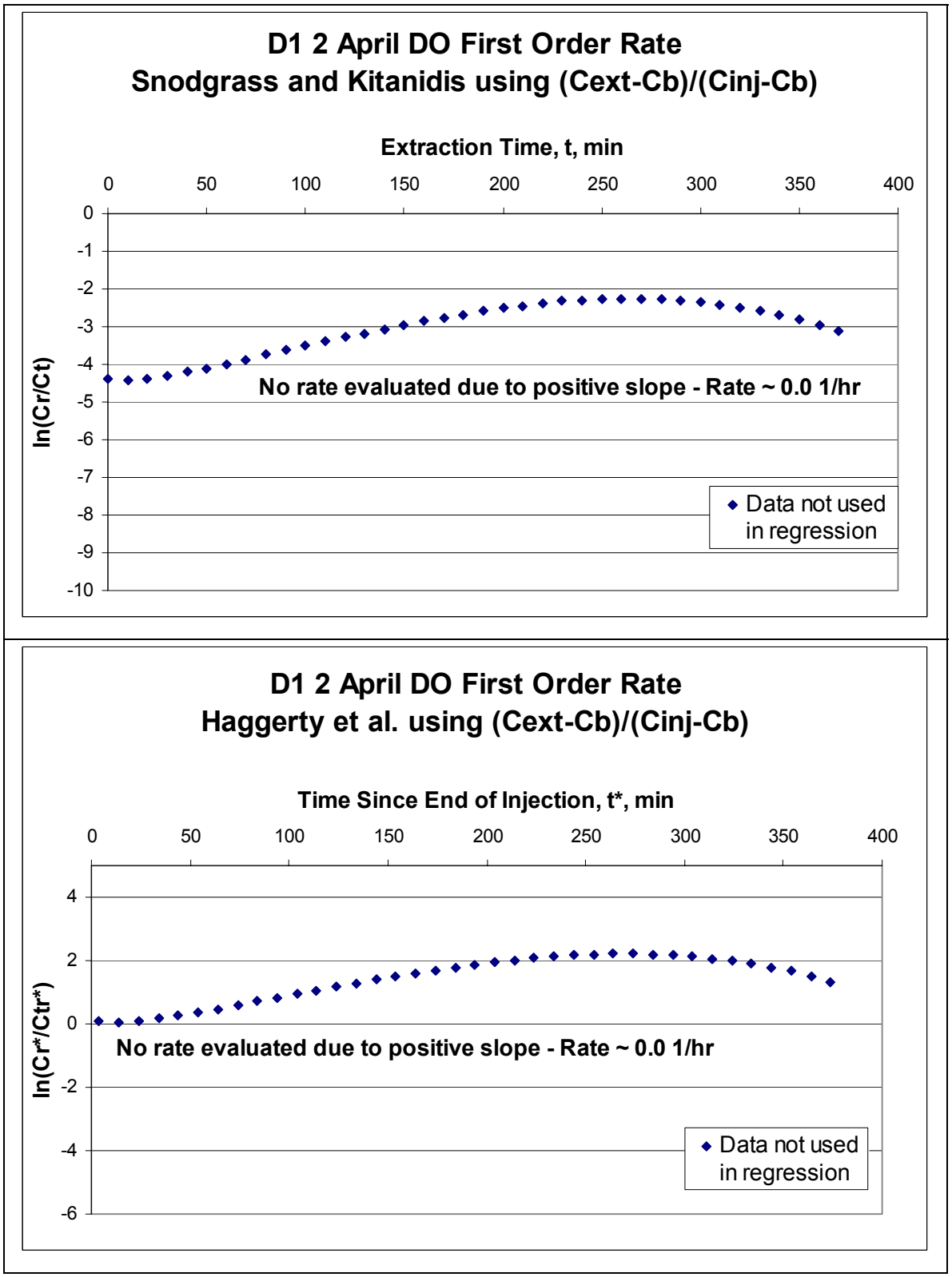

Figure C8 (cont.): Push-pull Test D1 2 April

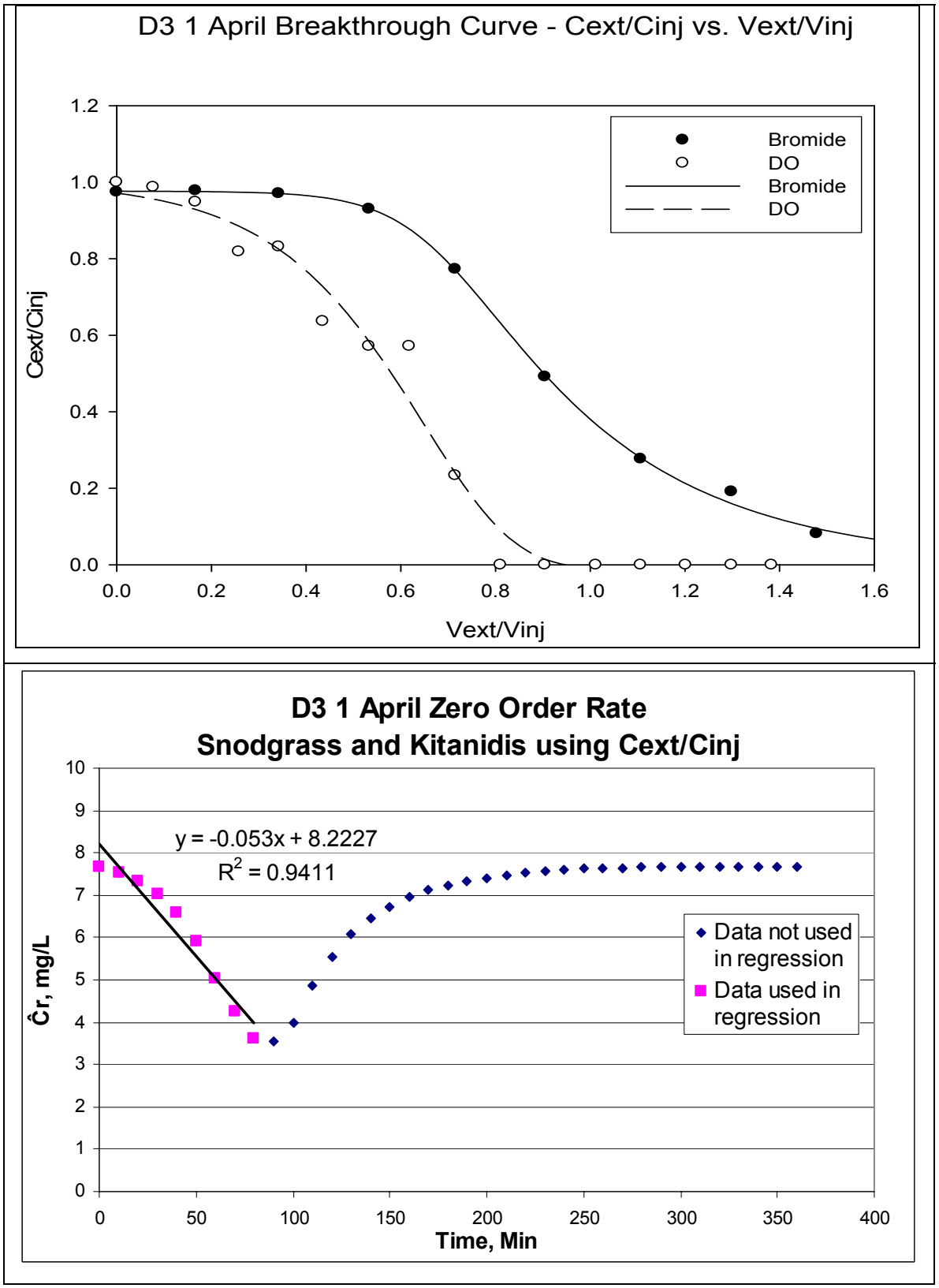

Figure C9: Push-pull Test D3 1 April

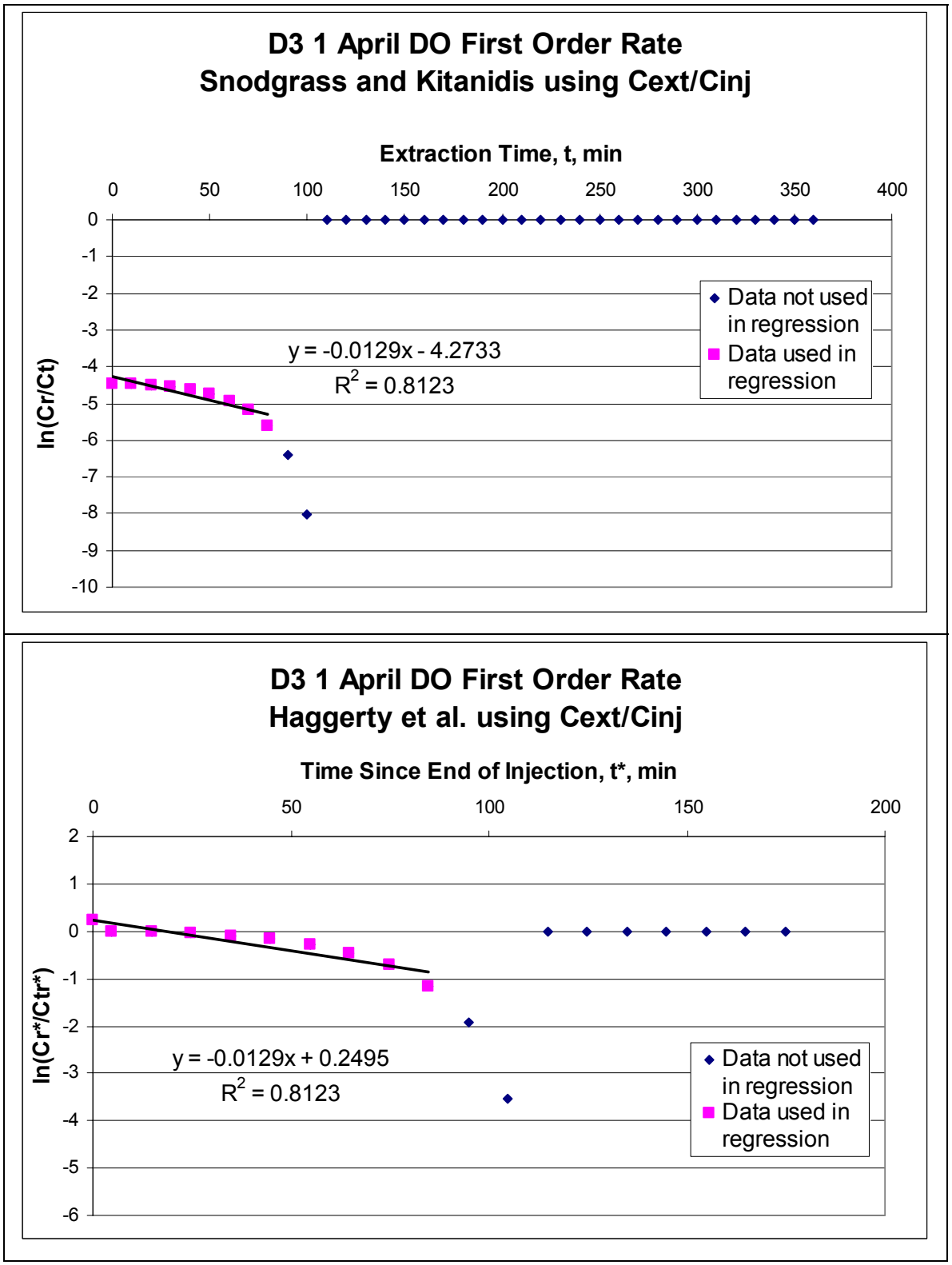

Figure C9 (cont.): Push-pull Test D3 1 April

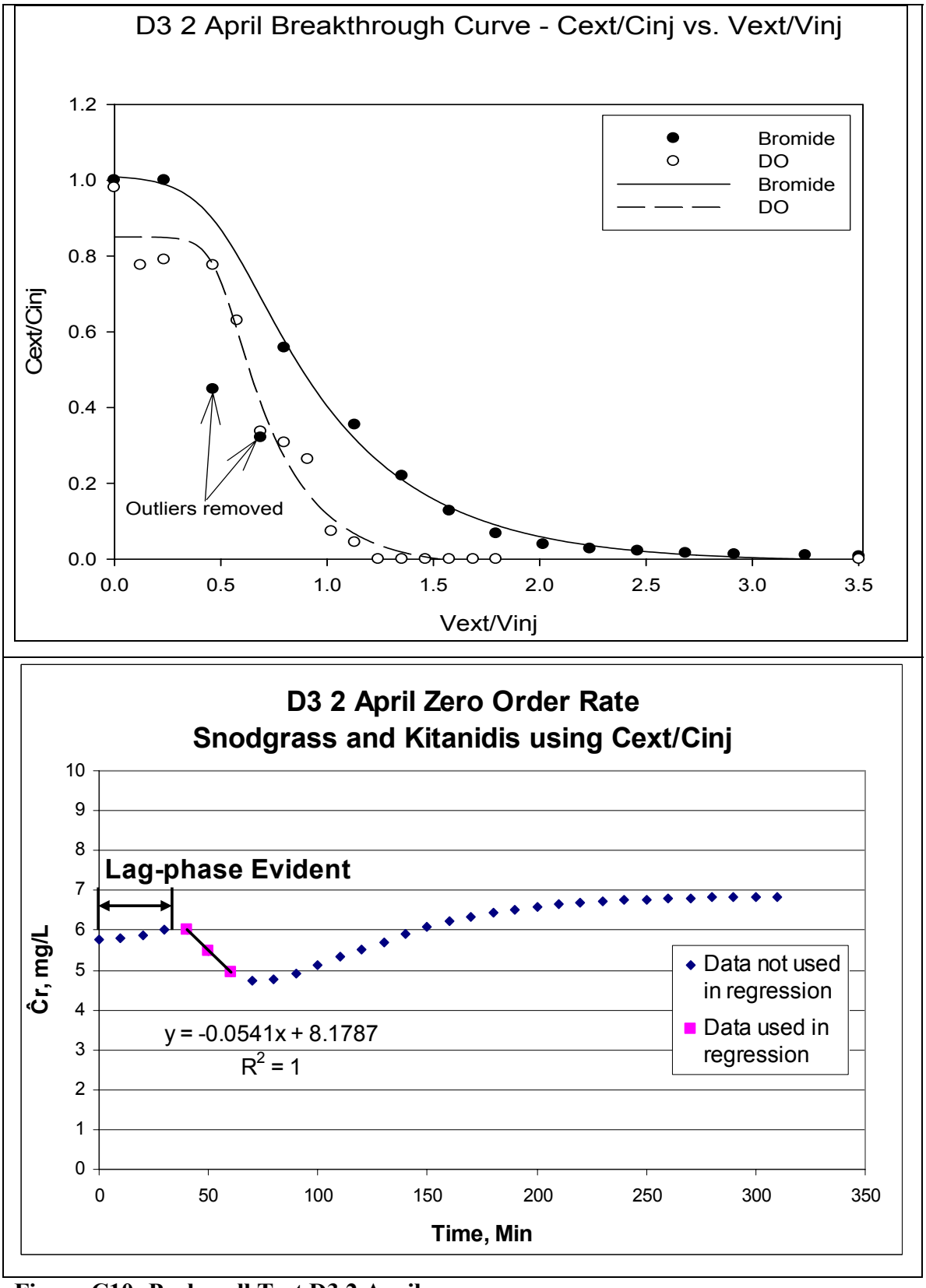

Figure C10: Push-pull Test D3 2 April

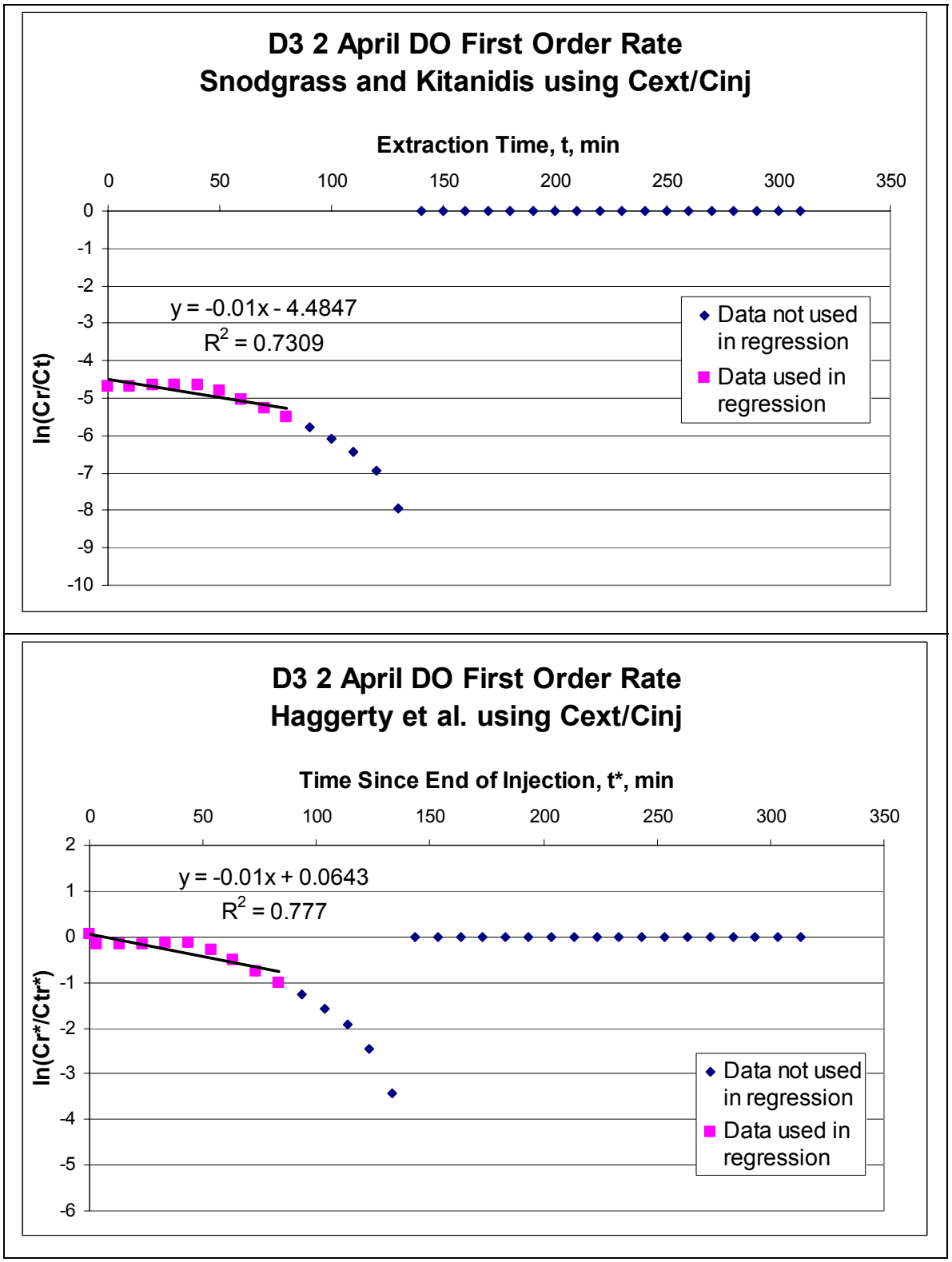

Figure C10 (cont.): Push-pull Test D3 2 April

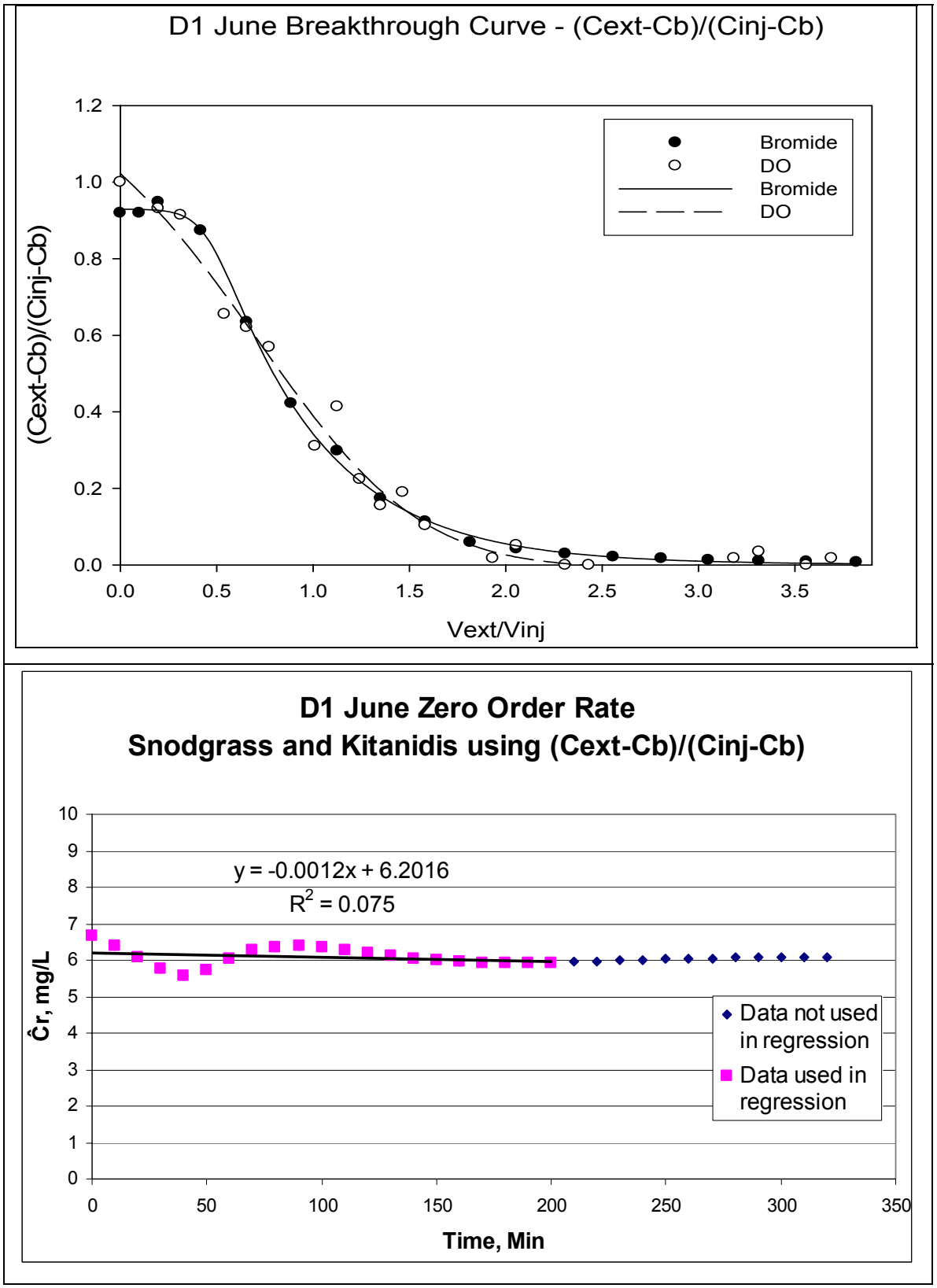

Figure C11: Push-pull Test D1 June

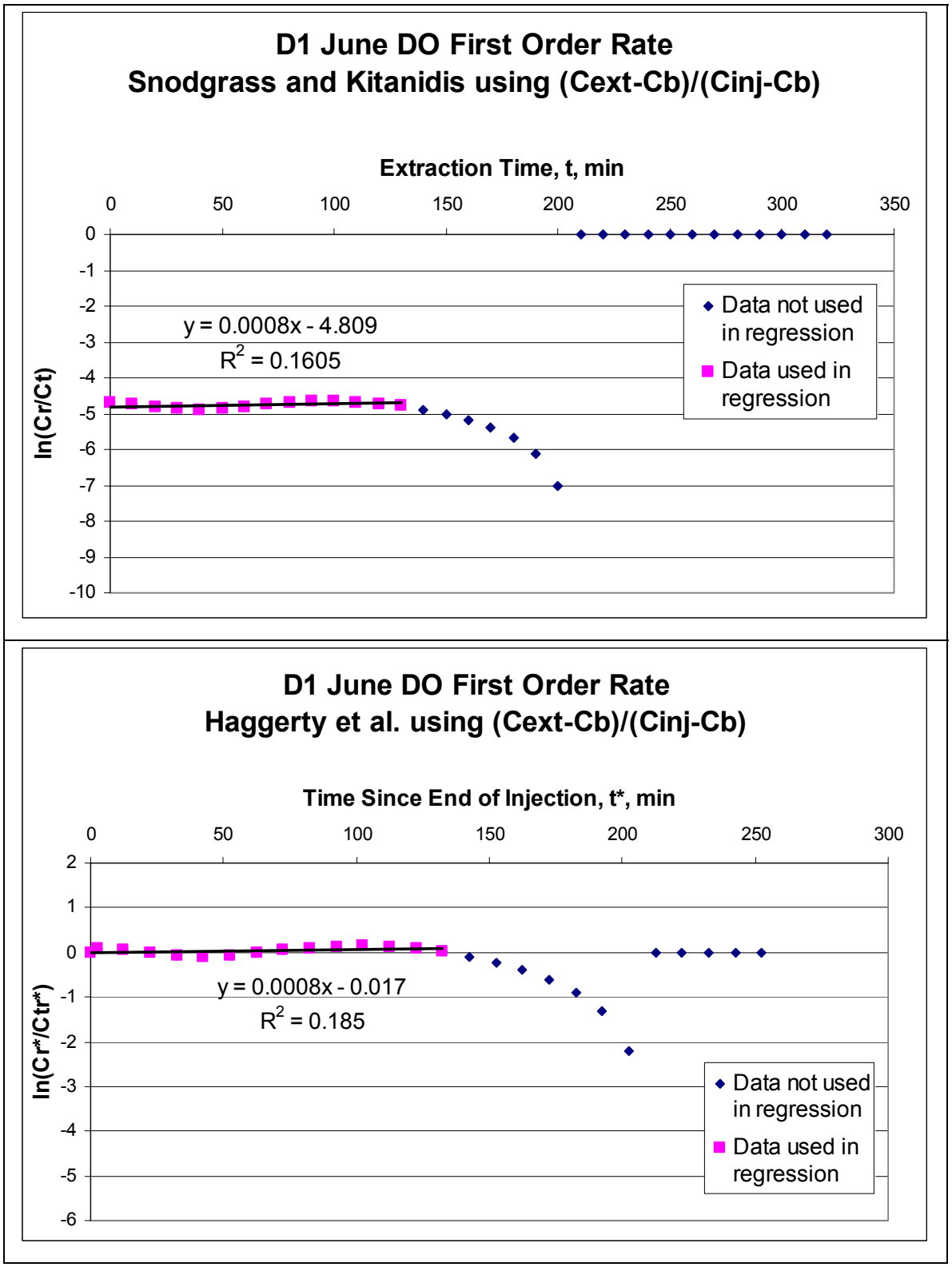

Figure C11 (cont.): Push-pull Test D1 June

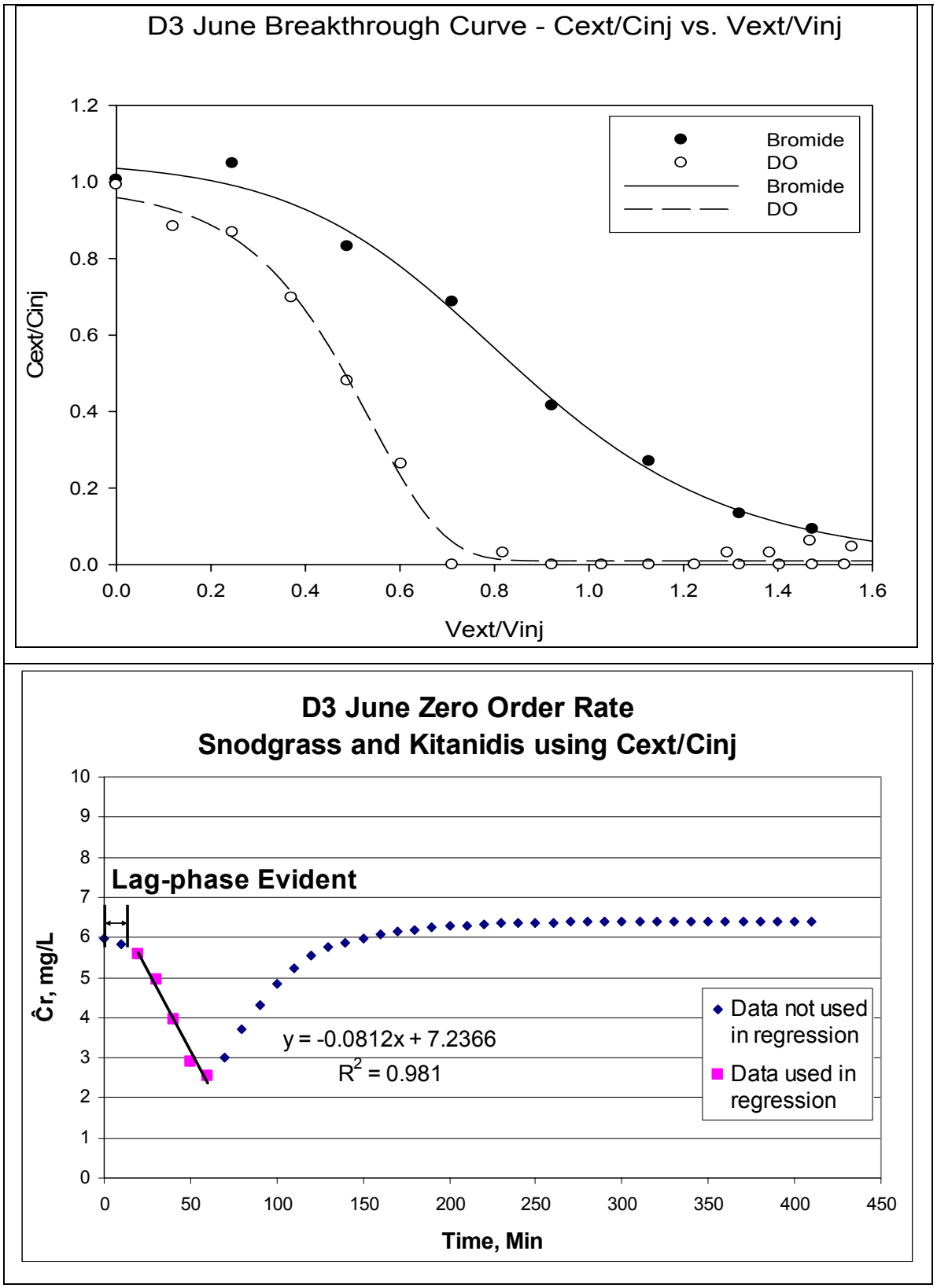

Figure C12: Push-pull Test D3 June

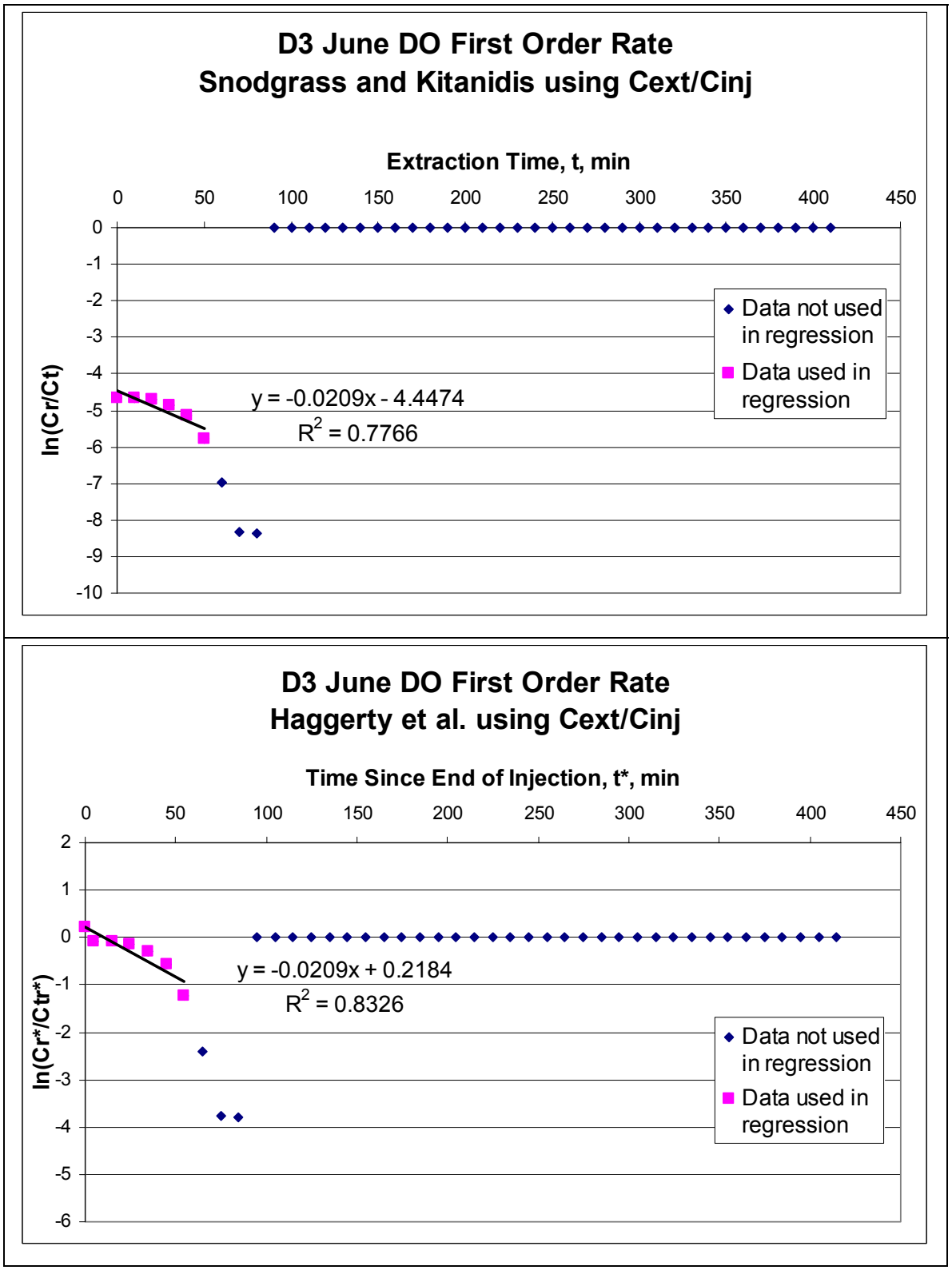

Figure C12 (cont.): Push-pull Test D3 June

VITA

Mark Thomas Pitterle was born on October 28, 1977 in Latrobe, PA. He graduated from Greensburg Central Catholic High School in 1996. He obtained his Bachelor of Science in Earth Science from Pennsylvania State University in 2000. He began his Master of Science degree in Environmental Engineering at Virginia Polytechnic and State University in 2001. In January 2004, he will begin a doctorate degree program in Civil and Environmental Engineering at the University of Colorado in Denver, CO working with the development of urban sustainable infrastructure.

At Work in the Field….

Oneida Poplar Tree Phytoremediation System

Getting to Know the Soils Used for Microcosms

Installment of Push-pull Wells. Wait a Minute….It's Not Raining!?!?

Field Analysis of Electron Donors During Push-pull Tests Knows No Hours

Wide Angle View of Oneida Poplar Tree Phytoremediation System

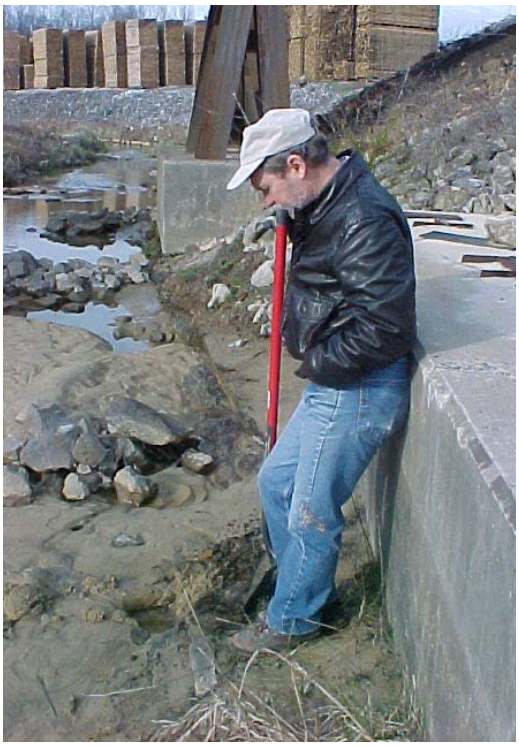

Deep Thoughts!

A Closer Look at the Oneida Monitoring System